



"Syntheses of high boron content
polyanionic multicluster
macromolecules for their potential use
in medicine"

Ana Maria Cioran

TESI DOCTORAL

Programa de Doctorat en Química

Director: Prof. Clara Viñas i Teixidor

Departament de Química

Facultat de Ciències

2013



Memòria presentada per aspirar al Grau de Doctor
per

Ana Maria Cioran

Vist i plau

Prof. Clara Viñas i Teixidor

Bellaterra, 10 de gener de 2013



Consejo Superior de Investigaciones Científicas
INSTITUT DE CIÈNCIA DE MATERIALS DE BARCELONA
Campus de la UAB. E-08193-Bellaterra, España
Tel. +34 93 580 18 53
Fax +34 93 580 57 29

La Professora Clara Viñas i Teixidor, Professora d'Investigació del *Consejo Superior de Investigaciones Científicas* a l'*Institut de Ciència de Materials de Barcelona*

CERTIFICA

Que n'ANA MARIA CIORAN, llicenciada en Enginyeria Química, ha realitzat sota la seva direcció el treball que porta per títol "*Syntheses of high boron content polyanionic multicluster macromolecules for their potential use in medicine*" que queda recollit en aquesta memòria per optar al títol de Doctor per la Universitat Autònoma de Barcelona.

I, perquè així consti i tingui els efectes corresponents, signa aquest certificat a Bellaterra, a 10 de gener de 2013.

Prof. Clara Viñas i Teixidor

ICMAB-CSIC

Aquest treball de recerca ha estat finançat per la *Comisión Interministerial de Ciencia y Tecnología*, CICYT mitjançant el projecte CTQ2010-16237 i per la *Generalitat de Catalunya* (projecte 2009/SGR/00279). Alhora, s'ha pogut realitzar gràcies a una beca per la *Formació de Personal Universitari* (FPU), referència AP2007-01723, concedida pel *Ministerio de Ciencia e Innovación*, des del juliol del 2008 al juliol del 2012. Tanmateix, en el marc de la beca FPU s'ha pogut realitzar una estada breu al Departament de Química de la Universitat de Liverpool des del gener a l'abril del 2012.

Aquest treball d'investigació, amb la data de defensa del 26 de febrer de 2013, té com a membres del tribunal a:

- President: Prof. Arben Merkoçi, Professor d'Investigació ICREA, Centre en d'Investigació Nanociència i Nanotecnologia, Campus UAB, Bellaterra.
- Vocal: Prof. Hiroyuki Nakamura, Professor of Chemistry and Life Science, Department of Chemistry, Gakushuin University, Tokyo 171-8588, Japan.
- Secretari: Dra. Rosa Maria Sebastian i Pérez, Professora titular de Química, Universitat Autònoma de Barcelona.

Com a membres suplents:

- Suplent 1: Prof. Joan Suades i Ortuño, Professor titular de Química, Universitat Autònoma de Barcelona.
- Suplent 2: Dra. Rosario Núñez Aguilera, Científica titular, Institut de Ciència de Materials de Barcelona (ICMAB-CSIC).

Acknowledgements

To begin with I would like very much to thank Prof. Clara Viñas who is also the supervisor of this Doctoral thesis for her extraordinary understanding and scientific support. It was very reassuring to know that I could always count on Prof. Viñas professional dedication but most of all, on her personal attention and concern. The hard work invested in this thesis became much easier, due to her energy and optimism, which proved to be somewhat contagious.

I would also like to thank to Prof. Francesc Teixidor for his constant interest and involvement in my research work, for his scientific advices and predisposition to solve any doubt of mine, at any moment. To both of them I would like to express my gratitude for accepting me within the research group.

To Dra. Rosario Núñez and Dr. José Giner for their kind spirit, not to mention the support they have been showing me ever since I arrived to Barcelona.

My sincere appreciation to Prof. Mathias Brust for his kindness and exceptional consideration he showed me during my short-term stage within his research group at the University of Liverpool. I would also like to thank him for giving me the opportunity to learn new and very interesting things regarding the world of nanoparticles. My thanks extend to Tania, Zeljka and Sam, from Prof. Brust's group, for their attention and collaboration.

Special thanks to Prof. Josefina Pons, from the Universitat Autònoma de Barcelona for accepting to be my tutor during the Doctoral program.

To Prof. Reijo Sillanpää (University of Jyväskylä) for the resolution of the crystalline structure presented in this research work.

I also want to thank Prof. Carles Miravittles and Prof. Xavier Obradors, ex-Director and Director of the *Institut de Ciència de Materials de Barcelona* (ICMAB-CSIC) for giving me the opportunity to make use of all the services within the *Institut* as well as to all the ICMAB's personnel (Trini, Vincente *et al.*) for the kind way they have been treating me.

To Anna Fernandez, who worked closely with us, helping us every single time by performing NMR and MALDI-TOF-MS analyses, but also for her joyfulness and wishful thinking.

También tengo muchas cosas que agradecer a Jordi Cortés que siempre se portó muy bien conmigo...gracias por escucharme cuando lo necesitaba y por estar a mi lado.

To my colleagues and also my friends with whom I have spent a lot of time both in and outside the lab: to Màrius Tarrés for performing and helping me interpret the results gathered from CV studies on several of my compounds and for your constant good humor; to Emilio, for all your help; to Pau, for your support and also for the sweet and quite special treats like rosmarine chocolate; to Ariadna, who has always been there for me; to Patricia, for charming us with her crystal-clear voice; to David, for our contradictory talks that heat up the spirits; to Radu, my Romanian comrade with whom I have started this adventure, to Ana and Marius for their affection and friendly chats (va doresc inca de pe acum casa de piatra!!); to Adnana, a very close friend, thank you for all the support and trust we have shared, for carrying so much about my happiness and wellbeing-it's been a pleasure sharing the hood with you!! To Victor, for being like a breath of fresh air to the group; to Ivy and Elena, the freshmen of the group, for your collaboration: I wish you the best with your research! To Justo, for his friendliness and good cheer; A Jordi y Mireia, por su amistad y soporte incondicional, ayudándome incluso antes de pedírselo (gracias!!).

I would also like to thank the persons who have spent less time alongside me during these last four years, but not for this reason less important: to Anca Stoica, for guiding me and helping me without preservation every time I needed; to Arantxa and Flor, for teaching me new things and for their advice in both work related as well as in personal topics; to Mònica, for her warmth and sweetness; to Elena M. for her friendship and also help in the laboratory; and to José, Noe, Yan, Will, Damien and Greg for their company and contagious happiness.

To the little, but joyful Romanian group from ICMAB (Roxana, Carmen, Costana), for being like a family to me.

To Ana Dobrișa, a wonderful person and a close friend, for all the precious moments spent together...for the special connection we share and for being always by my side.

My thoughts also carry me to the home I left behind, to the wonderful people I have back there. I want to thank all my friends (especially to Jenny, Rux and Dana) for helping and giving my dreams the wings they needed to get where I am now and on whom I know I can always count.

To my family: I have left you last, because you are the most important in my life. You have constantly been there for me, helping me fight for what I wanted. Thank you for all your patience, dedication and love that you have forever blessed me with. Bunicilor mei, pentru toata dragostea si bunatatea cu care m-au inconjurat mereu – imi doresc sa pot ajunge sa fiu pentru nepotii mei macar un sfert din tot ce insemnati voi pentru mine! Thank you for making me what I am today!!

Quiero expresamente dar las gracias a mi familia "adoptiva" de aquí, por haberme proporcionado todo (y mas!) cariño y ánimo que necesitaba y por hacerme sonreír. A vuestro lado me siento en casa!!

A mi Albert, la persona más importante de mi vida, tengo todo para agradecer: la paciencia que muestras cada día conmigo, el hecho de que siempre tienes cosas buenas por decirme, el saber cómo animarme cuando estoy en mis peores momentos, darme la confianza que necesito para seguir luchando por mis sueños...apenas he empezado, podría seguir durante paginas y paginas sin repetirme ni una sola vez...lo eres todo para mi!! Y como decía alguien hace tiempo, "noi te iubim foarte mult"!! Yo mas!!!

Thank you all for being there for me, with me, for good and bad!

The best is yet to come!!

Organització del Manuscrit

D'acord amb la normativa vigent i prèvia acceptació de la comissió de Doctorat de la Universitat Autònoma de Barcelona, aquesta Memòria es presenta com a recull de publicacions. Els treballs inclosos en aquesta memòria són:

Addendum: Articles publicats i presentats a la Comissió de Doctorat de la Universitat Autònoma de Barcelona al juliol de 2012:

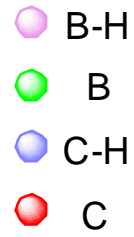
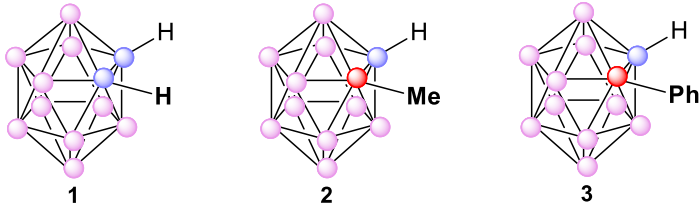
1. "Toward the synthesis of high boron content polyanionic multicluster molecules". Pau Farràs, Ana Maria Cioran, Václav Šícha, Francesc Teixidor, Bohumil Štíbr, Bohumír Grüner, Clara Viñas, *Inorganic Chemistry*, **2009**, *48*, 8210–8219, DOI: 10.1021/ic9006907.

2. "Mercaptocarborane-capped gold nanoparticles: electron pools and ion traps with switchable hydrophilicity". Ana M. Cioran, Ana D. Musteti, Francesc Teixidor, Jelka Krpeti, Ian A. Prior, Qian He, Christopher J. Kiely, Mathias Brust and Clara Viñas, *Journal of American Chemical Society*, **2012**, *134*, 212–221, DOI: 10.1021/ja203367h.

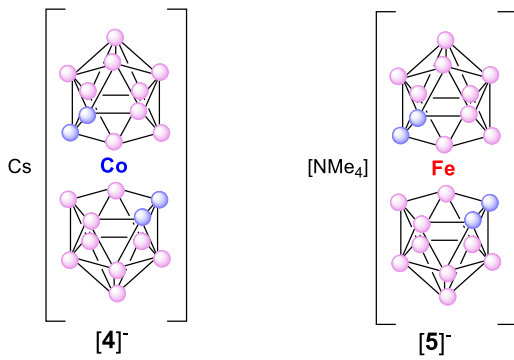
Figures



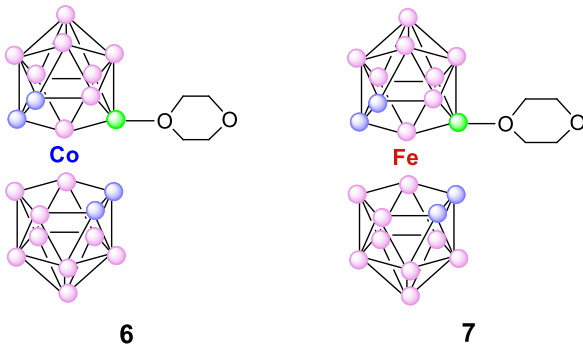
Neutral clusters



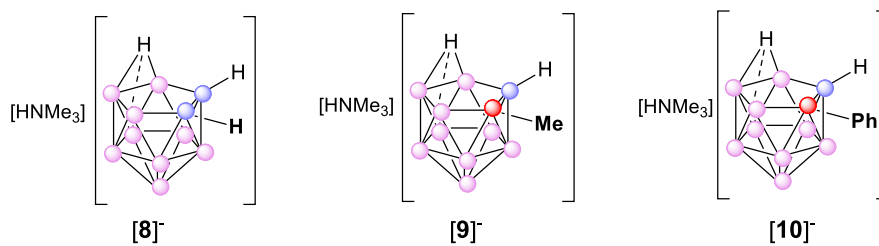
Anionic clusters



Zwitterionic clusters



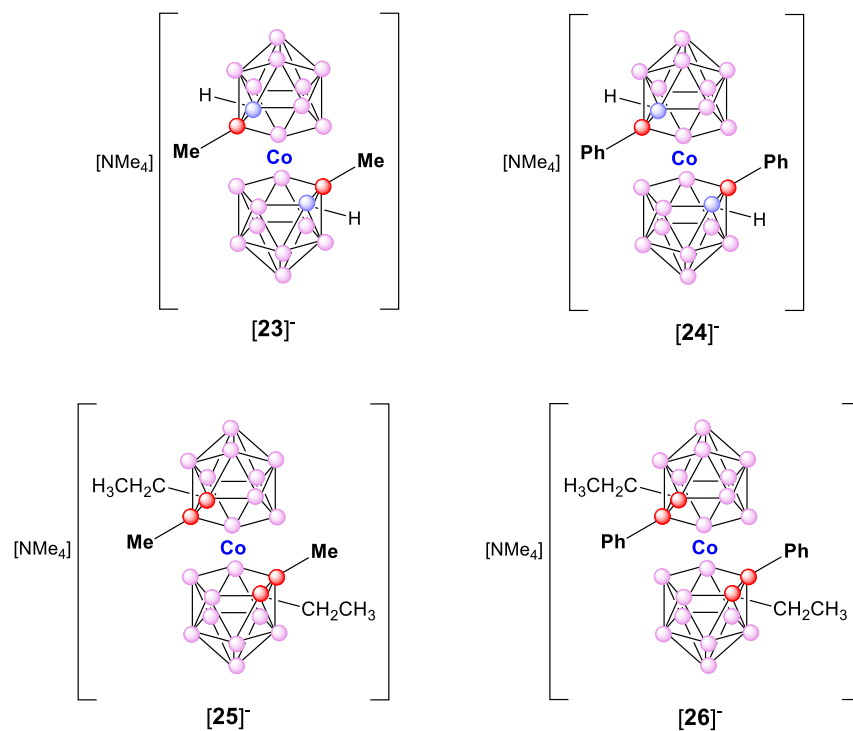
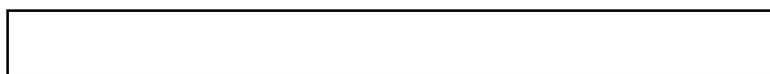
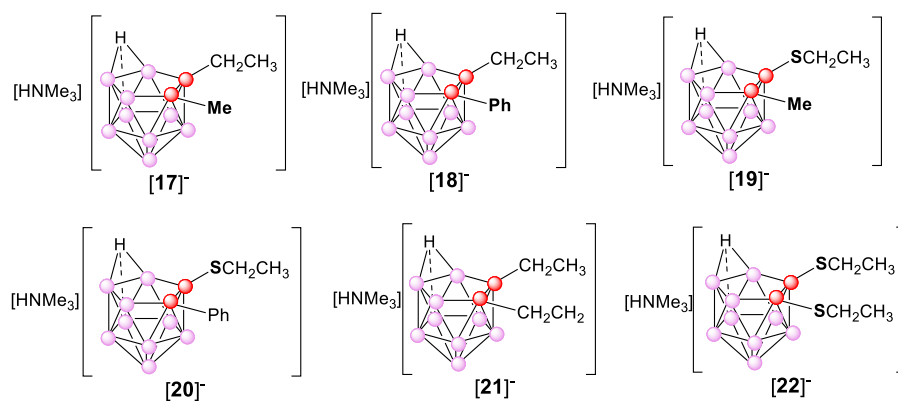
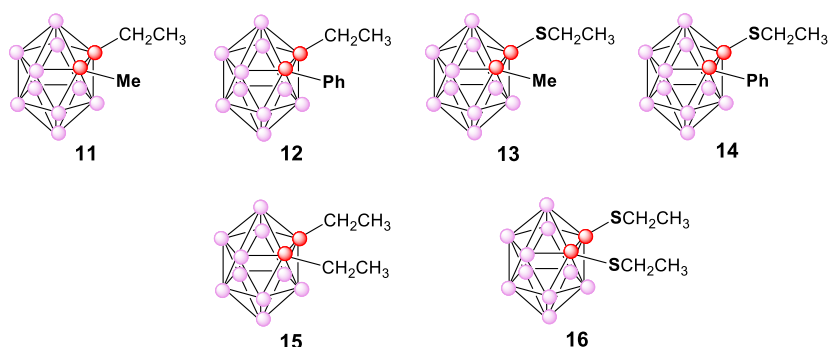
Anionic *nido*-carborane clusters

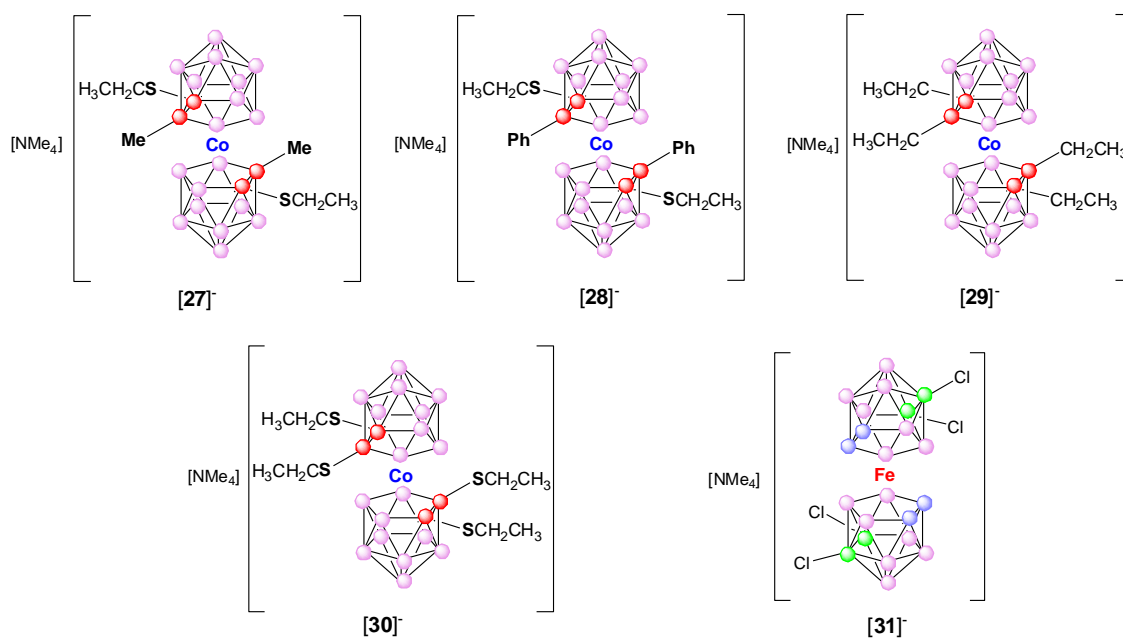


Compounds synthesized *via* a different procedure

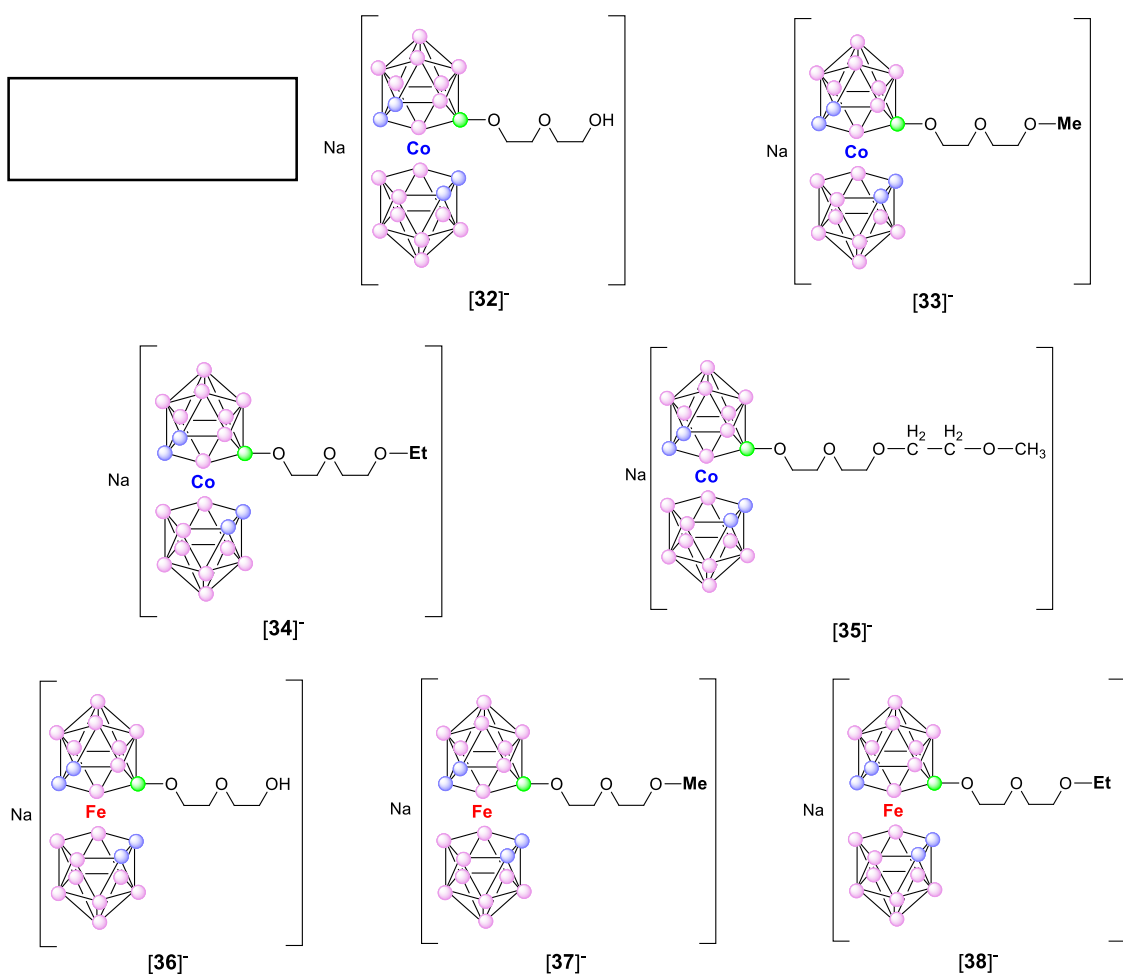
Already
reported
compounds

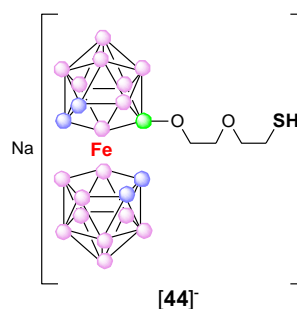
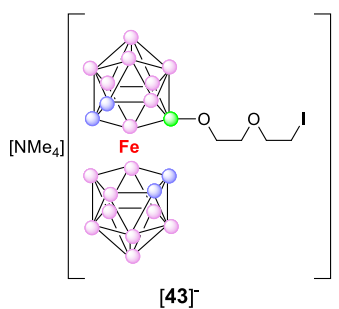
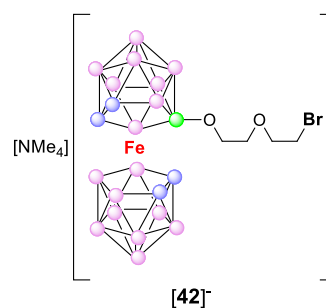
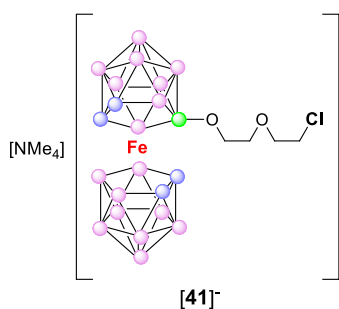
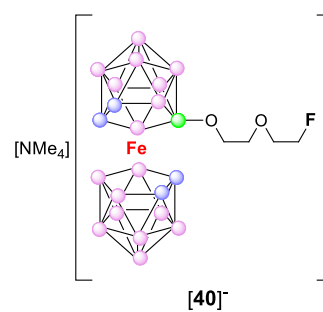
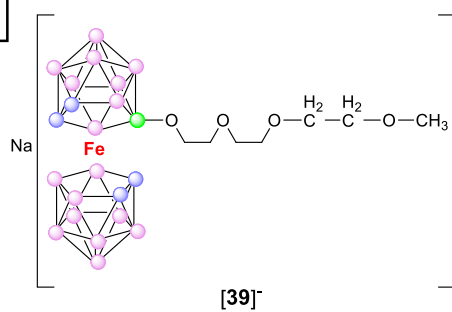
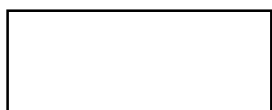
Chapter 2.1. Solid state complexation reactions



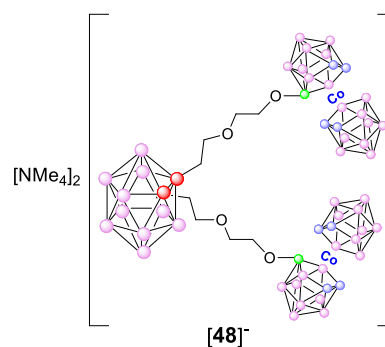
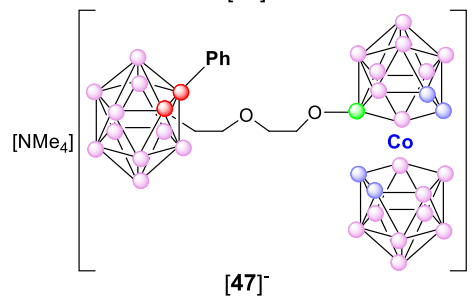
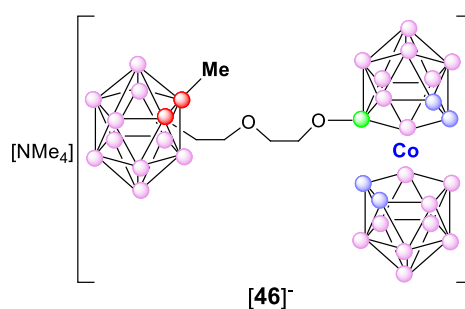
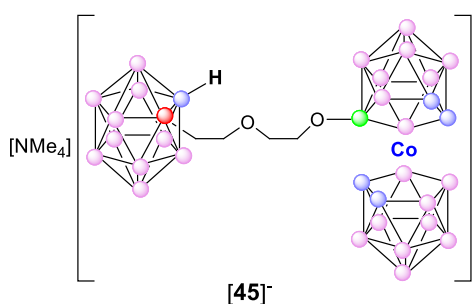
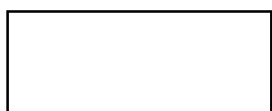


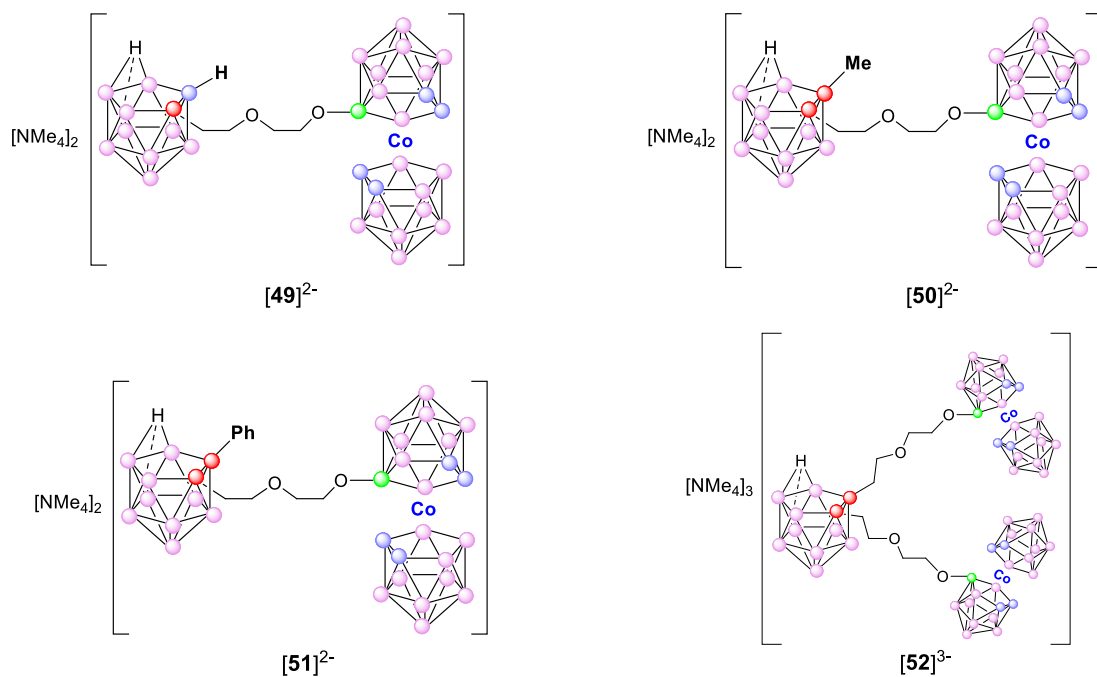
Chapter 2.2. 1,4-dioxane derivative of cobaltabis(dicarbollide) and ferrabis(dicarbollide) with various groups



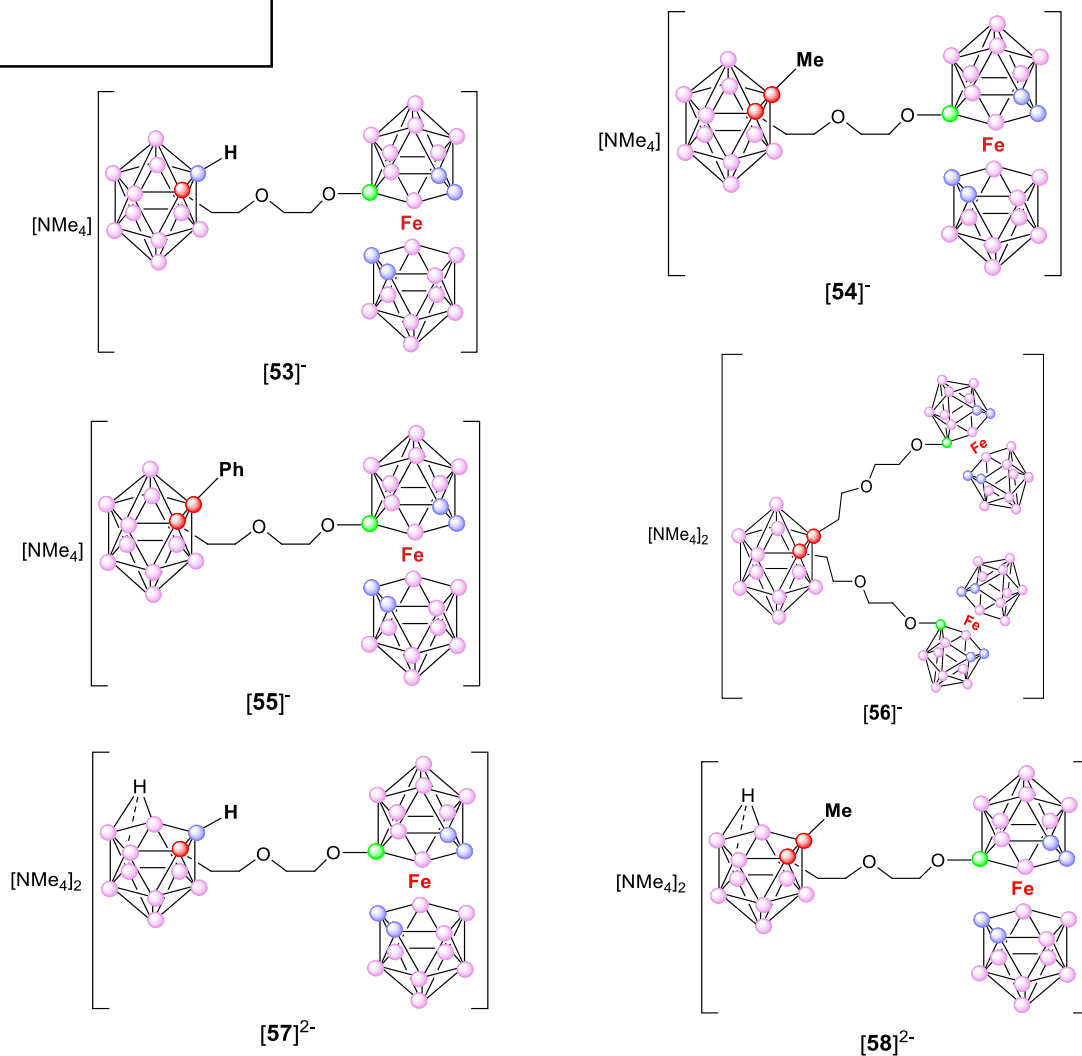


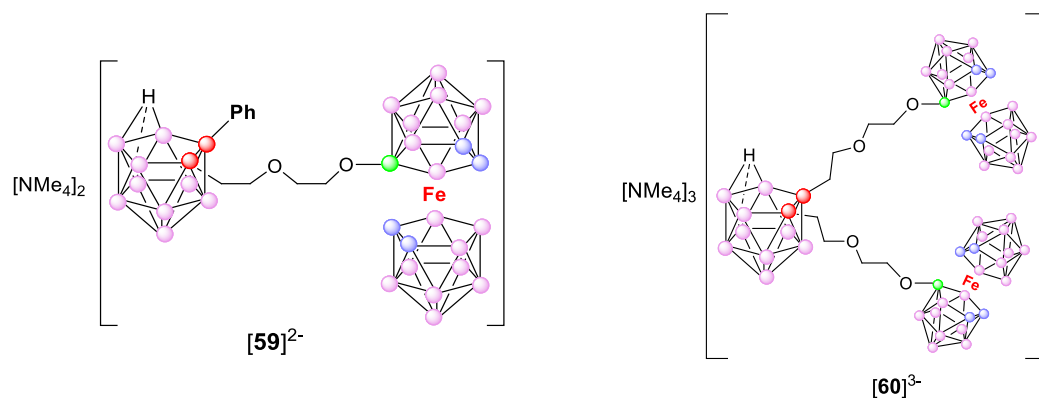
Chapter 2.3. *Closo* and *nido* cobalt(III) compounds substituted at the carbon vertices



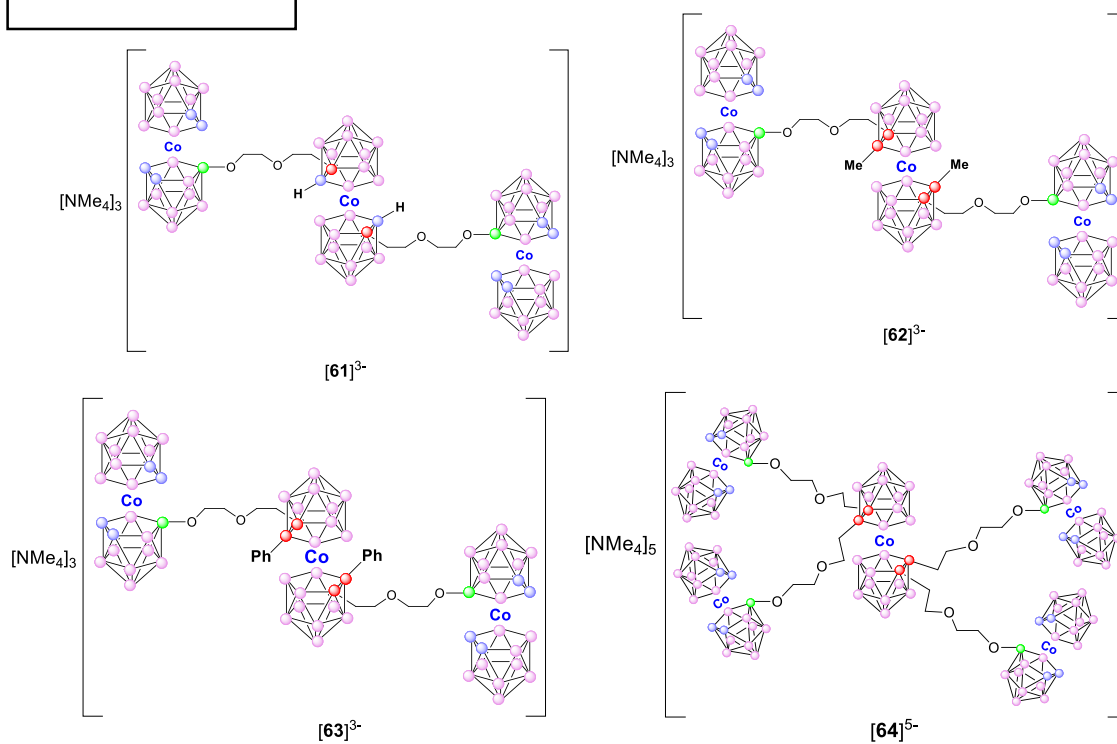
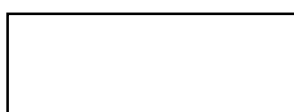


Chapter 2.3. *Closo* and *nido* ferra(III) compounds substituted at the carbon vertices

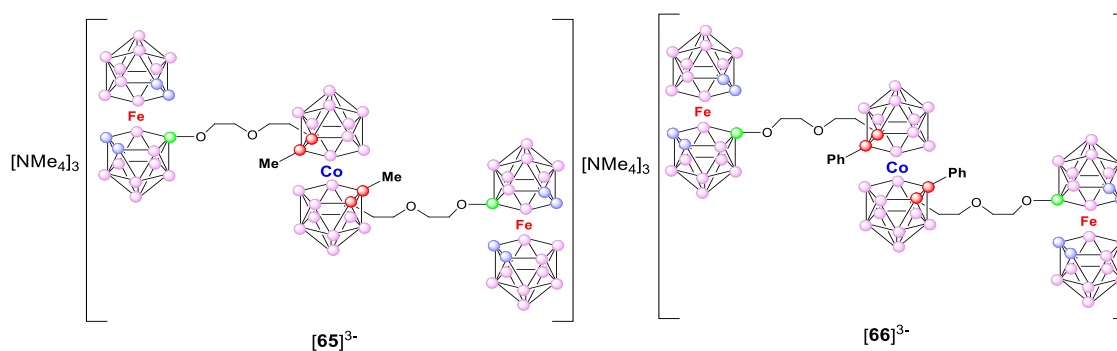
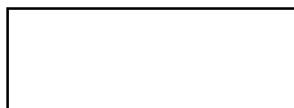


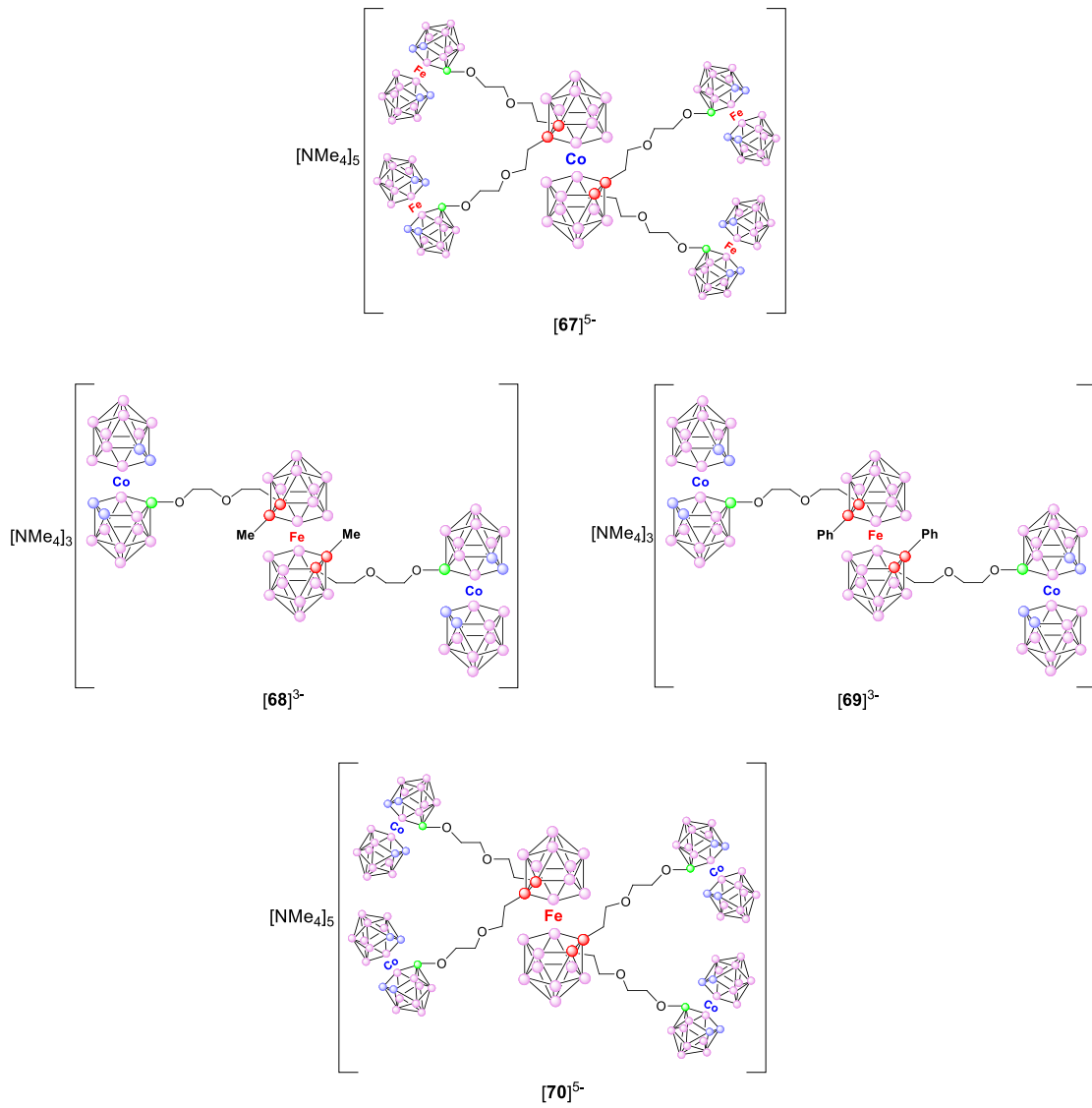


Subchapter 2.3.3. Synthesis of cobaltabis(dicarbollide) sandwich-type complexes

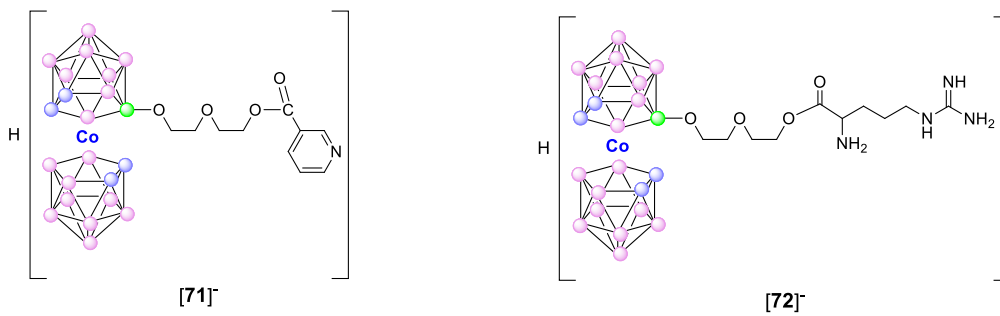


Subchapter 2.3.4. Synthesis of heterometal sandwich-type complexes

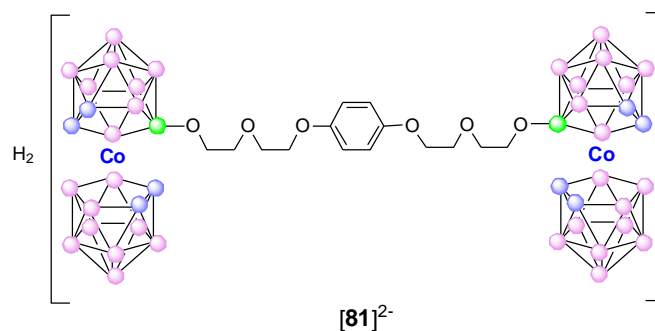
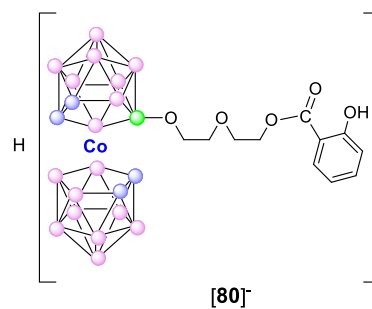
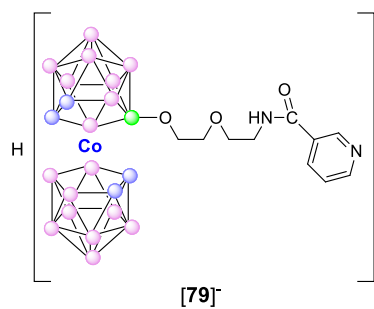
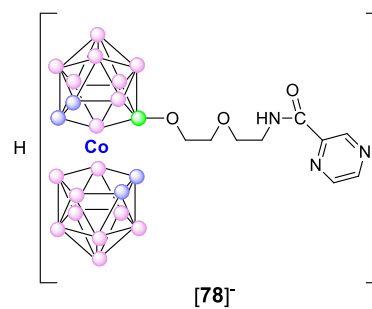
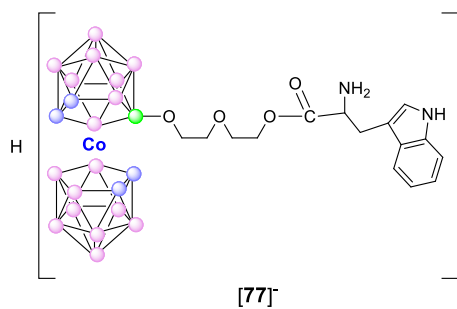
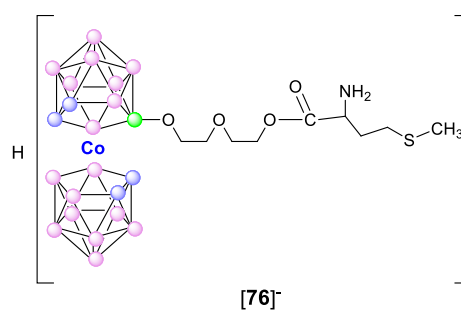
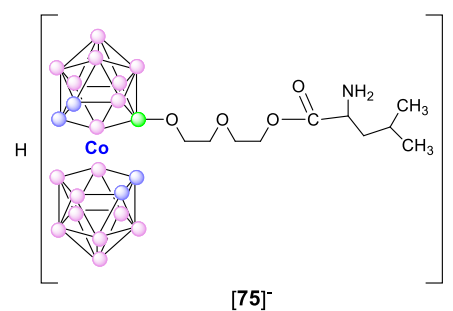
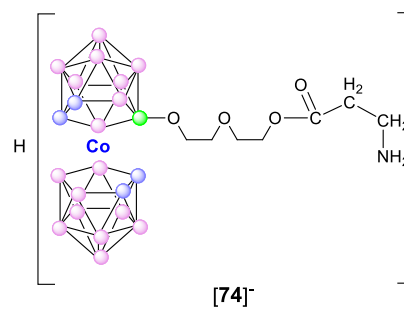
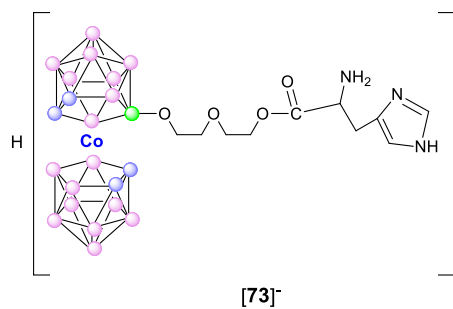




Chapter 2.4. 1,4-dioxane derivative of cobaltabis(dicarbollide) with biomolecules



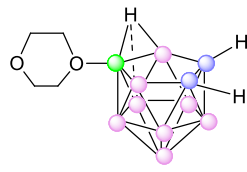
Already reported
compound



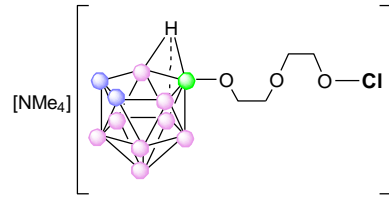
Innovative
compounds

Already reported
compounds

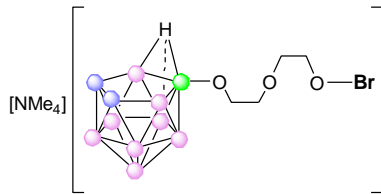
Chapter 2.5. Cyclic oxonium derivatives of polyhedral boron hydrides



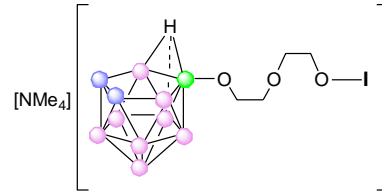
82



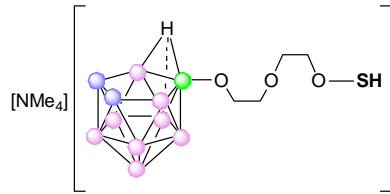
[83]⁻



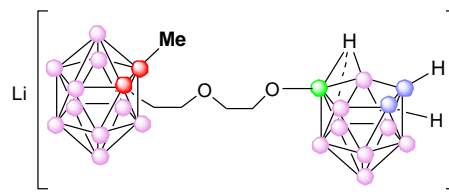
[84]⁻



[85]⁻

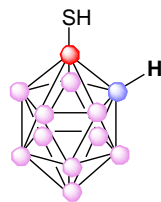


[86]⁻

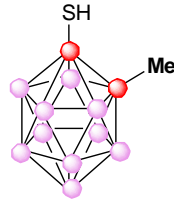


[87]⁻

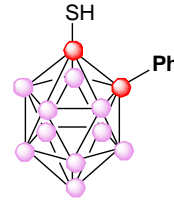
Chapter 2.6. Preparation and characterization of MPCs capped with thiol-based boron clusters



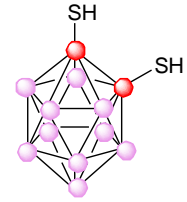
88



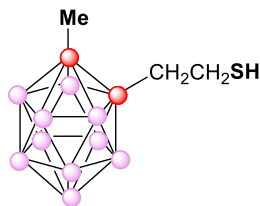
89



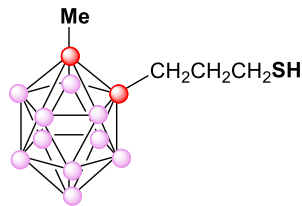
90



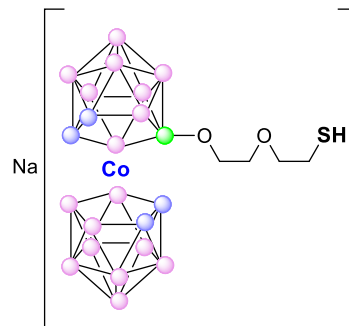
91



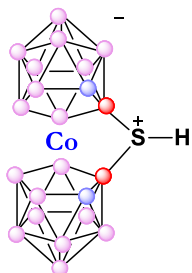
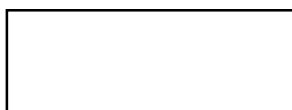
92



93



[94]⁻



95

Abbreviations

Me:	methyl group
Ph:	phenyl group
Et:	ethyl group
DME (Glyme):	DiMethoxyEthane
C _{carborane} :	carbon atom belonging to the carborane cluster
C _{cosane} :	carbon atom belonging to the cobaltabis(dicarbollide) complex
C _{fesane} :	carbon atom belonging to the ferrabis(dicarbollide) complex
H _{bridge} :	hydrogen atom bounded to a boron atom from the open face
H _{terminal} :	hydrogen atom bounded to a cluster boron atom
<i>o</i> -carborane:	<i>ortho</i> -carborane
<i>m</i> -carborane:	<i>meta</i> -carborane
<i>p</i> -carborane:	<i>para</i> -carborane
acetone-d ₆ (CH ₃ COCH ₃)	deuterated acetone
aq.:	aqueous
THF	tetrahydrofuran
LiCl	lithium chloride
<i>n</i> -BuLi:	<i>n</i> -butyllithium
<i>t</i> -Bu:	<i>tert</i> -butyl
BNCT:	Boron Neutron Capture Therapy
MPCs	Monolayer Protected Clusters
IR:	InfraRed
NMR:	Nuclear Magnetic Resonance
MALDI-TOF-MS:	Matrix Assisted Laser Desorption Ionization-Time of Flight–Mass Spectrometry
UV	UltraViolet
TGA	ThermoGravimetric Analysis
DSC:	Differential Scanning Calorimetry
XPS	X-ray photoelectron <i>spectroscopy</i>
CPS	Centrifuge Particle Sizing
TEM	<i>Transmission electron microscopy</i>
STEM-HAADF	High Angle Annular Dark Field (<i>HAADF</i>) Scanning Transmission Electron Microscopy (<i>STEM</i>)
ROS	Reactive Oxygen Species
m/ z:	mass/ charge

M	molar (mols ⁻¹ l ⁻¹)
S ₈	sulphur
PEG	polyethyleneglicol
BSSP	bis(4-sulfonatophenyl)phenylphosphane dihydrate dipotassium salt
CALNN	peptide sequence
ca.	circa
aprox.:	approximatly

For NMR spectra

δ (ppm):	chemical shifts in parts per million
s:	singlet
d:	doublet
t:	triplet
q:	quadruplet
m:	multiplet
ⁿ J(A,B):	coupling constant between A and B nuclei separated by <i>n</i> bonds
TMS:	TetraMethylSilane

For InfraRed spectra

I:	intense
vl:	very intense
ll:	low intensity
σ:	tension vibration
τ:	deformation vibration

Summary of the thesis

The research presented in this global summary illustrates the syntheses and characterization of the compounds obtained throughout the doctoral thesis as well as a section dedicated to the applications for some of the designed species.

1) The first chapter of the thesis deals with the syntheses of cobaltabis(dicarbollide) and ferrabis(dicarbollide) compounds *via* a rapid and environmental complexation reaction in solid state. The already reported in the literature syntheses of these compounds are performed in solution and moreover, are time consuming and quite difficult, requiring many reaction steps. The novelty that this new type of synthesis brings, besides time efficiency, is the fact that it requires no solvents which have measurable vapor pressure, and hence can emit volatile

organic compounds (VOCs). We have successfully synthesized the cobaltabis(dicarbollide) species in very high yields (83-90%), depending on the time of reaction and also proved our new method on cobaltabis(dicarbollide) and ferrabis(dicarbollide) derivatives possessing one or two substituents as well as on compounds bearing substituents with free pair of electrons. The gathered results indicate that the presence of a second substituent decreases the yield of the complexation reactions, and also that an organic group possessing either an element with a free pair of electrons or a π group within the molecule strongly diminishes the yield or even does not allow the reaction to take place.

2) Another subject of interest was the synthesis of alkyl-, halogen- and thiol-terminated synthons based on the oxonium derivative of ferrabis(dicarbollide). This is especially attractive, since breaking one carbon-oxygen bond should result in a moiety having a boron complex separated from a carbocationic center by 6 or more atoms (polyglycolic chain). The syntheses of halogen/thiol-terminated ferrabis(dicarbollide) synthons were of particular interest for their posterior covalent bonding to different platforms, leading to the obtaining of a wide variety of novel materials for new applications, such as surface functionalization. Our objective was to be able to synthesize, in a simple and rapid way, derivatives of ferrabis(dicarbollide) containing a terminal halide, and thus facilitating the applicability of metallocarboranes in a variety of different fields. The reaction conditions did not involve working with anhydrous solvents or in inert nitrogen atmosphere; it is simply the use of concentrated haloacids in organic solvents that led to the synthesis of the sought compounds, with yields greater than 80%.

Besides ring-opening with various haloacids, another high atomic efficient reaction was the synthesis of thiol-terminated ferrabis(dicarbollide) synthons, species that will prove to be very utile in groundbreaking applications, among which surface functionalization, by using these compounds as capping agents for nanoparticle stabilization. The functionalization of gold nanoparticles with this and other thiol-terminated carboranes and metallocarborane synthons opens the way to a wide variety of applications in catalysis, development of electronic devices and medicine to name only a few. Moreover, the fact that ferrabis(dicarbollide) has a rigid structure, restricted surface orientation and extensive possible modification chemistry, provides the axes for controlling their self-assembly, and therefore, will prove useful for enabling new applications.

3) One of the main goals of this doctoral work was the syntheses of polyanionic species as novel high-boron content molecules with enhanced water solubility using carboranyl anions as nucleophilic agents. The synthetic way was based on the use of *ortho*-carboranyl cluster and its respective derivatives (1-Me-*ortho*-carboranyl, 1-Ph-*ortho*-carboranyl) as nucleophiles in the 1,4-dioxane ring-opening reaction of cyclic oxonium [3,3'-M-8-(OCH₂CH₂)₂-1,2-C₂B₉H₁₀](1',2'-C₂B₉H₁₁)] (M = **Co**, **Fe**) compound to isolate mono- and di-anions of structures combining [3,3'-M(1,2-C₂B₉H₁₁)₂]⁻ and C₂B₁₀H₁₂ structural motifs, named *closo* compounds.

The *closo* carborane clusters are structures showing high stability with respect to strong acids but instead they react with Lewis bases (nucleophilic agents, such as potassium ethoxide) yielding more opened structures, known as *nido*, by a partial deboronation process. In this way

di- and tri-anionic macromolecules that combine $[3,3'-M(1,2-C_2B_9H_{11})_2]^-$ ($M = \text{Co}, \text{Fe}$) and $[C_2B_9H_{12}]^-$ clusters were synthesized, showing, due to their anionic character, water solubility, feature important for the future applications of these polyanionic macromolecules in medicine.

Starting from these previously obtained *nido* clusters, by a complexation reaction with either anhydrous $CoCl_2$ or $FeCl_2$, polyanionic organometallic compounds with sandwich-like structures can be synthesised, complexes where the metal coordinates two ligand units due to the disproportionation of the metal (II) into M (0) and M (III). Furthermore, we report in this doctoral thesis the syntheses of compounds containing either **Co**, **Fe** or both of them within the same molecule. Since these sandwich-type coordination complexes are polyanionic, they are more soluble in water and therefore could be important candidates for possible applications in the Boron Neutron Capture Therapy (BNCT), mainly in the treatment of tumor cells.

4) Another aim of this thesis was the ring-opening reaction of the zwitterionic cobaltabis(dicarbollide) derivative with biomolecules, such as aminoacids and antibiotics *via* a nucleophilic attack on the positively charged oxygen atom. In this particular case, the biomolecule moiety acts as a transport vector, delivering the boron-containing compound to the desired site (tumor), the following step being the irradiation with slow neutrons inducing the death of the cancerous cells. All the obtained cobaltabis(dicarbollide) complexes containing biomolecules have more boron atoms per molecule than either the carboranes or the *closo*-dodecaborate anion, making them more attractive from the BNCT point of view. Moreover, the presence of the biomolecules as well as the fact that they show increased water-solubility, convert these macromolecules into more biocompatible compounds, and hence better suited for medical applications.

5) Moreover, we attempted the dioxane ring-opening of oxonium derivative $[10-(OCH_2CH_2)_2-7,8-C_2B_9H_{11}]^+$ with nucleophiles such as halogen and thiol groups. However, with the exception of the reaction performed with concentrated hydrochloric acid, these reactions were not successful. The conclusion that can be drawn from these experiments is that the zwitterionic derivative of the cobaltabis(dicarbollide) species is more reactive since the halogen/thiol ending compounds did not were synthesized. This can be explained by electronic repulsions occurring between the negative charge located over the open pentagonal face of the $[10-(OCH_2CH_2)_2-7,8-C_2B_9H_{11}]^+$ and the nucleophilic agent.

6) And last but certainly not least, we have performed the enclavation of previously synthesized compounds bearing thiol groups to different platforms, such as gold nanoparticles (Point 2 above). In order to achieve this we first synthesized various types of capping ligands, both neutral and anionic, for a better study of the resulting properties. We expected that the use of anionic clusters, which possess different properties with respect to the neutral thioligands, would introduce quite unique and different properties to the resulting nanoparticles. In addition, we also pretended to investigate if the presence of an alkyl chain separating the thiol group from the boron cage would influence in any way on the properties of the prepared species, since the cluster will be further away from the gold core. We have started off with one of the simplest thioligand, namely mercaptocarborane, species showing a major advantage with respect to the

other ligands, namely the fact that we have C-H bond present within the molecule, moiety that would later on be useful for further substitutions. Using this compound as stabilizing agent, we prepared and characterized 3 nm gold nanoparticles, by reducing with sodium borohydrate. These newly obtained nanoparticles exhibit unique properties regarding phase transfer and cellular uptake. However, the gold nanoparticles functionalized with the other boron clusters did not possess any of the above described properties.

Moreover, we have synthesized 10 nm water soluble gold nanoparticles, by interchanging citrate stabilizing ligands with our thioligands and the resulting properties were quite exciting as well. We observed that when ether is added to an aqueous solution containing our nanoparticles capped with our thioligands, followed by a few drops of dilute HCl acid, the nanoparticles precipitate from water, redissolve readily in the etheric phase and end up forming a thin Au film at the interphase. If acetone is added to this mixture, the color of the solution changes from gray to dark red. This is a unique property of functionalized gold nanoparticles since the Au film, once formed, redissolves upon shaking in the aqueous mixture and the phenomenon repeats itself at infinitum.

In addition to the above mentioned nanoparticles synthesis, we came across an alternative route to the preparation of monodisperse gold nanoparticles, by sonicating the mercaptocarborane thioligand as a solid, with aqueous solution of Au-citrate solution. Using this method, after sonicating for 22 hours, we conceded the "fragmentation" of initial 16 nm gold nanoparticles to about 3 nm. On the other hand, none of the other boron-based compounds, neutral or anionic were able to reduce the size of initial nanoparticles by sonication.

For a more complete study, various ligands, different from boron-containing ones, were sonicated together with Au-citrate solution and analyzed by UV-vis. Sulphur (S₈), bis(□-sulfonatophenyl)phenylphosphane dihydrate dipotassium salt (BSSP), a peptide (CALNN) and PEG (these last three being water-soluble) were submitted to sonication after previous addition to the Au-citrate solution. The gathered results indicate that in presence of the water-soluble species, no "fragmentation" takes place, whereas with S₈ the decrease in size is observed, however, in a much lesser degree than for mercaptocarborane (from 12 nm to about 9.5 nm).

Table of contents

1. Introduction

1.1. Boron: Historic overview	pg. 1
1.2. Boranes, Carboranes and Metallocarboranes: Generalities	pg. 1
1.2.1. Chemical reactivity of <i>o</i> -carborane	pg. 2
1.2.2. Cobaltabis(dicarbollide) and ferrabis(dicarbollide)	pg. 4
1.3. Applications	pg. 6
1.3.1. Radionuclides extraction	pg. 6
1.3.2. Homogeneous catalysis	pg. 6
1.3.3. Smart materials	pg. 7
1.3.4. Medicine	pg. 7
1.4. Objectives	pg. 23

2. Results and discussions

2.1. Solid state complexation reactions	pg. 27
2.1.1. Complexation reactions of <i>nido</i> [7-R-8-R'-C ₂ B ₉ H ₁₀] ⁻ species with CoCl ₂	pg. 27
2.1.2. Complexation reactions of [7,8-C ₂ B ₉ H ₁₂] ⁻ species with FeCl ₂	pg. 32
2.1.3. Characterization of the <i>closo</i> species	pg. 33
2.1.4. Characterization of the <i>nido</i> clusters	pg. 35
2.1.5. Characterization of the cobaltabis(dicarbollide) species	pg. 36
2.2. Ring-opening reactions of 1,4-dioxane derivative of ferrabis(dicarbollide) with various groups	pg. 38
2.2.1. Syntheses of [3,3'-Fe(8-(OCH ₂ CH ₂) ₂ X-(1,2-C ₂ B ₉ H ₁₀)(1',2'-C ₂ B ₉ H ₁₁)] ⁻ (where X = RO ⁻ , X ⁻ and SH ⁻)	pg. 39
2.2.2. Characterization of starting materials [3,3'-Fe(C ₂ B ₉ H ₁₁) ₂] ⁻ and [3,3'-Fe(8-(OCH ₂ CH ₂) ₂ -(1,2-C ₂ B ₉ H ₁₀)(1',2'-C ₂ B ₉ H ₁₁)]	pg. 40
2.2.3. Characterization of [3,3'-Fe(8-(OCH ₂ CH ₂) ₂ X-(1,2-C ₂ B ₉ H ₁₀)(1',2'-C ₂ B ₉ H ₁₁)] ⁻ (where X = RO ⁻ , X ⁻ and SH ⁻)	pg. 43
2.3. Toward the synthesis of high boron content polyanionic multicluster macromolecules	pg. 49
2.3.1 Syntheses of <i>closo</i> derivatives <i>via</i> <i>exo</i> -cluster substitution reactions	pg. 50
2.3.2. Synthesis of <i>nido</i> compounds <i>via</i> a partial deboronation reaction of <i>closo</i> species	pg. 51
2.3.3. Synthesis of polyanionic multicluster cobaltabis(dicarbollide) sandwich-type complexes	pg. 52
2.3.4. Synthesis of polyanionic multicluster heterometal(III)-based sandwich-type complexes	pg. 53
2.3.5. Characterization of <i>closo</i> derivatives	pg. 55
2.3.6. Characterization of the <i>nido</i> derivatives	pg. 61
2.3.7. Characterization of polyanionic multicluster cobaltabis(dicarbollide) sandwich-type complexes	pg. 65
2.3.8. Characterization of the polyanionic multicluster heterocomplexes centered in cobalt	pg. 69
2.3.9. Characterization of the polyanionic multicluster heterocomplexes centered in iron	pg. 70
2.4. Ring-opening reactions of 1,4-dioxane derivative of	pg. 74

cobaltabis(dicarbollide) with biomolecules	
2.4.1. Syntheses of 1,4-dioxane derivative of cobaltabis(dicarbollide) with biomolecules	pg. 74
2.4.2. Characterization of 1,4-dioxane derivative of cobaltabis(dicarbollide) with biomolecules	pg. 75
2.5. Cyclic oxonium derivatives of polyhedral boron hydride	pg. 80
2.5.1. Syntheses and characterization of cyclic oxonium derivative of polyhedral boron hydrides	pg. 80
2.5.2. Syntheses of 7,8-dicarba- <i>nido</i> -undecaborate bearing different end groups	pg. 83
2.5.3. Characterization of 7,8-dicarba- <i>nido</i> -undecaborate bearing different end groups	pg. 84
2.6. Preparation and characterization of MPCs capped with thiol-based boron clusters	pg. 86
2.6.1. Synthesis and characterization of the neutral and anionic capping thioligands	pg. 87
2.6.2. Preparation of MPCs capped with boron clusters containing thioligands by reducing with sodium borohydride	pg. 90
2.6.3. Preparation of MPCs capped with thioligands <i>via</i> the method of sonication	pg. 101
2.6.4. Preparation of MPCs capped with thioligands <i>via</i> the acetone method	pg. 106
2.6.5 Applications of MPCs capped with boron-based thioligands	pg. 111
3. Conclusions	pg. 119
4. Bibliography	pg. 123
5. Addendum	

1. Introduction

1.1. Boron: Historic overview

The history of boron is placed almost 6000 years ago, when boron compounds were discovered for the first time; apparently, one of the first minerals to be exchanged in the times of the Ancient World was borax. Starting with the Babylonian people and going through Egyptians, Chinese, Romans and Arabians, the boron compounds were used in gold soldering, as mummification materials, and most of all, in the fabrication of glass (borosilicate). The first documented chemical research related to boron dates from 1702, when W. Homberg synthesized boric acid starting from borax and iron (II) sulphate. In 1808, the French chemists Gay-Lussac and L. J. Thenard, and independently, the English Sir Humphry Davy, obtained elemental boron, although none of them recognized the substance as a new element, that would later be acknowledged by Jöns Jacob Berzelius in 1824. It is only in the year 1912, when based on the investigation carried out by the German chemist Alfred Stock, the first hydrogen and boron based compounds, boranes, were synthesized.

Later on, in the sixties,^{1,2,3} the first carboranes were elaborated, which were polyhedral clusters of boron which incorporated carbon atoms as well in their structure. Based on previous studies, W. N. Lipscomb, who was awarded with the Nobel Prize,⁴ demonstrated that polyhedral boron clusters could be described as species with occupied orbitals and multicentric bonds in different resonant forms.⁵ In this way, boranes were no longer considered electron deficient and were soon called superatomics.⁶ No more than three years later, H. C. Brown and G. Wittig also received the Nobel Prize in Chemistry for their discoveries of the great reducing effect of BH units over unsaturated organic compounds.⁷ As a result, boron hydrides have had an important influence on the organic synthesis.⁸

1.2. Boranes, Carboranes and Metallocarboranes: Generalities

It is nowadays considered that the chemistry of boron clusters constitutes a bridge between organic, inorganic and organometallic chemistry, with influences that could reach theoretic chemistry, polymers and medicine. Boranes are neutral or anionic boron clusters formed by triangular faced polyhedral which contain for each vertex a B-H unit. The substitution of one of these vertices by a heteroatom⁹ gives rise to the family of heteroboranes, amongst which the carboranes, also known as carbaboranes, are the most studied ones, having at least one boron atom replaced by a carbon atom. The empiric formula of these compounds is: $[C_nB_mH_{n+m+p}]^{x-} = [(CH)_n(BH)_mH_p]^{x-}$, where n represents the number of C atoms within the vertices of the cluster, m is the number of B atoms within the cluster and p the number of bridging H (bridge H).

1. Introduction

These clusters, boranes as well as carboranes, are consistent with some electronic requirements, that were studied by Wade, Rudolph, Mingos and Williams and are commonly known as Wade rules.^{10,11,12} In this manner, starting from the number of occupied vertices and also on the number of electron pairs required to form the cluster skeleton, one can determine a tridimensional structure. Considering n to be the number of polyhedral vertices, if the number of electron pairs maintaining the cluster together is $n+1$, then the compound has a *closo* structure; if it is $n+2$, the compound is *nido*, whereas if it is $n+3$ the compound is *arachno*, as depicted in Figure 1. One vertex made up by a B-H unit gives two electrons to the cluster, from the boron atom. If one vertex consists of a C-H unit, the carbon will give three electrons to the cluster. Respectively, the bridge hydrogen would give only one electron.

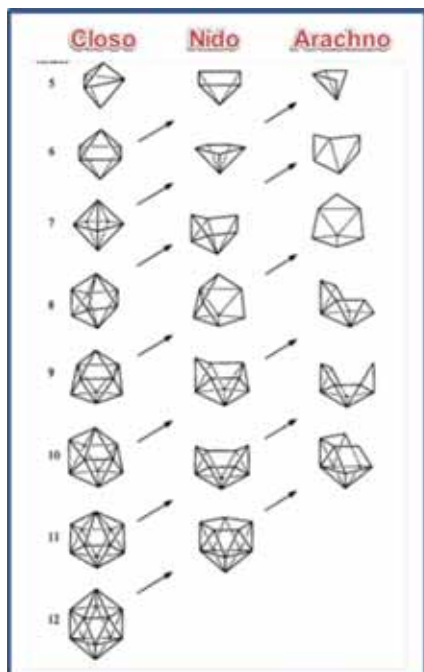


Figure 1. Structural relations between *closo*, *nido* and *arachno* boranes and heteroatomic boranes

Amongst all the carboranes, the most known is the group of the icosahedric clusters that possesses two carbon atoms, named dicarba-*closo*-dodecarboranes, which corresponds to the empirical formula $C_2B_{10}H_{12}$. The 1,2-dicarba-*closo*-dodecarborane, also known as *ortho*, with the carbon atoms in adjacent position (Figure 2) has been the isomer used in this doctoral thesis.



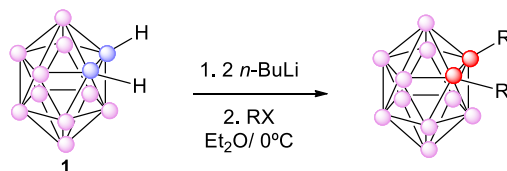
Figure 2. Numbering of the *closo ortho*-carborane cluster

1.2.1. Chemical reactivity of *o*-carborane

Although *ortho*-carborane shows high chemical stability in certain reaction conditions, it is also a compound exhibiting high synthetic versatility.

1.2.1.1. Deprotonation of C-H vertices and posterior substitution

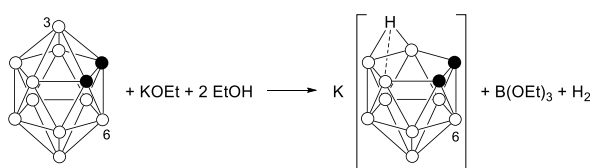
The hydrogen atoms of the C-H unit are more acids than the ones bonded to boron, due to the more electronegative character of carbon with respect to boron (2.5 and 2.0 respectively, according to Pauling scale). This relatively acidic character allows the easy substitution of the protons bonded to these carbon atoms by alkaline and alkaline-earth metals, in the presence of strong bases, like for example *n*-butyllithium, sodium hydride or Grignard reagents, opening the way to the introduction of new functional groups within the cluster, and modulating its properties, as shown in Scheme 1.



Scheme 1. Substitution of C-H vertices with various functional groups

1.2.1.2. Partial deboronation of the cluster by one vertex elimination

One of the structural modifications that the 1,2-*o*-C₂B₁₀H₁₂ cluster can undergo is the “decapitation” or partial deboronation, which consists in the elimination of one B-H vertex. This reaction dates back to 1964, when Wiesboeck and Hawthorne succeeded to isolate [7,8-*nido*-C₂B₉H₁₂]⁻ in high yield, implying EtO⁻ as a nucleophilic agent,¹³ as indicated in Scheme 2.

Scheme 2. *Ortho*-carborane partial deboronation reaction

The more electronegative character of the carbon atoms with respect to the one of the boron atoms induces the C_c-B bond polarization, and, as a consequence, a higher positive charge density over the boron atoms bonded directly to the two carbon ones. For what 1,2-*o*-C₂B₁₀H₁₂ is concerned, there are two boron atoms, B(3) and B(6), simultaneously bonded to a C_c, making these positions more susceptible to the attack of strong bases, such as potassium ethoxide, and leading to the obtaining of [7,8-*nido*-C₂B₉H₁₂]⁻. This species has formally lost one B⁺ fragment with respect to its precursor, allowing the formation of a cluster bearing one open pentagonal face, C₂B₉, where its remaining hydrogen is still present; this resultant *nido* cluster is a monoanionic species, as presented in Scheme 2 above. X-ray diffraction studies show that this H_{bridge} is more bonded to B(10) than to B(9) or B(11) and that it maintains itself equidistant to these last two.¹⁴

1.2.1.3. Complexation reactions

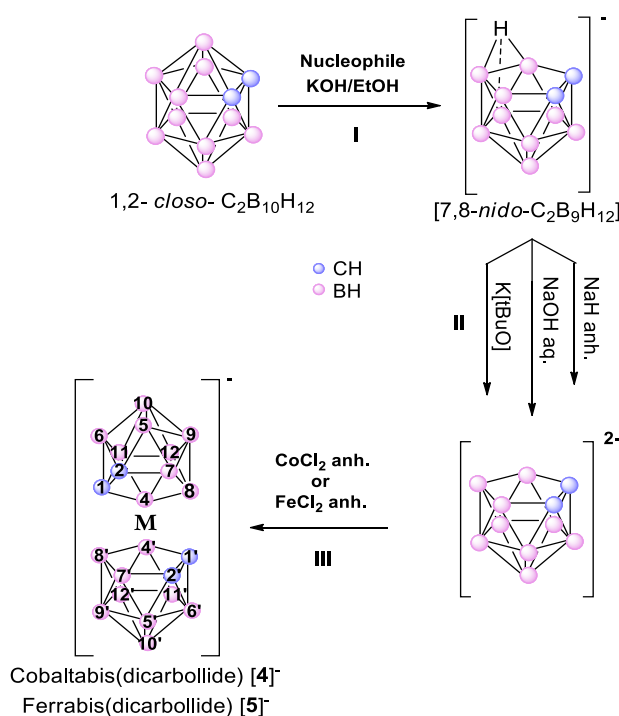
Starting from [C₂B₉H₁₂]⁻ or its conjugate base [C₂B₉H₁₁]²⁻, in the presence of metal-containing reagents, stable metallacarboranes were synthesized, in which the metal atom fills the vacancy and completes a 12-vertex *closo*-MC₂B₉ icosahedral cage. In this way the *closo* anionic icosahedral metallacarboranes, [3,3'-M(1,2-C₂B₉H₁₁)₂]ⁿ⁻, were generated where M = Co(III), Co(II), Fe(III), Fe(II), Ni(III), Cu(III), Au(III) and n = 1 or 2. The first metallacarborane to be synthesized was [3,3'-Fe(C₂B₉H₁₁)₂]⁻,¹⁵ obtained by Hawthorne and his research group in 1965, using two dicarbollide dianionic ligands.

1. Introduction

Shortly after, the synthesis of an analogous sandwich-type coordinated this time by cobalt, cobaltabis(dicarbollide), $[3,3'\text{-Co}(\text{C}_2\text{B}_9\text{H}_{11})_2]^-$, was reported.¹⁶

1.2.2. Cobaltabis(dicarbollide) and ferrabis(dicarbollide)

This research is mainly centred on the chemistry of $[3,3'\text{-M}(\text{C}_2\text{B}_9\text{H}_{11})_2]^-$, where $\text{M} = \text{Co}$, Fe . The structure of this *closo* compounds consists in a central metal atom, in oxidation state +3, bonded *via* σ bonds to two dicarbollide ligands, each of them contributing with two negative charges. The resulting negative charge is delocalized over the entire volume of the complex, this being the reason why the compound has a low charge density.¹⁷ Scheme 3 depicts the synthetic way for the $[3,3'\text{-M}(\text{C}_2\text{B}_9\text{H}_{11})_2]^-$ anions and indicates the corresponding vertex numbers.



Scheme 3. General scheme for the synthesis of cobaltabis(dicarbollide) and ferrabis(dicarbollide), $[3,3'\text{-M}(\text{C}_2\text{B}_9\text{H}_{11})_2]^-$

The synthesis of these compounds takes place in three steps, as indicated in Scheme 3: I) partial degradation of *closo* *o*-carborane by a strong nucleophile to *nido*- $[7,8\text{-C}_2\text{B}_9\text{H}_{12}]^-$; II) deprotonation of the previous obtained species to $[7,8\text{-C}_2\text{B}_9\text{H}_{11}]^{2-}$ and III) reaction with anhydrous CoCl_2 or FeCl_2 , yielding the corresponding sandwich-type metal-based compound. It should be mentioned that the formation of the dicarbollide by employing NaH presents various difficulties, starting from the dangers in manipulation and ending with the very complex removal from the reaction mixture. Moreover, it requires many synthetic steps and the yield is not very satisfactory. Another method reported in literature is the use of NaOH aqueous solution, but the main disadvantage is that it requires huge excess of NaOH , which also involves a large volume of sodium

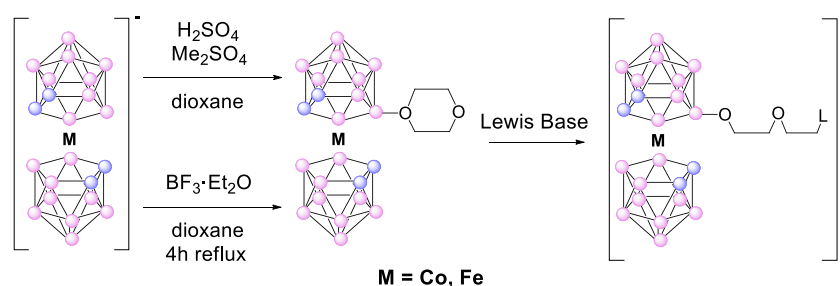
Scheme 4. Synthesis of zwitterionic species, followed by the functionalization of B(8) vertex by dioxane ring-opening by a Lewis base.

bicarbonate for the posterior neutralization of the reaction mixture.¹⁸ Therefore, the K[tBuO] method is the easiest and moreover, with good yields.

1.2.2.1. Reactivity of metallabis(dicarbollide)

These anions show two different reactivity points, the C-H and the B-H vertices. Little time ago, the substitutions at the metallabis(dicarbollide) $C_{cluster}$ atoms took place in a parallel way to the very synthesis of [4]⁻ and [5]⁻. Firstly, the $C_{cluster}$ substituted *o*-carborane was synthesized, then it was deboronated to the monoanionic species [7-R-7,8- $C_2H_9H_{11}$]⁻, followed by the H_{bridge} deprotonation to give rise to the dicarbollide anion; finally, the reaction with anhydrous $CoCl_2/FeCl_2$ took place, yielding the corresponding metallabis(dicarbollide) C-derivatives. Nevertheless, this method required many steps and involved many processes of purification, which led to low yields and only allowed the obtaining of identical substituents at the dicarbollide ligands. The major inconvenient, however, was that it did not permit the introduction of functional groups which did not resist to the alkaline conditions used for the synthesis of the dicarbollide anion. An alternative to this method was proposed by Chamberlin and collaborators in 1997,¹⁹ who uses the cobaltabis(dicarbollide) itself as starting material, and consists in the addition of *n*-BuLi to synthesize the corresponding lithiated salts by C_c -H deprotonation, followed by the reaction with halogenated derivatives to obtain C_c -R derivatives.

With respect to boron atoms substitutions, these were much more studied than the carbon atoms ones. Yet, they are more difficult since not all B-H vertices are equal, but not that different either; therefore, an adequate regioselectivity is hard to obtain. The more reactive vertices are those showing higher electronic density, namely boron atoms 8, 9 and 12. Halogenated derivatives of cobaltabis(dicarbollide) in positions 8-, 8,8'- and 8,8', 9,9', 12,12' were reported.²⁰ However, when high substitution is attempted, by-products with different halogenation degrees are also obtained.²¹ Even if these halogenated compounds were considered at first inert to substitution reactions, it was demonstrated that starting from the iodinated derivatives, different substitutions are possible.²²



1. Introduction

Another way of functionalization of the $[3,3'\text{-M}(\text{C}_2\text{B}_9\text{H}_{11})_2]^-$ boron vertices is based on the synthesis of the zwitterionic derivative, $[3,3'\text{-M}(8\text{-(OCH}_2\text{CH}_2)_2\text{-(1,2-C}_2\text{B}_9\text{H}_{10})(1',2'\text{-C}_2\text{B}_9\text{H}_{11})]$, $\text{M} = \text{Co, Fe}$.²³ The cobalt-based zwitterionic compound has been proven to be susceptible to nucleophilic attack on the CH_2 group bonded to the positively charged oxygen atom, e.g. by pyrrolyl,²⁴ imide, cyanide or amines,²⁵ phenolate, dialkyl or diarylphosphite,²⁶ alcoxides,²⁷ and nucleosides²⁸ resulting once again in one anionic species formed by the cleavage of the dioxane ring (Scheme 4). Recent publications^{29, 30} cover the synthesis of different oxonium derivatives of polyhedral boron hydrides.

1.3. Applications

Boron cluster compounds represent distinctive covalent species with a unique molecular architecture, nonconventional cluster bonding, and unusual chemistry.

The current applications for boron cluster compounds are based either on the unique properties of the molecules or on specific properties of the basic element itself, such as: the extreme acidity of acids conjugated to the polyhedral ions combined with a unique hydrophobicity of these anions; the exceptional stability of the polyhedral species due to their “aromaticity” and the unexpected ability of nearly all open-cage clusters to form sandwich metallic complexes.³⁰

1.3.1. Radionuclides extraction

Boron clusters were successfully used in the selective extraction of nuclear residues, radionuclides. The sandwich-type anion, $[3,3'\text{-Co}(\text{C}_2\text{B}_9\text{H}_{11})_2]^-$, which shows high stability in acidic medium in which the radioactive cations that are to be extracted are found, was the first compound to be used with such purposes.³¹ Due to its solubility in organic solvents, characteristic that makes them easily extractible from aqueous phases, its high chemical and thermal stability as well as resistance to radiation, the cobaltabis(dicarbollide) anion is ideal as extracting agent for metallic ions found in residual waters. For instance, the cobaltabis(dicarbollide) anion is used as selective extracting agent for ^{137}Cs and ^{90}Sr .³²

1.3.2. Homogeneous catalysis

In homogeneous catalysis, it is already known the catalytic activity of ruthenium and rhodium based carboranes in a wide variety of reactions such as terminal³³ and internal³⁴ alkenes' hydrogenation, hydrosilylation,³⁵ cyclopropanation³⁶ and Kharash CCl_4 addition reactions to olefins.³⁷

1.3.3. Smart materials

Boron clusters can also find application as doping agents for conducting organic polymers due to their low charge density, which improves the stability and in particular, their resistance to overoxidation.^{17,38} The first results concerning the luminescent properties of the carborane clusters were reported within our group of research.³⁹ Y. Chujo and collaborators demonstrated that the presence of boron clusters within the structures of organic polymers of polyphenylethynyl (PPE) favors the π conjugation within the polymer, increasing its photoluminescent properties and its resistance to the temperature of the material.⁴⁰ The use of boron clusters was also studied in several other applications, amongst which liquid crystals⁴¹ and ionic liquids.⁴² In addition to this, it is worth mentioning the importance of cobaltabis(dicarbollide) containing devices, such as sensors for H^+ , Na^+ and K^+ ions for their use in organ transport control for transplants,⁴³ selective electrodes for antibiotics and quiral aminoacids⁴⁴ or as sensors for neutrons.⁴⁵

1.3.4. Medicine

One essential characteristic for both boranes and carboranes is their biocompatibility⁴⁶ since they are artificially synthesized compounds and therefore, neither recognized nor metabolized by living organisms, displaying very low toxicity. On the contrary, some iron-based metallocarboranes having $[MeC_3B_7H_9]$ units, have shown to have cytotoxic properties on different tumor cell lines.⁴⁷ In addition to this, recent studies have proven that some cobaltabis(dicarbollide) derivatives can act as potent specific inhibitors of protease HIV-1.⁴⁸

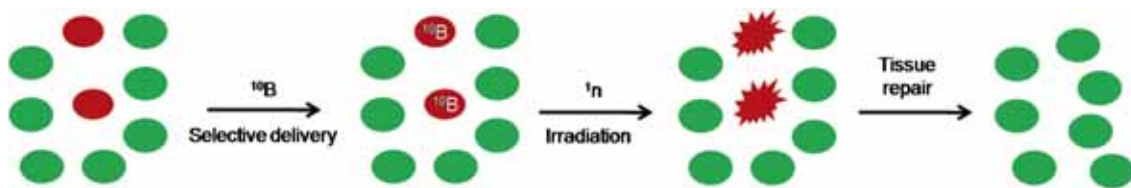
Contrast agents in X-rays

Highly iodinated molecules have been of interest for medical applications, especially in the field of radiodiagnosis, if one takes into account the iodine atom's elevated opacity in front of low-energy X-rays.⁴⁹ Contrast agents used currently consist in benzene derivatives with up to three iodine atoms and their corresponding dimers.⁵⁰ The research in this field is concerned with synthesizing more opaque contrast agents, and, at the same time, more innocuous. Species based on highly iodinated boron clusters⁵¹ are emerging as an alternative to organic contrast agents, due to several advantages: i) firstly, boron clusters display a lot of positions susceptible to iodination, up to a total of 90% of iodine in the molecule,⁵² fact that *a priori* enables high doses of radiopacity⁵³ and ii) secondly because B-I bonds are more stable in biological conditions than the C-I ones,⁵⁴ providing therefore stability in front of dehalogenation processes.⁵⁵

1. Introduction

Anticancer treatment based on Boron Neutron Capture Therapy (BNCT)

Figure 3. BNCT steps: selective delivery of ^{10}B -containing drugs to tumor cells followed by irradiation with slow neutrons (^1_0n), leading to tissue repair (figure from ref. 56). Applications associated with the properties of boron as the element within the deltahedral species primarily exploit the unusually high cross section of the ^{10}B isotope for neutron capture (20% natural abundance). This led to the development of lightweight neutron shields and in particular to the Boron Neutron Capture Therapy (BNCT) of tumors. Out of all boron clusters applications in medicine or pharmacology, the greatest number of publications refer to cancer treatment using BNCT.⁵⁶ This technique, discovered by Locher in 1936,⁵⁷ is currently in clinical trials in U.S.A., Japan and Europe.^{56a,58}



BNCT is a binary treatment modality (Figure 3)⁵⁹ that combines irradiation with a thermal or epithermal neutron beam with tumor-seeking, boron-containing drugs that are taken up preferentially by neoplastic cells to produce selective irradiation of tumor tissue. The high linear energy transfer (LET) alpha particles and recoiling ^7Li nuclei emitted during the $^{10}\text{B}(n, \alpha)^7\text{Li}$ reaction in tissue are known to have a high relative biological effectiveness (RBE) (the relative amount of damage that a fixed amount of ionizing radiation of a given type can inflict on biological tissues).⁶⁰ Their short path length in tissues (6-10 μm) limits their effect mostly to cells containing ^{10}B atoms, providing a strategy to damage tumor cells while protecting healthy tissue within the treatment volume.

For potential applications in BNCT, a therapeutic agent⁶¹ must i) possess low toxicity, ii) exhibit good tumor-cell selectivity, iii) persist intracellularly at constant concentrations during the course of neutron radiation, iv) be deliverable at 20-35 $\mu\text{g } ^{10}\text{B}$ per gram of tumor, v) be characterized by tumor: normal tissue and tumor: blood ratios higher than 3, and vi) have the capacity to reach the target site through the blood stream by penetrating biological barriers, such as the blood-brain barrier (BBB). Early-molecular-design approaches were guided by the observation that BBB is more permeable in the diseased state than it is in the healthy state, but therapeutics strategies that emerged from these approaches did not prove successful, mainly because isolated clusters of tumor cells protected by the normal BBB, retain the potential to become the centre for tumor recurrence.

1. Introduction

BNCT has been applied clinically for the treatment of patients with malignant brain tumors and malignant melanoma, using sodium mercaptoundecahydrododecaborate ($\text{Na}_2^{10}\text{B}_{12}\text{H}_{11}\text{SH}$; $\text{Na}_2^{10}\text{BSH}$)⁶² and L-p-(dihydroxyboryl)phenylalanine (L- ^{10}BPA)⁶³ respectively. In 1998, positron emission tomography (PET) using ^{18}F -BPA has been developed.⁶⁴ Some structures of boron compounds which have already been used for clinical treatment of BNCT are shown in Figure 4. The achievement of ^{18}F -BPA PET imaging enabled the prediction of tumor/blood and tumor/normal tissue ratios of L- ^{10}BPA before neutron irradiation. This PET technology also displayed selective accumulation of ^{18}F -BPA in various tumors. Thus, BNCT has been applied for various cancers including head and neck cancer, lung cancer, hepatoma, chest wall cancer, and mesothelioma.⁶⁵

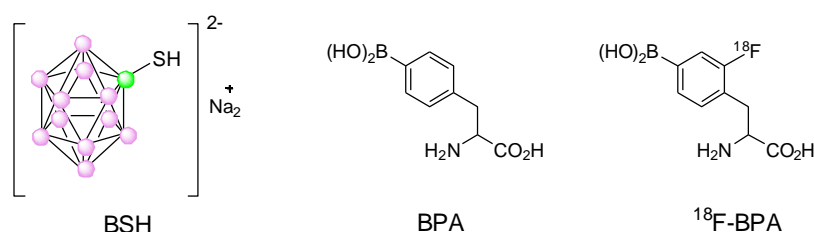


Figure 4. Boron compounds used in BNCT clinical treatment

Although the number of cases is increasing, development of new ^{10}B -carriers that deliver an adequate concentration of ^{10}B atoms to tumors is still an important requirement for effective and extensive cancer therapy in BNCT. Recent promising approaches that meet the requirement involve the use of small boron molecules,⁶⁶ such as porphyrins,⁶⁷ nucleosides,^{28c,68} aminoacids,⁶⁹ peptides,^{30,70} and boron-conjugated biological complexes, such as monoclonal antibodies,⁷¹ epidermal growth factors,⁷² carborane oligomers,^{66a,73} micells⁷⁴ and dendrimers.⁷⁵

In a study by Trivillin and coworkers⁷⁶ on hamster cheek pouch oral cancer model, it was shown that low-dose BNCT using BPA and $\text{Na}_2^{10}\text{B}_{10}\text{H}_{10}$ (GB-10) administered jointly induced significant tumor control with no radiotoxic effects on normal tissue and precancerous tissue (tissues with potentially malignant disorders, from which tumors may arise).⁷⁷

Boric acid [$\text{B}(\text{OH})_3$] and borane clusters (*closo*- $\text{B}_{12}\text{H}_{12}^{2-}$ or $\text{C}_2\text{B}_{10}\text{H}_{12}$) are the two main types of boron entities used so far in the synthesis of carrier molecules for BNCT. To a lesser extent boranes (BH^-) and cyanoboranes (BH_2CN^-) are used for synthesis of potential boron carrying drugs.⁷⁸

On the other hand, great interest is focused on synthesizing boron-rich drugs in order to raise the efficiency of generating highly energetic particles. One must take into account the fact that the therapeutic concentration is of 20-35 μg of ^{10}B per gram of tumor.⁷⁹ A commonly employed strategy for achieving such concentrations involves the

1. Introduction

design of therapeutic agents that incorporates polyhedral borane moieties.⁸⁰ Among these, the carboranes₂ (neutral lipophilic C₂B₁₀H₁₂) are of particular interest, not only because of their high ¹⁰B content, good catabolic stability and low toxicity⁸¹ but also because they are amenable to chemical functionalization.⁸²

Drug delivery systems

Tumor specific drug delivery has become increasingly interesting in cancer therapy, however, the clinical use of most conventional chemotherapeutics is often limited due to inadequate delivery of therapeutic drug concentrations to the tumor target tissue or due to severe and harmful toxic effects on normal organs.

Presently, one of the therapeutic applications that is constantly in development, associated with dendrimers, is drug delivery. The elevated level of control throughout dendrimeric structures synthesis as well as the power to modulate their surface with adequate number and type of charges, converts dendrimers in the optimal systems for penetrating cellular membranes and releasing of the drugs.⁸³

a) Dendrimers

Dendrimers are a class of monodisperse organic materials containing functionalities in the core, in the dendritic backbone, or on the surface.⁸⁴ The most important feature of dendrimer chemistry is the design of the structure and the possibility to insert selected chemical units in predetermined sites of the dendritic structure. The combination of dendrimers and other macromolecular topologies as building blocks is an attractive and promising approach in the development of molecular recognition,⁸⁵ and new catalytic systems⁸⁶ among others. A recent study on phosphorus dendrimers containing a triolefinic 15-membered macrocycle as a core and iminophosphane ligands on the surface up to the third generation has recently been reported.⁸⁷

During the last years, owing to their controllable architecture, monodispersity and capacity to accommodate large number of boron atoms, dendritic BNCT agents have received considerable attention. Barth *et al.* has shown that PAMAM “starburst” dendrimers containing isocyanato polyhedral borane (Na(CH₃)₃NB₁₀H₈NCO) exhibit preferential accumulation in reticuloendothelial system (RES) when tested *in vivo* against murine B16 melanoma.⁸⁸ Wu and coworkers attached an epidermal growth factor (EGF) inhibitor to a heavily boronated “starburst” dendrimer and obtained delayed cell proliferation, which together with the five-generation dendrimers structure must be responsible for the high level of boron accumulation (92.3 μg ¹⁰B/tumor) observed.^{88,89} The linking of boronated “starburst” dendrimers to EGF was first attempted by Capala *et al.*^{72a} who synthesized molecular structures each containing more than 1000 ¹⁰B atoms, but these dendrimers exhibited little affinity for epidermal

1. Introduction

growth factor receptor (EGFR). Barth *et al.*⁹⁰ were the first to publish *in vivo* data indicating the significant therapeutic benefit associated with EGF-boronated dendrimers, either alone or in combination with BPA, as demonstrated by the increase in life span of glioma-bearing mice.⁹¹ Although EGF targeting vehicles cannot act alone as boron delivery agents (because of the heterogeneity of receptor expansion in brain tumors) they can prove of value in therapies involving combination of drugs.⁹²

b) Gold nanoparticles

Metal NPs (Fe, Al, Si, Ti, Ag, Au and Cu), have received increasing interest due to their widespread medical, consumer, industrial, and military applications. NPs are being designed with chemically modifiable surfaces to attach a variety of ligands to improve biosensors, imaging techniques, delivery vehicles, and other useful biological tools.⁹³

Gold nanoparticles (Au NPs) and their wide spread use of in biological applications has been due to their simple synthesis methods,⁹⁴ ease of surface modification with peptides, DNA and antibodies,⁹⁵ and unique physicochemical properties such as excellent absorbance and scattering of light. On the basis of these properties, Au NPs have important applications for biological diagnostics,⁹⁶ cell labeling,⁹⁷ targeted drug delivery,^{98,99} medical imaging,^{100,101} synthetic inhibitors,¹⁰² cancer therapy,¹⁰³ and biological sensors.^{104,105,106}

Although gold is the subject of one of the most ancient themes of investigation in science, its renaissance now leads to an exponentially increasing number of publications, especially in the context of emerging nanoscience and nanotechnology.



The extraction of gold started in the 5th millennium B.C. near Varna (Bulgaria) and reached 10 tons/year in Egypt around 1200-1300 B.C. when the marvelous statue of Tutankhamen was constructed. In antiquity, gold was used for both aesthetic and curative purposes. Perhaps the most famous example is the Lycurgus Cup (Figure 5) that was manufactured in the 5th to 4th century B.C. It is ruby red in transmitted light and green in

reflected light, due to the presence of gold colloids.

In 1857, Faraday reported the formation of deep red solutions of colloidal gold by reduction of an aqueous solution of chloraurate (AuCl_4^-) using phosphorus in CS_2 (a two-phase system). The first use of gold in modern medicine was in 1890, after the German bacteriologist Robert Koch discovered that low concentrations of potassium gold cyanide, $\text{K}[\text{Au}(\text{CN})_2]$ had antibacterial properties against the tubercle bacillus.¹⁰⁷ In

1. Introduction

the 1920s gold therapy for tuberculosis was introduced¹⁰⁷ and in 1935 Jacque Forestier reported the use of gold to treat rheumatoid arthritis.¹⁰⁸

The next critical discovery was made in 1951 by Turkevitch *et al.*, namely the single-phase reduction of gold tetrachloroauric acid by sodium citrate in an aqueous medium, producing citrate stabilized Au NPs of about 20 nm in size (Figure 6a).¹⁰⁹ Later, seeking to produce Au NPs of a prechosen size, Frens *et al.* refined reaction conditions such as ratios,¹¹⁰ solution pH¹¹¹ and solvent,¹¹² allowing in this way better control of the gold nanoparticle size;¹¹³ however the distribution was still variable.

The last major contribution to the field of Au NPs syntheses is the Brust-Schiffrin method, published in 1994. It is based on a two-phase synthesis that exploits thiol ligands that strongly bind to gold due to the soft character of both S and Au. Initially, a gold salt is transferred into an organic solvent (toluene) with the help of a phase transfer agent (such as tetraoctylammonium bromide), then an organic thiol is added followed by a strong reducing agent (such as sodium borohydride) in excess, yielding thiolate protected Au NPs (Figure 6b).^{114, 115}

The major advantages of this method are the ease of synthesis, thermally stable NPs, reduced dispersity and control of size.¹¹⁶

In the last few years, producing of monodispersed nanoparticles was focused on exploring possible nanoparticle formation mechanisms. Natan *et al.* was an innovator for the investigation of seeded growth of Au NPs starting from the Frens *et al.* synthesis.¹¹⁷ Bastus *et al.* have successfully synthesized monodispersed citrate stabilized particles through kinetically controlled seed growth.¹¹³

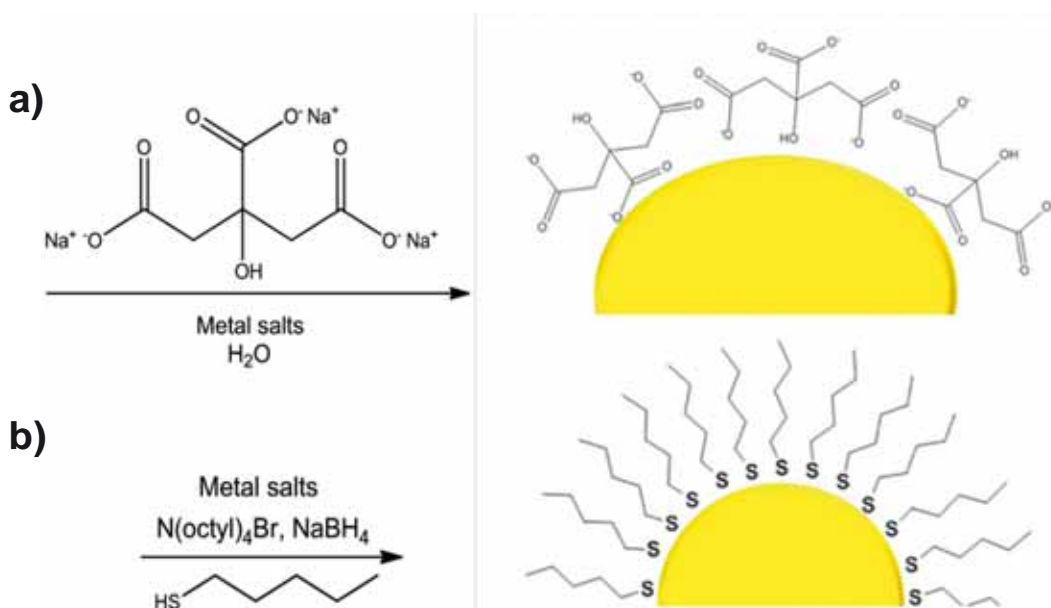


Figure 6. Scheme of chemical reduction for nanoparticle synthesis: a) reduction using sodium citrate that is also the capping agent, b) reduction and synthesis using thiol ligands (figure from ref. 113)

1. Introduction

Regarding their exploitation in medical applications, gold nanoparticles, due to their high stability in biological fluids, including blood, have become potential candidates to be used as tools for the controlled release of active agents.¹¹⁸ Studies¹¹⁹ concerning the use of radiolabelled drugs have revealed that appropriately designed nanoparticles are capable of overcoming the BBB and of depositing their therapeutic content in the brain. Reports claim that such structures afford up to a 10-fold increase in the concentration of drug in the brain, a lessened burst effect, slow clearance and improved half-life.

Au NPs multi-functionalized with BPA, folic acid and fluorescein isothiocyanate against three cancer cell lines that are known to overexpress folate receptor (FR) have been tested by Mandal *et al.*¹²⁰ and observed tumor: normal cell uptake ratios of 5 in the perinuclear region of cancer cells. Promisingly, a method for the low-temperature, solution synthesis of surface-functionalized boron nanoparticles has recently become available.¹²¹ In this method, the reduction of BBr₃ with sodium naphthalenide followed by the reaction of resulting bromide-capped intermediate with octanol, yields organo-capped boron nanoparticles.

In addition to all the above, due to their ease of synthesis, characterization and surface functionalization, noble metal nanoparticles, and in particular gold nanomaterials, have recently been demonstrated to possess another promising application, namely their action as self-therapeutics. Researches also showed that surface size, not surface charge, plays a large role in the therapeutic effect of Au NPs.¹²² Arvizo *et al.* studied how citrate reduced Au NPs (d = 5, 10 and 20 nm) had a dramatic effect on the vascular endothelial growth factor (VEGF) signaling events such as receptor-2 phosphorylation, intracellular calcium release and proliferation comparatively. Another report¹²³ showed that Ag NPs inhibited cell proliferation and migration in VEGF induced angiogenesis in bovine retinal epithelial cells. Further work described the anti-tumor effects of 50 nm Ag NPs *in vitro* and *in vivo*.¹²⁴

Independent on the size of NPs, several parameters play a dominant role in their enhanced magnetic, electrical, optical, mechanical, and structural properties. Many of these characteristics have potential implications in NPs toxicity, such as elemental composition, charge, shape, crystallinity, surface area, solubility, and surface chemistry/derivatization.¹²⁵

Cellular uptake of gold nanoparticles

The size and shape of nanoparticles also play a large role in relation to cellular uptake *in vitro*. As the size of a particle decreases, its surface area to volume ratio increases, allowing a greater proportion of its atoms or molecules to be displayed on the surface resulting in increased surface reactivity.¹²⁶ Oberdoerster *et al.*^{125d} reported that particles

1. Introduction

with greater specific surface area per mass were more biologically active and that their biological effects mainly depended on their surface area rather than particle mass.¹²⁷ As particle size shrinks, there is a tendency for toxicity to increase, even if the same material is relatively inert in a bulk form.¹²⁸ Several *in vitro* and *in vivo* studies with MPCs have demonstrated that smaller NPs are more toxic than larger NPs¹²⁹ and can induce immunological responses. Chan *et al.* has reported that 50 nm gold particles can enter into cell at a faster rate with higher amount relative to the other sizes.¹³⁰

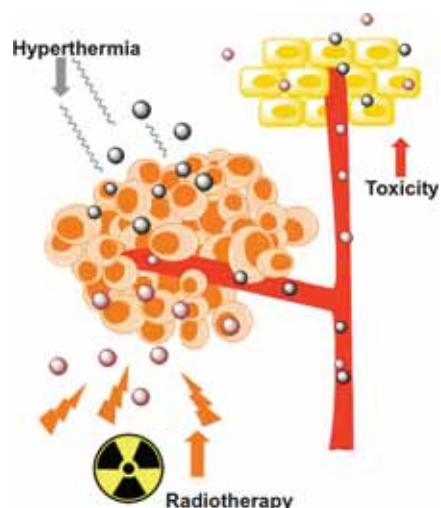
Most of the effects of shape have been studied in MPCs, which demonstrate that Au rods typically display greater toxicity than Au spheres.¹³¹ Spherical MPCs have higher cellular uptake than gold nanorods owing to variable biophysical properties.

Surface charge is also an important factor that moderates cellular uptake of nanoparticles: positively charged MPCs cause greater toxicity than those with negative surface charges.¹³² The functionality of the nanoparticle surface further allows specific or nonspecific interactions within the cellular lipid bilayer.¹³³ Since the cellular exterior is largely anionic, positively charged nanoparticles can easily transverse the cellular membrane *via* electrostatics.^{132a} Nonetheless, negatively charged nanoparticles have also been observed in the cytosol.^{132b} In addition, Rotello *et al.* have also reported that zwitterionic nanoparticles (effective overall neutral surface charge) can be highly efficient delivery system.¹³⁴

Recent innovations in nanotechnology have demonstrated that MPCs hold great promise as photodynamic therapy (PDT) and hyperthermic agents. Research has shown that the application of magnetic fields on metallic nanoparticles results in rapid heating.¹³⁵ In this heating process, electrical currents are produced in the gold particle by the oscillating magnetic field, resulting in rapid heating which quickly dissipates from the nanoparticle into the surrounding environment, incurring thermal ablation.¹³⁶

Although ionizing radiation is effective for controlling the proliferation rate of cancer cells, side effects are numerous and healthy tissue is often damaged. Metallic nanoparticles may offer an advantage in this area by exploiting their excellent optical properties, surface resonance, and wavelength tunability.¹¹⁵ For example, upon X-ray irradiation, MPCs can induce cellular apoptosis through the generation of radicals.¹³⁷ This treatment strategy has increased the killing of cancer cells without harming the surrounding healthy tissue.¹³⁸

This therapeutic method is depicted in Figure 7.

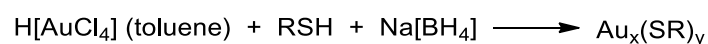


1. Introduction

Gold monolayer protected clusters (MPCs) modified with thiols

The modification of the surfaces of gold nanoparticles and macroscopic gold surfaces represents a chemical tool frequently used in the preparation of materials with properties that reflect a transitional phase between the molecular and bulk level.¹³⁹ These materials, which are called monolayer protected clusters (MPCs)^{114,140} and self-assembled monolayers (SAMs),¹⁴¹ have so far been studied essentially with a series of alkanethiol compounds, nanostructures showing unique and tunable properties effectuated by their small dimensions and adjustable chemical composition. Alkanethiol species are described in the literature as binding to gold surfaces as alkanethiolate units.^{141f} The adsorption of these thiol derivatives provides highly ordered monolayer films with well-defined structure, thickness, and wetting properties. It was shown that the alkanethiolate moieties pack densely on gold surfaces of nanoparticles.^{140b,141a}

A facile synthesis of nanoparticles composed of gold clusters coated with thiolate monolayers (or monolayer-protected gold clusters, Au MPCs), introduced by Schiffrin and coworkers,^{114,142} has attracted extensive use. The MPCs synthesis reaction is a two-step process that leads to modestly polydisperse (in core size) alkanethiolate protected Au clusters with average core diameters of 1.1- 5.2 nm.¹⁴³



The reaction's behavior is consistent with a nucleation-growth-passivation process: i) Larger thiol:gold mole ratios give smaller average MPC core sizes;¹⁴³ ii) fast reductant addition and cooled solutions produce smaller, more dispersive MPCs^{143,144} and iii) quenching the reaction immediately following reduction produces higher abundance of very small core sizes (< 2 nm).¹⁴⁵

Understanding reactivities of MPC monolayers and developing efficient strategies to functionalize them is key to their application in areas such as catalysis and chemical sensing. Templeton *et al.* have investigated^{140a} ligand place-exchanges (to form poly-homo- and -hetero-functionalized MPCs),¹⁴⁶ nucleophilic substitutions,¹⁴⁷ and ester and amide couplings¹⁴⁸ yielding MPCs with multiple functionalities, spherically organized around a central, metal core, arrangement similar to the one of dendrimers.¹⁴⁹ However, whereas dendrimers are typically denser at their perimeter than core, MPCs are "soft objects with hard cores". A study^{146c} of ligand place-exchange dynamics and mechanism shows that exchange (i) has a 1:1 stoichiometry, (ii) is an associative reaction, (iii) yields the displaced ligand in solution as a thiol, and (iv) does not involve disulfides or oxidized sulfur species.

c) Liposomal boron delivery in BNCT

In boron neutron capture therapy of tumors (BNCT), successful treatment requires a selective delivery of ^{10}B to tumor tissues to maximize damage to the tumor and to minimize damage to surrounding normal tissue.¹⁵⁰ High accumulation and selective delivery of ^{10}B into tumor tissue are the most important requirements to achieve efficient BNCT of cancers.^{79,151} The amount of ^{10}B necessary to realize fatal tumor cell damage is 20–35 $\mu\text{g/g}$ tumor tissue.¹⁵² At the same time, boron concentration in surrounding normal tissues and blood should be kept low to minimize damage to those tissues.

Recently much attention has been focused on the liposomal drug delivery system (BDS). Liposomes are efficient drug delivery vehicles, because encapsulated drugs can be delivered selectively to tumors. Therefore, liposomal boron delivery system is also considered to be effective for BNCT due to the possibility of carrying a large amount of ^{10}B compound. Two approaches have been investigated for liposomes as boron delivery vehicles: i) encapsulation of boron compounds into liposomes (Figure 8a) and ii) incorporation of boron-conjugated lipids into the liposomal bilayer (Figure 8b).¹⁵³

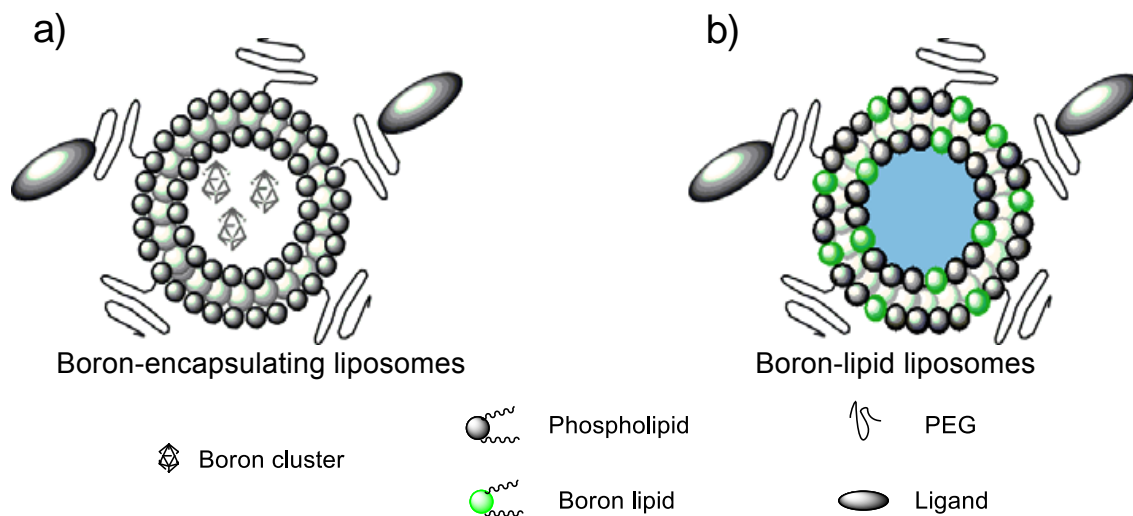


Figure 8. Approaches of liposomal boron delivery system (image from ref.¹⁵³)

Encapsulation

Boron compounds-encapsulated liposomes are attractive vehicles to deliver adequate quantities of boron to the tumor cells for BNCT.

Yanagie *et al.*¹⁵⁴ were the first to employ liposomes for the delivery of encapsulated boronated compounds *in vitro*. Selective delivery of the therapeutic agent was achieved by the encapsulation of BSH into immuno-liposomes that had been conjugated to monoclonal antibodies (mAbs). The *in vitro* experiments show that thermal-neutron irradiation at 5×10^{12} neutrons/cm² inhibited tumor-cell growth, whereas *in vivo*

1. Introduction

experiments at 2×10^{12} neutrons/cm² demonstrated the capacity to suppress tumor growth. Hawthorne^{151b} encapsulated a variety of hydrolytically stable polyhedral borane anions into unilamellar liposomes and the formulation was tested on tumor-bearing mice. Although the polyhedral anions did not exhibit any selectivity towards tumor cells, the employed liposome formulations were shown to be capable of effecting the selective delivery of borane anions to tumors (peak boron concentration = $40 \mu\text{g } ^{10}\text{B/g}$ tumor tissue; tumor: blood ratio = 5).

Various boron compounds-encapsulated BDSs have been developed including passive targeting liposomes¹⁵⁵ and/or active targeting liposomes by conjugating tumor specific ligands, such as folate receptor (FR),¹⁵⁶ epidermal growth factor receptor (EGFR),¹⁵⁷ and transferrin (TF) receptor.¹⁵⁸ Pan *et al.*¹⁵⁶ demonstrated that FR-targeted liposomes afford an almost 10-fold increase in the accumulation of ^{10}B in cancerous tissue. The concept of FR-targeting liposomes has also been exploited by Maruyama *et al.*^{158a} in the formulation of Na₂BSH with FR-PEG liposomes. Doi *et al.*¹⁵⁹ illustrated the superior selectivity of FR-PEG liposomal carriers of BSH as compared to PEG-liposomes or BSH alone.

Incorporation

In contrast to the encapsulation, the development of lipophilic boron compounds embedded within the liposome bilayer is an attractive means to increase the overall incorporation efficiency of boron-containing species, as well as to raise the gross boron content of the liposome in the formation.

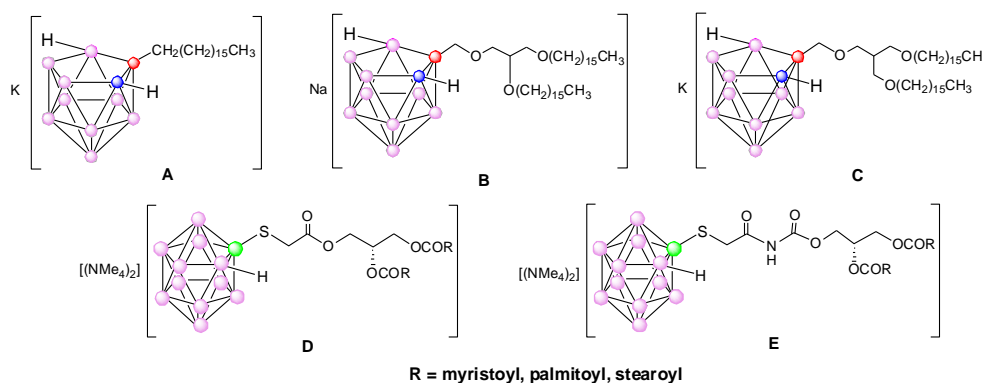
Nido-carborane lipids

The carboranyl cage is characterized by extremely high lipophilicity. This feature is recently being exploited in the application of some borane clusters as hydrophobic component (pharmacophore) in biologically active molecules providing them with capacity to interact hydrophobically with other molecules such as proteins or lipids of cellular membranes. Carborane pharmacophores may also improve the ability of modified molecules to penetrate lipid bilayers and potentially increase the cellular uptake.¹⁶⁰

A system involving the accumulation of boron in the liposomal bilayer is highly potent because drugs can be encapsulated into the vacant inner cell of a liposome. Furthermore, functionalization of liposomes is possible by combination of lipid contents. Therefore, boron and drugs may be simultaneously delivered to tumor tissues for BNCT and chemotherapy of cancers. Hawthorne and coworkers first introduced *nido*-carborane as a hydrophilic moiety into the amphiphile **A** (Figure 9) and examined liposomal boron delivery in mice using **A** and distearoylphosphatidylcholine (DSPC).¹⁶¹

1. Introduction

Nakamura *et al.* reported the first synthesis of *nido*-carborane lipid having a double-tailed moiety conjugated with *nido*-carborane as a hydrophilic moiety and its vesicle formation from **B**.¹⁶² Furthermore, they investigated the possibility of actively targeting boron liposomes to solid tumor by conjugating transferrin (TF) to the surface of the liposomes. Boron concentration of 22 $\mu\text{g } ^{10}\text{B/g}$ tumor was observed in mice injected with the boron liposomes at 7.2 mg $^{10}\text{B/kg}$ body weight. However, the injection of a higher boron concentration (14 mg $^{10}\text{B/kg}$ body weight) resulted in acute toxicity to the mice.¹⁶³ Hawthorne and co-workers also recently reported similar acute toxicity in mice injected with *nido*-carborane lipid **C**. They found that the liposomes were very toxic already at dosages of 6 mg boron per kg body weight.¹⁶⁴ *Nido*-carborane lipids might therefore be problematic as agents for boron delivery in BNCT, since the high toxicity may be caused by the *nido*-carborane structure, although the mechanism of *nido*-carborane cytotoxicity has not been studied in detail.



Closo-dodecaborate lipid liposomes

The problem of toxicity shown by *nido*-carborane lipids can be overcome by using $(\text{B}_{12}\text{H}_{11}\text{S})^{2-}$ -containing lipids, since BSH, a water soluble divalent anion cluster, is the only acceptable boron cluster compound that can be used at the present time in clinical trials in Japan, Europe, or the USA. Other suitable target species are under rapid development, but $\text{B}_{12}\text{H}_{11}\text{SH}^{2-}$ will probably remain the baseline compound for clinical studies conducted in the future.^{151b} Absence of toxicity in patients has later been proven in clinical trials.¹⁶⁵ The boron compounds that are used as capture agents for BNCT should be nontoxic when administered in amounts required to obtain sufficient tumor concentrations and thus sustain a lethal $^{10}\text{B}(n, \alpha) ^7\text{Li}$ reaction.

However, few synthetic examples of BSH derivatives as boron carriers have been reported so far due to the difficulty of their functionalizations.¹⁶⁶ In a study by Nakamura and coworkers,¹⁶⁷ the toxicity of boron liposomes **D** and **E** (Figure 9) was investigated, showing that for a dose of 15 mg of boron per kilogram of weight no mouse died after

1. Introduction

injection with the boron liposomes for up to three weeks, although 50% of the mice injected with the boron liposomes prepared from the lipid **C** died at a dose of 14 mg of boron per kilogram of weight within 48 hours.¹⁶⁷

d) Metallacarboranes as boron carriers for BNCT

The persistent interest in the design and synthesis of boron-containing nucleosides is that such compounds may be selectively accumulated in rapidly multiplying tumor cells, and end up trapped within the cell or ideally, incorporated into nuclear DNA of tumors.¹⁶⁸

Metallacarboranes contain about 1.5 times as much boron as BSH and 18 times more boron atoms than boric acid. They are characterized by high lipophilicity, property which may facilitate transport of the carrier molecules across the blood–brain-barrier (BBB) and improve cellular uptake. The ability of deltahedral ligands to form stable complexes with metals allows incorporation of various metals with different properties into boron carrier molecule and provides an additional advantage to high boron load.

The study on anti-tumor activity of metallacarboranes was originally initiated more than 20 years ago. Toxicity and pharmacokinetics of potassium salt of cobaltabis(dicarbollide) ion were tested¹⁶⁹ and was observed that it exhibited cytotoxic, but not mutagenic activity in the system used. The *in vitro* anti-tumor activity of a tin-meta-carborane derivative $\{[(1,7\text{-C}_2\text{B}_{10}\text{H}_{11}\text{-1-COO})\text{Bu}_2\text{Sn}]_2\text{O}_2$ has been described.¹⁷⁰ Anti-tumor activity of metallacarboranes other than based on dicarba-closo-dodecaboranes has also been described.¹⁷¹ *In vitro* cytotoxicity of these complexes against selected human tumor cell lines ranged from moderate to high. Detected cytotoxicity of the above compounds makes some of them candidates for further studies as potential anti-tumor agents, but also excludes them as boron carriers for BNCT.

In contrast, Plešek *et al.* found that conjugates of metallacarborane complex type of cobaltabis(dicarbollide) ion with nucleoside unit, and in some cases simple nonnucleoside derivatives are characterized by low cytotoxicity.^{28b}

In conclusion, nucleoside/metallacarborane conjugate and some simple metallacarborane derivatives substituted at B(8) have shown low toxicity and high lipophilicity, an advantageous and preferred property for potential boron delivering drugs.

Tumor specific drug release

It was observed that particle size, surface charge¹⁷² and liposome composition had a strong influence on the clearance profile (e.g., incorporation of phosphatidylinositols or monosialogangliosides prolongs liposome circulation in the blood).¹⁷³ Moreover, by

1. Introduction

coating the liposomal surface with PEG-polymers, the liposome clearance by the macrophages can be delayed. Thus the liposomes can to some extent pass in and out of the liver and spleen without being cleared whereas they remain in the tumor tissue due to the depleted lymphatic drainage¹⁷⁴ and a leaky vasculature.¹⁷⁵ This results in selective liposome accumulation in tumors through passive diffusion.

While significant advances have been made in overcoming many of the barriers with liposomal drug delivery, there still remains the problem of obtaining a high local drug bioavailability specifically in the cancerous tissue while maintaining the stability of the liposomes in circulation. There are two general directions within drug delivery cancer research focusing on solving this problem. (i) Site-specific delivery by targeting which can be achieved by coating the liposomes with ligands or antibodies that target receptors in the tumor tissue. By incorporating an active and site-specific release mechanism into the liposomes, it may be possible to dramatically increase the release and therapeutic efficacy of the carried drug.¹⁷⁶

Enhanced accumulation by targeting

The use of site-specific triggers that can release drugs specifically in diseased tissue is one way of increasing drug bioavailability at the tumor target site. Another way of optimizing drug bioavailability is to obtain a higher degree of liposome accumulation by active targeting. Furthermore, the combination of active targeting with active triggering can potentially lead to significantly enhanced and specific drug release at the tumor target site. Several critical issues exist: i) when liposomes accumulate in the interstitial compartment due to extravasation and bind to the first line of target cells, liposomes with strongly binding ligands may obstruct the way for more liposomes to accumulate,¹⁷⁷ ii) immunoliposomes show enhanced liposome clearance¹⁷⁸ and iii) internalization by endocytosis is the normal strategy associated with active targeting.

Enhanced delivery via triggered release

Several strategies have been proposed to accomplish site-specific triggered drug release in tumor tissue. Liposomes triggered by acid,¹⁷⁹ small changes in temperature¹⁸⁰ and light¹⁸¹ have all been shown to be useful concepts for releasing encapsulated drugs. Yet, liposomes designed with these specific trigger mechanisms have not yet reached clinical trials. A more recently proposed principle for site-specific drug release is the enzymatically triggered approach.¹⁸²

However, so far none of these approaches are in clinical use and there is a well-recognized need for effective triggered release. In 2007, Gabel *et al.* showed that liposomes consisting of dipalmitoyl phosphatidylcholine (DPPC) release their contents upon addition of the negatively charged boron cluster $\text{Na}_2\text{B}_{12}\text{H}_{11}\text{SH}$ (BSH).¹⁸³ According

1. Introduction

to their study, BSH triggers release of liposome content in a dose-dependent manner. Concentrations of 1 mM BSH are sufficient to noticeably increase the release rate of carboxyfluorescein (CF) encapsulated in liposomes prepared from dipalmitoyl phosphatidylcholine (DPPC). At higher BSH concentrations, leakage is complete within minutes. At low BSH concentrations, inclusion of PEG lipids leads to more pronounced leakage rates, whereas at higher BSH concentrations the rate is lower.

Another way of triggering the release of liposomal contents could be achieved by using surface cross-linked micelles (SCMs). The click reaction used in the cross-linking and postfunctionalization makes the SCMs extremely versatile and easy to prepare. A particular attractive feature of the SCMs is their rapid breakage upon cleavage of surface cross-links, enabling fast delivery of surface-active materials using specific chemical stimuli. As demonstrated by the leakage experiments performed by Zhao and Li,¹⁸⁴ the SCMs could trigger the release of liposomal contents upon cleavage and different mechanisms of leakage could be obtained, depending on the types of surfactants released.

Shi *et al.* reported¹⁸⁵ folate-receptor targeted pH-sensitive liposomes based on cationic /anionic lipid pair, with the appropriate composition, can facilitate highly efficient intracellular drug delivery. Moreover, the fact that the pH-sensitivity of cationic/anionic liposomes is maintained in the presence of serum, confers these liposomes the potential of being suitable agents for systemic administration (since serum's retaining activity is required for use in systemic delivery).

To conclude, the targeting strategies to improve accumulation and internalization by coating the liposomes with antibodies or other ligands will significantly improve the liposome bioavailability in the future.

1.4. Objectives

The main objective of this doctoral thesis was the syntheses of high boron content polyanionic macromolecules, for their potential use in a wide variety of medical applications. The metallacarborane complexes have more boron atoms per molecule than either the carboranes or the *closo*-dodecaborate anion, making them more attractive from the BNCT point of view. Moreover, the fact that they are anionic, increases their water-solubility, that “a priori” could facilitate their biodistribution.

The cobaltabis(dicarbollide) has been chosen as starting metallacarborane compound. The syntheses of monoanionic going to polyanionic ($n = 1-5$) multicluster derivatives has been performed, since the main goal of this doctoral thesis was to obtain high boron content, water-soluble, macromolecular compounds for their medical use in Boron Neutron Capture Therapy (BNCT).

The functionalization of gold nanoparticles (Au NPs) with either neutral or anionic boron-based thioclusters was performed, yielding boron-enriched polyanionic multicluster macromolecules, displaying a host of interesting properties, among which, increased water solubility. This is a vital property for the further study of cellular uptake and intracellular fate. Moreover, we want to find out if the size of the monolayer protected clusters (MPCs) obtained by capping of the Au NPs with our thioligands, have any influence on the properties as well as on the interactions they have with biological cells.

2. RESULTS and DISCUSSIONS



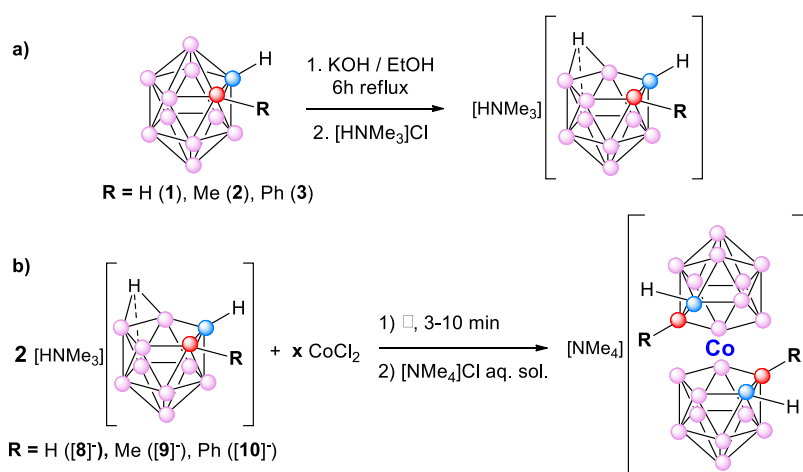
2.1. Solid state complexation reactions

As previously described cobaltabis(dicarbollide) and ferrabis(dicarbollide) have attracted significant attention because of their high content in boron, great stability, water-solubility, but also because they can be functionalized both on boron^{23a,25a,26,186,187} and on carbon atoms,^{19,188} opening the way to a wide variety of applications. However, in spite of all these interesting properties, their synthesis is quite difficult, requiring many reaction steps as shown in the Introduction section (Subchapter 1.2.1). Therefore, we thought of a much easier complexation reaction for the obtaining of these metallocarboranes, since their syntheses are quite time consuming. Furthermore, as reported so far in the literature, these complexation reactions are performed in solution and take more than 24 hours, depending on the substituents present in the molecule.

2.1.1. Complexation reactions of *nido* [7-R-8-R'-C₂B₉H₁₀]⁻ species with CoCl₂

We thought of designing a rapid and efficient method for the synthesis of metallocarborane complexes, since, as previously explained, the ones available at the moment require difficult intermediary reaction steps.

We first wanted to try out this new procedure using as starting material a compound already in hand, such as the *ortho*-carborane **1**. *Ortho*-carborane **1** was partially deboronated before being subjected to complexation, as indicated in Scheme 5a below. Based on the results obtained by the complexation reactions of this *nido* species, this reaction procedure was set-up.



Scheme 5. General synthetic route: **a)** partial deboronation reaction; **b)** complexation reaction of the *nido* species with CoCl₂

One of the most important features of the complexation reaction is that the starting compounds were always the trimethylammonium salts of the respective *nido* species. In this way, when heated in solid state, hydrogen and trimethylammonium are generated as gases, and by leaving the system, the equilibrium is shifted towards the

formation of the final cobalt-coordinated compounds. The presence of the trimethylammonium can be easily detected only by smell, since this gas has a characteristic pungent odor.

For the complexation reaction of $[\text{HNMe}_3][\mathbf{8}]$, various parameters, such as temperature, time of reaction, excess of CoCl_2 , as well as the nature of the CoCl_2 reagent (either anhydrous or hydrated) were tried out, in order to find the optimal parameters for the reaction procedure. As indicated in Table 1 (entries 1-5), only the time of heating proved to have some influence on the complexation reaction of species $[\text{HNMe}_3][\mathbf{8}]$.

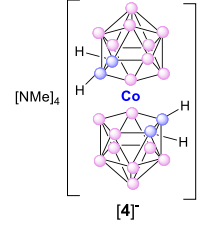
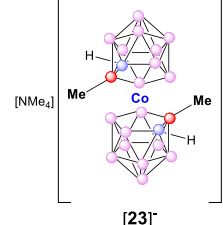
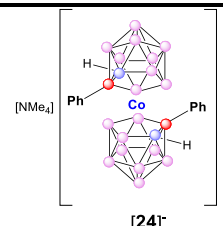
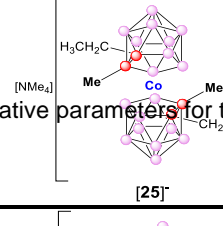
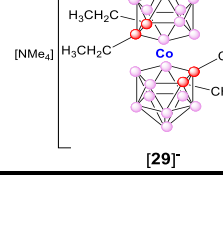
Complex	Entry	Working conditions		CoCl_2 excess	Yield %
		Time (minutes)	Temperature ($^{\circ}\text{C}$)		
 [4]	1	3'	350	1.5 CoCl_2 anh.	83
	2	5'	350	1.5 CoCl_2 anh.	85
	3	7'	350	1.5 CoCl_2 anh.	88
	4	7'	350	1.5 $\text{CoCl}_2 \cdot 6\text{H}_2\text{O}$	90
	5	8'	350	1.5 $\text{CoCl}_2 \cdot 6\text{H}_2\text{O}$	88
 [23]	6	2'	350	5 CoCl_2 anh.	42
	7	3'	350	5 CoCl_2 anh.	46
	8	3'	470	5 CoCl_2 anh.	68
	9	5'	350	5 CoCl_2 anh.	75
	10	10'	350	5 CoCl_2 anh.	90
	11	2' + 6'	350/470	1.5 $\text{CoCl}_2 \cdot 6\text{H}_2\text{O}$	87
 [24]	12	2' + 6'	350/470	1.5 $\text{CoCl}_2 \cdot 6\text{H}_2\text{O}$	88
	13	2' + 6'	350/470	2.5 $\text{CoCl}_2 \cdot 6\text{H}_2\text{O}$	94
	14	2' + 6'	350/470	25 CoCl_2 anh.	60
	15	10'	350	5.5 CoCl_2 anh.	83
 [25]	16	2' + 6'	350/470	2.5 CoCl_2 anh.	82
	17	2' + 6'	350/470	2.5 CoCl_2 anh.	68
 [29]					

Table 1. Representative parameters for the synthesis of cobaltabis(dicarbollide)-based complexes

The boron spectra of the above presented species confirm the conversion of the *nido* cluster into its corresponding complex. Moreover, the boron signals characteristic for

the *nido* species disappear with the formation of the new complex, since the two dicarbollide units are coordinated by the cobalt atom, resulting in a complex in a *close* form. In all of these experiments (entries 1-5), [4]⁻ was obtained in very high yields.

Once we have demonstrated that the solid state complexation reaction starting from 1 yielded the desired complex [4]⁻ in a matter of minutes and without the use of any solvent, we looked for the optimal parameters for the complexation reactions of the *nido* species that possess one substituent on the carbon atom, namely the *ortho*-carborane derivatives [9]⁻ and [10]⁻.

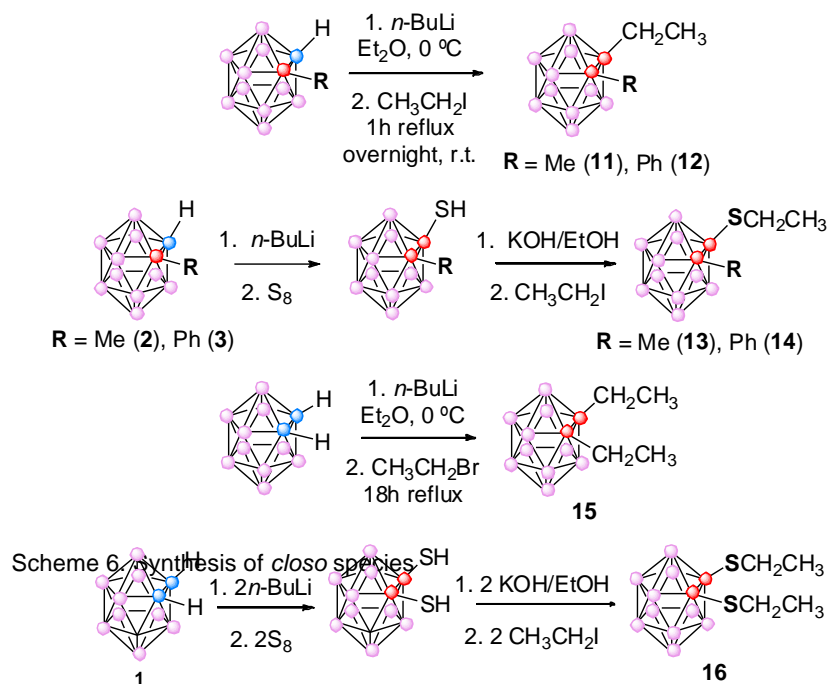
Regarding time of reaction, we can clearly see that the presence of one substituent on each of the dicarbollide units influences on the final yield of the corresponding complexes. Take for example entries 1 and 7 of Table 1 above. It clearly indicates that when some degree of steric hindrance is involved, using the same heating time and temperature, the yield is drastically reduced from 83% for complex [4]⁻ to 46% for species [23]⁻. Moreover, we can observe the importance of the time of reaction within the same class of complexation reactions only by looking at entries 9 and 10 for complex [23]⁻. After only 5 minutes of heating at 350 °C, the yield obtained is of only 75%, whereas by increasing the number of heating minutes, at the same temperature of 350 °C, the yield is significantly improved to 90%.

With respect to the temperature used for complexation, it can also be seen how it influences the final yield by checking entries 7 and 8 for the values of 350 °C and 470 °C respectively, for compound [23]⁻. The increase in temperature by 120 °C, while maintaining the time of heating and the CoCl₂ excess constant, induces an increase in the final yield of about 50%. Another parameter that we took into account when running the complexation reaction was the nature of the CoCl₂, either anhydrous or hydrated. However, to our surprise, we also obtained very good results when using the hydrated CoCl₂, as presented for compound [24]⁻. Likewise, concerning the number of excess equivalents of CoCl₂, we can observe that when using large excesses, as it is the case illustrated in entry 14 of Table 1, the result was a important decrease in the yield of compound [24]⁻.

Now that we have proven that our new method does work for species with one substituent on each dicarbollide unit, allowing us to obtain in a easier and much faster way carbon-disubstituted cobaltabis(dicarbollide) complexes, we wanted to see if we could apply the same procedure for the synthesis of complexes having substituents present at both carbon atoms within the same dicarbollide unit. In order to follow our theory, we firstly had to synthesize the disubstituted C_c derivatives, as well as the ones bearing substituents with free pair of electrons. These species were obtained in two steps: i) the first step was the metallation reaction of *o*-carborane derivatives, 2 and 3,

Results and discussions

2.1. Solid state complexation reactions

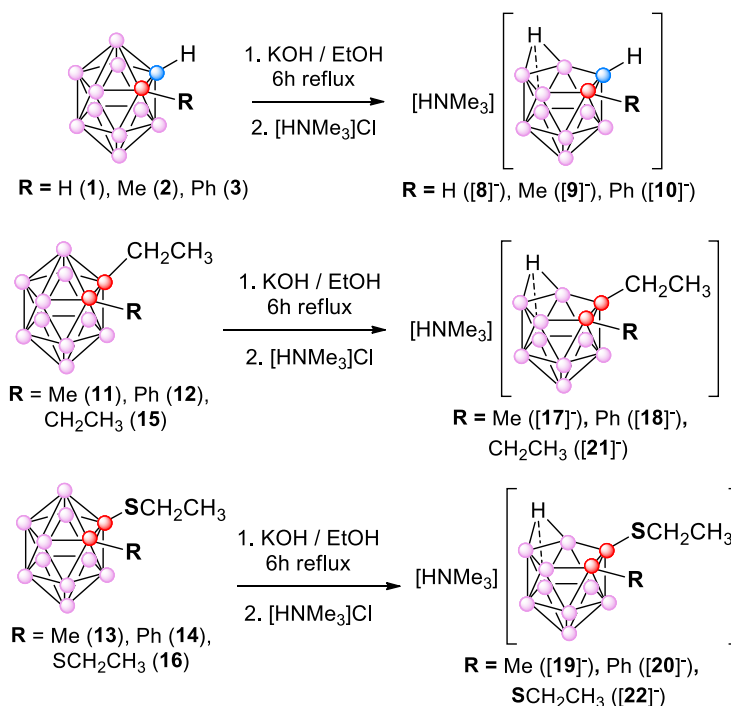


and the thiol derivative of **2** and **3**, with one or two equivalents of *n*-BuLi, depending on the desired compound; and ii) the second step consisted in a nucleophilic substitution of the lithium/potassium ion, yielding the *closo* clusters as indicated in Scheme 6. It is worth mentioning that when the bromoethane was used as a source of the organic group instead of

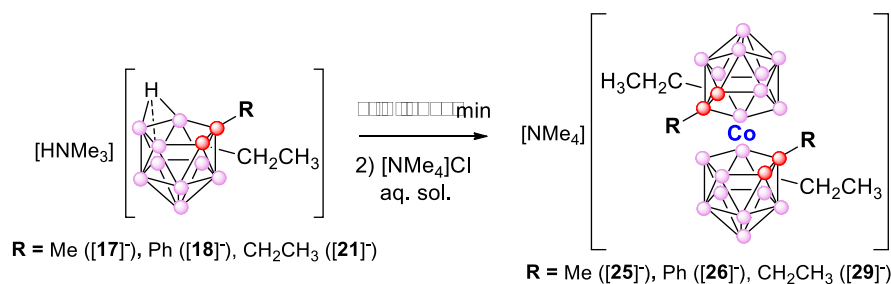
its corresponding iodine-derivative, the yields were quite unsatisfactory (no more than a 20%).

The following step was the partial deboronation reaction of the previously synthesized *closo* species. The general procedure consists in a nucleophilic attack on B(3) or B(6) by EtO^- under 6 hours of reflux.

After extraction with dilute HCl, all the compounds were precipitated as trimethylammonium salts, namely $[\text{HNMe}_3][\mathbf{17}]$ - $[\text{HNMe}_3][\mathbf{22}]$. The synthetic way is presented in Scheme 7.



Next, we were seeking to determine if the presence of a second alkyl or aryl substituent at the C_2B_3 open-face of a *nido* species cluster will hinder the formation of the complex. The new procedure to obtain the cobaltabis(dicarbollide) complexes was applied by heating the corresponding *nido* salts with $CoCl_2$, yielding the desired cobaltabis(dicarbollide) complexes, as shown in Scheme 8.

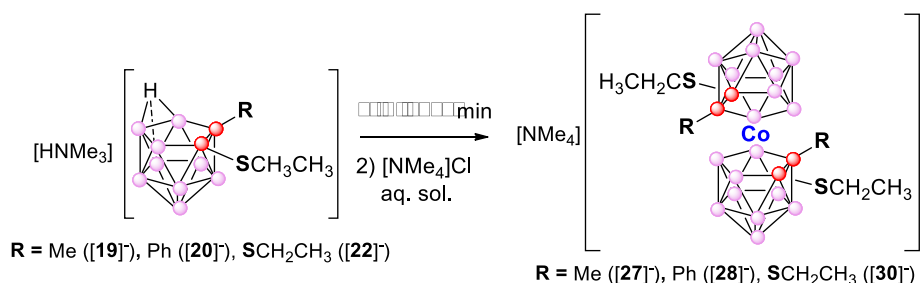


Scheme 8. Complexation reaction yielding monoanionic species $[25]^-$, $[26]^-$ and $[29]^-$

In the case of the alkyl substituents, the different synthetic procedures are presented in Table 1 (entries 16 and 17).

However, in the case of the phenyl-containing cluster, the NMR characterization of the final complex indicated that after 8 minutes of heating at an average temperature of 440 °C, there was still a large amount of starting material present. Therefore, more reactions are to be performed, varying the reaction conditions, in order to find the optimum parameters for the complexation of this type of compounds.

After determining that the steric hindrance does not dramatically affect the complexation reaction in the case of the alkyl substituents, we were curious to determine if the presence of elements bearing free pair of electrons will have any influence on the formation of the complex. For this we first synthesized the *closo*-thioethers of the *ortho*-carborane derivatives **13**, **14**, **16**, followed by partial deboronation of the *closo* cluster to the corresponding *nido* species $[19]^-$, $[20]^-$ and $[22]^-$ and finally ran the proper complexation reaction with $CoCl_2$, as indicated in Scheme 9.



Scheme 9. Complexation reaction of C-tetrasubstituted derivatives

Out of these three compounds, only the *nido* species $[19]^-$, which has a Me group bonded to the C_c , gave rise to the desired complex; however, the yield was significantly lower than for the previously obtained species, namely 50%. The complexation

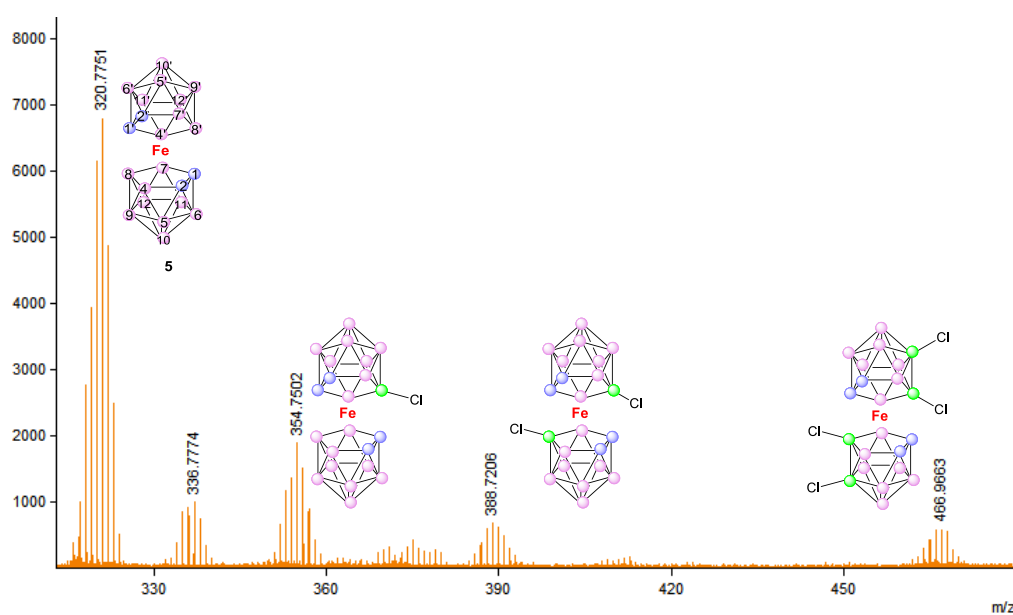
reactions for the *nido* species with **R** = Ph or **SCH₂CH₃** did not work, and the *nido* clusters were recovered after 8 minutes of heating. This could be explained either by electronic or steric effects of the C_c substituents.

2.1.2. Complexation reactions of [7,8-C₂B₉H₁₂]⁻ species with FeCl₂

After obtaining such satisfactory yields by using the innovative solid state complexation reaction, the next step was to determine if we can apply the procedure we developed for the cobaltabis(dicarbollide)-based complexes to synthesize the corresponding iron-containing species, since iron is a more biocompatible oligoelement than cobalt, and therefore, should find more use in medical applications.

Starting from the same trimethylammonium salt of **[8]**, we heated it in solid with FeCl₂ for 8 minutes at 350 °C, then added HCl 1M and ether, extracted the organic layer and precipitated it as tetramethylammonium salt for a better characterization. We were expecting to find the ferrabis(dicarbollide) species, however, the results obtained after processing the reaction were quite surprising. First of all, since the brown-greenish precipitate was showing a yield of only 55% (whereas the yield obtained for the synthesis of cobaltabis(dicarbollide) complex, **[4]**, using the same conditions, was 88%). Secondly, we did not obtain the sandwich-type compound, but substituted some hydrogen atoms for chlorine atoms on the ferrabis(dicarbollide) complex, probably due to the fact that this metallacarborane species is more reactive than its homologue, the cobaltabis(dicarbollide). This information was extracted from the corresponding MALDI-TOF-MS spectrum, that showed us the presence of ferrabis(dicarbollide) complex and other clusters, as represented in Figure 10. MALDI-TOF-MS is a method of mass spectrometry in which an ion's mass-to-charge ratio is determined *via* a time

Figure 10. Chlorination during solid state complexation reaction



measurement. This ionization technique by laser desorption, is one of the most efficient characterizing methods of the synthesized anionic clusters in solid state. The confirmation of the obtaining of monoanionic species lays in the peaks separation in the isotopic distribution, which is of one m/z unit. The most probable chlorination positions are the B(8) and B(10), the former because since it is one of the boron atoms situated in the C_2B_3 face, further from the two carbon atoms, therefore bearing a more negative charge, and the latter because of the superposition of the hybrid sp orbitals of both cobalt and B(10).

As indicated by mass spectrometry, four different ferrabis(dicarbollide) complexes are present within the same sample. The molecular peak at 467 cm^{-1} fully agrees with the tetrachlorinated species. Nevertheless, this cluster's chlorination reaction does not occur for the cobaltabis(dicarbollide), clearly showing the more reactive character of the ferrabis(dicarbollide) complex, that, once formed, undergoes electrophilic substitution, yielding some halogenated derivatives. The peak at 354.75 m/z corresponds to the monochlorinated derivative, whereas the one at 388.72 m/z illustrates the presence of the dihalogenated species within the analyzed sample, [31].

In conclusion, now that we have established a new procedure for the synthesis of cobaltabis(dicarbollide) and ferrabis(dicarbollide) complexes, using a solvent-free method, we should carry on further studies on other *nido* species and determine if we can extrapolate this procedure to the obtaining of different complexes, all by using this rapid, easy and environmental-friendly method. Moreover, we also determined that the presence of a second substituent decreases the yield of the complexation reactions, and also that an organic group possessing either an element with a free pair of electrons or a π group within the molecule strongly diminishes the yield or even does not allow the reaction to take place.

2.1.3. Characterization of the *closo* species

The *closo* species were characterized employing techniques such as FTIR, MALDI-TOF-MS and ^1H , $^1\text{H}\{^{11}\text{B}\}$ -NMR, $^{11}\text{B}\{^1\text{H}\}$ -NMR and ^{11}B -NMR.

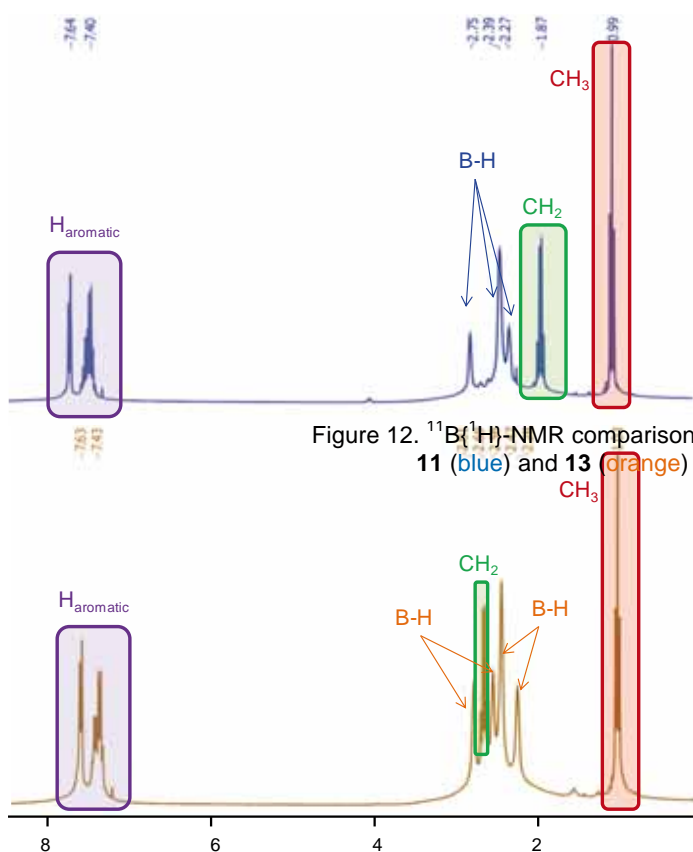
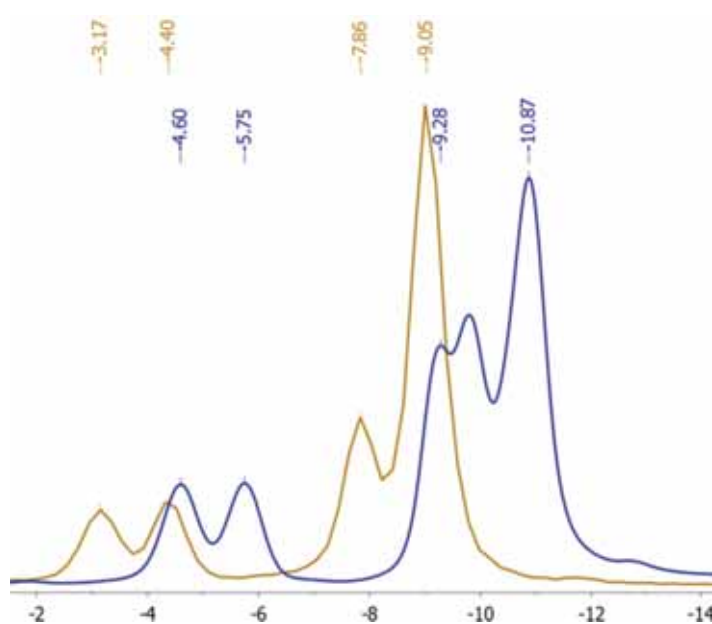


Figure 12. $^1\text{H}\{^{11}\text{B}\}$ -NMR comparison between **11** (blue) and **13** (orange)

$^1\text{H}\{^{11}\text{B}\}$ -NMR spectra of compounds **12** and **14** indicate the synthesis of the desired compounds. As expected, since the only difference is the presence of the sulphur atom within our molecule **14**, there would be not much change in the $^1\text{H}\{^{11}\text{B}\}$ -NMR spectrum, but for changes in the chemical shifts of the constituent groups. This is illustrated in Figure 11 in which one can observe the shift of the CH_2 - group from 1.87 ppm to 2.69 ppm when bonded to the sulphur atom. This is due to the more electronegative character of the sulphur atom, which deshields the CH_2 -

group, shifting it to lower field values. The aromatic hydrogens and the CH_3 - group are too far to be influenced by this effect, so practically there is no change in their chemical shifts. The broad singlets that appear in the region 2.75 - 2.27 ppm belong to B-H bonds. The integration of the main groups verifies, confirming once again the synthesis of the sought compounds.

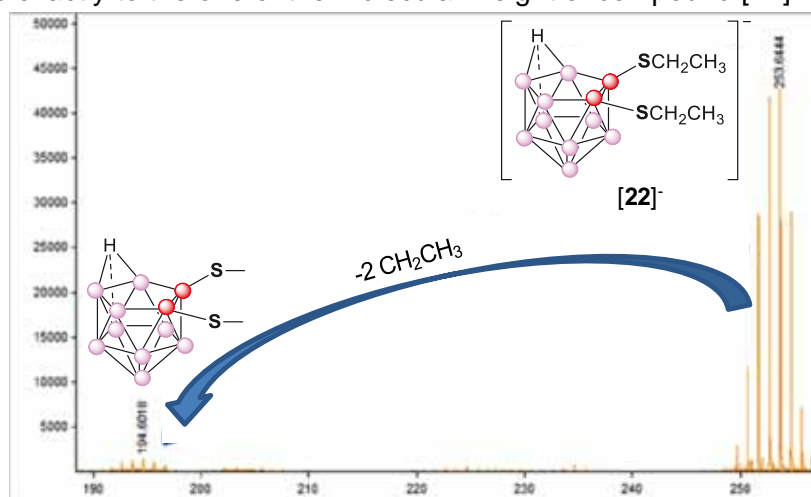
The effect of the sulphur atom is also visible in the $^{11}\text{B}\{^1\text{H}\}$ -NMR spectra. When comparing compound **11** with **13**, one can see that the presence of a more electronegative element (sulphur) determines a shift towards lower field values. This is clearly shown in Figure 12.



2.1.4. Characterization of the *nido* clusters

The *nido* species [17]⁻-[22]⁻ were characterized using the same techniques as the *closo* compounds presented above, namely by FTIR, MALDI-TOF-MS and ¹H, ¹H{¹¹B}-NMR, ¹¹B{¹H}-NMR and ¹¹B-NMR.

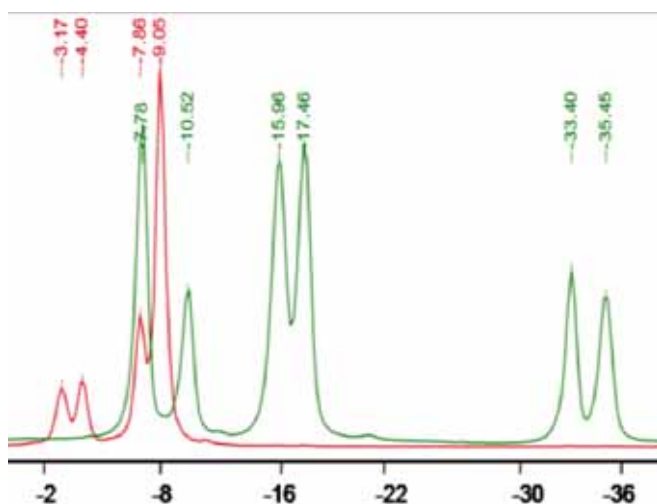
The MALDI-TOF-MS presented in Figure 13 confirms the fact that there were no by-products resulting from the deboronation reaction. The molecular peak at 253.6 m/z corresponds exactly to the one of the molecular weight of compound [22]⁻.



The ¹H{¹¹B}-NMR spectra of the compounds of the above synthesized *nido* species are presented in Table 2.

Compound	R	R'	δ (C-Me) (ppm)	δ (CH ₂ CH ₃) (ppm)	δ (CH ₂ CH ₃) (ppm)	δ (B-H) (ppm)	δ (H _{bridge}) (ppm)
[17] ⁻	Me	CH ₂ CH ₃	1.39	1.76/1.61	0.99	1.95-0.46	-2.62
[19] ⁻	Me	SCH ₂ CH ₃	1.51	2.56/2.51	1.14	2.37-0.58	-2.54
[21] ⁻	CH ₂ CH ₃	CH ₂ CH ₃	-	1.78/1.59	0.96	2.00-0.49	-2.64
[22] ⁻	SCH ₂ CH ₃	SCH ₂ CH ₃	-	1.75/2.69	1.11	2.38-0.62	-2.50

Table 2. ¹H{¹¹B}-NMR chemical shifts of *nido* compounds [17]⁻, [19]⁻, [21]⁻, [22]⁻



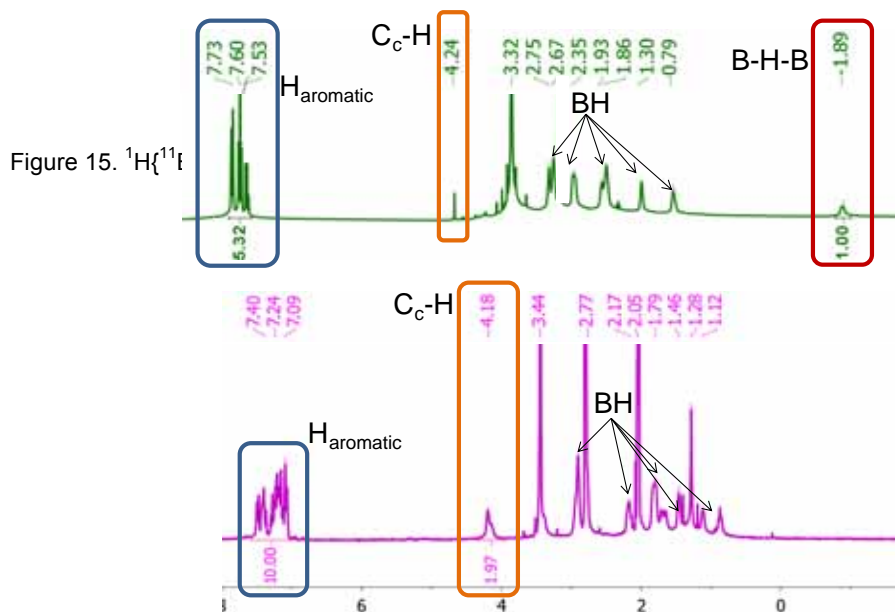
The influence on the chemical shift of the thiolate group is very well shown in Table 2. We can observe a downfield shift of the CH₂- group that is immediate bounded to the sulphur atom, namely of about 0.9 – 1 ppm.

Figure 14 presents the ¹¹B{¹H}-NMR spectra before (red) and after (green) the partial deboronation

reaction of compound **13**, bearing one thiolate group within its structure. The pattern and the chemical range of the boron signals showing at -33 and -35 ppm are a clear indication that the degradation reaction did occur, and that no other by-products are formed during the degradation process.

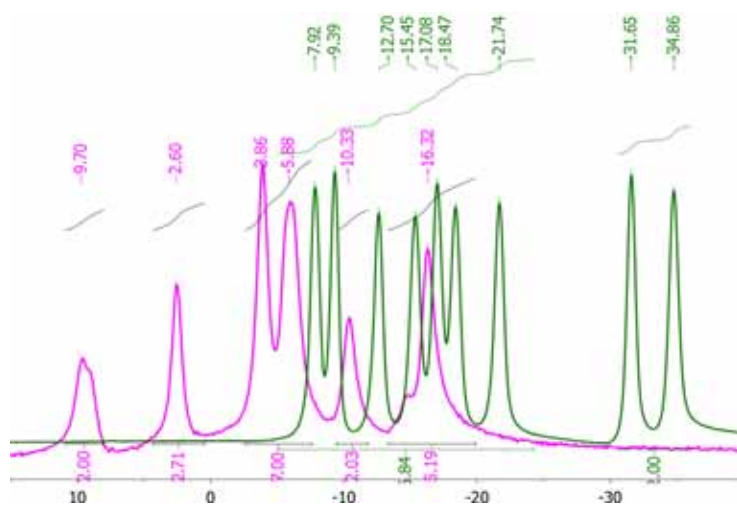
2.1.5. Characterization of the cobaltabis(dicarbollide) species

Regarding the process of the complexation reaction, Figure 15 shows the comparison between the $^1\text{H}\{^{11}\text{B}\}$ -NMR spectra of compounds **[10]** and **[24]** where we can clearly see the disappearance of the bridged hydrogen of the *nido* species at about -2.42 ppm with the formation of the \square^5 cobaltabis(dicarbollide) sandwich complex.



the complex **[24]**, the proton signals at 7.40 – 7.09 ppm correspond to the aromatic phenyl groups within the molecule, the ones present at 4.18 and 4.11 ppm belong to the proton from the $\text{C}_c\text{-H}$ bonds, whereas the peaks appearing from 2.77 until 1.12 ppm are characteristic for the B-H bonds. Furthermore, the bridged H peak appearing in the $^1\text{H}\{^{11}\text{B}\}$ -NMR spectrum of the *nido* compound at -2.42 ppm is no longer present

once the complexation reaction takes place, fact indicated in the $^1\text{H}\{^{11}\text{B}\}$ -NMR spectrum of **[24]** complex (Figure 15 purple). The $^{11}\text{B}\{^1\text{H}\}$ -NMR spectra of the above presented *nido* species (Scheme 7) confirm the conversion of the *nido* cluster into its corresponding complex, as presented in Figure 16. The boron signals characteristic for the *nido* species disappear



with the formation of the new complex, since the two dicarbollide units are coordinated by the cobalt atom, resulting in a *closo* form. This, together with a small shift to lower field values, is illustrated in Figure 16.

The complexation of the *nido* species [17]⁻, [19]⁻, [21]⁻ was also achieved, fact confirmed by the disappearance of the peaks indicating the *nido* form at about -32 and -35 ppm; however, further purification is essential for a characterization beyond any reasonable doubt of the corresponding complex structures. Moreover, the complexation reaction starting from the *nido* salt of species [30]⁻ was not possible, independent on the change in parameters and reaction conditions, due to electron repulsion effect.

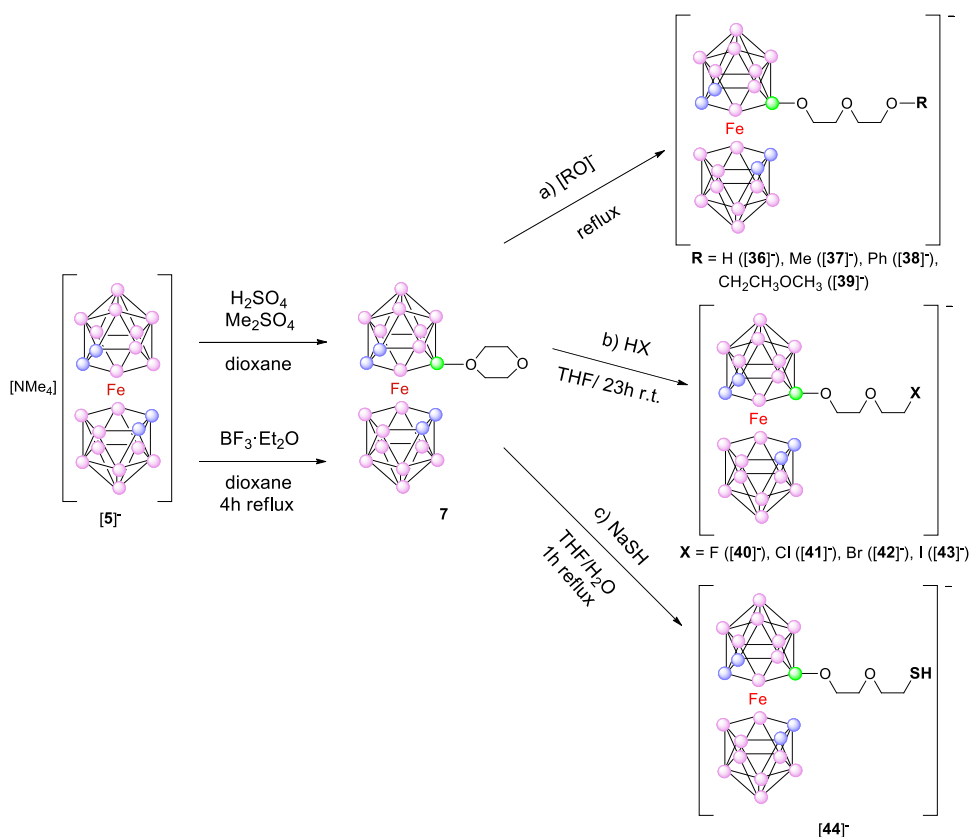
Results and discussions

Scheme 10. General scheme for the syntheses of [3,3'-Fe(8-(OCH₂CH₂)₂X-(1,2-C₂B₉H₁₀)(1,2'-C₂B₉H₁₁))] 2.2. Ring-opening reactions of 1,4-dioxane derivative of ferrabis(dicarbollide) with various groups

2.2. Ring-opening reactions of 1,4-dioxane derivative of ferrabis(dicarbollide) with various groups

As previously mentioned in the Introduction section, our main goal was the syntheses of boron-enriched compounds for their applications in medicine. Having in mind the fact that iron is a more biocompatible oligoelement than cobalt is, and also based on prior reported 1,4-dioxane ring-opening of cobaltabis(dicarbollide) with alcoxides²⁷ as well as with halogen and thiol groups,¹⁸⁹ we became concerned with the obtaining of ferrabis(dicarbollide) with the above mentioned synthons for the potential binding to various platforms. Our interest in the syntheses of these classes of compounds is justified by the fact that these innovative boron species could be delivered into tumor cells using different strategies for tumor targeting or could be used as building blocks for synthesis of boron-containing biomolecules.

Here we report the synthesis of alkyl-, halogen- and thiol-terminated synthons based on the oxonium derivative of ferrabis(dicarbollide) **7** (Scheme 10). This is especially attractive, since breaking one carbon-oxygen bond should result in a moiety having a boron complex separated from a carbocationic centre by 6 or more atoms (polyglycolic chain). In such a way, molecules with a reasonable length spacer between the boron cage and the property-determining part of the molecule could be prepared.



The first step was the synthesis of the zwitterionic derivative, $[3,3'\text{-Fe}(8\text{-(OCH}_2\text{CH}_2)_2\text{-}(1,2\text{-C}_2\text{B}_9\text{H}_{10})(1',2'\text{-C}_2\text{B}_9\text{H}_{11})]$ zwitterionic species, **7**. The procedure reported so far in the literature^{23b} implies the use of a Bronsted acid, namely H_2SO_4 to subtract a hydride from the C_2B_3 face unit, followed by the nucleophilic attack of the dioxane ring on the remaining positive B(8) atom. However, we wanted to determine if the synthetic procedure reported by our group for the obtaining of **6**^{23a} will also prove efficient for the synthesis of **7**, so $\text{BF}_3\cdot\text{Et}_2\text{O}$, a Lewis acid, was used as the electrophilic agent that will induce the nucleophilic substitution. After refluxing the reaction mixture for four hours, the solvent is evaporated and the desired compound separated by TLC; using silica gel plates and dichloromethane as eluent, the open-ring species remains as baseline. The yield obtained following this procedure, namely 52%, is comparable to the one already present in the literature, using concentrated sulphuric acid, dimethylsulphide and 1,4-dioxane.^{23b}

2.2.1. Syntheses of $[3,3'\text{-Fe}(8\text{-(OCH}_2\text{CH}_2)_2\text{X-}1,2\text{-C}_2\text{B}_9\text{H}_{10})(1',2'\text{-C}_2\text{B}_9\text{H}_{11})]^-$ (where X = RO^- , X^- and SH^-)

Once the zwitterionic species **7** was synthesized, the following step was the ring-opening reaction with various nucleophiles, as illustrated in Scheme 10a above.

Compounds **[36]**⁻ - **[39]**⁻ described here were obtained using alkoxides as nucleophiles, namely sodium methoxide, ethoxide and 2-methoxyethoxide. The preparation of the alkylferracarborane species was achieved in very satisfactory yields (92-96%), in an atom efficient and environmentally friendly transformation. After the nucleophilic attack of the RO^- group on the positive oxygen atom from the 1,4-dioxane ring, the resulting compounds were purified by TLC, using a dichloromethane:hexane 1:1 mixture. The base line was separated and passed through a cation-exchange resin to yield the sodium salt.

Other subject of interest alongside this doctoral thesis was the preparation of haloalkylferracarboranes **[40]**⁻ - **[43]**⁻, in order to complete a previous synthetic method developed by our research group yielding cobaltabis(dicarbollide) bearing halogen end moieties.¹⁸⁹ The syntheses of halogen/thiol-terminated ferrabis(dicarbollide) synthons were of particular interest for their posterior covalent bonding to different platforms, leading to the obtaining of a wide variety of novel materials for new applications, such as surface functionalization. Our objective was to be able to synthesize, in a simple and rapid way, derivatives of **[5]**⁻ containing a terminal halide, and thus facilitating the applicability of metallocarboranes in a variety of different fields.

The reaction conditions did not involve working with anhydrous solvents or in inert nitrogen atmosphere; it is simply the use of concentrated haloacids in organic solvents

that led to the synthesis of the sought compounds, with yields greater than 80% (Scheme 10b).

Besides ring-opening with various haloacids, another high atomic efficient reaction was the synthesis of thiol-terminated ferrabis(dicarbollide) synthons, species that will prove to be very utile in groundbreaking applications, among which surface functionalization.

Following the procedure described by our group for the synthesis of thiol-terminated $[3,3'\text{-Co}(\text{C}_2\text{B}_9\text{H}_{11})_2]^-$,¹⁸⁹ we prepared its iron analogous with the intention of using them as capping agents for nanoparticle stabilization. After purification by silica-gel chromatography, the final compounds were precipitated as tetramethylammonium salts for a better characterization.

The functionalization of gold nanoparticles with this and other thiol-terminated carboranes and metallacarborane synthons opens the way to a wide variety of applications in catalysis (dihydroxylation reactions,¹⁹⁰ carboxylic ester cleavage¹⁹¹), development of electronic devices and medicine to name only a few.

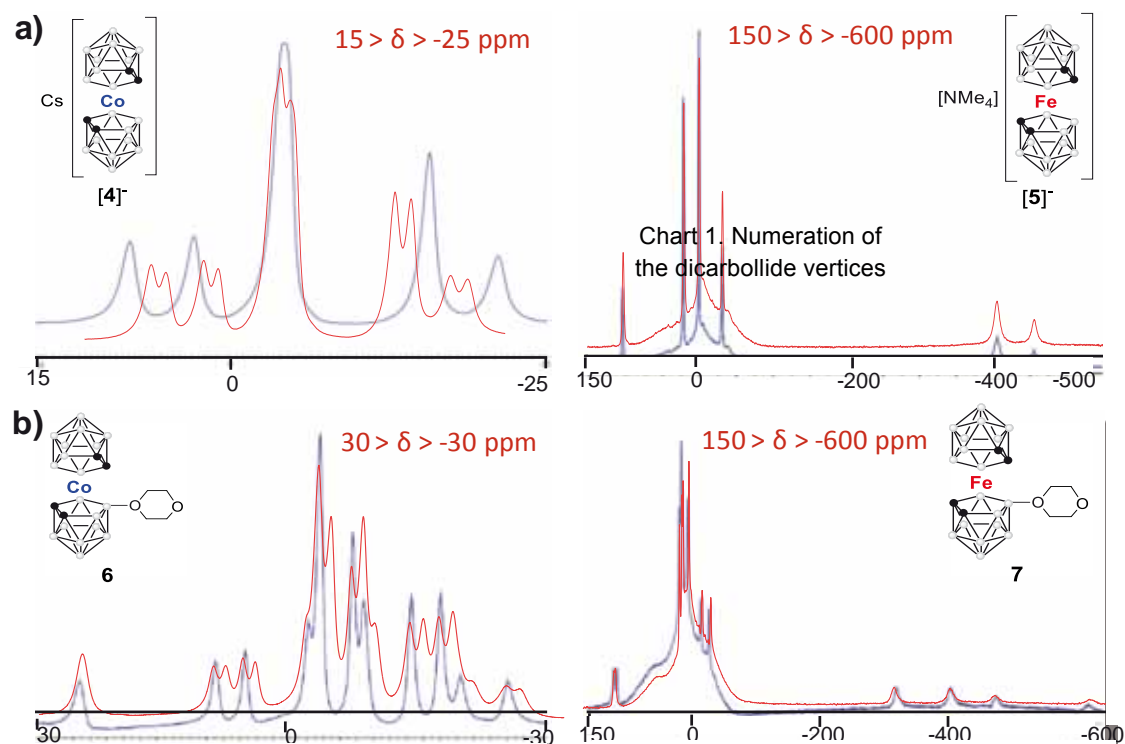
Moreover, the fact that ferrabis(dicarbollide) has rigid structure, restricted surface orientation and extensive possible modification chemistry, provides the axes for controlling their self-assembly, and therefore, will prove useful for enabling new applications.

2.2.2. Characterization of starting materials $[3,3'\text{-Fe}(\text{C}_2\text{B}_9\text{H}_{11})_2]^-$ and $[3,3'\text{-Fe}(\text{8}-(\text{OCH}_2\text{CH}_2)_2-(1,2\text{-C}_2\text{B}_9\text{H}_{10})(1',2'\text{-C}_2\text{B}_9\text{H}_{11}))]$

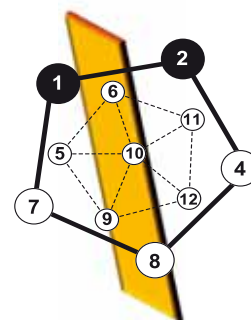
Since the ferrabis(dicarbollide) compounds are Fe(III) paramagnetic species, paramagnetic shifting with respect to the corresponding cobaltabis(dicarbollide) derivatives should be expected. This is why precautions have to be taken when running ^1H and ^{11}B -NMR regarding the extent of the spectral window; this is not the case for cobaltabis(dicarbollide) derivatives, which are diamagnetic molecules. This extensive spectral range of the ferrabis(dicarbollide)-containing species was from +80 to -20 ppm for the ^1H -NMR and from +110 to -500 ppm for the ^{11}B -NMR. This range was imposed by the paramagnetic character of Fe(III). Moreover, the same paramagnetic character prevents the coupling between the B and the H nuclei in the ^{11}B -NMR spectra (Figure 17a). The ^{11}B -NMR spectra of the zwitterionic species **6** and **7** show symmetry splitting of each signal present in the parent ferrabis(dicarbollide) ion into two peaks due to the presence of two symmetrically inequivalent dicarbollide ligands, as presented in Figure 17b. Likewise, since every subunit of the zwitterionic species is different, additional peaks appear in the ^{11}B -NMR spectrum of these compounds when comparing them with **[4]** and **[5]**. For instance, in the case of B(8), the boron directly bonded to the oxonium atom, a shift towards higher field values is observed, due to shielding.

Results and discussions

One obvious characteristic of $^{11}\text{B}\{^1\text{H}\}$ -NMR spectra of these paramagnetic compounds is the broadening of the chemical shift range from 40 ppm (Figure 17a left) to 750 ppm (Figure 17a right).



Another special feature of the iron-containing metallocarborane spectra is the fact that they show no coupling with the hydrogen (Figure 17a, right). Additionally, in the case of [5], ^{11}B -NMR spectrum allows us to perfectly identify the boron atoms most affected by the presence of the Fe(III) centre: the one that resonates at the lower field (≈ 110 ppm) and the ones that appear at high field values (≈ -400 and ≈ -450 ppm). To notice that their peak pattern is 1:2:1. Chart 1 displays the vertices number of the dicarbollide unit. From it, we can observe that there are two groups of boron vertices: i) the ones belonging to the \square^5 bonding C_2B_3 face (B(8), B(4) and B(7)) and ii) the one antipodal to the Fe(III) vertex, B(10) that interacts with Fe(III) by superposition of the hybrid sp orbitals.



The symmetry plane of the ligand that is perpendicular to the C_2B_3 face and bisects the $\text{C}_c\text{-C}_c$ bond, gives rise to two types of boron atoms: on one hand, B(8) and on the other hand, B(4) and B(7), which are equivalents. So, it is expected that the three boron atoms on the C_2B_3 face equally bonded to the Fe(III), will be affected in the same way, resonating close to one another, and showing a 2:1 peak pattern. So, "a priori" it was assigned B(10) at the lowest field and B(8), B(4) and B(7) at the highest field.

Results and discussions

2.2. Ring-opening reactions of 1,4-dioxane derivative of ferrabis(dicarbollide) with various groups

Figure 18. ^{11}B -NMR peaks distribution of cobaltabis(dicarbollide) (blue) and ferrabis(dicarbollide) (red) respectively

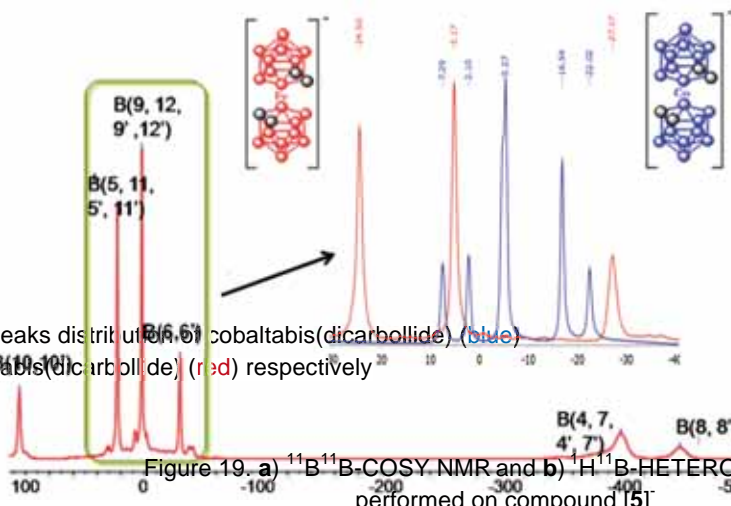
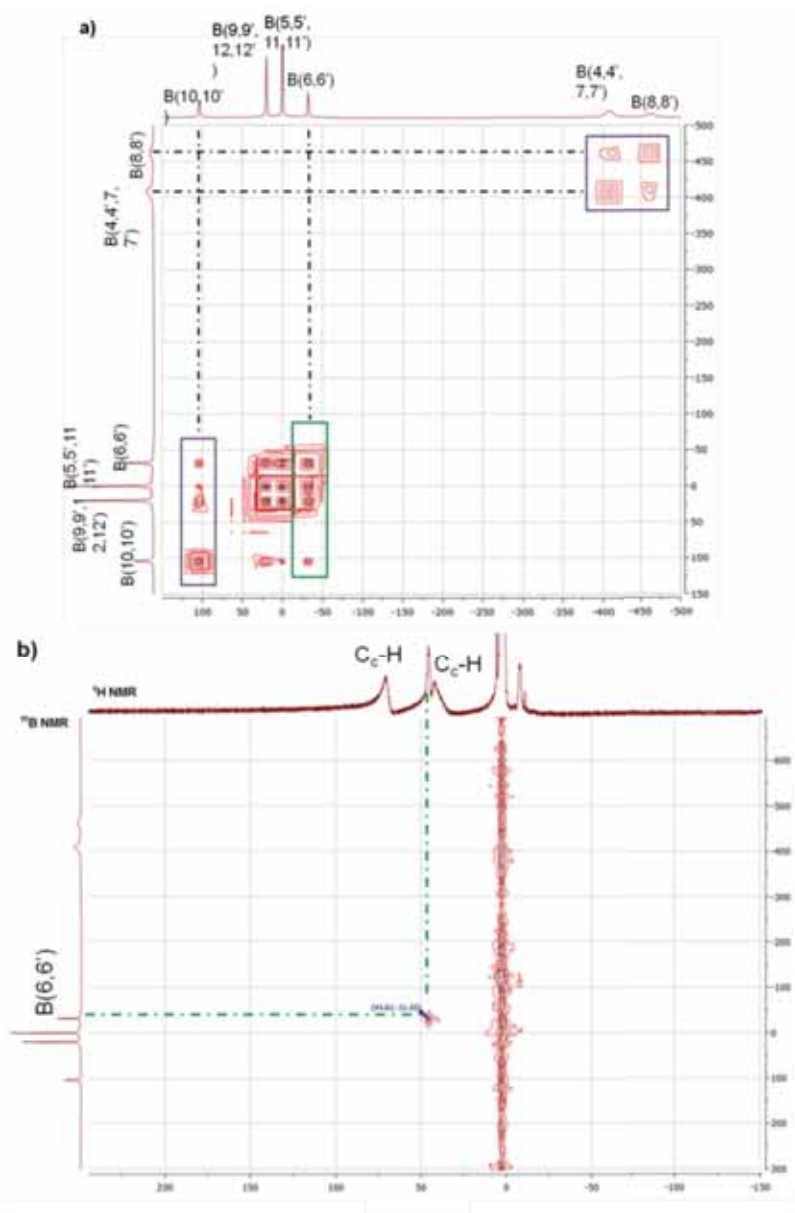


Figure 19. a) ^{11}B - ^{11}B -COSY NMR and b) ^1H - ^{11}B -HETEROCOSY NMR performed on compound [5]



In order to confirm the assignment of the peaks suggested above, we performed ^{11}B -COSY NMR, presented in Figure 19a. From this figure, we observed that the two boron peaks appearing at high field values interact only between themselves and additionally, their

integration values give 2:1. This, together with the facts depicted in Chart 1, indicates that these boron atoms correspond to the ones from the C_2B_3 face, B(4) and B(7) overlapping and therefore integrating 2, and to B(8), respectively.

The extremely deshielded peak, appearing at very low field values ($\approx +110$ ppm), interacts with the remaining B_5 plane boron atoms (B(5), B(6), B(9), B(11), and B(12)), but shows no interactions with the ones situated on the C_2B_3 face. This reconfirms that this peak

can be no other but the antipodal B(10).

Another very interesting aspect is the fact that the interactions of B(6), boron atom connected to both carbon atoms, with the other borons from the B₅ plane can also be observed. This is quite unique since there are no reported cases in the literature where B(6) cross coupling interactions can be so clearly noticed.

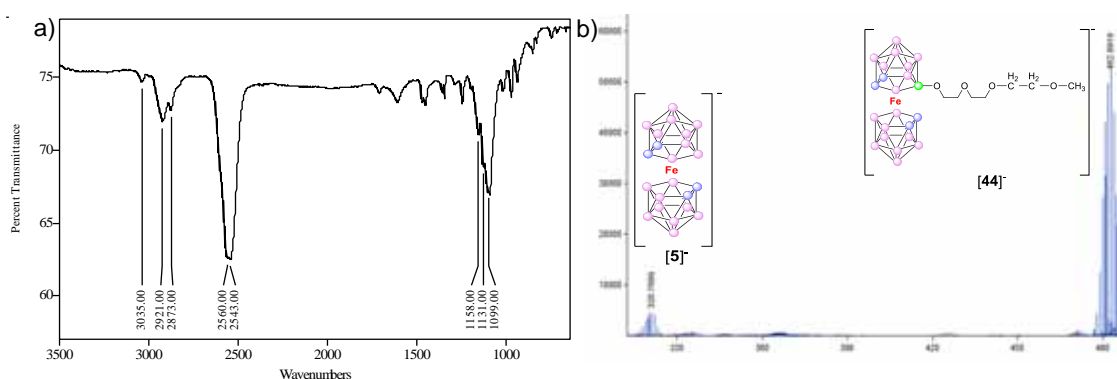
Regarding the assignment of the C-H peaks, as indicated in Figure 19b, one can distinguish 2 signals for the ¹H-NMR spectrum, the broad ones at about +70 and +45 ppm that present no interaction with any of the boron peaks. We assign these signals to the H atoms bonded to C_c within the [3,3'-Fe(C₂B₉H₁₁)₂] molecule. On the other hand, the sharp proton peak in between these 2 signals (at approximately +50 ppm) interacts only with the peak previously assigned as B(6). In conclusion, this C_c-B(6)-C_c face acts in a very peculiar way, and so far we are not able to explain the shift to low field values of the H atom bonded to B(6) with respect to all the other H atoms, as illustrated in ¹H-¹¹B HETEROCOSY NMR (Figure 19b).

Figure 20. a) FTIR and b) MALDI-TOF-MS confirming the synthesis of compound [39]

2.2.3. Characterization of [3,3'-Fe(8-(OCH₂CH₂)₂X-(1,2-C₂B₉H₁₀)(1',2'-C₂B₉H₁₁)]⁻ (where X = RO⁻, X⁻ and SH⁻)

These ferrabis(dicarbollide) derivatives [36]⁻ - [44]⁻ containing various ending groups were characterized employing spectroscopic and spectrometric techniques such as FTIR, MALDI-TOF-MS, ¹H, ⁷Li and ¹¹B-NMR analysis techniques, and, in some cases, cyclic voltammetry, based on our experience for the characterization of the paramagnetic species.

FTIR spectroscopy for compounds [36]⁻ - [39]⁻ helps confirming the obtaining of the desired species. The absorption band at 3035 cm⁻¹ corresponds to the existence of C_c-H bonds within the molecule, whereas the ones belonging to OCH₂- groups from the polyetheric chain are visible from 1472 to 1092 cm⁻¹. In addition, the peaks in the range of 2560-2543 cm⁻¹ are a clear indicator of the presence of B-H bonds (Figure 20a).



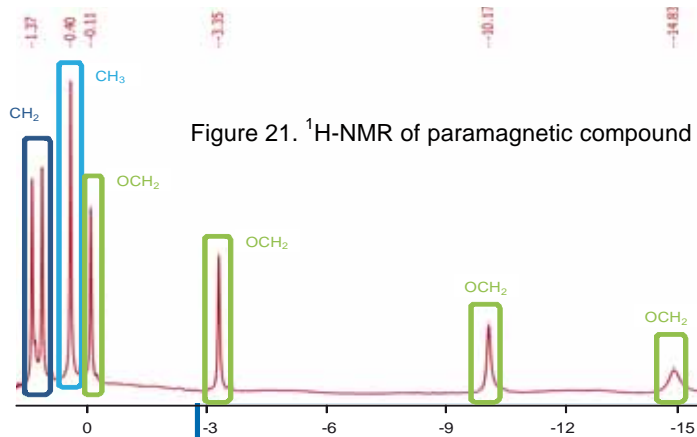
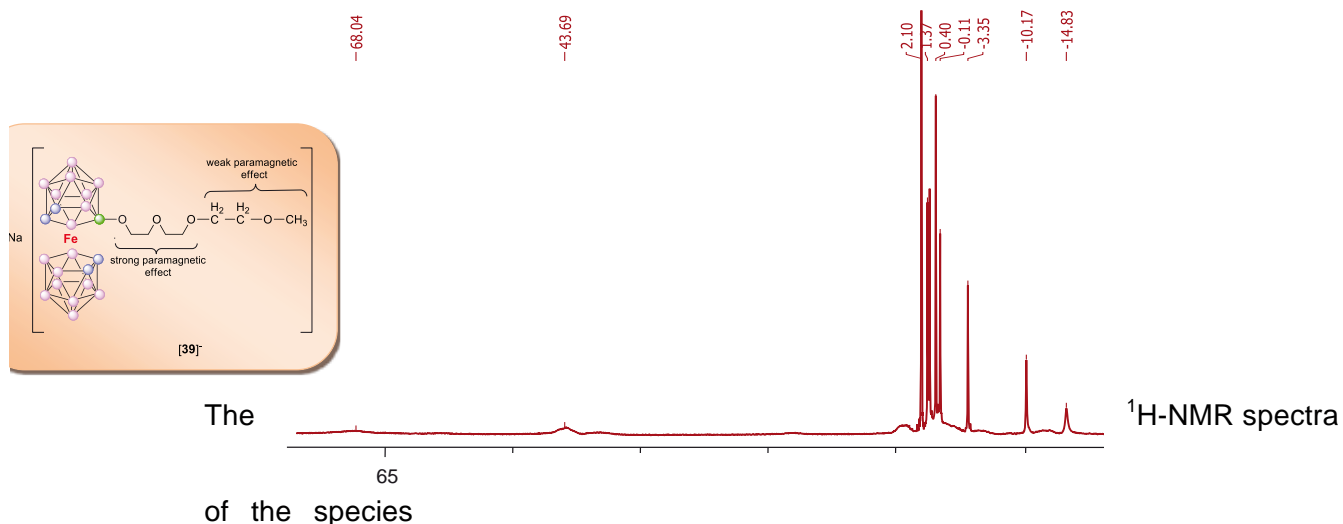


Figure 21. $^1\text{H-NMR}$ of paramagnetic compound [39]

2.2. Ring-opening reactions of 1,4-dioxane

derivative of ferrabis(dicarbollide) with various groups confirms our structure is MALDI-TOF-MS the molecular peak that appears 482.8 m/z. The small peak showing at 320.78 m/z is actually corresponding to the ferrabis(dicarbollide) molecule itself.



The $^1\text{H-NMR}$ spectra

of the species

described in this section of the doctoral thesis exhibit considerable paramagnetic shifting of all signals, most pronounced being the broad signal of $\text{C}_c\text{-H}$ protons found in the range of 68 and 43 ppm. No apparent $^1\text{H-}^1\text{H}$ coupling can be seen (Figure 21). Another interesting observation is the influence of the closeness of the $\text{OCH}_2\text{-}$ groups

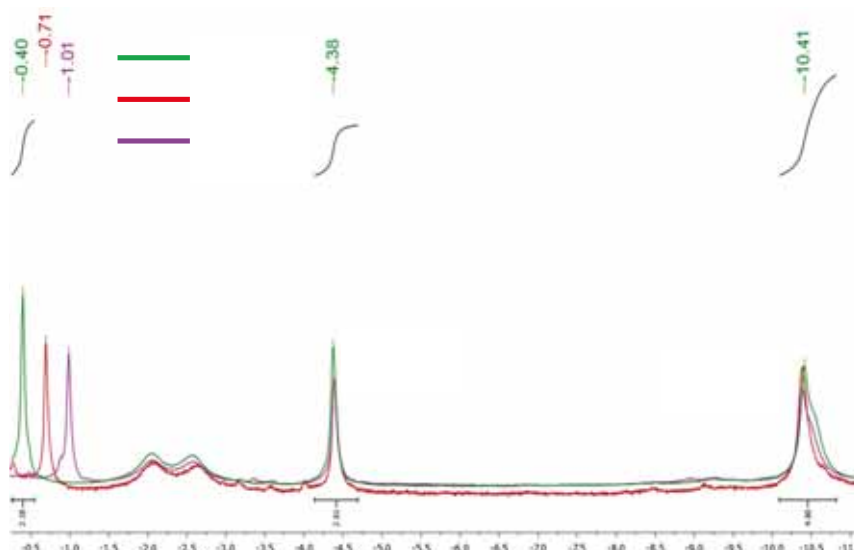
Figure 22. Comparison between $^1\text{H-NMR}$ spectra of compounds [41]⁻ - [43]⁻

Results and discussions

2.2. Ring-opening reactions of 1,4-dioxane derivative of ferrabis(dicarbollide) with various groups

to the Fe (III) centre: the closer situated, the more shifted to higher field values, as indicated in the $^1\text{H-NMR}$ of the paramagnetic species [39]⁻ in Figure 21. The CH_2 - and CH_3 - groups situated far from the metal centre are less altered by the paramagnetic effect and more or less appear at normal chemical shifts (1.37 and 0.4 ppm respectively).

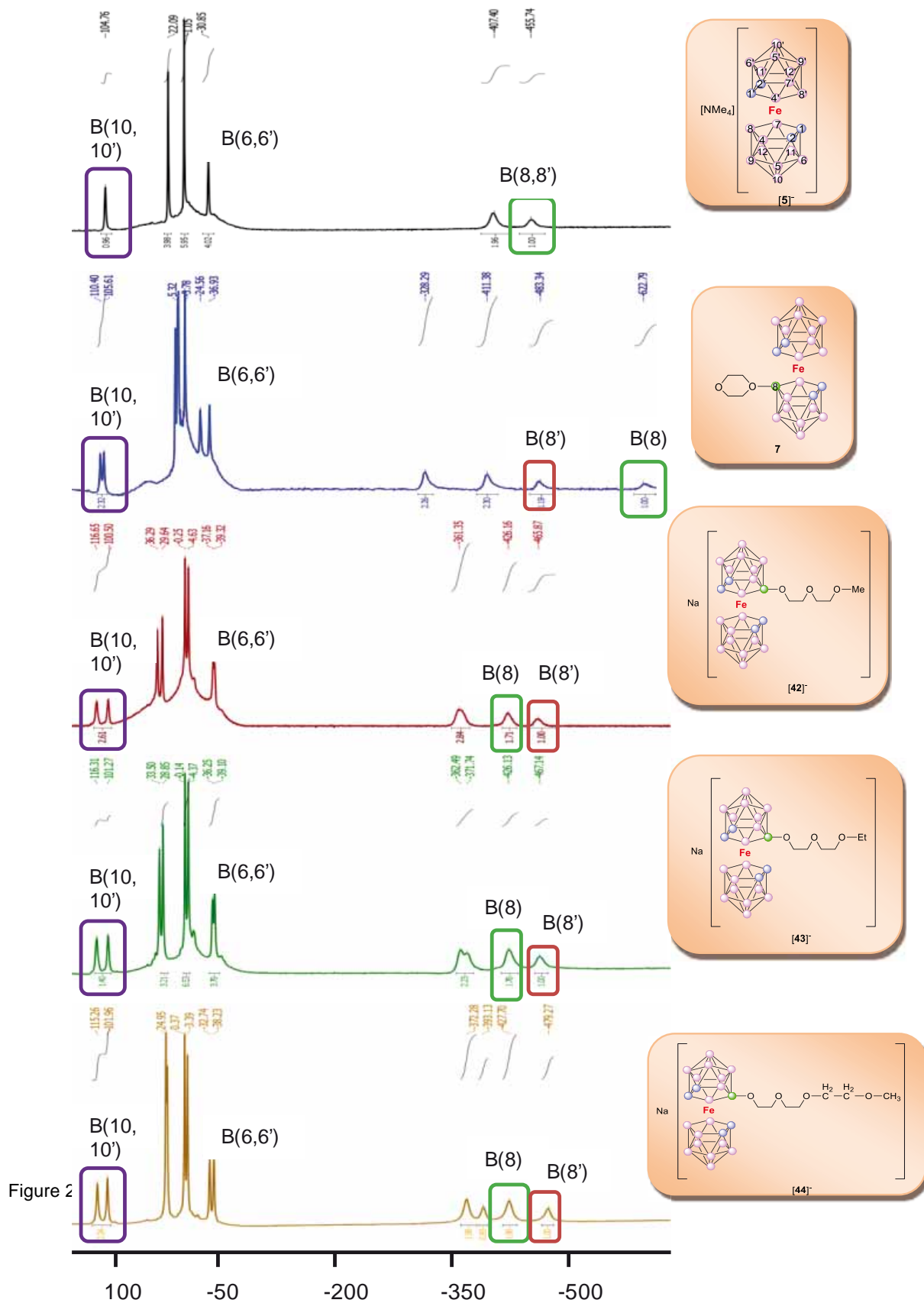
As indicated in Figure 22, the $^1\text{H-NMR}$ spectra of species [41]⁻ - [43]⁻ are compared, in order to draw the attention on the influence of the halogen group on the shift of the protons in its immediate proximity. Basically, as the electronegativity of the halogen substituent increases, the CH_2 - group bonded directly to it shifts to upfield values. However, no such influence can be seen in the case of the OCH_2 - groups within the molecule.



Noteworthy is the extreme upfield shift of the B(8) resonance in the starting zwitterionic species with respect to the anionic parent [5]⁻ and compounds [37]⁻ - [39]⁻. One possible explanation could be the fact that in the case of the closed-ring system presented by the neutral species, **7**, the negative charge is localized over the metallocarborane only, whereas once the dioxane ring is open, the charge is localized over the entire molecule, leaving the boron atoms “more deshielded” and therefore the shift to lower field values exhibited by the ferrabis(dicarbollide) derivatives, [37]⁻ - [39]⁻.

Results and discussions

2.2. Ring-opening reactions of 1,4-dioxane derivative of ferrabis(dicarbollide) with various groups



Results and discussions

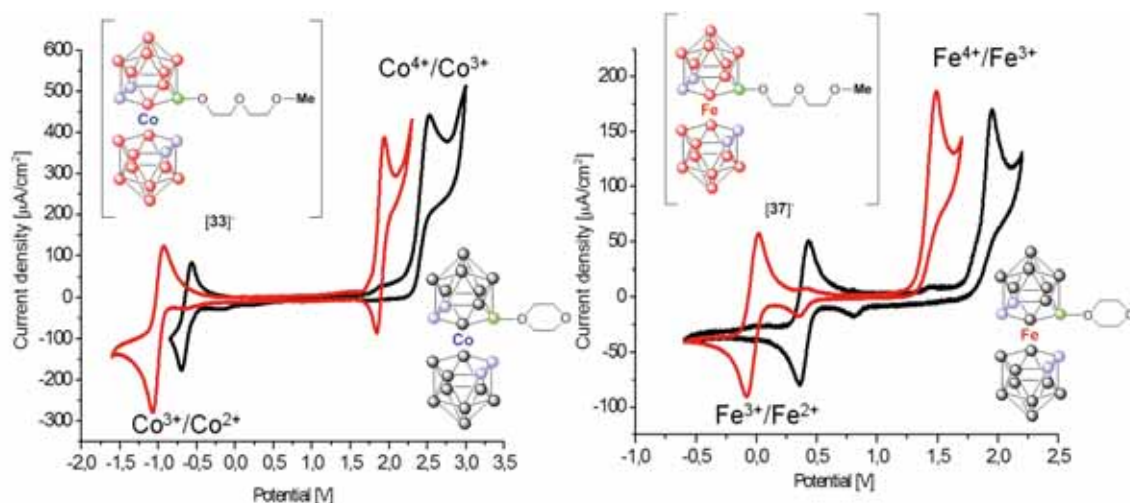
2.2. Ring-opening reactions of 1,4-dioxane derivative of ferrabis(dicarbollide) with various groups

Additionally, cyclic voltammetry was explored to be used in a qualitative manner. This can be done since all cobaltabis(dicarbollide) and ferrabis(dicarbollide) derivatives are electroactive species and also because their oxidation/reduction potentials are sufficiently separated to make a clear distinction.

Cyclic voltammetry was used for the first time in order to determine the type of metallacarborane present, as well as to differentiate between a closed 1,4-dioxanate ring system and an open chain.

Figure 24. Cyclic Voltammetry of parent compounds **6** and **7** and the corresponding alkoxides

By running this cyclic voltammetry analysis, we firstly wanted to determine if the metal reduction from M(III) to M(II) was dependent on the compounds nature, namely if it was zwitterionic or anionic species. Secondly, we were looking to find the $E_{1/2}$ different reduction values, depending on the metal, Co or Fe. And lastly, once we had determined the $E_{1/2}$ values of the corresponding species, the following step was to see if one could use this cyclic voltammetry technique as a quantitative method.



From Figure 24 one can observe that the potentials of open-ring systems for cobaltabis(dicarbollide) and ferrabis(dicarbollide) derivatives differ by about 1 Volt. In this way, one can determine without any doubt which one of the two metallacarborane, neutral or anionic, is present in an unknown sample.

Table 3 shows the half wave potentials ($E_{1/2}$) of neutral and anionic compounds. The electrochemical cell contained glassy carbon electrode as working electrode, a reference $Ag/AgCl/KCl_{sat}$ electrode and platinum wire as auxiliary electrode. All experiments were performed at room temperature using $[NBu_4]Cl$ 0.1 M acetonitrile solution. The solutions were deoxygenated with analytical grade nitrogen at the start of each experiment to prevent oxygen interference. All the potential values were referred to the Fc^+/Fc couple [$E_{1/2}(Fc^+/Fc) = 0$ V].

Results and discussions

2.2. Ring-opening reactions of 1,4-dioxane derivative of ferrabis(dicarbollide) with various groups

Compound	$E_{1/2}(M^{3+}/M^{2+})$ (V)	$E_{1/2}(M^{4+}/M^{3+})$ (V)	Metal
6	-1.288	1.773	Co
[33]⁻	-1.759	1.131	Co
7	-0.369	1.141	Fe
[37]⁻	-0.792	0.678	Fe

Table 3. Half wave potentials of compounds **6**, **[33]⁻**, **7**, **[37]⁻** with respect to a Ag/AgCl electrode

The immediate conclusion that could be drawn from Table 3 is that the presence of the oxonium cation close to the metallic centre (for compounds **6** and **7**), shifts with about 0.5 Volts the potential to more anodic values (compounds are easier reduced). This affirmation is in agreement with Coulomb's law on similar chemical surroundings, which states that it is always easier to reduce a neutral species than a similar one bearing a negative charge as it is the case of our compounds for M^{3+}/M^{2+} .

To sum up, the results presented so far embody a synthetic strategy based on ring-opening reactions of **7** which may be seen as a multi-purpose tool, since it opens new routes to a variety of more sophisticated products than just compounds **[36]⁻**-**[44]⁻**. Moreover, this exceptionally clean reaction could be used to generate novel iron-containing compounds otherwise unavailable by other conventional methods.

2.3 Toward the Synthesis of High Boron Content Polyanionic Multicluster Macromolecules

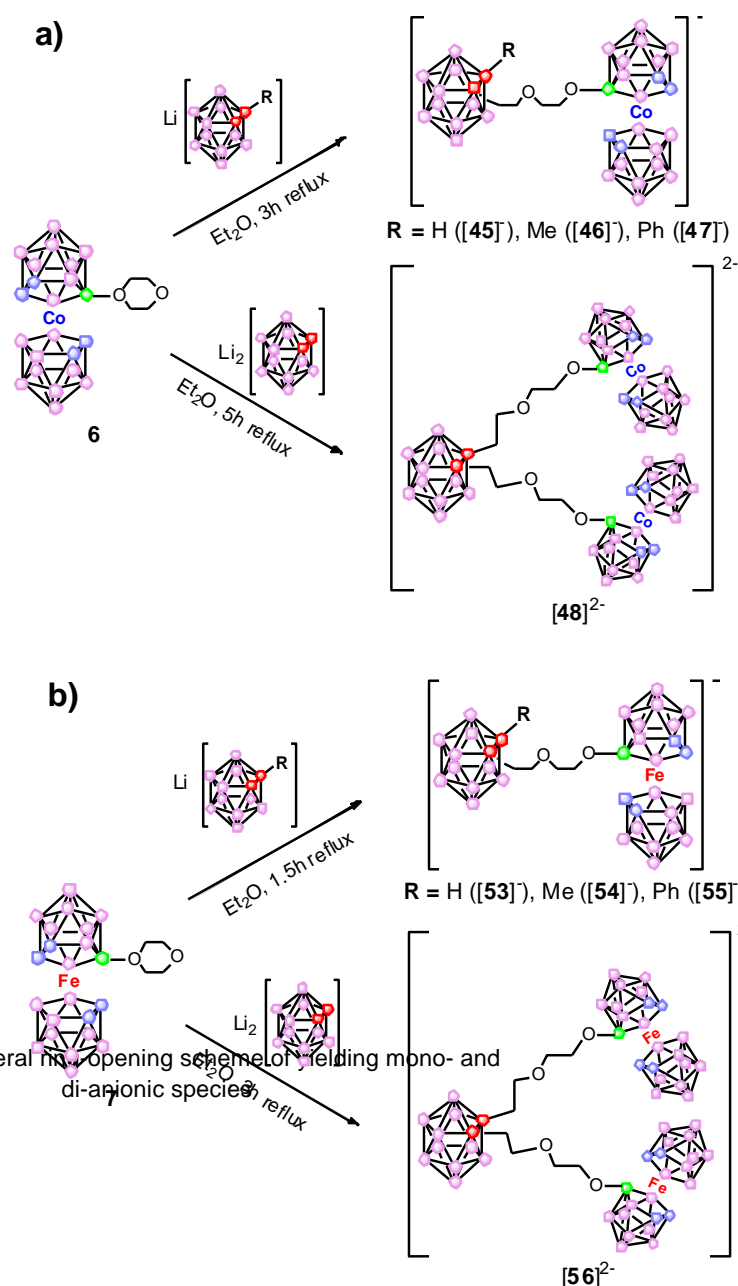
The synthetic strategy based on the attack of oxonium derivatives of borane¹⁹² and metallacarborane^{25a,26,187a,193} anions in the presence of nucleophilic agents was first reported in 1976.^{187c,194} The discovery of the nucleophilic ring-opening reaction in boranes¹⁹² and metallacarboranes^{26,187a,193} has been one of the most important features in boron chemistry over the past several years. A review on this field has been published recently, summarizing some of the nucleophiles that have been used so far.²⁹ The derivatization of boranes and metallacarboranes may open the way for new possible applications of these anions.

The use of a variety of ring-opening nucleophiles on [3,3'-Co(8-(OCH₂CH₂)₂-1,2-C₂B₉H₁₀)(1',2'-C₂B₉H₁₁)], **6**, has led to the synthesis of compounds of promising practical uses in various fields, including solid electrolytes, strong nonoxidizing acids,³⁰ weakly coordinating anions,¹⁹⁵ ionic crystals⁴² and enzyme inhibitors.⁴⁸

Sivaev *et al.*¹⁹⁶ demonstrated that the tetrahydrofuran (THF) ring in the [B₁₂H₁₁ 3THF]⁻ anion can be opened by all three isomers (1,2-, 1,7- and 1,12-) of Li[C₂B₁₀H₁₁]. Additionally, in a preliminary communication,¹⁹⁷ our group briefly outlined the synthesis and isolation of mono- and di-anion species combining the [3,3'-Co(1,2-C₂B₉H₁₁)₂]⁻ and [C₂B₁₀H₁₂] structural motifs.

In this doctoral thesis, this viable concept of multicage boron chemistry was extended by giving full experimental details and complete structural data. Moreover, the deboronation of the *closo*-carborane moieties followed by their complexation allowed the preparation of a novel type of polyanionic water-soluble high boron content macromolecules that could be good candidates for increasing BNCT techniques' efficiency.

This chapter has been divided in three different parts; the first one corresponds to the study of the ring-opening reaction of [3,3'-M(8-(OCH₂CH₂)₂-(1,2-C₂B₉H₁₀)(1',2'-C₂B₉H₁₁)] (M = Co (**6**), Fe (**7**)) by the *ortho*-carboranyl (**1**) and its monosubstituted derivatives, the 1-Me- (**2**) and 1-Ph-carboranyl (**3**) as nucleophilic agents, giving rise to what will be generally called *closo* compounds. In the second part, partial degradation reactions of the previously synthesized clusters were conducted, leading to the corresponding *nido* derivatives. The third part is centred on the complexation reactions of these *nido* species, yielding polyanionic sandwich-type complexes. The corresponding characterization techniques for each type of syntheses are also reported in this section.

2.3.1. Syntheses of *closo* derivatives via *exo*-cluster substitution reactions

Scheme 11. General nucleophilic opening scheme of yielding mono- and di-anionic species.

Following our studies on cobaltabis(dicarbollide) direct substitution¹⁹⁷ to obtain novel high boron content polyanionic species with enhanced water solubility, we have explored the possibility of using lithiated boron clusters as nucleophiles to produce a new family of high boron content polyanionic macromolecules.¹⁹⁸ This has been, in part, stimulated by the high water solubility of the cobaltabis(dicarbollide) salts of potassium, sodium, or lithium.¹⁹⁹ With these two points in mind, we studied the nucleophilic behaviour of the lithiated salt of 1,2-*closo*-carborane and its Me and Ph derivatives toward [3,3'-M(8-(OCH₂CH₂)₂)-(1,2-C₂B₉H₁₀)(1',2'-C₂B₉H₁₁)] (M = Co, Fe).

In the case of *ortho*-carborane, the C_c-H bond is highly polarised due to a significant difference in electronegativity between the two atoms, 2.55 and 2.20 respectively. This is why the hydrogen atoms from C_c-H can be easily extracted by a strong base such as *n*-butyllithium.

The strong electronwithdrawing character of the *ortho*-carborane unit favours this type of metallation reactions, where lithium atoms replace the protons bonded to the C_{cluster} yielding the corresponding *ortho*-carborane salts.²⁰⁰ In this case, the metallation

reactions carried out yielded monolithiated salts for compounds **1** and **2** and dilithiated species for **3**, by the addition of one or two equivalents of *n*-BuLi respectively.

All reactions were carried out using standard vacuum and inert-atmosphere techniques, although some operations, such as column chromatography, were carried out in air.

The next step was the nucleophilic attack of the C_c (which is considered a carbanion) on the dioxane ring of compounds **6** and **7**, producing their opening. As shown in Scheme 11a the synthesis of compounds [45]⁻ - [48]²⁻ as well as the ones of their iron-based were carried out.

The synthetic procedure for the obtaining of iron-based homologues species [53]⁻ - [56]²⁻ (Scheme 11b) compounds is very similar with the one used for the obtaining of the cobalt-containing species, with the only difference that the reflux time is reduced from 3 hours to 1 hour and 30 minutes in the case of the monoanionic species, and from 5 to 3 hours for the dianionic compound respectively, indicating that the iron zwitterionic species is more reactive than its cobalt-based analogous.

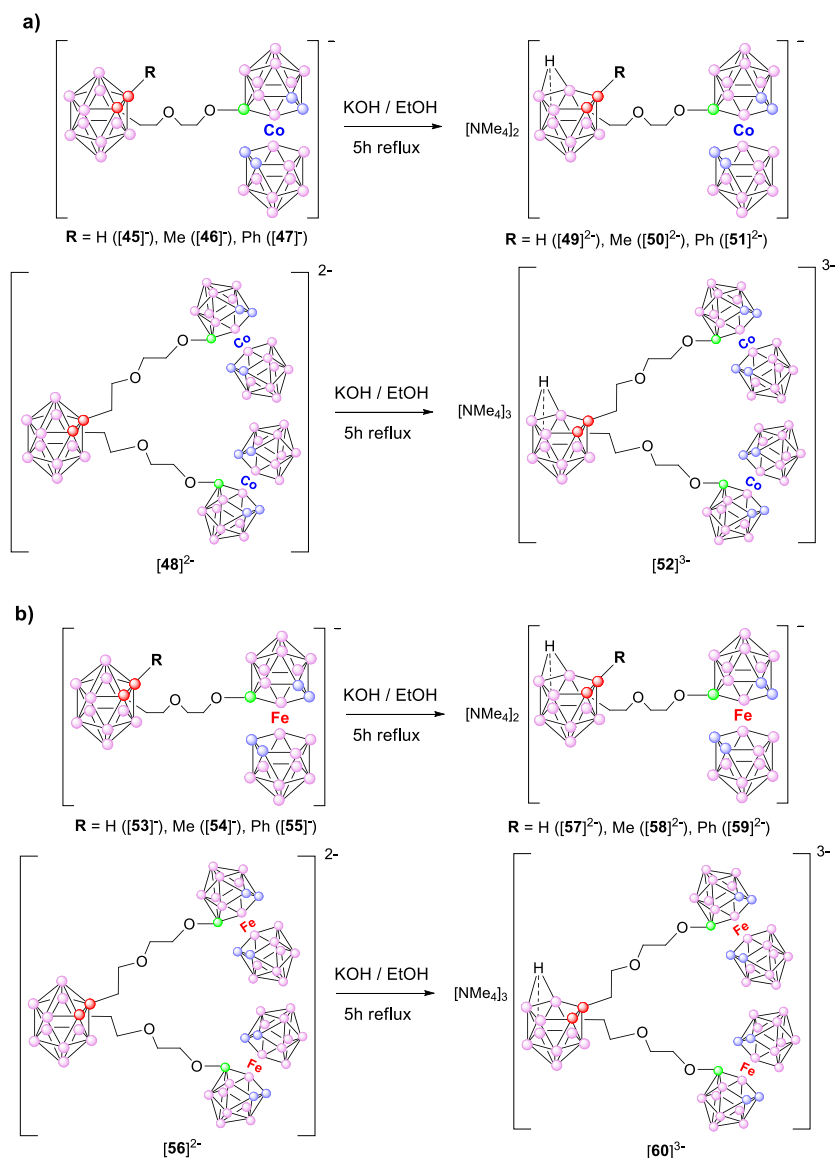
The purification of the above presented compounds was performed by TLC, using silica gel as stationary phase and a mixture 1:1 of dichloromethane:hexane as elutant; in this way, the unreacted zwitterionic starting material elutates, leaving the desired anionic compound on the base line.

2.3.2. Synthesis of *nido* compounds *via* a partial deboronation reaction of *closo* species

The *closo* carborane clusters are structures showing high stability with respect to strong acids but instead they react with Lewis bases (nucleophilic agents) yielding more opened structures, known as *nido*, by a partial deboronation process that implies the loss of a vertex.

In this subchapter the partial degradation reactions for the *closo* compounds [45]⁻ - [48]²⁻ (Scheme 12a) and [53]⁻ - [56]²⁻ (Scheme 12b) previously obtained were performed, using potassium etoxide as nucleophilic agent at reflux. The nucleophilic attack takes place at the boron atoms directly bounded to both carbon atoms, the B(3) or its equivalent, B(6), since they both present electronic deficiency. With this reaction a boron vertex (B⁺) is formally eliminated. The species obtained after refluxing the reaction mixture for 5 hours are dianionic ([49]²⁻ - [51]²⁻ and [57]²⁻ - [59]²⁻) and trianionic ([52]³⁻ and [60]³⁻).

Results and discussions



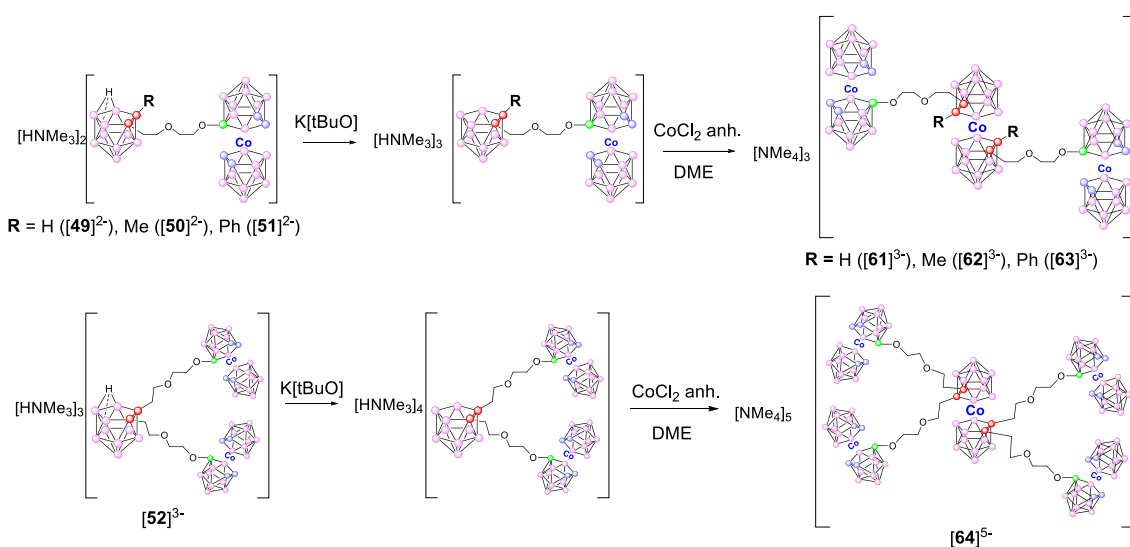
2.3.3. Synthesis of polyanionic multicluster cobaltabis(dicarbollide) sandwich-type complexes

As previously explained in the Introduction part, the *nido* species [7,8-C₂B₉H₁₂]⁻ possess a bridged H over the C₂B₃ open face of the dicarbollide unit. This bridged hydrogen is acidic enough as to be extracted by a strong base, such as *n*-buthyllithium, potassium *tert*-butoxide or sodium hydride, to give the dicarbollide species of [7,8-*nido*-C₂B₉H₁₁]²⁻. The absence of this bridged hydrogen determines an open pentagonal C₂B₃ face, favouring η⁵-coordination to a metal. Ligands [49]²⁻ - [52]³⁻ contain one *nido* cluster within their molecule and therefore can form complexes with η⁵ metals. In this way, once the *nido* species are formed, 2 potassium *tert*-butoxide equivalents are added to extract both the bridged hydrogen and the proton from the trimethylammonium cation, yielding the corresponding dicarbollide ligands as showed in Scheme 13. The following

step is the reaction of the dicarbollide unit with anhydrous CoCl_2 , yielding Co(III) sandwich-like coordination complex $[\mathbf{61}]^{3-}$ - $[\mathbf{63}]^{3-}$ and $[\mathbf{64}]^{5-}$, where the metal coordinates two ligand units due to disproportionation of the Co(II) to Co(0) and Co(III) . From this reaction, the lithium salts of the corresponding metallocarboranes were obtained; therefore, a metathesis reaction with $[\text{NMe}_4]\text{Cl}$ in aqueous medium is performed, resulting in the complexes precipitation as orange solids, with yields higher than 65%.

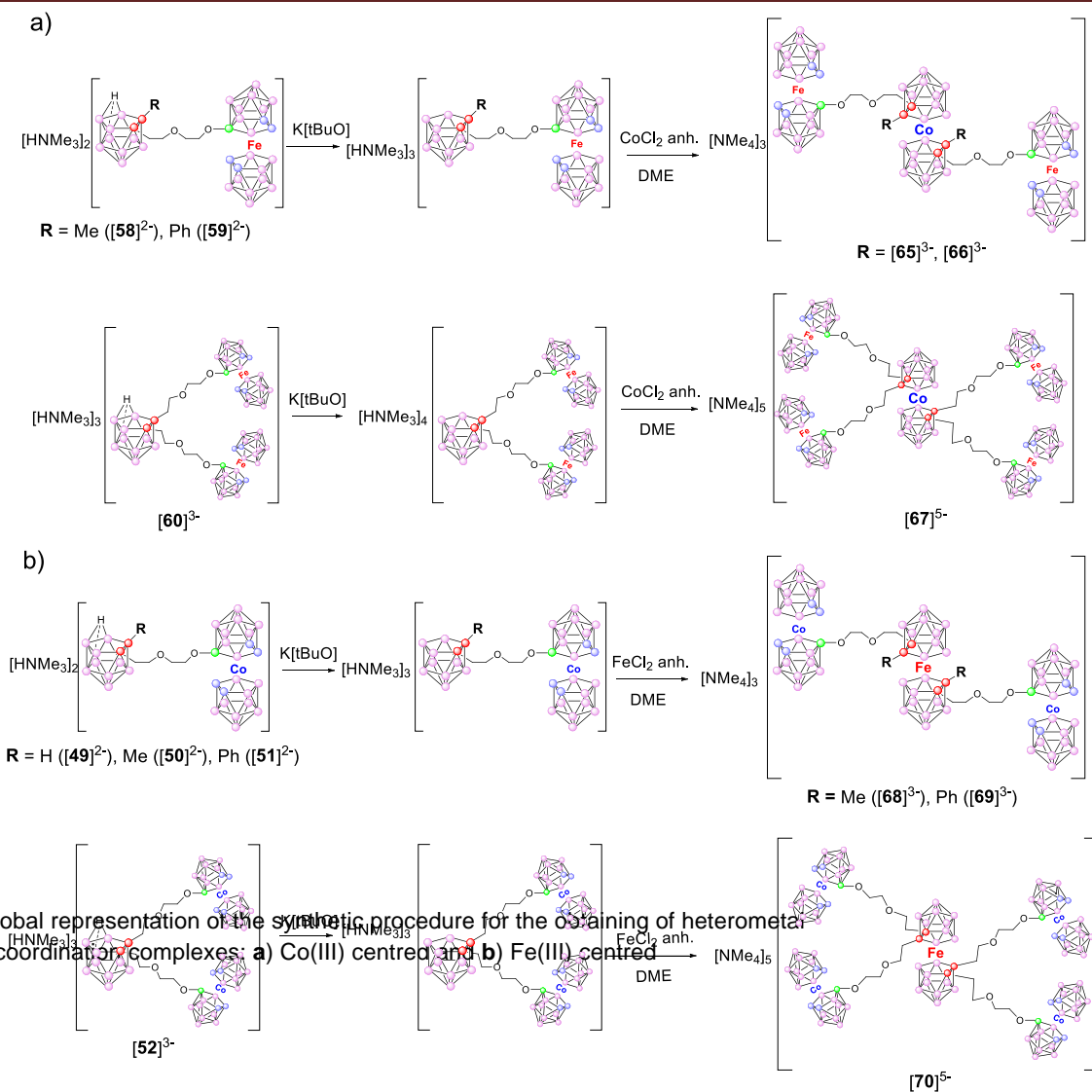
These organometallic sandwich-type complexes, due to their elevated boron-content and the fact that they are polyanionic compounds, and therefore water soluble, are promising candidates as drugs in BNCT, especially of tumor cells.

Scheme 13. Syntheses of cobaltabis(dicarbollide) sandwich-type complexes



2.3.4. Synthesis of polyanionic multicluster heterometal(III)-based sandwich-type complexes

Following the same synthetic procedure previously described in Subchapter 2.3.3, we obtained coordination complexes containing both Co and Fe within their molecule, as shown in Scheme 14. The procedure is similar to the one described for the synthesis of homo cobalt-centred coordination complexes. In the first step, the hydrogen bridge of the *nido* species is extracted with a strong base, potassium *tert*-butoxide, followed by the addition of this reaction mixture over anhydrous CoCl_2 or FeCl_2 in DME. After reflux, the complex is extracted with ether and purified by thin layer chromatography.



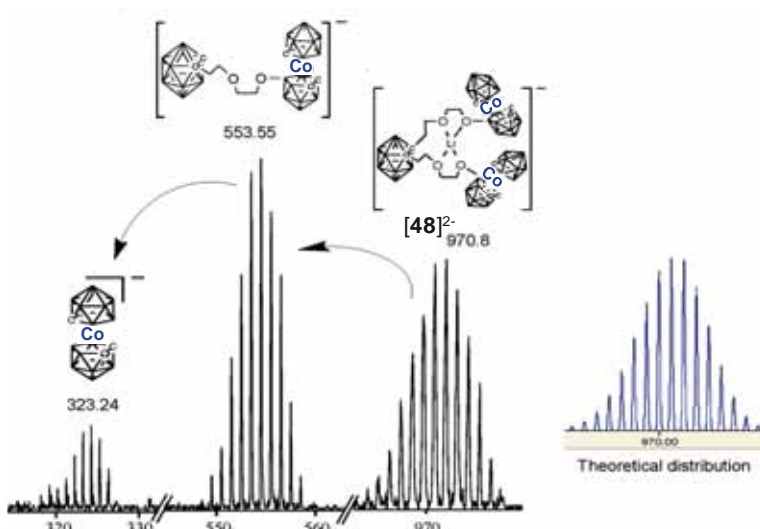
Scheme 14. Global representation of the synthetic procedure for the obtaining of heterometal coordination complexes: **a)** Co(III) centred and **b)** Fe(III) centred

By complexation with anhydrous CoCl_2 or FeCl_2 , the corresponding coordination complexes, showing both cobalt and iron within their molecule were synthesized. The only difference with respect to the previous homo cobalt-centred complexes, is that after refluxing the reaction mixture over several days (from 1 to 3, depending on the bulkiness of the substituents), the mixture was left under air, so that the Fe(II) species formed to be oxidized to the desired Fe(III)-centred complexes.

2.3.5. Characterization of *closo* derivatives

The FTIR analysis of the mono- and dianionic *closo* species presented above confirms their synthesis. The broad absorption band at about 2560 cm^{-1} supports the existence of B-H, while also sustaining a *closo* structure for our compounds.

Compound	$\nu(\text{C-H})$	$\nu(\text{C-H})_{\text{alkyl}}$	$\nu(\text{B-H})$	$\nu(\delta(\text{CH}_2))$	$\nu(\text{C-O-C})$
[45] ⁻	3057	2955, 2920, 2871	2556, 2539	1481	1131, 1096
[46] ⁻	3041	2934, 2880	2569	1448, 1531	1251, 1214, 1157, 1088
[47] ⁻	3043	2929, 2873, 2838	2564	1447	1244, 1155, 1096
[48] ²⁻	3058	2932, 2882, 2833	2566	1471, 1452	1158, 1081
[53] ⁻	3036	2957, 2922, 2872	2545	1448, 1367	1124, 1090
[54] ⁻	3054	2975, 2921, 2873	2562	1463, 1369, 1322	1116
[55] ⁻	3045	2953, 2920, 2872	2552	1417, 1363	1151, 1087
[56] ²⁻	3036	2957, 2925, 2866	2552	1483, 1417	1158, 1128, 1092

Table 4. FTIR spectroscopy for compounds [11]⁻ - [48]²⁻ and [53]⁻ - [56]²⁻

Another method used for the characterization of these newly synthesized high boron content anionic compounds was matrix-assisted laser desorption/ionization (MALDI)²⁰¹ spectrometry. The MALDI-TOF-MS (TOF = time of flight) spectrum of compound [48]²⁻ is taken as a representative example of the divalent

closo family of ions, with the properly isotopic distribution showing a peak at 970.80, which corresponds to $[\text{M} + \text{Li}^+]$ and the fragmentation peaks at 553.55 and 323.24, respectively (Figure 25). As shown in this figure, the experimental isotopic pattern was in good agreement with the calculated isotopic plot (Molecular Weight Calculator for Windows 9x/NT/00/ ME/XP, version 6.83). In agreement with MALDI-TOF-MS spectra, the polyanionic species [48]²⁻ appears as a monovalent compound, by adding a lithium cation, coordinated by the oxygen atoms present in the molecule.

Figure 26 shows the MALDI-TOF-MS spectrum of compound [54]⁻ in which one can clearly see the signals of the starting material **7** but the peak dominating the spectrum is the one belonging to the sought monoanionic compound.

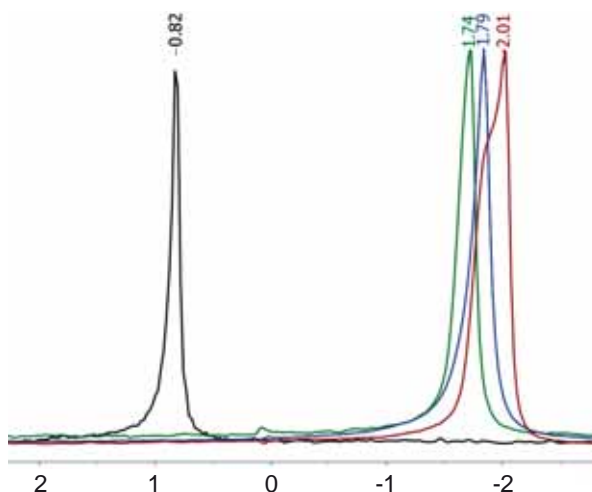
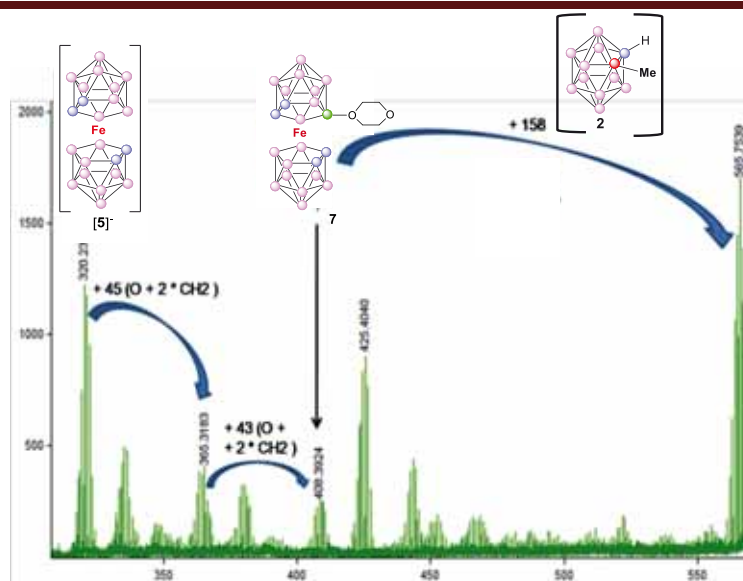
To prove the presence of the lithium cation within our molecules, ⁷Li-NMR

spectrum was performed on both monoanionic compounds [46]⁻ and [47]⁻ and dianionic compound, [48]²⁻. Since these species are not water soluble, the standard reference for

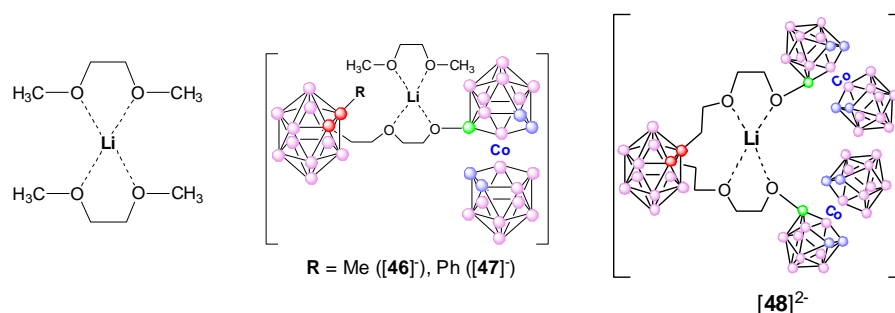
⁷Li-NMR, namely 1M LiCl aqueous solution, could not be used. A 1M LiCl in DME (Figure 27 black) was prepared and used as reference for this type of analysis, the other compounds being prepared using the same solvent.

Another reason for running ⁷Li-NMR was to determine if the presence of different surroundings of the lithium cation would end in inducing different chemical shifts (results illustrated in Figure 27).

As it has previously been reported by our group, anionic clusters containing electron-rich *exo*-cluster substituents (S or P) dissipate electron density into the electron-rich element.^{33,202} This element becomes a strong Lewis base and a very good coordinating ligand.^{33,34,203} Most probably the oxygen atom in the B(8)-O bond in compounds [46]⁻ - [48]²⁻ can play the same role as S and P atoms, dissipating the negative charge and becoming a strong Lewis base. Thus, the anionic species can coordinate to a Lewis acid (Li⁺) through the oxygen atom at the B(8) position. The anionic charge of the metallocarborane cluster dissipates through the oxygen atom bonded to B(8); moreover, the existence of a second oxygen atom deeply favors the interaction with a lithium cation, forming an O·····Li·····O interaction (Figure 28).



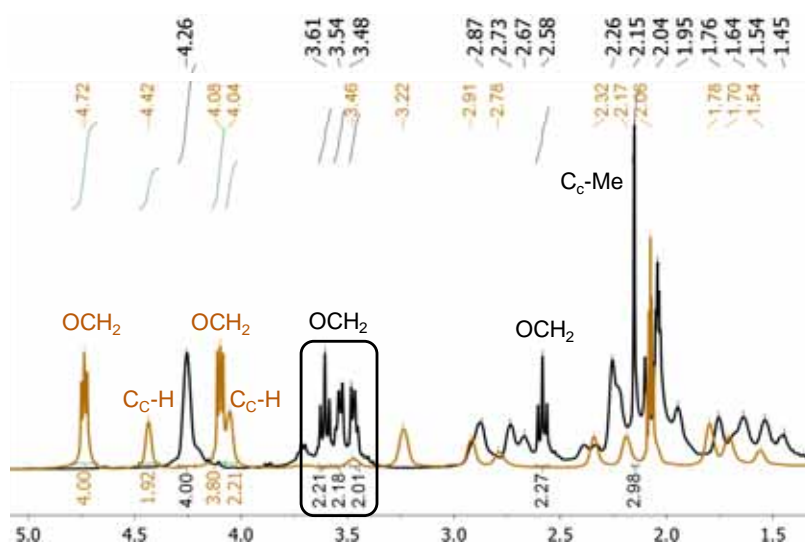
Results and discussions



This is perfectly supported by the ⁷Li-NMR spectra shown in Figure 27, in which the Li cation coordinated to compounds [46]⁻ - [48]²⁻ appears, as expected at higher field values with respect to the reference. These data are corroborated by the previously presented MALDI-TOF-MS in Figure 25, clearly indicating the presence of coordinated lithium to oxygen in the case of compound [48]²⁻ that produces a global monovalent species.

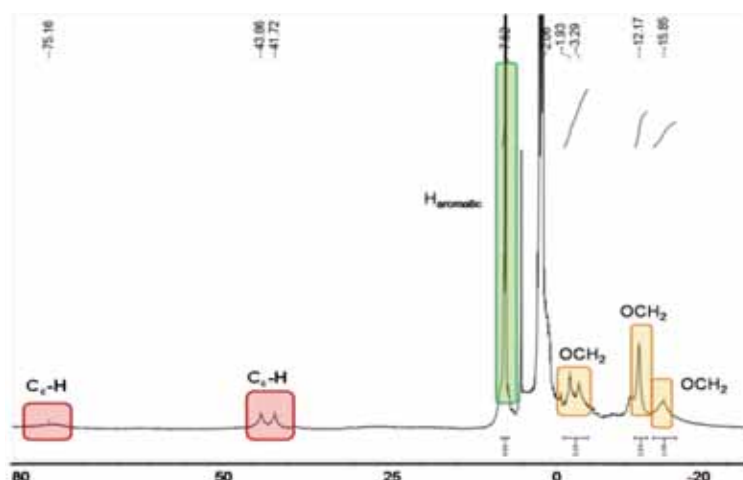
Figure 29 displays the ¹H{¹¹B}-NMR spectra of the starting neutral compound **6** and anionic compound [46]⁻. As presented in this figure, in the case of the starting compound, **6**, the C_c-H of each dicarbollide unit appear as two separated peaks, at 4.4 and 4.03 ppm while in the case of compound [46]⁻, the C_c-H appears as a singlet.

The same effect is observed in the case of the OCH₂- groups from the polyetheric chain: the ones from **6** are present at lower field values (4.7 and 4.06 ppm) than the ones corresponding to the anionic species [46]⁻ (3.61, 3.52, 3.48 and 2.58 ppm). Another observation is that the OCH₂- groups from **6** appear as two triplets, each integrating 4, due to the symmetry in the 1,4-dioxane ring.



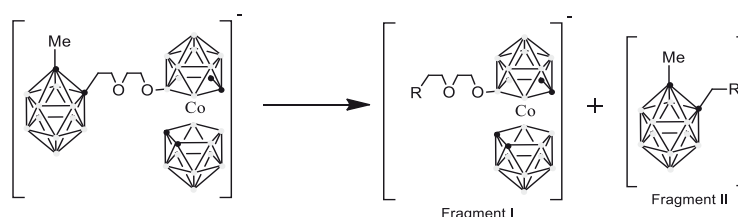
Furthermore, the signals of the BOCH₂⁻, -CH₂OCH₂⁻, and -CH₂-carborane units of the interconnecting 1,4-dioxane chain appear within the range $\delta \approx 2.89$ -1.45 ppm.

^1H -NMR spectrum of compound [55] (Figure 30) shows that the H signals are altered by the paramagnetic character of Fe, since the CH_2 - groups appear in the range 0 - -12 ppm.



Regarding the $^{11}\text{B}\{^1\text{H}\}$ -NMR, we observed²⁰⁴ that the spectrum of the monosubstituted derivatives of $[3,3'\text{-Co}(1,2\text{-C}_2\text{B}_9\text{H}_{11})_2]^-$ is the result of plain addition of the spectra of the two individual halves. In a similar manner, Figure 31 shows how the $^{11}\text{B}\{^1\text{H}\}$ -NMR spectrum of [46]⁻ can be analyzed as two fragments. The spectrum of fragment I is approximated by that of the anion and the one of fragment II by the spectrum of 1- CH_3 -1,2-*closo*- $\text{C}_2\text{B}_{10}\text{H}_{11}$ or more precisely by the one of the model compound 1- CH_3 -2- $\text{CH}_3\text{OCH}_2\text{CH}_2$ -1,2-*closo*- $\text{C}_2\text{B}_{10}\text{H}_{10}$, that was synthesized for this purpose only.

In order to understand the spectrum and assign the peaks corresponding to each fragment, we have used the DM2008 program.²⁰⁵ The latter has been used almost exclusively for modelling solid-state NMR spectra of noncluster compounds. We used this program for the first time on the computational disarticulation of the $^{11}\text{B}\{^1\text{H}\}$ -NMR spectra in solution to analyze the multicenter compounds isolated.



These species contain either 28 or 46 boron atoms of different degrees of symmetry. Table 5 and Figure 32a exemplify the disarticulation of the ^{11}B -NMR spectrum of the methylated anion [46]⁻, for which it is possible to find 14 different Gaussian-type curves fitting experimental spectra. Figure 32b represents the typical 1:1:1:1:2:2:(2+2):2:2:1:1 $^{11}\text{B}\{^1\text{H}\}$ -NMR spectrum of a fragment I $[3,3'\text{-Co}(8\text{-(OCH}_2\text{CH}_2)_2\text{-(1,2-C}_2\text{B}_9\text{H}_{10})(1',2'\text{-C}_2\text{B}_9\text{H}_{11})]^-$ anion with a C_s symmetry (12 different signals, two overlapped). This leaves

Results and discussions

As seen in Figure 32c, the theoretical spectrum of 1-CH₃-2-CH₃OCH₂CH₂-1,2-*c/oso*-C₂B₁₀H₁₀ is in excellent agreement with its experimental data with 1:1:2:2:4 resonances at -4.28, -5.82, -9.25, -9.90 and -10.54 (see Figure 32d).

About the paramagnetic Fe(III) species, from the superposition of the ¹¹B{¹H}-NMR spectra of the starting *o*-carborane **1** and the *c/oso* Fe(III) compound [**56**]²⁻ one can point exactly the signals corresponding to the paramagnetic iron-based moiety and the fragment of the molecule represented by *o*-carborane, which appears between 5 and -20 ppm, as shown in Figure 33.

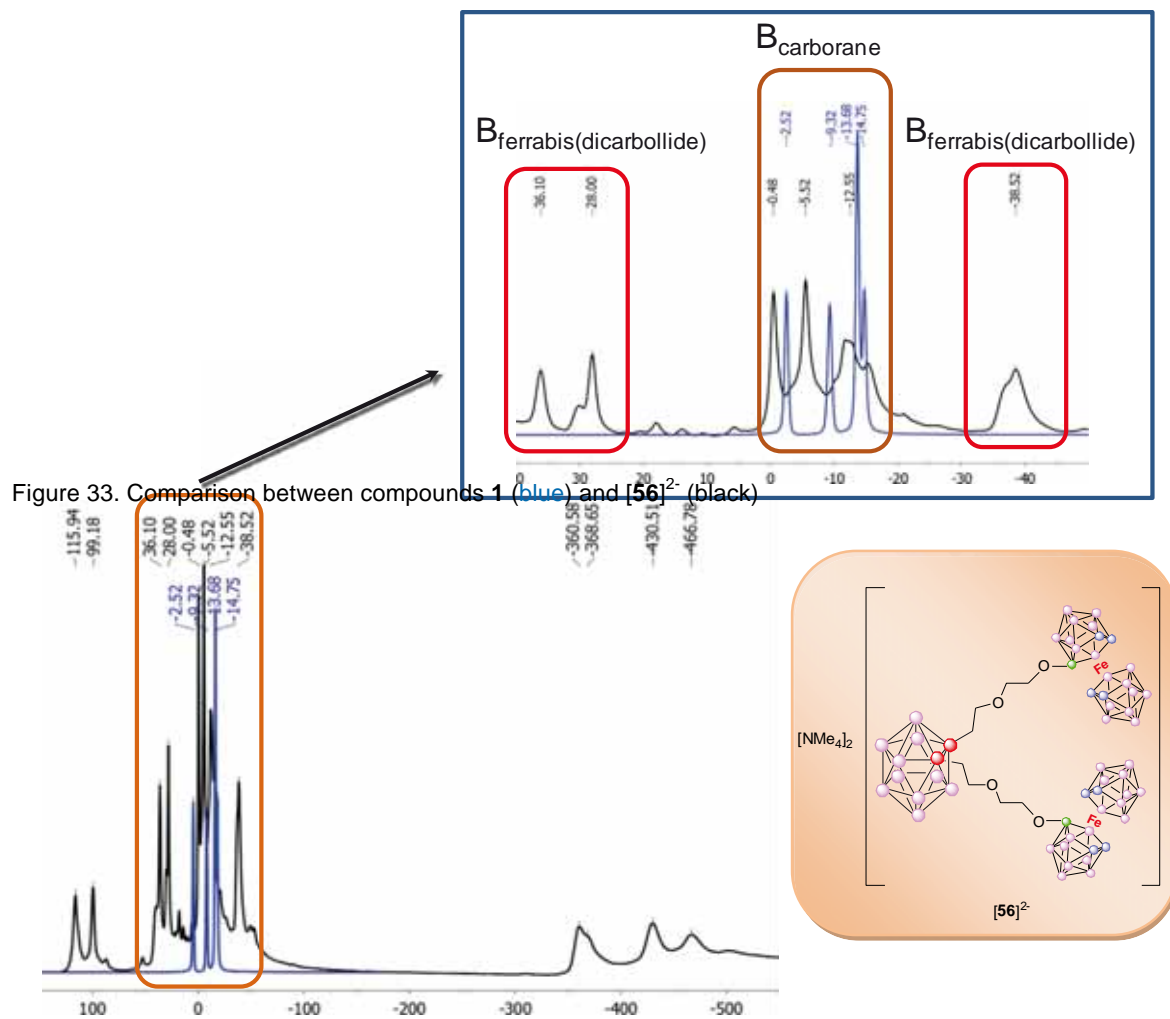


Figure 33. Comparison between compounds **1** (blue) and [**56**]²⁻ (black)

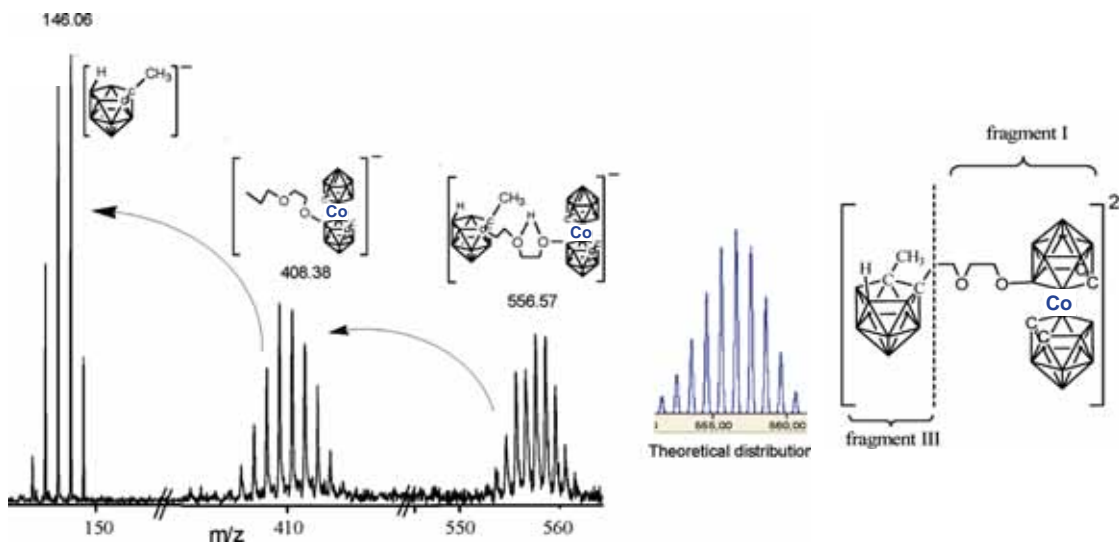
2.3.6. Characterization of the *nido* derivatives

FTIR spectroscopy performed on compounds $[57]^{2-}$ - $[59]^{2-}$ and $[60]^{3-}$ confirms the deboronation of the *closo* species since some B-H absorption values appear at values lower than 2550 cm^{-1} . The appearance of the B-H bond vibration to lower frequencies than their corresponding *closo* clusters, namely between 2500 and 2550 cm^{-1} ,²⁰⁶ is a characteristic of the *nido* carboranes (Table 6).

Compound	$\nu(\text{C}_c\text{-H})$	$\nu(\text{C-H})_{\text{alkyl}}$	$\nu(\text{B-H})$	$\nu(\delta(\text{CH}_2))$	$\nu(\text{C-O-C})$
$[57]^{2-}$	3044	2966, 2927, 2868	2542	1480, 1454	1158, 1115
$[58]^{2-}$	3038	2963, 2927, 2869	2536	1480, 1453	1167, 1115, 1091
$[59]^{2-}$	3032	2954, 2928, 2882	2526	1444, 1383	1090, 1067

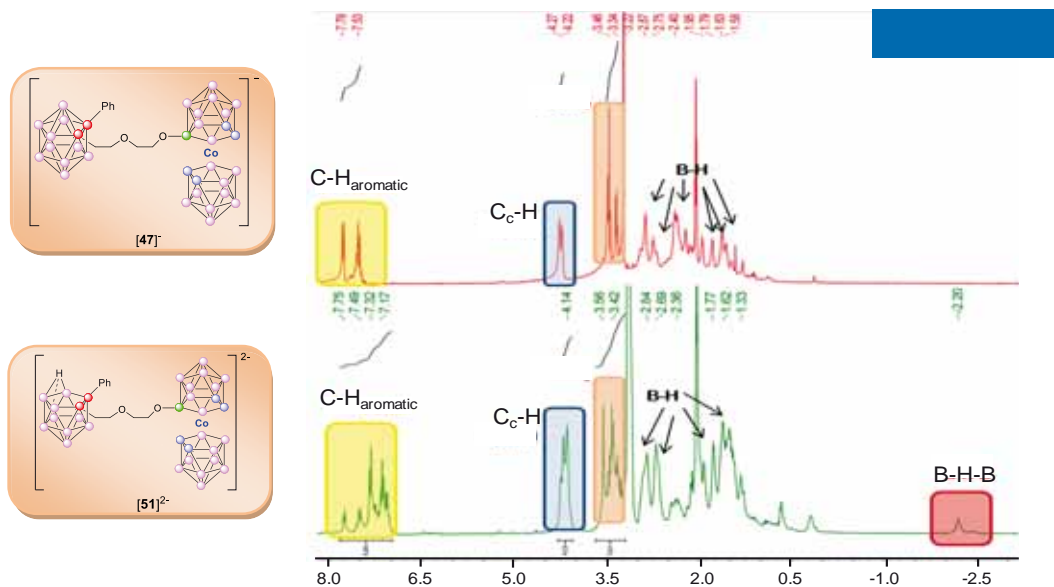
Table 6. FTIR spectroscopy of *nido* iron-based compounds

The MALDI-TOF-MS spectrum of compound $[50]^{2-}$, taken as a representative example of the divalent *nido* family of ions, displays a signal group centred at m/z 556.57 corresponding to the molecular peak $[\text{M} + \text{H}^+]^-$ and peaks at 408.38 and 146.06, similar with fragments I and III, respectively (Figure 34).

Figure 34. a) The MALDI-TOF-MS spectrometry of compound $[\text{NMe}_4]_2[50]$; b) fragmentation of the dianionic methyl derivative $[50]^{2-}$.

$^1\text{H-NMR}$ performed on the cobalt-containing *nido* compounds, confirms their synthesis due to the presence of the bridged hydrogen which remains at the open $[\text{C}_2\text{B}_9]$ pentagonal face; the peak corresponding to this acidic hydrogen appears at quite higher field values as compared to the other B-H bonds, namely at about -2.2 ppm (Figure 35).

Results and discussions

Figure 35. $^1\text{H}\{^{11}\text{B}\}$ -NMR comparison between *closo* [47]⁻ and *nido* [51]²⁻

Regarding ^1H -NMR of the iron-based species, we attribute the peak present at approximately -45 ppm to the bridged hydrogen remaining after the nucleophilic attack on either B(3) or B(6) bonded to both carbon atoms of the *o*-carborane cage, as depicted in Figure 36. We assume this shift to high field values is due to the influence of the paramagnetic iron-based moiety as well as to the fact that once the *o*-carborane cluster has been deboronated, the negative charge is no longer delocalized over the entire cage, but localized on the C_2B_3 pentagonal face. This is also the reason for the acidic character of the bridged hydrogen that can now be easily extracted by strong bases, such as potassium *tert*-butoxide.

With respect to $^{11}\text{B}\{^1\text{H}\}$ -NMR characterization, considerations similar to the ones involved in analyzing the *closo* clusters were used for interpreting the spectra of the corresponding *nido*-[C_2B_9] counterparts. The typical differences between the spectra of *closo* compounds and their eleven-vertex *nido* counterparts are exemplified for the methylated species [46]⁻ and [50]²⁻ in Figure 37.

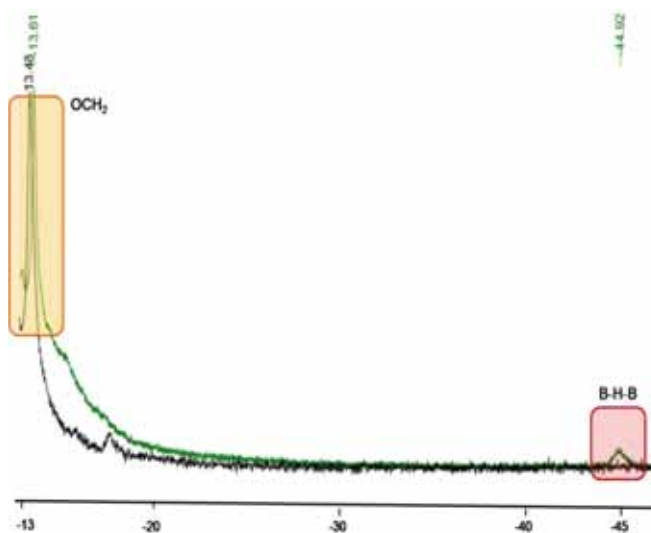
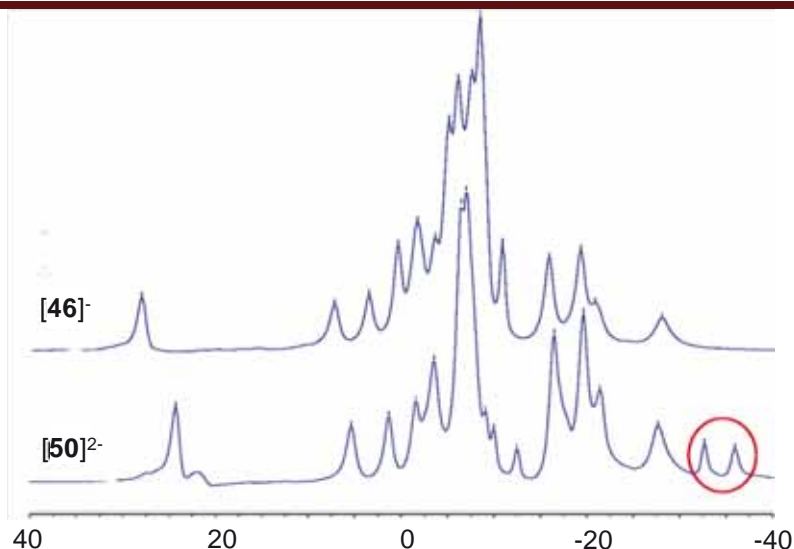
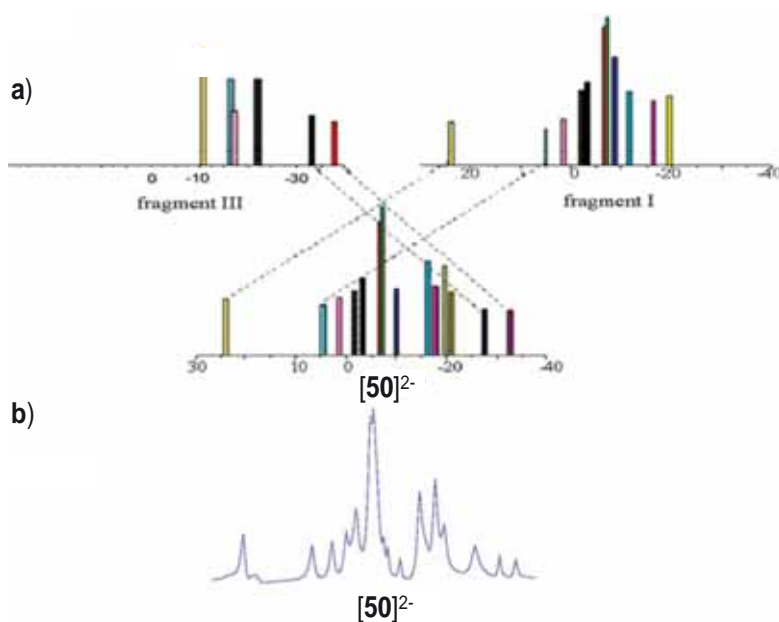


Figure 37. Comparison between $^{11}\text{B}\{^1\text{H}\}$ -NMR spectra of the *closo* compound [46]⁻ and its *nido* isomer [50]²⁻.

Results and discussions



The NMR analysis used for the characterization of all of the above presented compounds gives valuable information regarding the differences between the *closo* and the *nido* species. As presented in Figure 37, additional peaks for the *nido* compounds with respect to the corresponding *closo* species appear in the experimental $^{11}\text{B}\{^1\text{H}\}$ -NMR spectra in the range $\delta \approx -34/-36$ ppm, which clearly confirms the deboronation of the neutral *closo* $[\text{C}_2\text{B}_{10}]$ cluster to the anionic *nido* $[\text{C}_2\text{B}_9]^-$ one. As shown in Figure



32b, the methylated *nido* dianion $[\text{50}]^{2-}$ could be considered as the sum of fragment I and fragment III.

Figure 38a presents the schematic representation of the $^{11}\text{B}\{^1\text{H}\}$ -NMR spectrum of the methylated *nido* dianion $[\text{50}]^{2-}$ consists of 12 resonances from fragment I plus 9 resonances of fragment III. Its experimental

$^{11}\text{B}\{^1\text{H}\}$ -NMR spectrum (Figure 38b) confirms it. The only difference with respect to the corresponding *closo* species is the appearance of the two extra peaks, at ≈ -34 ppm

Results and discussions

and ≈ -36 ppm respectively. These peaks come from the *nido* carborane (fragment III), as depicted in Figure 36a.

Regarding ^{11}B -NMR, the chemical shift of the boron atoms from the iron-based fragment is not affected by the deboronation reaction; this only influences the shifts of

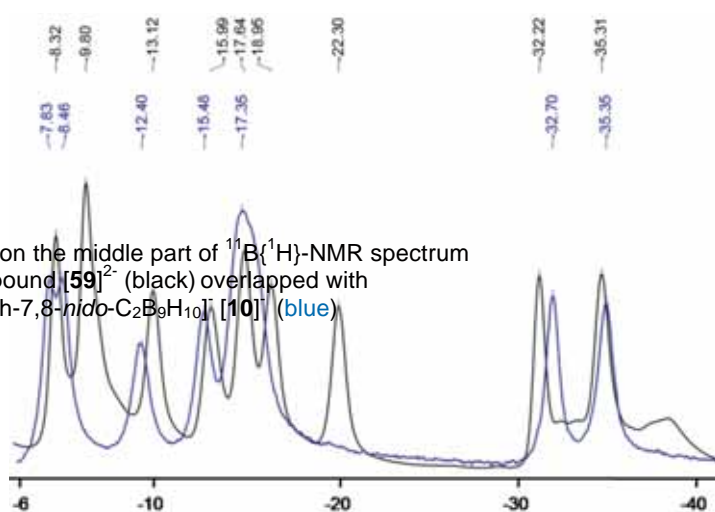


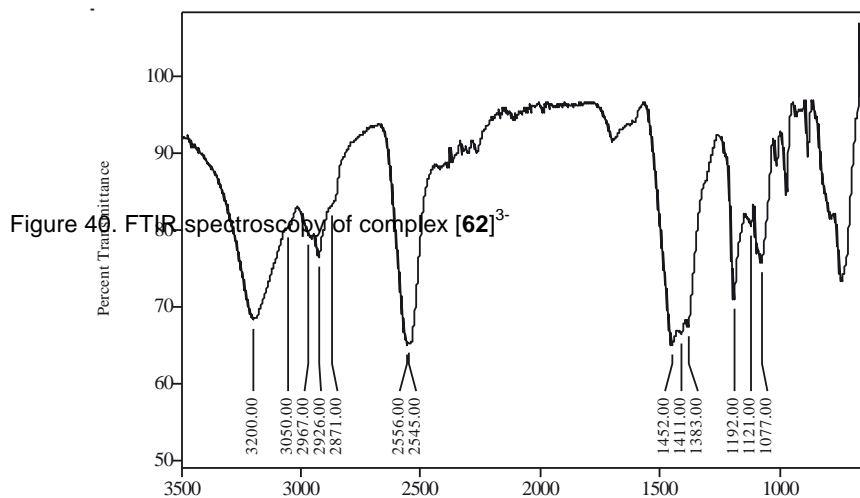
Figure 39. Zoom on the middle part of $^{11}\text{B}\{^1\text{H}\}$ -NMR spectrum of compound $[\mathbf{59}]^{2-}$ (black) overlapped with $[\mathbf{7-Ph-7,8-nido-C_2B_9H_{10}}]^+ [\mathbf{10}]^-$ (blue)

the borons from the carboranes cage, namely the appearance of the two peaks confirming the obtaining of the corresponding *nido* species, the signals from -32 and -36 ppm as presented in Figure 39. Once more, the presence of the negative charge over the open cluster face induces a quite remarkable effect on the boron magnetic resonance spectrum, by provoking an

important shift to high field values.

It should be concluded that the reactions shown in Schemes 11 and 12 lead to mono-, di-, and trianionic compounds containing both metal cobaltabisdicarbollide and carborane structural motifs within the same molecule. The presence of carborane subclusters may add new properties to boron clusters and, in fact, give rise to new species which can be used potentially in various fields of chemistry, biology, and medicine. Moreover, the deboronation of the *closo*-carborane moieties allowed the obtaining of a novel type of high boron content (almost 50%) polyanionic macromolecules. Likewise, the fact that these compounds are polyanionic makes them more soluble in water, which therefore increases their potential for biological uses. Furthermore, the carborane subunits can be easily modified by attaching variable substituents onto the carbon and boron vertex, making out of these structurally flexible compounds potential candidates for BNCT^{81,151,207} of cancer and HIV-protease inhibition.

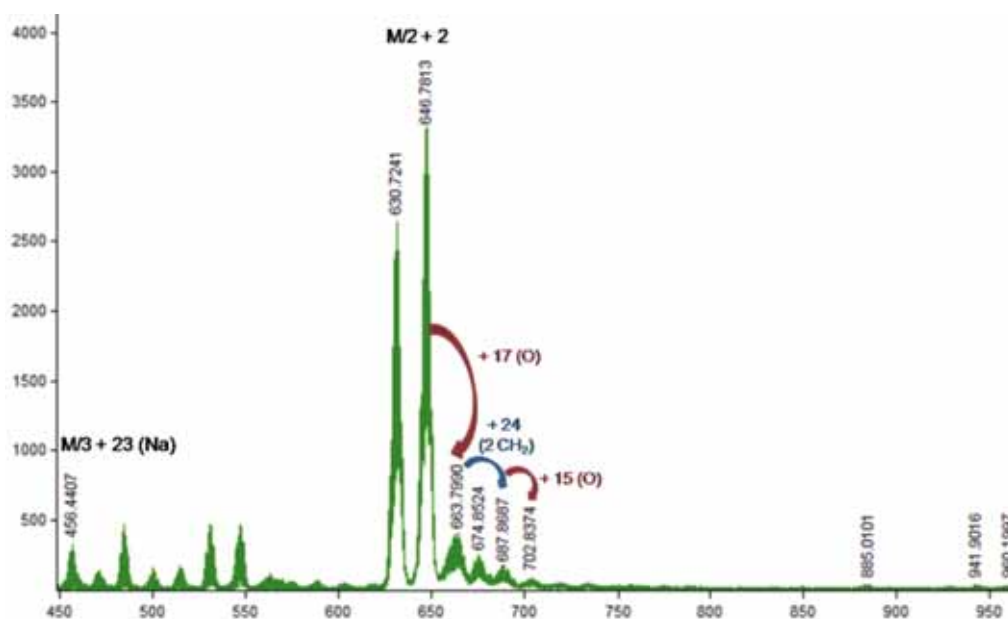
2.3.7. Characterization of polyanionic multicluster cobaltabis(dicarbollide) sandwich-type complexes

Figure 40. FTIR spectroscopy of complex $[62]^{3-}$

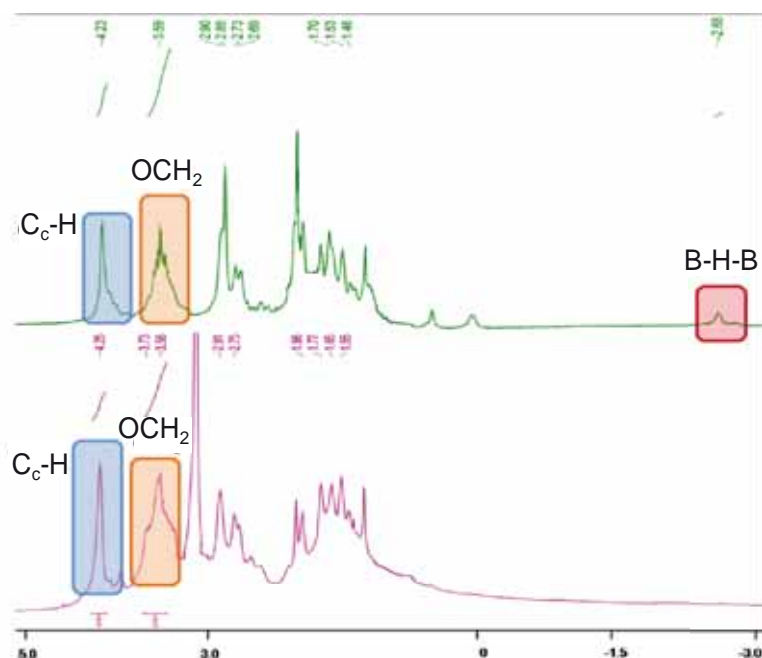
From the FTIR spectroscopy in Figure 40, one can clearly see the B-H absorption band at 2556 and 2545 cm^{-1} which dominates the spectrum as well as the band corresponding to the C-H absorption value. The 2556 cm^{-1} value of the B-H band comes from its actual

closo structure, whereas the 2545 cm^{-1} value refers to the two dicarbollide units coordinated by Co(III). The bands at 1192-1077 cm^{-1} indicate the presence of C-O-C bonds within the complex.

MALDI-TOF-MS spectrometry, even if it does not show the peak corresponding to the total trianionic molecular peak, it does indicate the presence of the di- and monoanionic species of compound $[63]^{3-}$ as depicted in Figure 41. As already described in previous subchapters, we have encountered that the polyanionic species appear as monovalent compounds, by adding either lithium, potassium or hydrogen cations among others. In this case, the monovalent form coordinated a sodium cation as it appears in the MALDI-TOF-MS spectrum.



The $^1\text{H}\{^{11}\text{B}\}$ -NMR spectra (Figure 42) bring the confirmation of the complexation



reaction, since the bridge hydrogen peak from -2.6 ppm disappears as it is eliminated by the $\text{K}[\text{tBuO}]$ during the reaction, indicating the formation of a formal “*closo*” complex $[\mathbf{64}]^{5-}$.

From Figure 43 one can observe the disappearance of the boron signals left at the open pentagonal face for $[\mathbf{50}]^{2-}$ (namely the ones at -34 and -36 ppm) with

the formation of the cobalt-based coordination complex, since formal bounds can be imagined between the 2 “*nido*” units and cobalt yielding in fact a *closo* form).

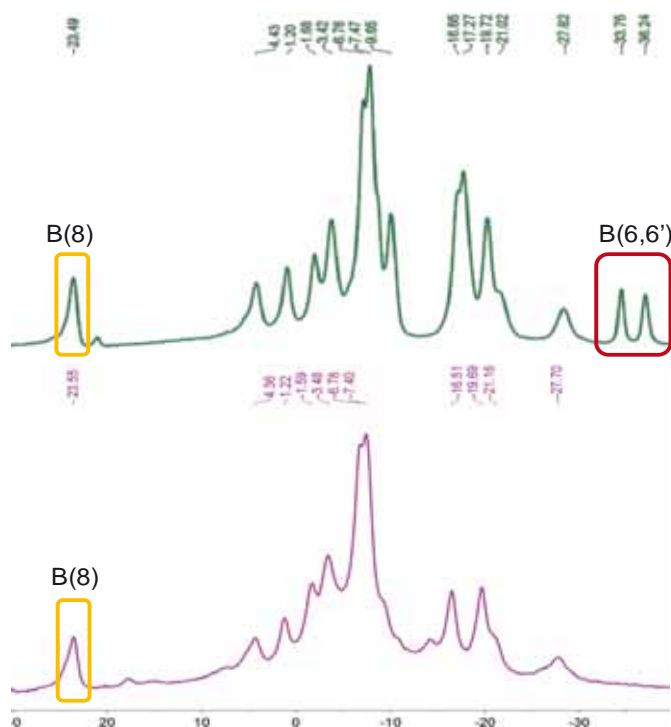


Figure 43. $^{11}\text{B}\{^1\text{H}\}$ -NMR of compounds $[\mathbf{50}]^{2-}$ (green) and $[\mathbf{62}]^{3-}$ (purple)

Besides FTIR, MALDI-TOF-MS and NMR analysis, another method that brings additional information with respect to the synthesis of our complexes is UV-Vis spectroscopy. In order to confirm our theory with respect to the synthesis of the

complexes, some UV/Vis studies on cobaltabis(dicarbollide) anion were performed. Previously, Hawthorne and co-workers²⁰⁸ have reported that the UV/Vis spectrum of $[3,3'\text{-Co}(1,2\text{-C}_2\text{B}_9\text{H}_{11})_2]^-$ in methanol consists of four absorptions peaks at 216, 293, 345 and 445 nm, which is essentially in agreement with the one subsequently reported in 1982 by Matel and co-workers^{20c} showing one main absorption band at $\lambda_{\text{max}} = 287$ nm ($\epsilon = 30000 \text{ Lcm}^{-1}\text{mol}^{-1}$). Based on these previous researches^{22b,209} we have recorded the UV/Vis spectrum of four compounds (two chosen as references for the others two) using the same solvent for all measurements, namely ethanol.

The aim of our study was to demonstrate that the cobaltabis(dicarbollide) unit is the chromophoric group of the complex and to see if there is any correlation between the values of the absorbance and the number of cobaltabis(dicarbollide) units present in the molecule. The spectra showed 3 peaks, two of them not well defined, but one can observe that the peak from 314 nm is present in all 3 compounds (reference with an open dioxane ring and two complexes) and in accordance with the Lambert Beer law (respects a linear dependence between absorbance and concentration). Therefore, relevant comparisons can be made.

Two compounds, one with a closed-dioxane ring (**6**) and the other with an open-dioxane ring ($[33]^-$) were chosen as reference. For these compounds the calibration curves were plotted in ethanol (Figure 44).

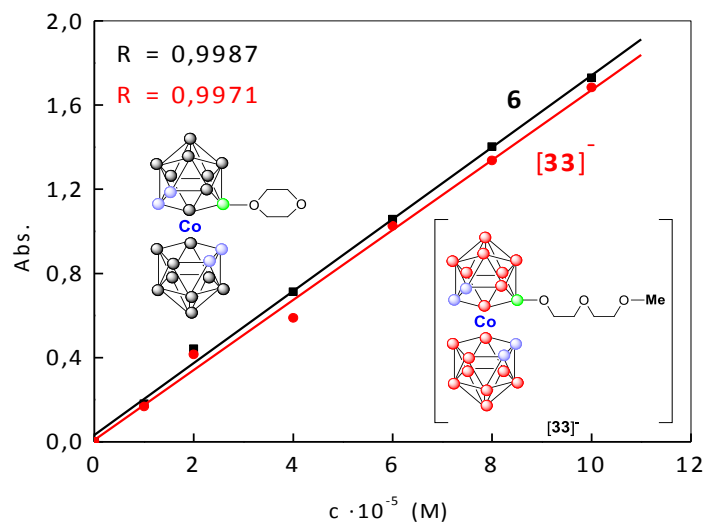


Figure 44. Calibration curves for reference compounds **6** and $[33]^-$

The following step was to measure the absorbance of compounds $[63]^{3-}$ and $[64]^{5-}$ exhibiting the same open-ring sandwich type structure as compound $[33]^-$, at a certain concentration. As indicated in Figure 45a, in the case of $[3,3'\text{-Co}(8\text{-(OCH}_2\text{CH}_2)_2\text{-(1,2-C}_2\text{B}_9\text{H}_{10})(1',2'\text{-C}_2\text{B}_9\text{H}_{11}))]$, **6**, which is a zwitterion (neutral molecule) our theory is valid, since the value of the absorbance is 3 times and 5 times respectively, higher than the

Results and discussions

one of the reference compound; however, the maximum of absorbance appears at slightly different wavelength, 287 nm for **2** and 314 nm for $[63]^{3-}$ and $[64]^{5-}$. This can be explained based on the fact that the reference compound exhibits a closed dioxane ring whereas compounds $[63]^{3-}$ and $[64]^{5-}$ are anions with open-ring systems. As shown in Figure 45b, the 3 compounds, the reference (compound $[33]^-$) and the analytes (compounds $[63]^{3-}$ and $[64]^{5-}$), present open-dioxane rings and therefore, the maximum of absorbance appears at the same wavelength (314 nm). Another observation is that the nature of the nucleophile present in the molecule (Ph-*o*-carborane for $[63]^{3-}$ and *o*-carborane for $[64]^{5-}$) does not influence the wavelength at which the absorbance has the maximum value.

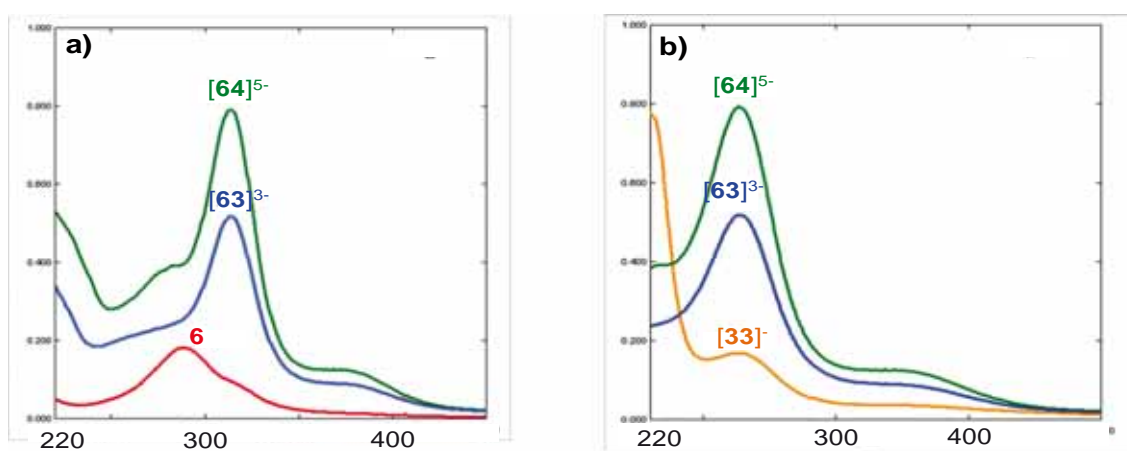


Figure 45. a) Comparative study on UV spectra for compounds **6**, $[63]^{3-}$ and $[64]^{5-}$ ($10\ \mu\text{M}$) and b) for compounds $[33]^-$, $[63]^{3-}$ and $[64]^{5-}$ ($10\ \mu\text{M}$)

Having the straight-line equation and knowing the absorbance's (314 nm), the concentrations were computed. It was observed that even if the concentrations of the references and of compounds $[63]^{3-}$ and $[64]^{5-}$ were the same, the value of the absorbance was 3 times higher for $[63]^{3-}$ (containing 3 cobaltabis(dicarbollide) units in its structure) and 5 times for $[64]^{5-}$ (exhibiting 5 cobaltabis(dicarbollide) units) (Table 7).

Comp. no.	Reference conc. (μM)	Calibration curves equation (linear fit)	R	Complex $[63]^{3-}$ conc. (μM)	Complex $[64]^{5-}$ conc. (μM)
6	10.00	$y = 0.033 + 0.171 \cdot x$	0.9987	28.50	44.40
$[33]^-$	10.00	$y = 0.009 + 0.166 \cdot x$	0.9971	30.70	47.20

Table 7. Analysis data recorded by UV-Vis spectroscopy

In conclusion this method can be successfully used to quantify the number of cobaltabis(dicarbollide) units within the macromolecule since we have proved that there is a direct dependence between the number of cobaltabis(dicarbollide) units and the absorbance's intensity.

2.3.8. Characterization of the heterocomplexes centred in cobalt

In this subchapter we took the iron-based *nido* compounds $[57]^{2-}$ - $[60]^{3-}$ and complex them with anhydrous CoCl_2 . We were quite astonished to find that the ^{11}B -NMR of the final molecule actually looked like ferrabis(dicarbollide) spectrum, with only two peaks at extremely high field values and only one signal downfield, at about +110 ppm. No B-H-B signal is present either in the ^1H -NMR as it was the case with the corresponding *nido* species, so we can safely conclude that the complexation reaction was successful (Figure 46).

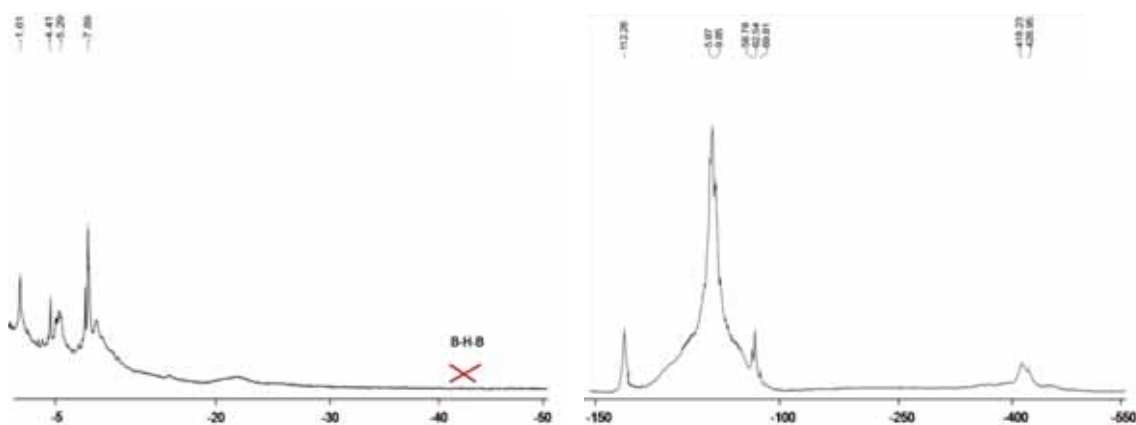
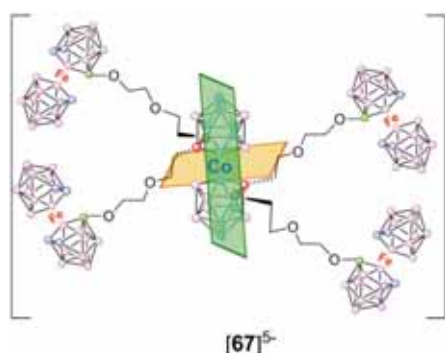


Figure 46. a) ^1H -NMR and b) ^{11}B -NMR spectra of complex $[67]^{5-}$

The Co(III)-based complexes obtained in this section, even if they are polyanionic as their *nido* species, do not have such significant shifts as the *nido* clusters do, because of the high delocalization of the negative charges over the entire molecule. This information can be validated if we look at the medium values of the ^{11}B -NMR spectra of the *nido* compounds $[59]^{2-}$ and $[60]^{3-}$ which are around -280 ppm and the one of the



corresponding sandwich-type complexes $[66]^{3-}$ and $[67]^{5-}$ at approximately -264 ppm.

In addition, we also observe two symmetry planes: one found parallel to the C_2B_3 faces, making the two central dicarbollide units and the up and down branches equivalent, and another symmetry plan perpendicular to this one, going horizontally through the central Co(III) atom and bisecting the $\text{C}_c\text{-C}_c$ bonds (Figure 47), making the above and below branches equivalent.

Results and discussions

Figure 48. $^1\text{H}\{^{11}\text{B}\}$ -NMR comparison between the *nido* species [51]²⁻ (green) and its iron-centred complex [69]³⁻ (purple)

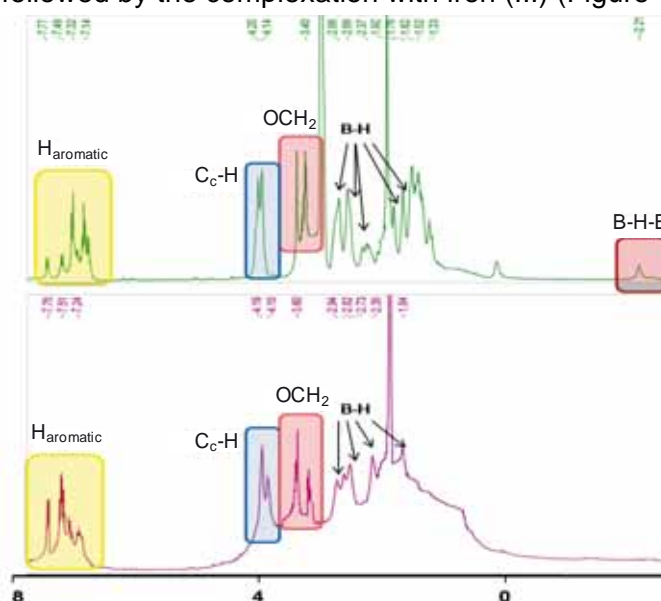
2.3.9. Characterization of the polyanionic multicenter heterocomplexes centred in iron

To our surprise, the resulted complex did not exhibit paramagnetic properties, but a regular, diamagnetic character as the one presented by the cobalt-based species. This was revealed by NMR, since the signals appeared in a normal +25 to -30 ppm range and not at extreme both high and low fields as it happens with the family of paramagnetic compounds.

Table 8 shows the complexation reaction with FeCl_2 since the B-H absorption band which in the case of the *nido* derivatives appeared around 2540 cm^{-1} shifts to higher frequencies once the complex was synthesized, namely to about 2566 cm^{-1} , an indicative of the formation of a “*closo*” compound.

Compound	$\nu(\text{C}_c\text{-H})$	$\nu(\text{C-H})_{\text{alkyl}}$	$\nu(\text{B-H})$	$\nu(\delta(\text{CH}_2))$	$\nu(\text{C-O-C})$
[50] ²⁻	3032	2923, 2865	2543	1481	1241, 1159, 1102
[51] ²⁻	3035,	2921, 2865	2533	1482, 1446	1247, 1168, 1099
[52] ³⁻	3036	2922, 2865	2533	1481, 1420	1249, 1163, 1098
[68] ³⁻	3043	2954, 2926, 2856	2566	1463, 1374	1197, 1164, 1098
[69] ³⁻	3047	2958, 2930, 2872	2562	1447, 1417, 1367	1232, 1164, 1097
[70] ⁵⁻	-	2973, 2902	2559, 2538	1479, 1453, 1408, 1369	1231, 1163, 1077

In addition to the FTIR data, $^1\text{H}\{^{11}\text{B}\}$ -NMR gives us clear information about the fact that the complexation reaction did take place, therefore confirming the extraction of the bridged hydrogen followed by the complexation with iron (III) (Figure 48).



Moreover, the $^1\text{H}\{^{11}\text{B}\}$ -NMR comparison between the *nido* species [52]³⁻ and the corresponding iron-centred complex [70]⁵⁻ indicates the synthesis of the sought compounds, since the boron signals which are characteristic for the *nido* clusters are no longer present once the formation of the complex. In addition, the $^{11}\text{B}\{^1\text{H}\}$ -NMR spectrum shows that the peaks continue in a +25 to -30 ppm range and there was no need for extensive spectral range

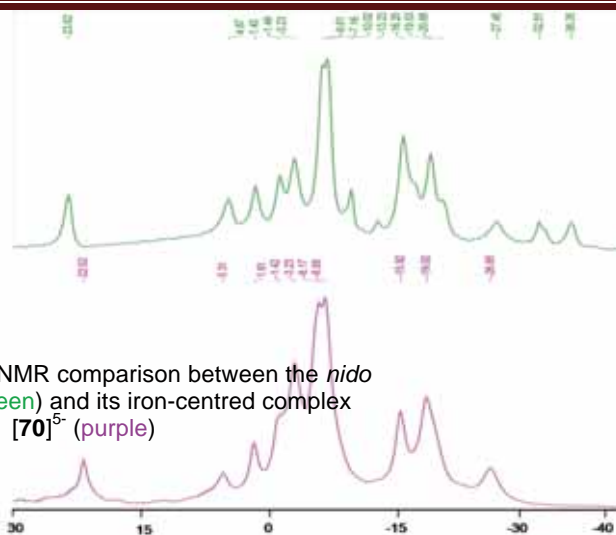


Figure 49. $^{11}\text{B}\{^1\text{H}\}$ -NMR comparison between the *nido* species [52]³⁻ (green) and its iron-centred complex [70]⁵⁻ (purple)

as thought before hand, given the fact that the central metal atom is iron, and therefore should, in agreement with our previous experience, exhibit paramagnetic properties (Figure 49). The fact that the iron-centred species was a diamagnetic compound was a surprising finding. A reasonable explanation can be that the four polyglycol chains ended in four cobaltabis(dicarbollide) units prevents the Fe(II) to oxidize to Fe(III) as it happens with the plain pristine unit [3,3'-Fe(1,2-C₂B₉H₁₁)₂]⁻.

Based on the results obtained by using UV-visible analysis in order to establish the number of cobaltabis(dicarbollide) units present in the molecule, we thought of applying the same method for species containing both types of metallacarborane. Still, in this case where we have two different metals present, the adsorption bands overlapped and it was impossible to assign which absorption was from cobaltabis(dicarbollide) and which belonged to the ferrabis(dicarbollide) units. We should perform deconvolutions in order to exactly know how many cobaltabis(dicarbollide) and ferrabis(dicarbollide) units we have, and therefore, this method is not very reliable.

However, other techniques proved to be very useful in previous analysis, namely Cyclic Voltammetry (CV) and Square Wave Voltammetry (SWV). These resulted to be the only accurate techniques for the determination of different types of metallacarboranes present within the same molecule, since between cobaltabis(dicarbollide) and ferrabis(dicarbollide) derivatives there is a difference of about 1 volt, when taking into account the $E_{1/2}$ of $\text{M}^{3+}/\text{M}^{2+}$. What is more, we can quantify the ratio between these two different metals, as presented in the CV and SWV images shown in Figure 48. This is due to the fact that the intensity of each peak is directly proportional to the concentration of the electroactive species (considering the number of electrons, area, diffusion factor and scan rate, constant for all the measurements). The working

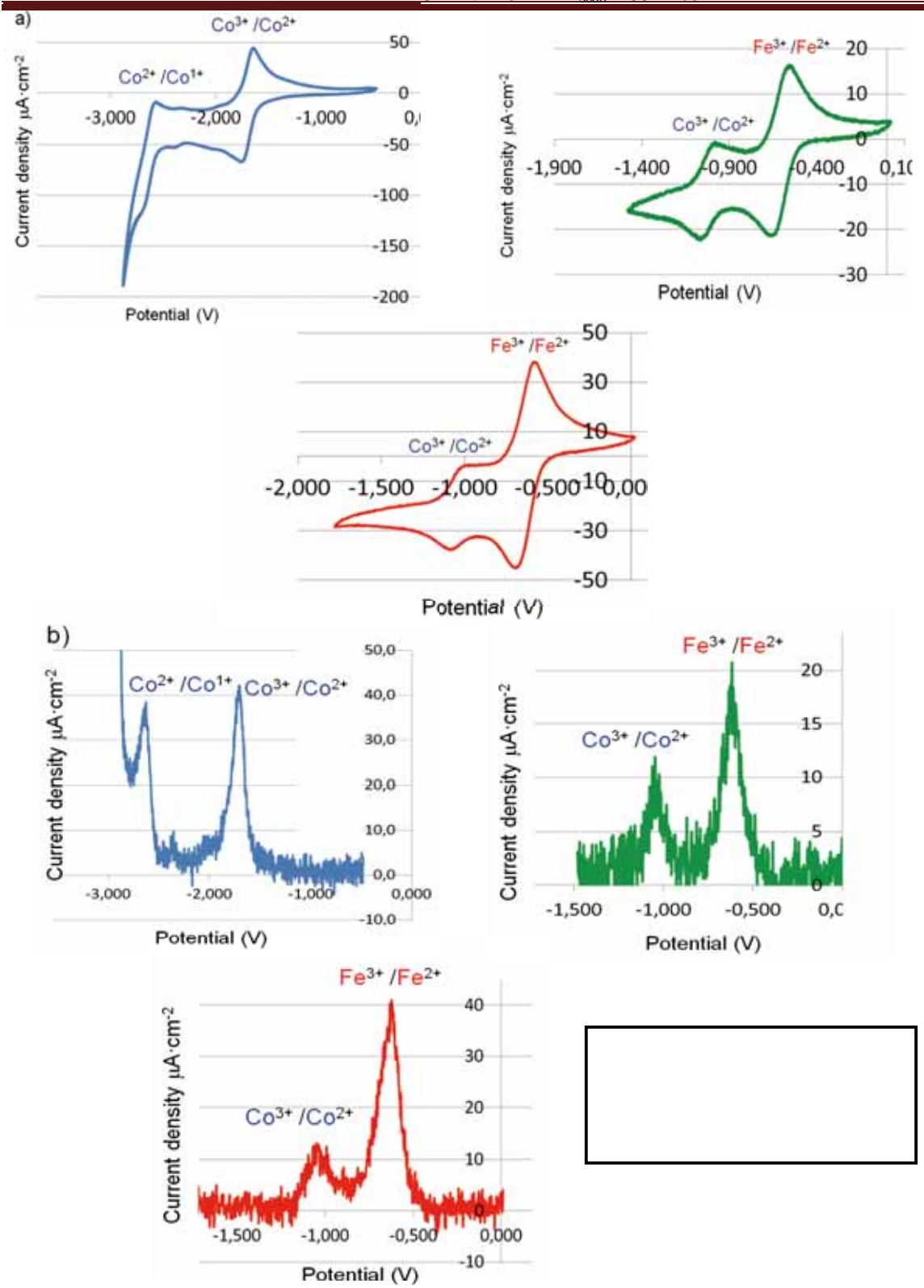
conditions were glassy carbon electrode as working electrode, as reference electrode a Ag wire (always referenced to the couple Fc^+/Fc in order to compare the obtained values with the previous ones, Chapter 2.2) and platinum wire as auxiliary electrode, using a $[NBu_4]PF_6$ 0.1 M acetonitrile solution.

As indicated by the SWV in Figure 50b, we can exactly determine the ratio between Co and Fe atoms, simply by looking at the current density. Let us take as example compound $[65]^{3-}$ having one cobalt and two iron atoms within its molecule, fact supported by its SWV (Figure 50b green). This measurement clearly depicts the potential related to the Co atom at about $10 \text{ mA}\cdot\text{cm}^{-2}$, and the peak intensity of the iron atoms, which exactly doubles the one of the cobalt. Furthermore, the SWV of $[67]^{5-}$ (red) complex, also indicates in an accurate manner that the value of potential corresponding to the cobalt atom is around $10 \text{ mA}\cdot\text{cm}^{-2}$, whereas the intensity for the iron atoms is exactly four times greater, namely $40 \text{ mA}\cdot\text{cm}^{-2}$, in perfect agreement with the 1Co:4Fe content within its molecule.

In order to determine the exact number and nature of metallacarborane units present in a molecule, we should make a calibration curve (different concentrations of a very well known compound containing just one metallacarborane unit) and use it as reference to be able to get the precise concentration and therefore, the precise number of units within an unknown sample.

However, since this has only been a preliminary study, follow-up studies have to be run in order to acquire the data necessary for an accurate interpretation of the CV analysis. Regarding the Figure 50, the data for the cobalt-containing species $[61]^{3-}$ are in agreement with the potential values obtained for compound $[33]^{3-}$ and basically with all the cobaltabis(dicarbollide) potential values present in the literature.²¹⁰ A surprising finding was the potential values of compounds $[65]^{3-}$ and $[67]^{5-}$ as referred to species $[61]^{3-}$ showing only cobaltabis(dicarbollide) units within its molecule (0.8 volt shift respectively, to the anodic direction). Although we have not yet elaborated a concrete theory, we consider it to be due to the presence of the surrounding paramagnetic species (ferrabis(dicarbollide)). The CV data are gathered in Table 9 below.

Compound	$E_{1/2}(\text{Co}^{3+}/\text{Co}^{2+})$ (V)	$E_{1/2}(\text{Fe}^{3+}/\text{Fe}^{2+})$ (V)	Metal
$[61]^{3-}$	-1.712	-	3 Co
$[65]^{3-}$	-1.029	-0.611	1 Co : 2 Fe
$[67]^{5-}$	-1.066	-0.641	1 Co : 4 Fe



To sum up, all the polyanionic species presented so far have showed increased water-solubility, detail that makes them attractive as potential candidates for BNCT tumor treatment. Moreover, the different metal-centres described up to this point (Co, Fe) might bring about new dimension to the subject of new boron carriers for BNCT.

2.4. Ring-opening reactions of 1,4-dioxane derivative of cobaltabis(dicarbollide) with biomolecules

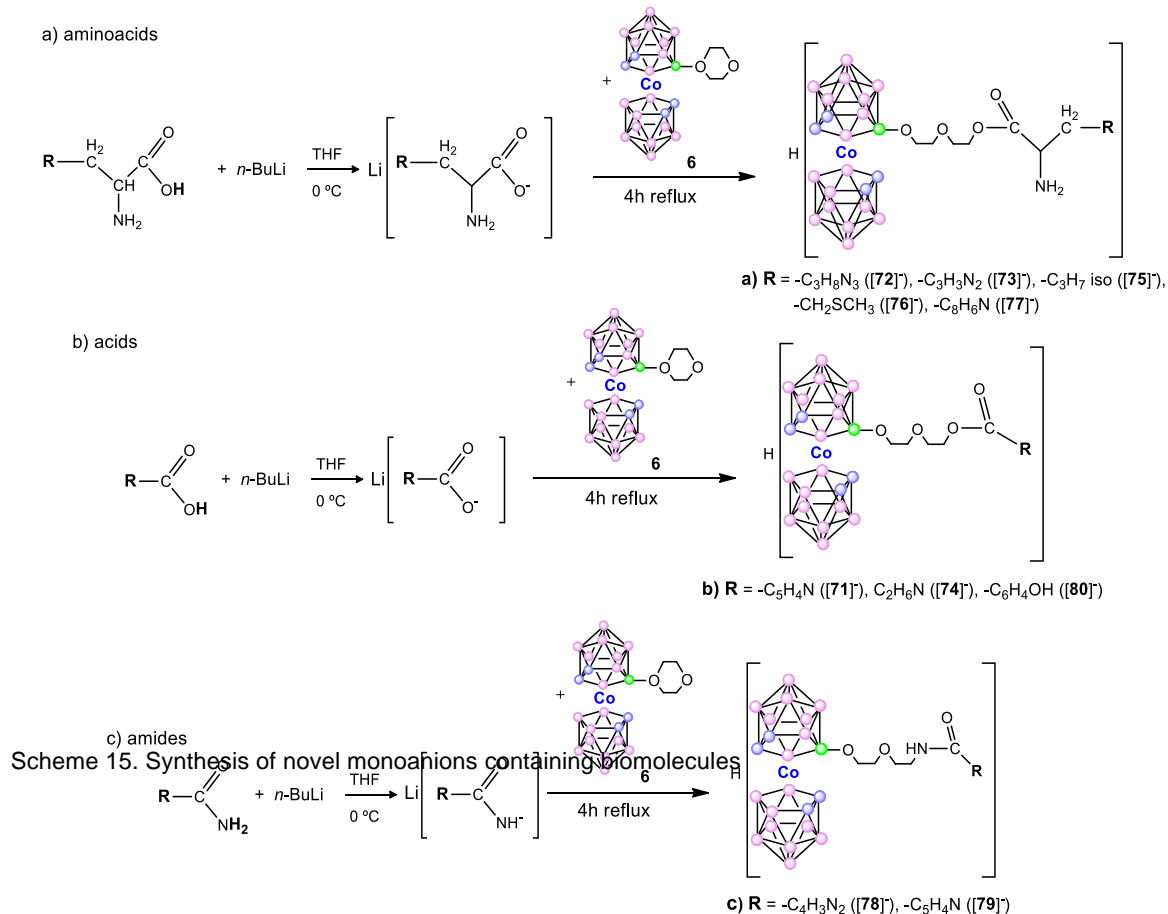
The cobaltabis(dicarbollide) anion, $[3,3'\text{-Co}(1,2\text{-C}_2\text{B}_9\text{H}_{11})_2]^-$, is among the boron moieties proposed for use in medicinal chemistry relatively recently.^{44b,48,211} The sodium salt of this metallocarborane cluster demonstrates good solubility in water; however, the anion itself is rather lipophilic and that could have some advantages in medical applications. As it has been explained in previous sections, the problem related to the synthesis of monosubstituted functional derivatives of cobaltabis(dicarbollide) was solved when nucleophilic opening of 1,4-dioxane oxonium derivative was reported.^{23a,187a} This neutral oxonium derivative of cobaltabis(dicarbollide) has received increased interest in these last years due to its ability to be easily attached to various substrates, including biomolecules such as porphyrines^{67g,h,212} or nucleosides,^{28,68,213} *via* a nucleophilic attack on the positively charged oxygen atom (see Introduction). In this part of the thesis we were concerned with the use of biomolecules as vectors for the transport of boron-enriched compounds to the specific site (cancerous cells). The following step would be the irradiation with slow neutrons-BNCT (as described in the Applications part of the Introduction), leading to the death of the tumor cells.

2.4.1. Syntheses of 1,4-dioxane derivative of cobaltabis(dicarbollide) with biomolecules

In this chapter, $\text{Co}(8\text{-(OCH}_2\text{CH}_2)_2\text{-(1,2-C}_2\text{B}_9\text{H}_{10})(1',2'\text{-C}_2\text{B}_9\text{H}_{11})]$ is cleaved by employing biomolecules derivatives. The starting biomolecules are aminoacids and vitamins such as sodium salicylic acid, nicotinamide, nicotinic acid, pyrazinamide, arginine, α -alanine, leucine, histidine and tryptophan.

The first step for this dioxane ring-opening reaction was the nucleophilic synthesis. The nucleophilic species of the respective biomolecules were obtained by an acid/base reaction. The acidic hydrogen of an OH or NH_2 group was removed by using *n*-BuLi as base. Once the lithiation process is completed, an anhydrous THF solution of **6** is added. The mixture was left under reflux for four hours of reflux, followed by extraction with dilute HCl and then purification by separation on TLC plates (Scheme 15).

All the obtained cobaltabis(dicarbollide) complexes containing biomolecules have more boron atoms per molecule than either the carboranes or the *clos*o-dodecaborate anion, making them more attractive from the BNCT point of view. Moreover, the presence of the biomolecules as well as the fact that they show increased water-solubility, convert these macromolecules into more biocompatible compounds.



2.4.2. Characterization of 1,4-dioxane derivative of cobaltabis(dicarbollide) with biomolecules

The final compounds were characterized using FTIR, MALDI-TOF-MS and ¹H, ¹¹B and ¹³C-NMR techniques, confirming the synthesis of the desired species, with very good yields.

The fundamental vibrations of the attached to different substrates are depicted in Table 10.

Compound	ν (C _c -H)	ν (C-H) _{alkyl}	ν (B-H)	ν (C-O-C)
[71] ⁻	3085, 3052	2954, 2927, 2870	2561	1292, 1256, 1172, 1100
[72] ⁻	3043	2954, 2930, 2873	2565	1287, 1250, 1120, 1098

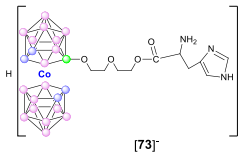
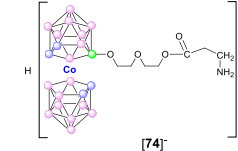
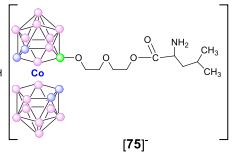
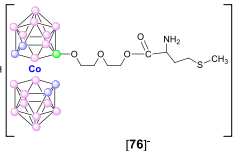
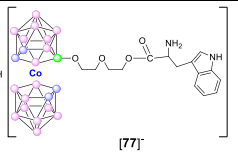
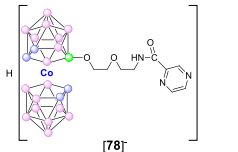
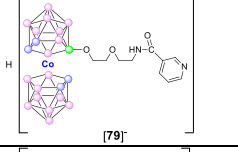
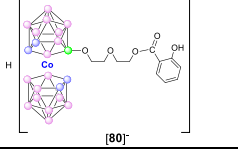
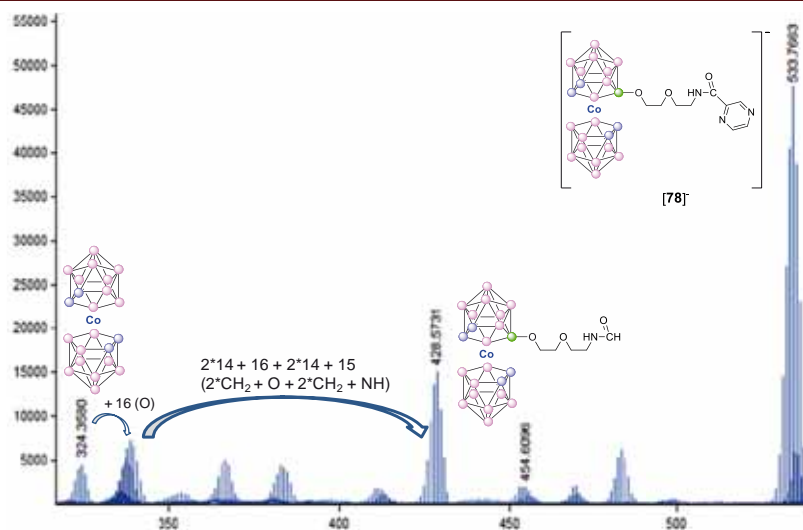
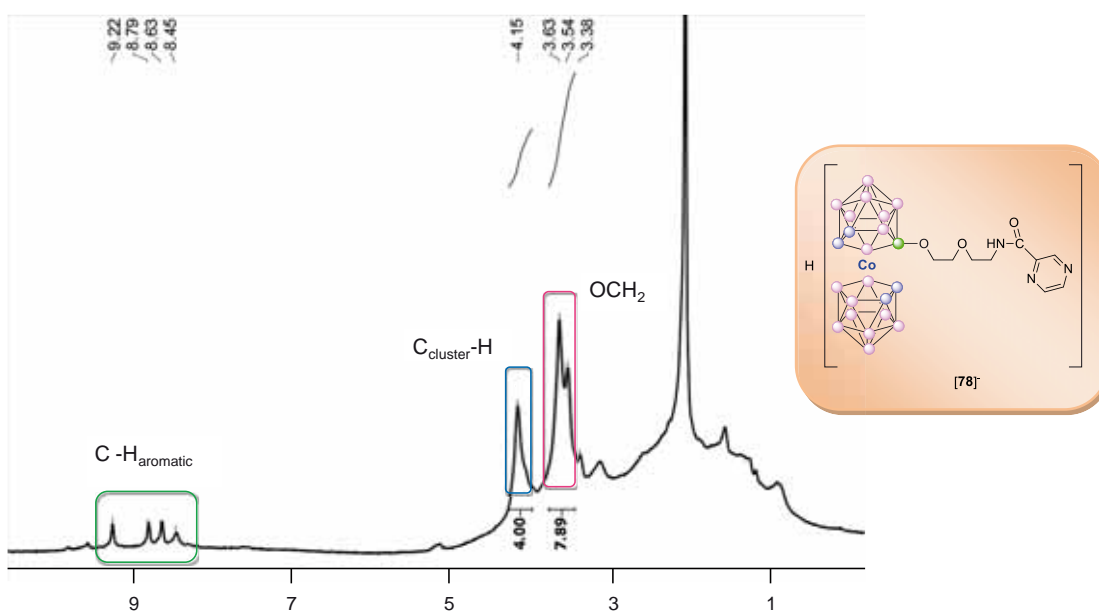
Compound	ν (C-H)	ν (C-H) _{alkyl}	ν (B-H)	ν (C-O-C)
 [73] ⁻	3042	2942, 2930, 2873	2565	1285, 1250, 1121, 1098
 [74] ⁻	3042	2924, 2873	2563	1231, 1156, 1123, 1099
 [75] ⁻	3043	2927, 2873	2564	1234, 1120, 1098
 [76] ⁻	3042	2953, 2925, 2872	2563	1232, 1122, 1098
 [77] ⁻	3043	2952, 2927, 2872	2564	1248, 1122, 1099
 [78] ⁻	3043	2928, 2871	2562	1250, 1162, 1118, 1098
 [79] ⁻	3044	2926, 2870	2562	1164, 1122, 1098
 [80] ⁻	-	2989, 2901	2564	1250, 1076

Table 10. FTIR spectroscopies of compounds [71]⁻ - [80]⁻

MALDI-TOF-MS also indicates the obtaining of the desired species [78]⁻, since the experimental molecular peak, corresponding to the monoanionic species, at 533.7 m/z matches the theoretical one expected for this compound, namely at 532.58 m/z. The peak showing at 454.6 m/z belongs to the species without the pyrazine ring within its molecule, whereas the one at 324.3 m/z is the starting monoanion itself, as depicted in Figure 51.

Figure 51. MALDI-TOF-MS spectrum of monoanionic compound $[78]^-$

Measurements of $^1\text{H-NMR}$ spectra not only complement knowledge of the individual B-H vertices, but also provide information on the presence of $\text{C}_c\text{-H}$ vertices and on the existence of proton-bearing substituents, as OCH_2 in the molecules described in this chapter. As indicated in the $^1\text{H-NMR}$ spectrum presented in Figure 52 below, the reaction did take place since we find the characteristic aromatic signals for the phenyl ring, as well as the ones corresponding to the PEG chain of the species and the $\text{C}_c\text{-H}$ peaks.

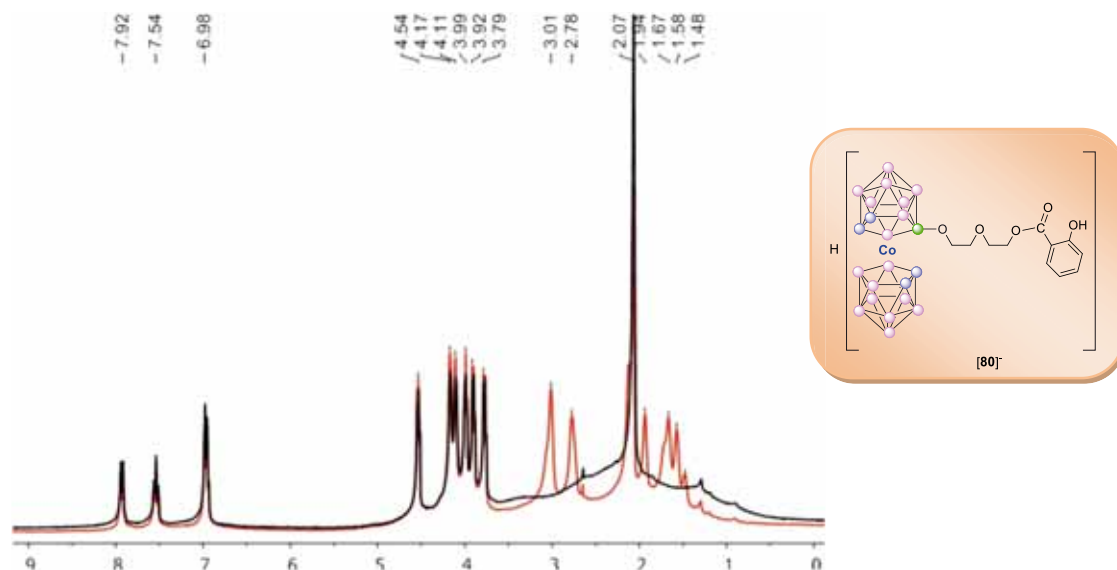
Figure 52. $^1\text{H-NMR}$ spectrum of compound $[78]^-$

By overlapping the coupled (black) and decoupled (red) $^1\text{H-NMR}$ spectra, one can clearly see the signals belonging to B-H bonds within the molecule, as presented in Figure 53. The fact that the peaks corresponding to the hydrogen atoms bounded to

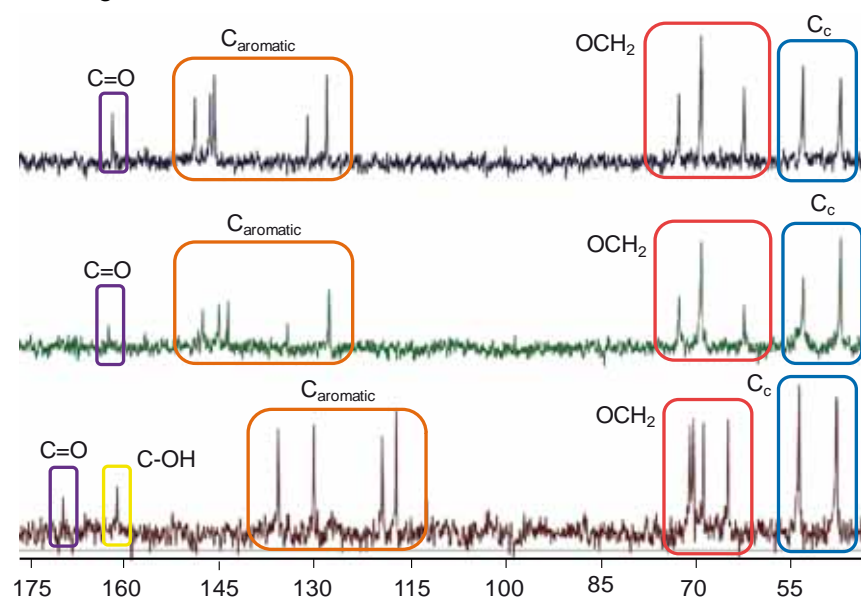
Results and discussions

2.4. Ring-opening reactions of 1,4-dioxane derivative of cobaltabis(dicarbollide) with biomolecules

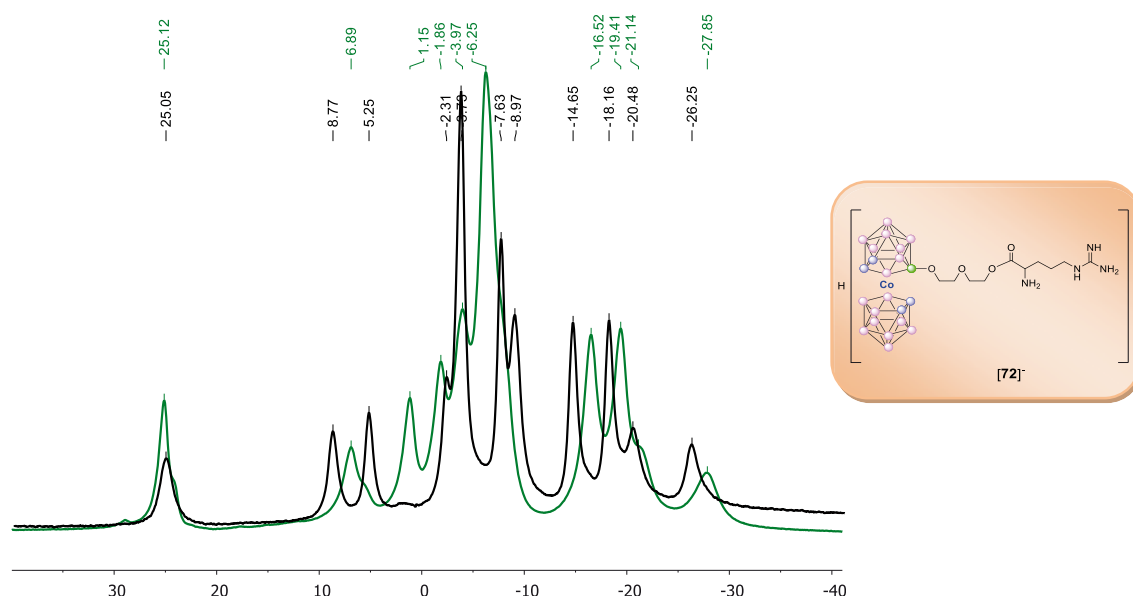
Figure 54. $^{13}\text{C}\{^1\text{H}\}$ -NMR spectra of monoanionic $[3,3\text{-Co}(\text{C}_2\text{B}_9\text{H}_{10})_2(\text{OCH}_2\text{CH}_2)_2\text{-}(1,2\text{-C}_2\text{B}_9\text{H}_{10})(1,2\text{-C}_2\text{B}_9\text{H}_{11})]$ bearing biomolecules [75] (blue), [78] (green), [79] (red) and [80] (black). The borons are wide is due to the coupling to boron itself, since its two isotopes have different spins and abundance (80% $^{11}\text{B} = 3/2$, 20% $^{10}\text{B} = 3$).



From the $^{13}\text{C}\{^1\text{H}\}$ -NMR spectra represented in Figure 54 one can clearly see that there is practically no difference between the chemical shifts of the above, due to the fact that the organic moiety and the cobaltabis(dicarbollide) complex are separated by the polyethylene glycol chain. One slight difference is in the shift of the C=O group of compound [80], owed to the more electronegative character of the aromatic fragment, with respect to the ones of species [71] and [79]. Another difference refers to the number of signals corresponding to the OCH₂ groups within the polyglycolic chain, namely the overlapping of two signals in the case of compounds [78] and [79] due to similar surroundings.



Regarding the $^{11}\text{B}\{^1\text{H}\}$ -NMR spectra (Figure 55), the fact that the resulting compounds are very similar since the substituents have no significant influence in the cluster, is translated in an unique change that is the passage from the reagent to the product; in the first case we have a boron atom, the B(8), bounded to an oxonium atom and in the final product this boron is bounded to an etheric oxygen, due to ring cleavage. This difference is corresponding to a slight shift in the position of the boron atoms bounded to B(8).



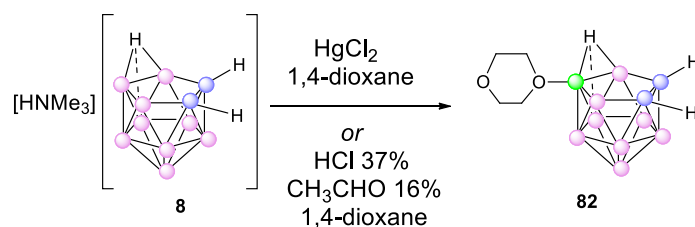
2.5. Cyclic oxonium derivatives of polyhedral boron hydrides

Since polyhedral boron hydrides are commonly considered as three-dimensional aromatic systems,²¹⁴ it is reasonable to assume that substitution reactions in these systems can be described in the framework of the mechanisms of electrophilic aromatic substitution. However, in the same time, considering the hydride character of the hydrogen atoms belonging to the polyhedral boron clusters another mechanism exist, which involves the primary attack of the electrophilic agent, resulting in the simultaneous elimination of hydride and electrophile to form a carbocation-like centre on the boron atom, which is then subjected to the attack of a nucleophilic species. This mechanism is called electrophile-induced nucleophilic substitution (EINS). In the absence of a strong nucleophilic agent, even weak nucleophiles, such as ether solvent molecules, can attack the positive boron atom, leading to the formation of the corresponding oxonium derivatives.²⁹

2.5.1. Syntheses and characterization of the starting cyclic oxonium derivative of polyhedral boron hydrides **82**

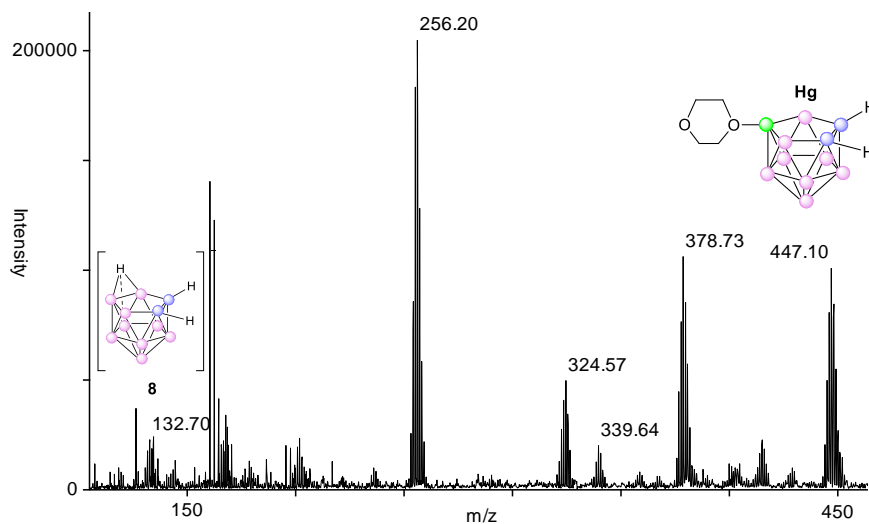
The synthesis of the first oxonium derivatives dates from 1969, when the preparation of two isomeric tetramethylene oxonium derivatives was reported in the reaction of the parent 7,8-dicarba-*nido*-undecaborate anion with FeCl_3 in tetrahydrofuran.²¹⁵ The selective synthesis of symmetrical oxonium derivative [10-(OCH_2CH_2)₂-7,8- $\text{C}_2\text{B}_9\text{H}_{11}$] was reported in be obtained in two ways, starting from the same parent compound, 7,8-dicarba-*nido*-undecaborate, either by i) reaction with HgCl_2 and 1,4-dioxane or by ii) treatment with acetaldehyde in a mixture of toluene, concentrated HCl and 1,4-dioxane,²¹⁶ as described in Scheme 16.

We have synthesized compound **82** by applying the methodology described at point ii), and leaving the reaction mixture under stirring at room temperature for 4 hours. After this period, the solvent was evaporated to dryness followed by extraction with toluene, leading to the obtaining of a light-yellow precipitate with a yield of 61%.



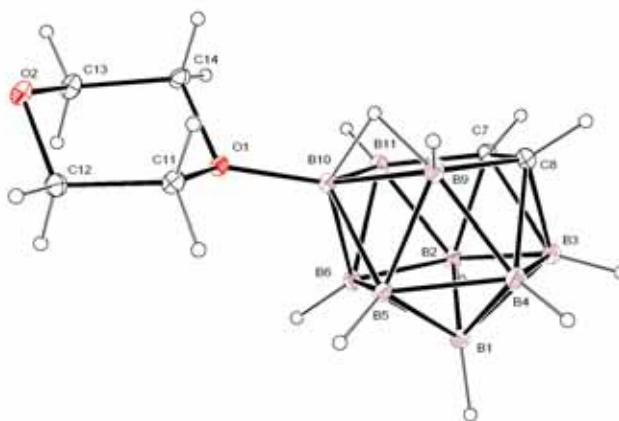
The reason why we did not use the procedure involving HgCl_2 was because even if the data gathered from ^{11}B -NMR indicated that we have synthesized what we thought to be the final neutral compound the sought compound, the results obtained from MALDI-

TOF-MS analysis revealed that the species we synthesized was in fact a compound possessing one Hg atom within its molecule, as indicated in Figure 56 below. The molecular peak corresponding to the zwitterionic species should appear around 220.5 m/z; yet, not such peak is to be found when applying procedure i). Instead, we get the peak confirming the existence of a Hg atom within our structure.



Once we have established which methodology is to be used in order to obtain the desired species, the following step was the characterization of what we wanted to be the starting material for a range of reactions, namely compound **82**.

What is more, we have also obtained a crystalline structure of species **82**, illustrated in Figure 57.



For a better assignment of the peaks, we overlapped the NMR spectra of the parent trimethylammonium salt of 7,8-dicarba-*nido*-undecaborate anion with the ones of the resulted zwitterionic species, illustrated in Figures 58 and 59.

Figure 58. ${}^1\text{H}\{^{11}\text{B}\}$
(blk)

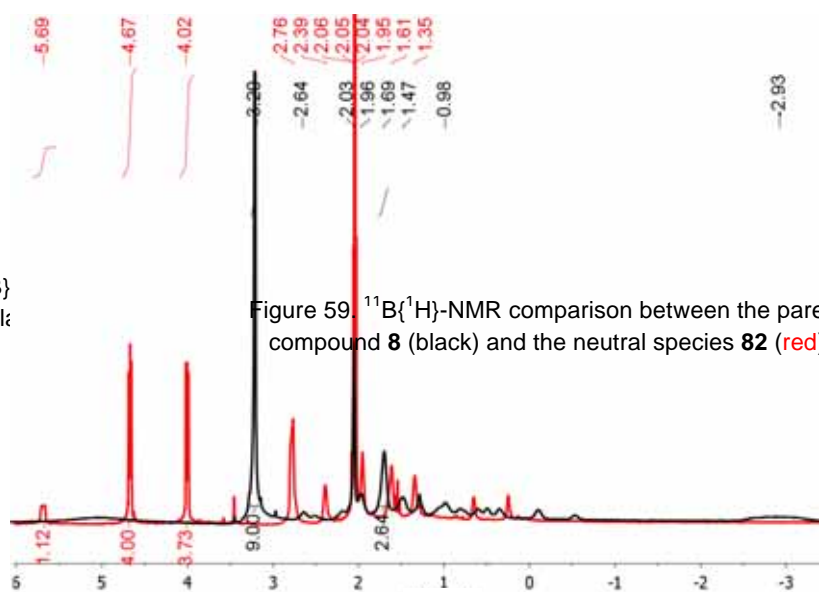
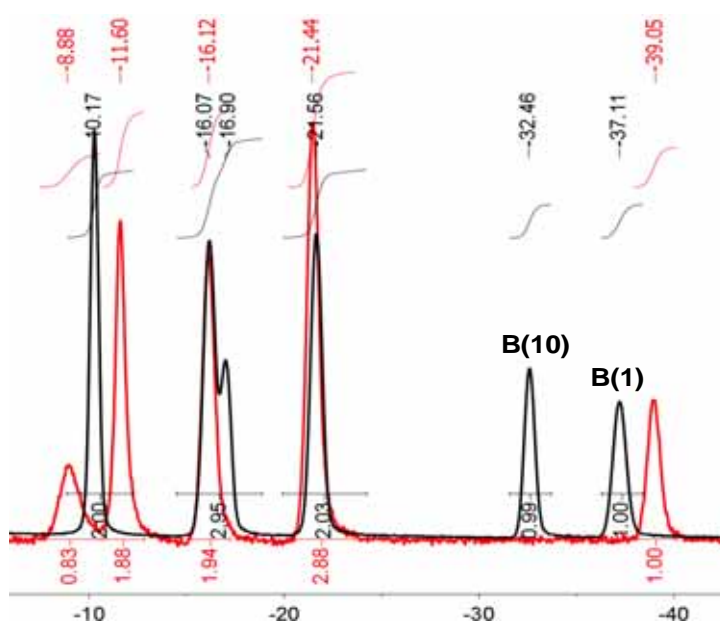


Figure 59. ${}^{11}\text{B}\{^1\text{H}\}$ -NMR comparison between the parent compound **8** (black) and the neutral species **82** (red)

The main conclusion that can be drawn from the ${}^1\text{H}\{^{11}\text{B}\}$ -NMR comparison is the significant chemical shift to lower field values suffered by the bridged hydrogen remaining at the open C_2B_3 pentagonal face regarding species **82**. Initially, in the starting compound, this hydrogen appears at -2.93 ppm, but following the nucleophilic attack on the oxygen atom, it becomes more acidic and shifts about 8.6 ppm to lower field values, namely at +5.69 ppm. Moreover, this particular peak is a quadruplet with equal intensities due to the two equivalent neighboring boron atoms. The $\text{C}_c\text{-H}$ bonds have more or less at the same chemical shift, showing at 1.69 ppm in the case of compound **8** and at 1.61 ppm for species **82**, respectively. The other signals in the range 2.74 to 1.35 ppm belong to the B-H bonds.

With respect to the ${}^{11}\text{B}\{^1\text{H}\}$ -NMR analysis, one can clearly observe the effect of the introduction of the dioxane ring within the molecule. First of all, the boron atom directly bonded to the 1,4-dioxane ring (B(10)) becomes more deshielded and suffers significant chemical shift to lower field values, from -39.05 to -8.88 ppm.



The main conclusion that can be drawn from the ${}^1\text{H}\{^{11}\text{B}\}$ -NMR comparison is the significant chemical shift to lower field values suffered by the bridged hydrogen remaining at the open C_2B_3 pentagonal face regarding species **82**. Initially, in the starting compound, this hydrogen appears at

Secondly, due to the same electronwithdrawing effect of the positive oxygen atom on the dioxane ring, the boron atom bonded to both carbons, B(3), shifts about 5 ppm to higher field values, from -16.90 to -21.56, fact confirmed also by the integration value.

2.5.2. Syntheses of 7,8-dicarbano-*nido*-undecaborate bearing different end groups

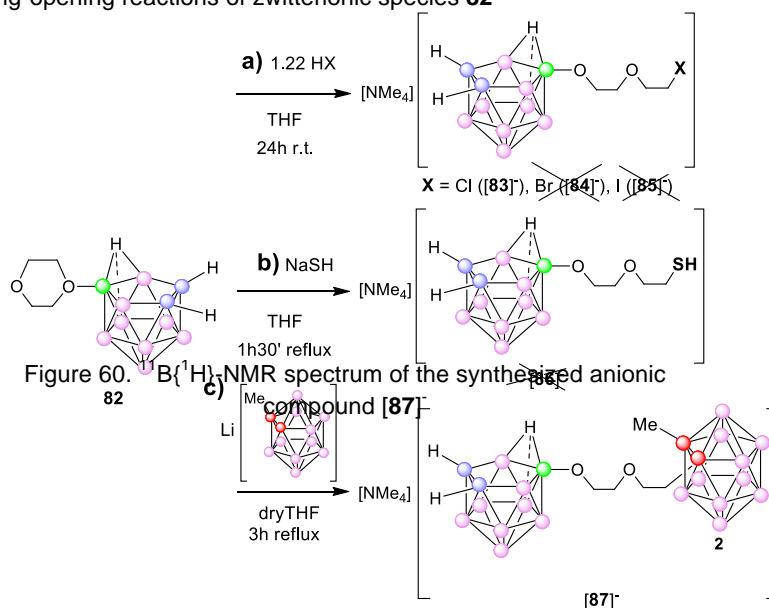
Now that we have fully characterized our starting compound **82**, we wanted to determine if it possesses the same chemical activity as its metallocarborane analogous, the zwitterionic species of cobaltabis(dicarbollide), **6**.

The fact that despite their high stability oxonium derivatives were proven to act as alkylating agents is especially attractive in the case of cyclic oxonium species, where breaking one carbon-oxygen bond would result in a moiety having a carboranes cluster separated from a carbocationic centre by a chain of 6 atoms. In this way, molecules with a reasonable length spacer between the carboranes cage and the property-determining fragment of the molecule could be prepared. Although this type of synthesis seems simple enough to occur with halogens as nucleophilic agents, the only example of oxonium ring-opening with halide ions is the reaction of pentamethylene oxonium derivative of *closo*-dodecaborate with fluorides, whereas the similar reaction with chlorides results in the recovery of the starting material.²¹⁷ The ring-opening reactions of cyclic oxonium compounds with sulphur nucleophiles are rare and include the ring-opening reactions of cyclic oxonium species of the *closo*-dodecaborate²¹⁸ and *closo*-decaborate²¹⁹ anions with hydrosulphide.

Based on the results described so far, we report in this chapter the attempts of ring-opening reactions of 1,4-dioxane ring with nucleophiles such as halogens and thiol groups.

Nonetheless, applying the same reaction conditions, the 1,4-dioxane ring-opening using bromine, iodine (Scheme 17a) or thiolate groups (Scheme 17b) as nucleophiles did not give rise to the sought compounds, but to a recovery of the starting material. However, by succeeding in opening the oxonium ring with chlorine, we showed that these type of reactions do occur; therefore, further studies are required to synthesize the other halogen derivatives, such as increasing the reflux time or changing the solvent in order to be able to increase the temperature of reflux.

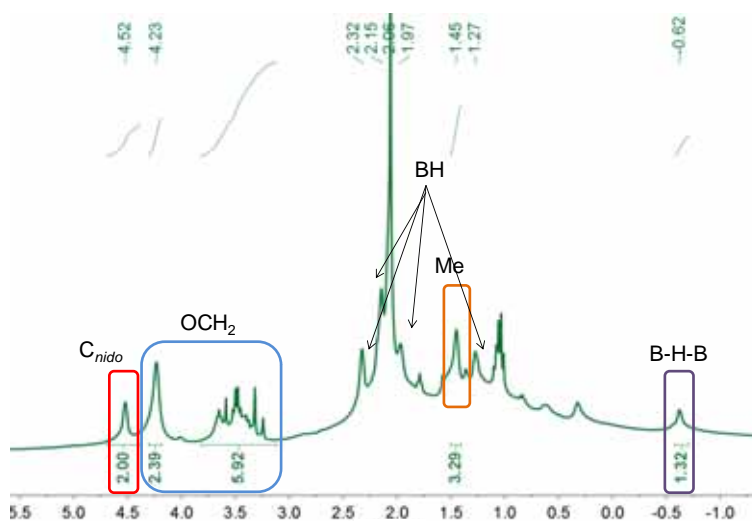
Another point of interest was the ring-opening reaction of **82** using the carboranyl anion as nucleophilic agent. The first step is the lithiation reaction of the Me-*o*-carborane cluster, substituting the hydrogen atom with a lithium one. Then, the attack of the resulting carboranyl anion on the positive oxygen atom belonging to the neutral closed-dioxane ring compound, gives rise to the desired species [**87**], as depicted in Scheme 17c.

Scheme 17. Ring-opening reactions of zwitterionic species **82**

2.5.3. Characterization of 7,8-dicarba-*nido*-undecaborate bearing different end groups

As presented before, the ring-opening reaction for compound **82** proved to be quite difficult, and the nucleophilic agents used

Regarding ring-opening with the Me-*o*-carborane-based derivative one can observe from the $^1\text{H}\{-^{11}\text{B}\}$ -NMR spectra for compound **[87]**, the peak that appears at 4.52 ppm and integrates 2 belongs to the $\text{C}_c\text{-H}$ bonds from the *nido*-carborane cage, whereas the ones at 4.23 and 3.3-3.7 ppm correspond to the OCH_2 groups (Figure 60).



Regarding the $^{11}\text{B}\{^1\text{H}\}$ -NMR spectra comparison for the halogen-terminated synthons, the analysis indicates that only the species resulted from the reaction with concentrated HCl is obtained as final compound, whereas for the other ring-opening reactions, the starting material is recovered.

The $^{11}\text{B}\{^1\text{H}\}$ -NMR for compound **[87]** perfectly illustrates the presence of both *closo* and *nido* carborane clusters within the same molecule, as shown in Figure 61. This is also supported by the integration values, which clearly indicate that there are 9 boron atoms belonging to the *nido* cluster and 10 borons coming from the *closo* Me-carborane cage.

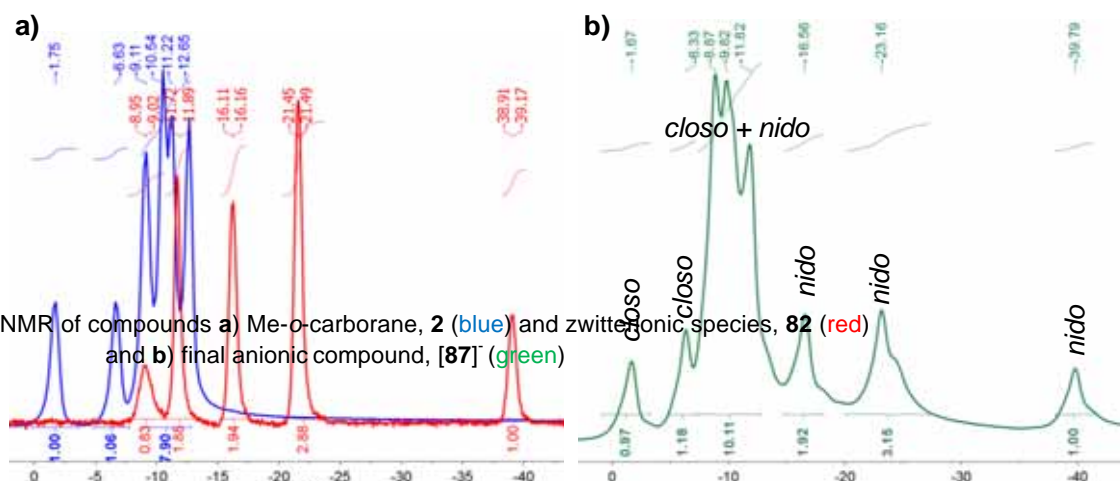


Figure 61. $^{11}\text{B}\{^1\text{H}\}$ -NMR of compounds a) Me-o-carborane, **2** (blue) and zwitterionic species, **82** (red) and b) final anionic compound, **[87]** (green)

The general conclusion is that compound **82** is not as chemically active as zwitterionic metallacarborane species **6** since it does not give rise to the same open-ring derivatives as the latter. This can be explained since in the case of the former, the negative charge is localized over the open C_2B_3 pentagonal face, and therefore, the approaching nucleophile is subjected to electronic repulsions. For the metallacarborane derivative, which presents the negative charge delocalized over the entire molecule, such repulsions do not exist, and therefore the nucleophilic attack takes place quite easily, yielding, among many others, the species presented in chapter 2.2.

2.6. Preparation and characterization of MPCs capped with thiol-based boron clusters

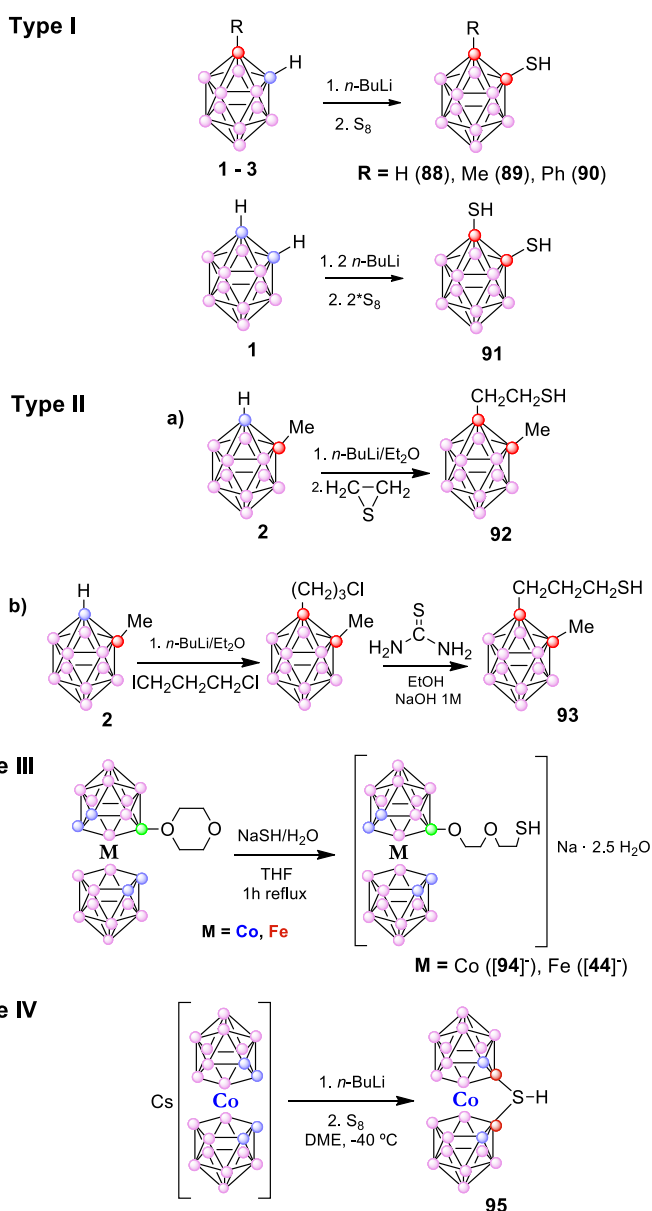
As shown in Chapter 2.2, one of the reasons of ring-opening of **7** with thiol groups was the posterior enclave to different platforms, such as gold nanoparticles, yielding boron-enriched materials with applications in BNCT. Thiolate-stabilized gold nanoparticles, now commonly referred to as monolayer protected clusters (MPCs), have been studied with unabated enthusiasm since the initial report of a simple two-phase liquid/liquid protocol in 1994, which enabled the gram scale preparation of dodecanethiolate-capped particles in the 1.5 to 4 nm size range that were stable under ambient conditions as isolated solids and readily redispersible in nonpolar solvents.²²⁰

The practical importance of MPCs is evidenced, for example, by their current role in the development of artificial nose-type gas sensors with potential applications in lung cancer diagnostics based on breath analysis.²²¹ The first crystal structure of a typical representative of this class of materials stabilized by mercaptobenzoic acid (MBA), $\text{Au}_{102}(\text{MBA})_{44}$, was published in 2007,²²² and others such as $[\text{Au}_9(\text{PPh}_3)_8(\text{NO}_3)_3]$,^{223a} $\text{Au}_{25}\text{L}_{18}$,^{223b,223d} $\text{Au}_{38}\text{L}_{18}$,^{223c} (L = $\text{SC}_2\text{H}_4\text{Ph}$), $[\text{Au}_{25}(\text{PPh}_3)_{10}(\text{SCET})_5\text{Cl}_2]^{2+}$,²²⁴ $[\text{Au}_{20}(\text{PPhpy})_{10}\text{Cl}_4]^{2+}$,²²⁵ $[\text{Au}_{39}(\text{PPh}_3)_{14}\text{Cl}_6]^{2+}$ ²²⁶ followed, generally suggesting that the stability of the clusters stems partly from their electronic closed shell structure²²⁷ as previously observed in series of alkali metal clusters with so-called magic numbers of electrons.²²⁸ Recently, much MPC work has focused on the use of water-soluble clusters for biomedical applications, such as drug and gene delivery and photodynamic therapy.²²⁹ Hydrophilic thiols successfully used as capping agents for this purpose include sugars,²³⁰ peptides,²³¹ polymetacrylate,²³² and polyethylene glycol (PEG) derivatives.²³³ Solubility is a general problem that often poses limits to the chemical versatility of MPCs, which, in principle, could be prepared with any combination of chemical and/or biomolecular functionalities in the ligand shell. In practice, many ligand shell modifications compromise the particles' colloidal stability and cause aggregation. While the chemical properties of MPCs are dominated by those of the functional groups present in the ligand shell, it is well established that the metal core can accept or donate a number of electrons in discrete steps, as evidenced by electrochemical charging experiments.²³⁴ At the cathodic limit this leads, under certain conditions, to the destabilization of the particles by reductive loss of thiolate ligands.²³⁵ The vast majority of electrochemical experiments with MPCs, beginning with Murray's pioneering work that introduced the concept of quantized capacitance charging, have been carried out in nonaqueous media using MPCs stabilized by short chain alkanethiols to enable electron transfer across the ligand shell.²³⁴ The compared to water low dielectric constants of such media implies low double layer capacitances and hence allows the

observation of single electron charging steps at the expense of limiting the amount of charge that can be stored on each cluster. In water, colloidal metals acting effectively as electron pools have been known for some time and were first reported by Henglein and co-workers,²³⁶ but charge-dependent transfer of metallic particles across the water/oil interface has not been observed in any system reported to date.

2.6.1. Synthesis and characterization of the neutral and anionic capping thioligands

The first step for the obtaining of the MPCs was the synthesis of the capping ligands. Two different families of capping thiolate ligands were designed: neutral (**Type I** and **II**)



and anionic (**Type III** and **IV**).

The procedure was somewhat different depending on the type of the nature of ligands. These are presented in Scheme 18.

Type I: Formation of C_c-SH bonds. This type of reactions consist in a nucleophilic substitution reaction, S_N2. The first step is the removal of an H atom by a strong base, such as *n*-BuLi, followed by the nucleophilic attack of the *o*-carboranyl lithiated salt on the sulphur atom, to yield the corresponding thiol group.

Type II: There is an organic spacer present between C_c and the SH group. Two different reactions were designed.

a) These reactions resemble **Type I**, with the only difference in the choosing of the electrophile, which, in this case, is a cyclic thioether. The final thiol group is obtained

from the lithium thiolate moiety, by extracting the reaction mixture with dilute hydrochloric acid.

b) The procedure in this kind of reactions is based on the same nucleophilic attack of the carboranyl group on the C-I bond, with the formation of lithium iodine salt, which shifts the equilibrium to the obtaining of the chlorinated derivative as an intermediate. This compound was then treated with thiourea in ethanol and refluxed for four hours, at which point, sodium hydroxide solution was added. After another two hours of reflux, the desired thiol was extracted with ethylic ether.

Type III: reactions suppose, as previously explained in Subchapter 2.2.2, the nucleophilic attack on the positively charged oxygen atom by the thiolate group,¹⁸⁹ leading to the monoanionic thioligands [44] and [94].

Type IV: to obtain carbon derivatives, by direct deprotonation of the C_{cluster}-H groups of cobaltabis(dicarbollide) using a strong base, such as *n*-BuLi. The synthesis of this compound consists in a deprotonation reaction of 4, at -40 °C leading to a dark-blue solution of the corresponding dilithiated species.^{22b} Following this reaction, elemental sulphur, S₈, is added. While the reaction mixture is stirred at room temperature for about two hours, and then refluxed overnight, the carbanions formed attack, as nucleophiles, the S₈ cycle. After this period, the C_{cluster}-S bond is formed and the compound was precipitated as tetramethylammonium salt, and purified by several thin layer chromatographies, leading to a dark-orange compound. This reaction does not proceed in the same manner that in the case of *o*-carborane, since the final product does not contain a thiol moiety (even if excess of acid was added, in order to protonate the sulphur), but a different species, with a sulphur atom bonded to both of the dicarbollide units, yielding in fact a zwitterionic species.

The resulting compounds, both neutral and anionic, were characterized employing techniques such as FTIR, ¹H, ¹¹B, ¹³C-NMR, and MALDI-TOF-MS. FTIR absorption bands values are presented in Table 11.

Compound	$\nu(\text{C}_c\text{-H})$	$\nu(\text{C-H})_{\text{alkyl}}$	$\nu(\text{B-H})$	$\nu(\delta(\text{CH}_2))$	$\nu(\text{C-O-C})$
88	3063	2987, 2902,	2567	1456	1122, 1134, 1070
89	-	2941, 2856	2570	1442	1105, 1049
90	-	2987, 2903	2596, 2566	1495, 1446	1076, 1004
91	-	2988, 2902	2565	1487, 1461	1079, 1014
92	-	2988, 2886	2593, 2569	1442, 1418	1250, 1173, 1078
93	-	2988, 2902	2593, 2560	1442, 1390	1250, 1173, 1078, 1028
[94]	3037	2934, 2875	2555, 2521	1455	1246, 1132, 1095, 1054
[44]	3032	2930, 2872	2527	1455, 1352	1246, 1113, 1090, 1057
95	3069	2931, 2873	2576, 2540, 2506	1458	1106, 1036

Results and discussions

Table 11. FTIR spectroscopy of compounds [44], 88-95

Figure 63. Comparison between ^{11}B -NMR and $^{11}\text{B}\{^1\text{H}\}$ -NMR for compound 95
 A comparison between the ^1H -NMR spectra coupled (black) and decoupled (gray) of neutral compound 93 is illustrated in Figure 62.

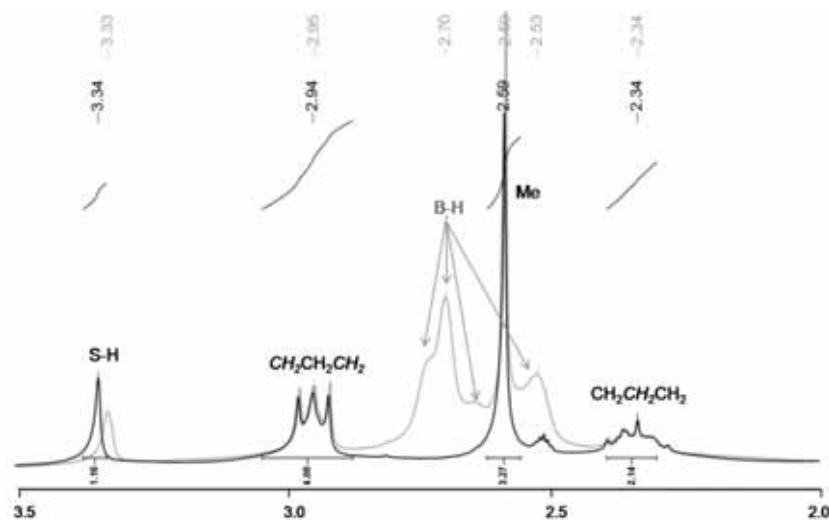
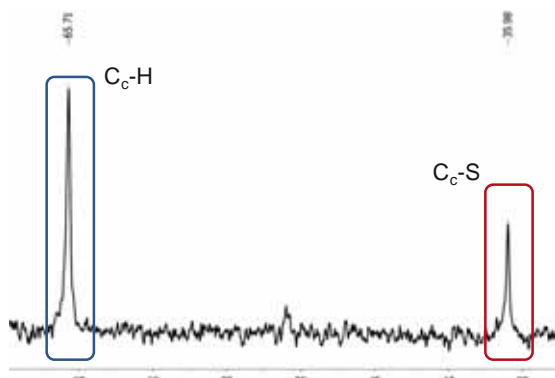
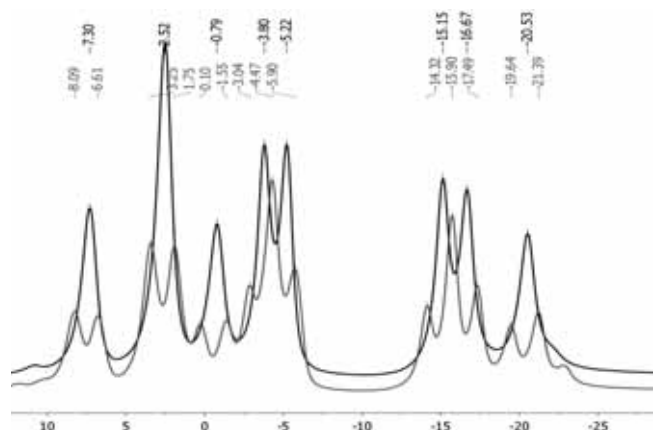


Figure 62. Comparison between ^1H -NMR and $^1\text{H}\{^{11}\text{B}\}$ -NMR for compound 93 run in CDCl_3

The signal which appears at the lowest field value, 3.34 ppm, belongs to the H bonded to sulphur, whereas the peak at 2.94 ppm is characteristic to the CH_2 - groups bonded to the two electronwithdrawing moieties within the cluster, namely the *o*-carborane unit and the sulphur atom. The proximity to these fragments determines the deshielding of the CH_2 - groups and, as a direct consequence, the downfield shift.

Figure 61 presents a comparison between the ^{11}B - and $^{11}\text{B}\{^1\text{H}\}$ -NMR spectra of compound 95, in order to illustrate the fact that the substitution did not take place at neither one of the boron atoms, since every single peak appears decoupled, but at the carbon atoms within the cluster.

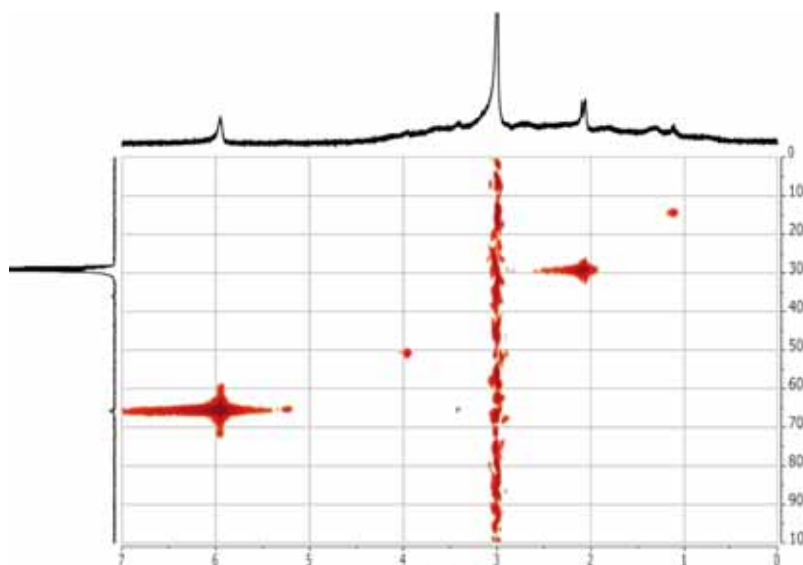


The $^{13}\text{C}\{^1\text{H}\}$ -NMR spectrum brings additional information about the obtaining of the desired species. As indicated in Figure 64, the two peaks corresponding to the $\text{C}_c\text{-S}$ and to $\text{C}_c\text{-H}$, respectively, appear

Results and discussions

at 36 and 65 ppm, signals registered using deuterated acetone.

This information was extracted after performing a $^1\text{H}^{13}\text{C}$ -HETEROCOSY NMR, which allowed us to precisely assign the carbon signals corresponding to the C-H bonds and the ones belonging to the C-S bridge (Figure 65). One can clearly see how the carbon signal at 65 ppm interacts with the hydrogen peaks appearing at about 6 ppm, peak that corresponds to the C-H bonds within the neutral metallacarborane species **95**. Therefore, the remaining carbon peak was assigned to the C-S bond, since no interaction with the sandwich complex was present.



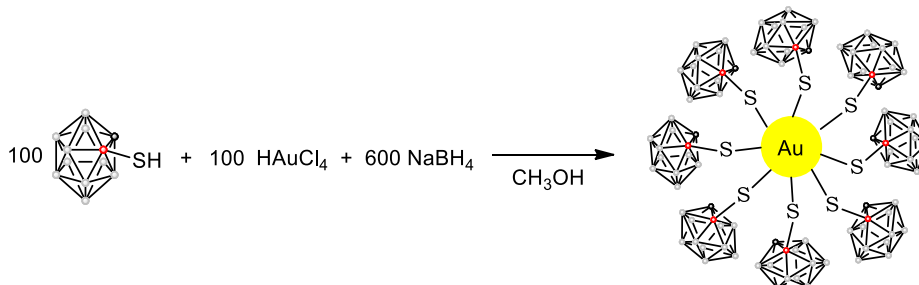
2.6.2. Preparation of MPCs capped with boron clusters containing thioligands by reducing with sodium borohydride

In order to develop the synthetic procedure, we chose *o*-carborane monothiol substituted species, **88**, because of its perfect icosahedral geometry as well as for its extreme chemical and thermal stability. However, the main drawback of this cluster, like its derivatives, is highly hydrophobic and generates water-insoluble structures with limited bioavailability being therefore unsuitable for application in BNCT.^{56,151a,237} The choosing of the mercaptocarborane ligand was also very helpful for the development of the synthetic procedure, since it has the simplest structure among the presented thioligands. However, a major advantage of this species with respect to the other

Results and discussions

ligands is that we have C-H bond present within the molecule, moiety that would later on be useful for further substitutions.

The preparation of the MPCs consists in dissolving of the mercaptocarborane in



methanol, followed by the addition of the same number of equivalents of chloroauric acid. Immediately after, this yellow solution was treated with a 6-fold excess of sodium borohydride, also dissolved in methanol. After stirring for ten minutes at room temperature, the solvent was removed by rotary evaporation, as presented in Scheme 19.

While in previously reported single- and biphasic preparations of MPCs any excess of borohydride appears to be tolerated, this system here is very sensitive to the amount of borohydride added, so that once a threshold of more than 6-fold stoichiometric excess with respect to Au(III) reduction is reached, the clear brown solution of nanoparticles turns abruptly into a black slurry followed by irreversible precipitation of the entire gold content as a black powder. Also as purified particles, the MPCs remain prone to decomposition in the presence of a large amount of borohydride. This property indicates that unlike other MPCs, these are amenable to further reduction by borohydride and eventually suffer reductive loss of the protective thiolate ligands, which has previously only been observed in electrochemical experiments using MPCs capped with hexanethiol.²³⁵ We attribute this to the necessary openness of the ligand shell resulting from the fact that it is impossible to cover a sphere (Au core) with smaller spheres (carboranes) without leaving gaps and to the very small diameter of the carborane of about 0.5 nm, which may still allow electron transfer from borohydride to

the gold core across the ligand shell. Given the size of the carborane, the gaps will not be narrower than 0.25 nm, even at closest packing of carborane spheres, and thus will permit most ions and small molecules direct access to the gold surface.

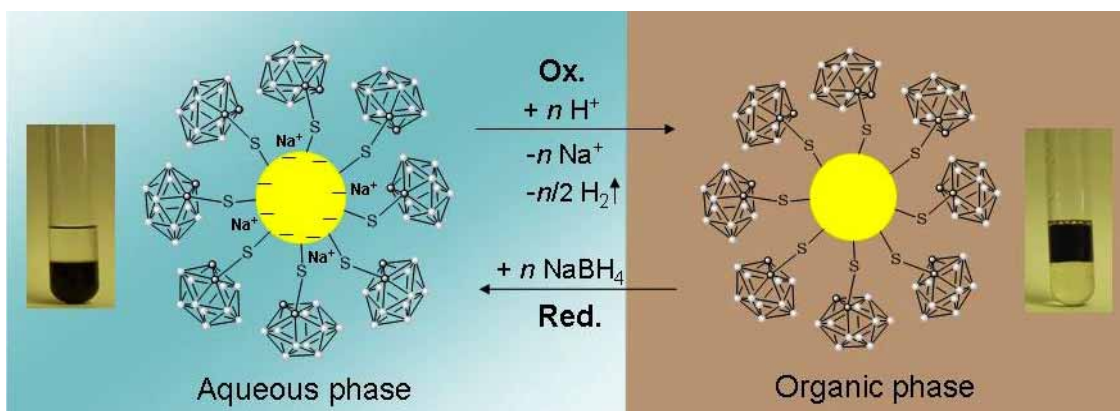
The dark-brown residue was first thoroughly washed with diethyl ether to remove excess mercaptocarborane and then dissolved in isopropanol and filtered to remove the remaining sodium borohydride and other insoluble contaminants. After rotary evaporation of the isopropanol, the final product was obtained as a dark-brown solid.

To our surprise, this newly obtained material dissolves not only in alcohols and acetone but also in water, while it is insoluble in diethyl ether and less polar solvents. In theory, MPCs consisting only of a gold core and a shell of mercaptocarborane ligands should be very hydrophobic and hence completely insoluble in water. Hence, their solubility in polar solvents therefore is a much unexpected finding.

The perhaps more interesting property of the particles is their reversible transfer from water to diethyl ether achieved by acidification of the aqueous phase with dilute hydrochloric acid. Upon addition of the acid, the particles precipitate from the aqueous phase under evolution of a small amount of gas, presumably hydrogen (also in the absence of borohydride), and redissolve readily in the organic phase. In a two-phase system direct extraction from the aqueous to the organic phase is observed. Re-

Scheme 20. Model illustrating the nanoparticles both as electron and ion storage devices

extracting the particles into an aqueous phase is possible by addition of sodium borohydride but cannot be achieved simply by an alkaline aqueous phase. This demonstrates that it is not an acid–base reaction but a redox reaction that switches the solubility of the particles. The process is completely reversible, and the same particles can be isolated as a solid, redissolved, and moved back and forth between diethyl ether and water phases without any evidence of aging effects. A simple model that describes the particles as both electron and ion storage devices is presented in Scheme 20.



In the presence of sodium borohydride, the core charges up negatively by storing a number of excess electrons, which are counter balanced by sodium ions occupying the voids between the carborane spheres on the surface of the particle. The cathodic limit of this charge storage process is the observed decomposition of the material by reductive desorption of ligands, for example, after addition of excess borohydride. This structural model also explains the observed anionic behavior of the particles.



As illustrated in Scheme 21, the dissociation of sodium ions from the core leads to the formation of giant polyanions, which can be extracted into nonpolar solvents with tetraoctylammonium bromide,

as shown in Scheme 21. Positive charging of the core by reaction with suitable oxidizing agents has not been attempted but should be an interesting goal of future work along with a full electrochemical characterization of these materials. The stored electrons are removed from the gold core by mild oxidation in dilute acid under evolution of hydrogen, as also shown in Scheme 20. Concurrently, sodium ions desorb, and the particles become much less hydrophilic and either precipitate or transfer to the organic phase if present.

Finally, a simple experiment was conducted in order to demonstrate that the voids between the carboranes could be irreversibly filled by a suitable molecular stopper, such as octanethiol. A day after addition of a small amount of octanethiol to a solution of MPCs in diethyl ether, the transfer the particles to water by addition of borohydride was no longer possible. Also, the particles were now tolerant to a large excess of borohydride in the aqueous phase and did not decompose, suggesting that charging of the metal core by direct access of the reducing agent through voids in the ligand shell was no longer possible.

The purified MPCs obtained as dark-brown solids were subjected to a number of complementary analytical techniques typically employed for the characterization of such materials. We have characterized these new MPCs by UV-vis, infrared, and NMR spectroscopy, centrifugal particle sizing (CPS), transmission electron microscopy (TEM), and in some cases by scanning transmission electron microscopy-high-angle annular dark field (STEM-HAADF), thermogravimetric analysis (TGA), differential scanning calorimetry (DSC), quantitative analysis of boron, gold, and sulfur by X-ray photoelectron spectroscopy (XPS), and atomic emission spectroscopy (AES).

Results and discussions

Figure 66 shows the FTIR spectra of mercaptocarborane **88** (red) and that of the corresponding MPCs (black). The main characteristic bands are labeled in both cases. Strong broad absorptions at $2596\text{--}2573\text{ cm}^{-1}$ in both the pure mercaptocarborane and the final MPCs, due to B-H stretches, dominate the FTIR spectra and support that the *closo* cluster structure is preserved in the MPCs.²⁰⁶ In addition, the FTIR spectrum of MPCs exhibits C(H) stretch absorption at 3063 cm^{-1} confirming the presence of C_{cluster}-H bond²³⁸ in the gold nanoparticles. Comparison of the spectra demonstrates that mercaptocarborane is the effective component of the MPCs.

The presence of the mercaptocarborane in the ligand shell of the nanomaterial was further confirmed by ¹H and ¹¹B-NMR spectroscopy in deuterated acetone, as depicted in Figure 67a and 67b, respectively. The ¹H-NMR clearly shows the absence of the S-H proton after attachment of the ligand to the gold nanoparticle surface. Furthermore, the broad single resonance corresponding to C_{cluster}-H bond²³⁹ moves from 4.84 to 4.42 ppm once the ligand coordinates to the gold nanoparticle.

Figure 67b shows a comparison between the ¹¹B-NMR spectrum of our MPCs and the NMR spectrum of mercaptocarborane alone. While there are clear differences in the peak patterns indicating a strong interaction between the ligand and the metal core, the range of the chemical shifts fully coincides in both spectra giving further

evidence that the *closo* structure is retained in the final MPCs. Most notably, the peak at $\delta 5.5$ ppm in the spectrum of the pristine mercaptocarborane shifts upfield in the MPCs as a result of the gold bonding.

This has been reported before for the corresponding carboranylthiolates after coordination to metal, in which the sulfur provides a bridge to transfer electron density

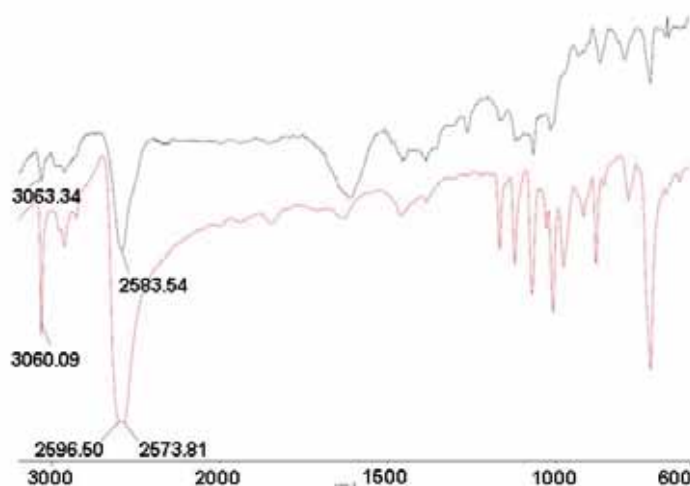
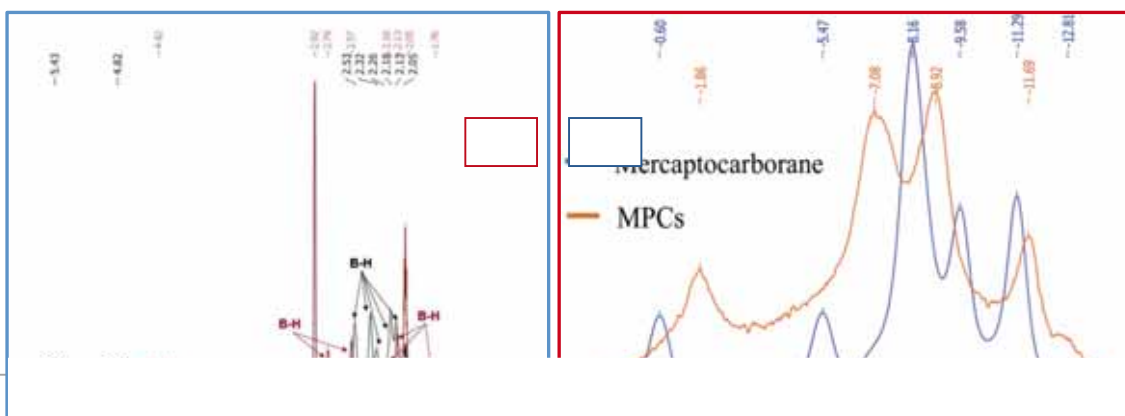
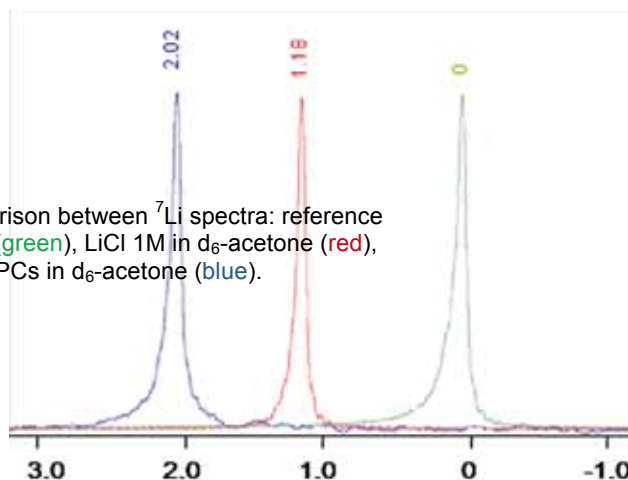


Figure 67. a) Comparison between ¹H/¹¹B-NMR spectra of **88** (black) and MPCs (red); in Figure 67a and 67b, respectively. The ¹H-NMR clearly shows the absence of the S-H proton after attachment of the ligand to the gold nanoparticle surface. b) Comparison between ¹¹B-NMR spectra of **88** (blue) and **88** attached to MPCs (orange).



from the rich transition metal to the electron-deficient carborane cage.²⁴⁰ Thus, the carborane electron density in the MPCs is higher than in the parent thiol.

In order to demonstrate the ability of the MPCs to store ionic charge, we passed a sample dissolved in water through a lithium ion exchange column²⁴¹ and subsequently analyzed by ⁷Li-NMR spectroscopy, as shown in Figure 68. Using acetone as solvent, a single sharp peak at 2.02 ppm in the ⁷Li NMR spectrum of the MPCs was observed. This is clearly indicative of the presence of lithium ions in the



MPCs. In addition, by comparison with a reference solution of lithium chloride in acetone, the Li resonance in the MPCs is about 1 ppm deshielded. This evidence that the lithium in MPCs is not so thoroughly solvated by acetone as it is in the case of lithium chloride in the same solvent and that lithium ions polarize electron density from its surroundings, either from the gold nanoparticle or the hydrogen B-H vertexes, that possess a partial hydride character or both. One should take into consideration the fact that in aqueous medium sodium ions are strongly associated with the MPCs and are probably located in the voids between adjacent mercaptocarborane cages. In the exchange column, they are replaced stoichiometrically by lithium ions, which are now sitting inside the voids in contact with or close proximity to the gold surface.

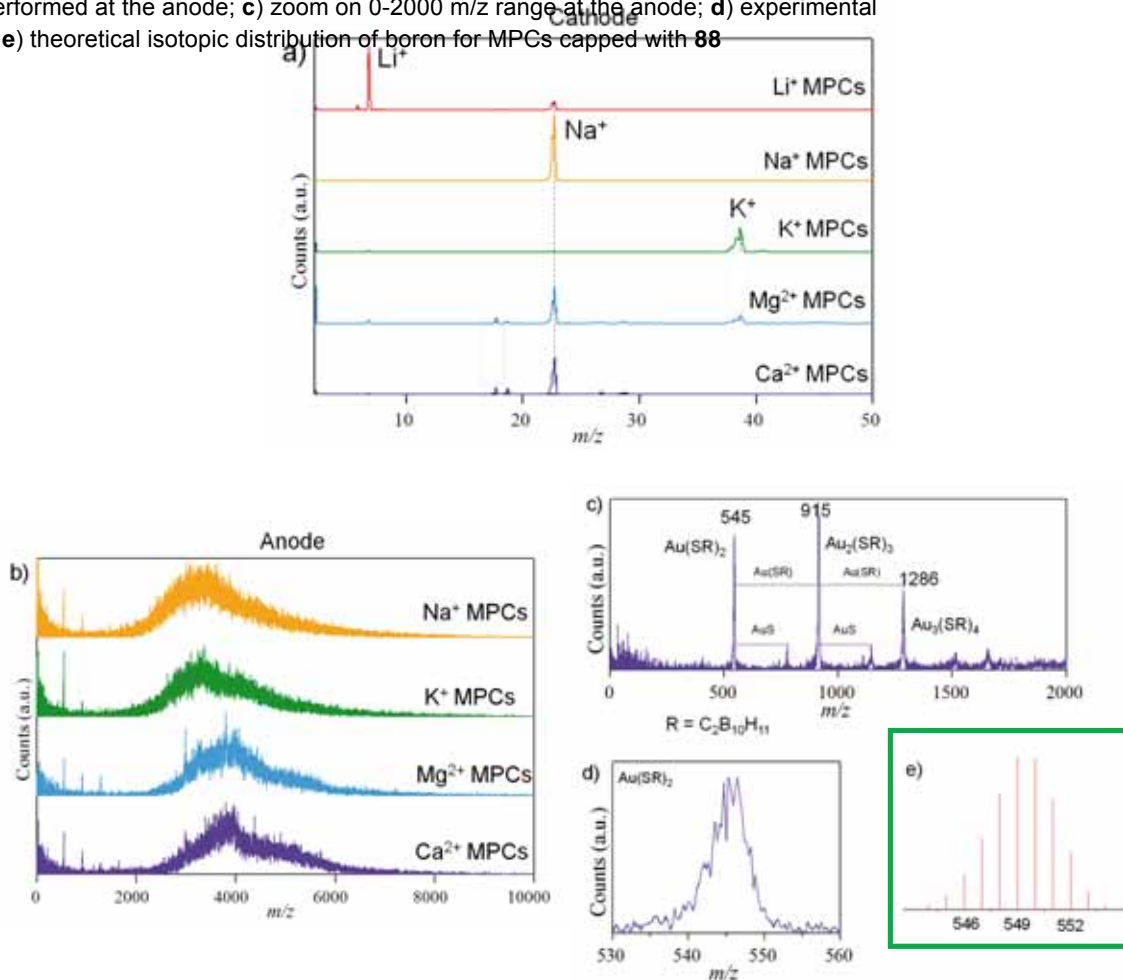
Moreover, we interchanged the initial Na⁺ cation with Li⁺, K⁺, Mg²⁺ and Ca²⁺, by passing a solution of water soluble MPCs through a cation-exchange resin charged with the corresponding cation, to determine if the cation itself had any influence on the MPCs. MALDI-TOF-MS performed at the cathode showed that only Na⁺ can be interchanged by other alkali metals such as Li⁺ or K⁺. With alkali-earth metals, such as Mg²⁺ and Ca²⁺, there is no cation-exchange even if the aqueous solution of the MPCs is passed more than 7 times through the resin as represented in Figure 67a.

MALDI-TOF-MS performed at the anode (Figure 69b) shows two distinctive parts: the peak in the range 3000-5000 m/z correspond to the molecular weight of the MPCs, whereas the range 500-1300 m/z indicates the formation of smaller MPCs. As indicated in Figure 69c, the lowest peak appearing at 545 m/z indicates a Au(SC₂B₁₀H₁₁)₂ unit, the one at approximately 915 m/z corresponds to Au₂(SC₂B₁₀H₁₁)₃ and the peak at 1286 represents the Au₃(SC₂B₁₀H₁₁)₄ unit, all in agreement with recent reported units

Results and discussions

covering a Au₂₃ gold cluster.²⁴² Likewise, the isotopic distribution presented in Figure 69d further confirms the functionalization of the MPCs with boron-based clusters, **88**.

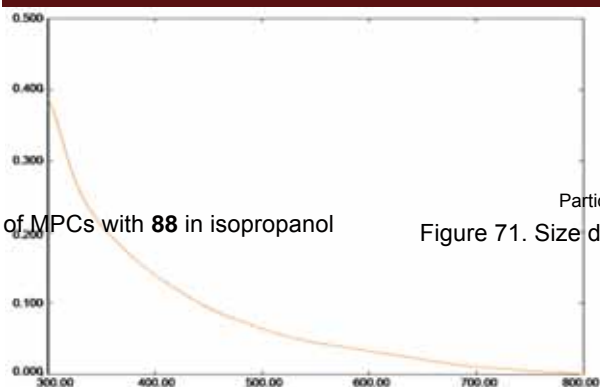
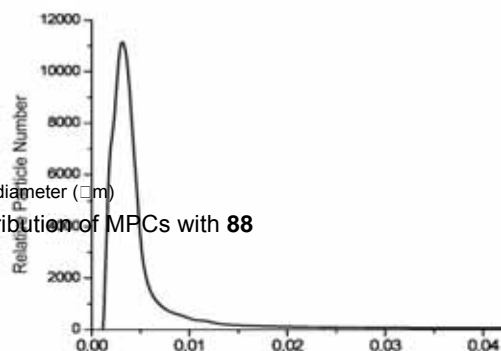
Figure 69. a) MALDI-TOF-MS performed at the cathode on MPCs functionalized with thioligand **88**; b) MALDI-TOF-MS performed at the anode; c) zoom on 0-2000 m/z range at the anode; d) experimental and e) theoretical isotopic distribution of boron for MPCs capped with **88**



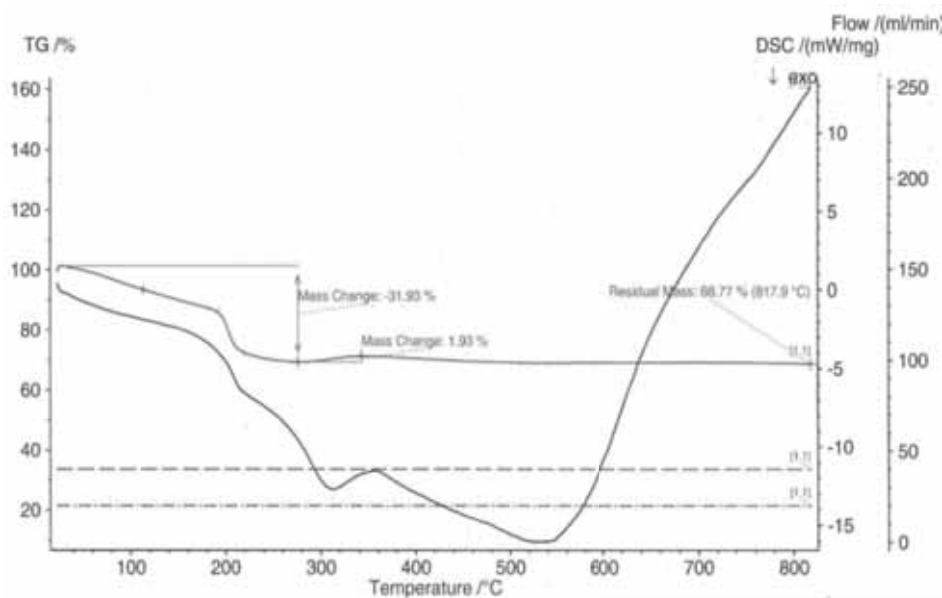
Another technique typical for nanoparticles characterization is UV-vis spectroscopy. This technique gives the typical featureless spectra indicative of particles with a core diameter below 3 nm showing in the UV range strongly increasing absorption with decreasing wavelength due to d-band transitions, while a plasmon band is absent, as illustrated in Figure 70.

Moreover, the absence of a plasmon band in the UV-vis spectrum of the material confirms that the typical gold core size is below 3 nm.

Results and discussions

Figure 70. UV-vis. of MPCs with **88** in isopropanolFigure 71. Size distribution of MPCs with **88**

This is further confirmed by the centrifugal particle sizing (CPS), a technique that reaches its limitation at the 5 nm and below range. As presented in Figure 71, a mean particle size including the ligand shell of 3.2 nm was estimated. Taking into account the known diameter of the carborane cage of near 0.5 nm,²⁴³ a total gold particle diameter of 2.1 nm would be expected as presented above. Partial elemental analysis was also carried out for Au and B by ICP-AES and for Au, B, and S by XPS. By ICP-AES, a Au:B molar ratio of 1:6.5 was found, while a Au:B:S relative molar content of 2.17:16.15:1.31 was obtained by XPS. TGA gave a weight loss of 31.93% attributable to the loss of mercaptocarborane ligands, as shown in Figure 72.



These results are all in good agreement with each other and indicate an average proportion of 0.6 ligand molecules per gold atom. This empirical ratio is rather large in comparison to that of well-known MPCs of gold, such as $\text{Au}_{102}(\text{SR})_{44}$ ²⁴⁴ or $\text{Au}_{144}(\text{SR})_{60}$,²⁴⁵ but can be explained by the minority presence of a significant population

of extremely small clusters and even complexes that only contain a single gold atom, probably of the type $\text{Au}(\text{SR})_2$, as evidenced by STEM-HAADF images (Figure 73). In addition, mercaptocarboranes differ significantly from the typically used alkanethiols, and it can be argued that they should favor a somewhat higher ligand coverage. Conventional thiols do not exhibit the same acidity, volume, self-organization possibilities, and coordinating character of the sulfur atom nor the same possibility to generate interactions between each other as do mercaptocarboranes.²⁴⁶ The rigid and

globular form of the *o*-carborane ligand is very different from that of an alkane. Among typical organic ligands, the closest shape to that of the *o*-carborane cluster would be a rotating benzene moiety,²⁴⁷ but even in

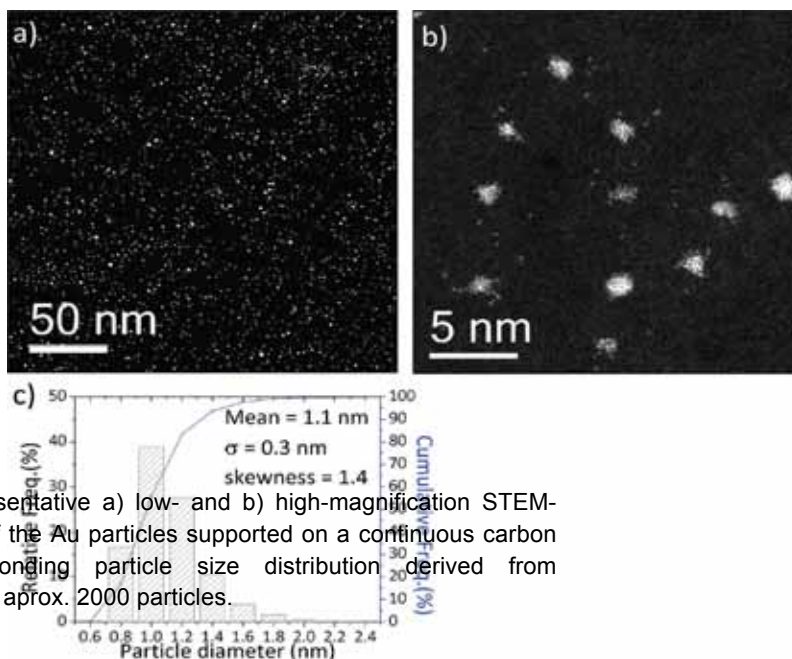
this case, neither the possibility of self-interactions nor the

packing efficiency would be comparable.

The *o*-carborane via its acidic $\text{C}_{\text{cluster}}\text{-H}$ bond

gives rise to hydrogen or dihydrogen interactions with neighboring clusters B-H groups ($\text{C}_{\text{cluster}}\text{-H}\cdots\text{H-B}$).²⁴⁸ These interactions are not possible for alkanes. Thus it is not unreasonable to expect a slightly higher packing density of ligands for the mercaptocarborane MPCs in comparison with organic groups, e.g., alkanes. Moreover, the *o*-carborane attracts electrons through the cluster carbon atoms more readily than benzene.²⁴⁹

This research was completed with the stabilization of MPCs with other thio-carborane clusters shown on Scheme 19. Once the procedure was defined and the ratios of the reagents established for monothiol carborane **88**, we applied the same procedure for the preparation of 3 nm MPCs capped with either neutral or anionic boron-based thioligands, **89-93**. The anionic compounds [**44**], [**94**] and **95** are water-soluble, and therefore their synthesis was performed using water instead of methanol. However, these nanomaterials, although soluble in water, acetone, or isopropanol, did not display



the same phase transfer properties as the ones functionalized with the mercaptocarborane, **88**, namely the reversible transfer of the particles from water to diethyl ether, achieved by acidification of the aqueous phase with dilute hydrochloric acid or from ether to water by addition of sodium borohydride. These newly obtained MPCs were characterized by FTIR, ^1H and ^{11}B -NMR, UV-vis, CPS, ICP-AES and, in some cases, TGA.

The comparison between FTIR spectra of the starting material **90** and its corresponding MPCs is depicted in Figure 74 (*left*). FTIR spectroscopy confirms the presence of the boron-based ligands in the structure of MPCs due to strong broad absorptions at $2557\text{--}2576\text{ cm}^{-1}$, a typical indicative of the presence of B-H bonds of a *closo* cluster confirming that the thioligands retain the initial *closo* structure throughout the MPCs preparation. In addition to this, one can observe the presence of C-H bonds (in the case of sandwich-type ligand, [**94**] $^-$), both in the starting material and in the MPCs indicated by $\nu(\text{C-H})$ stretch absorption at about 3030 cm^{-1} and 3047 cm^{-1} correspondingly, as presented in Figure 74 (*right*).

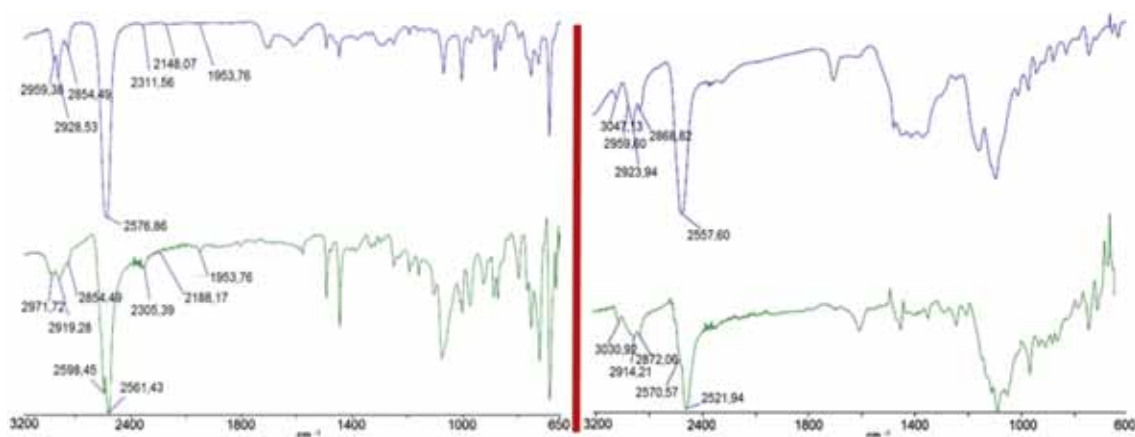


Figure 74. *Left*: Comparison between the FTIR spectra of neutral thioligand **90** (green) and its corresponding MPCs (blue); *Right*: FTIR spectra of anionic thioligand [**94**] $^-$ (green) and its MPCs (blue)

It is also interesting to see the effect of the sodium cation on the MPCs, represented by the coordination of sodium with 2.5 water molecules (determined by TGA), fact that is indicated by the appearance of the absorption bands at about 1400 cm^{-1} .

The NMR analysis completes the characterization of the MPCs, by showing how the S-H is no longer present in the ^1H -NMR spectra after the functionalization of the gold nanoparticles, demonstrating that the bonding of sulphur to the gold core did indeed take place. Regarding the ^{11}B -NMR comparison, the broadening of the boron signals as well as the shift of about 2 ppm towards higher field values indicates the interaction between the ligand and the gold core. Moreover, the spectrum also confirms the fact that the *closo* structure is maintained throughout the preparation procedure (Figure 75).

Results and discussions

2.6. Preparation and characterization of MPCs capped with thiol-based boron clusters

As illustrated in Figure 76, the UV-vis spectra of the MPCs stabilized with ligands **88-91** do show, in agreement with the theoretical calculations performed by Mulvaney,²⁵⁰ that we are dealing with MPCs smaller than 3 nm (no surface plasmon band) for neutral ligands, except ligand **91**, which leads to the synthesis of somewhat larger MPCs. In addition, according to the experimental results reported Hais *et al.* in their tables,²⁵¹ the particle size in this case is of about 4 nm.

Furthermore, for the MPCs modified with ligand **91**, there is a slight shift from 520 nm to approx. 550 nm that may be due

to interactions between the two sulphur atoms and the gold core (Figure 76).

In the case of the MPCs capped with metallacarborane-based ligands, we can see a small plasmon peak, which indicates that the size of the nanoparticles is also larger than 3 nm.

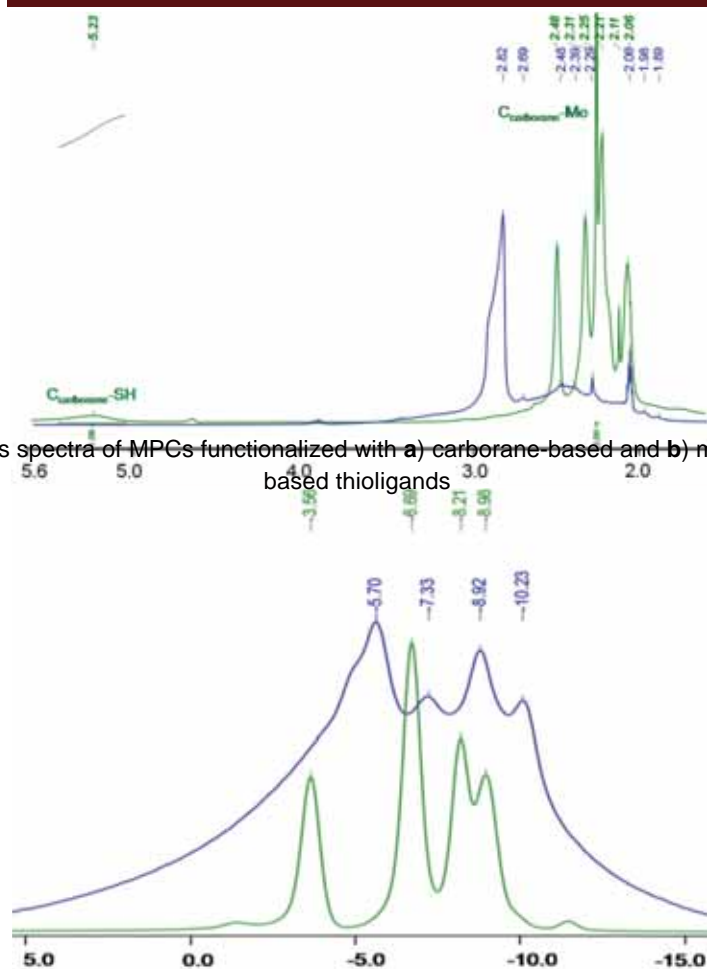
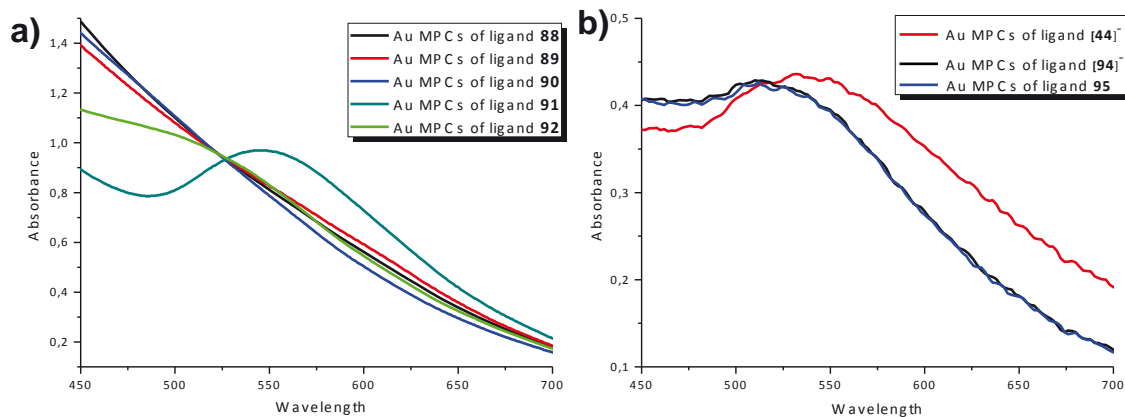


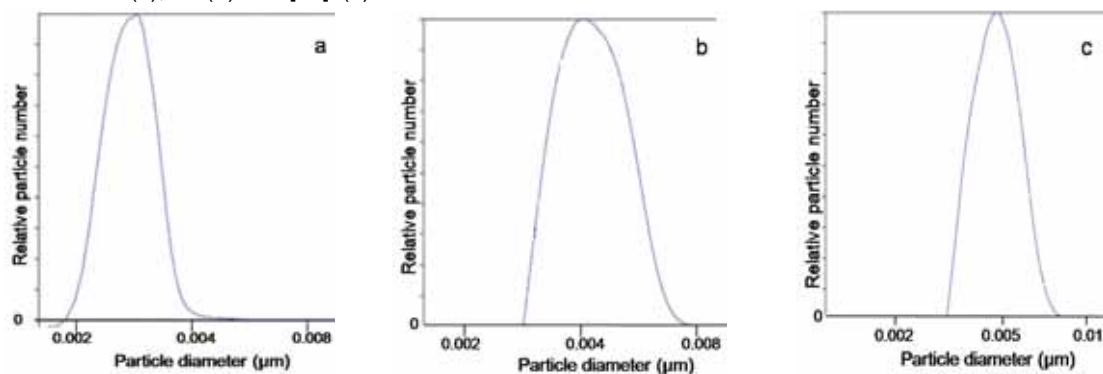
Figure 76. UV-vis spectra of MPCs functionalized with a) carborane-based and b) metallacarborane-based thioligands



Results and discussions

This is also confirmed by the CPS analysis (Figure 77), showing a particle diameter of more than 5 nm. The size distribution shows a mean particle diameter of about 3-4 nm for MPCs functionalized with carborane-based ligands (**a** and **b**), whereas the MPCs capped with metallacarborane-based thioligands are slightly larger, namely 6-7 nm (**c**).

Figure 77 shows the size distribution of MPCs functionalized with **89** (**a**), **91** (**b**) and **[94]⁻** (**c**)



As indicated in Table 12, there is an average of 3 Au atoms for every neutral cluster (**89-91**), and about 4 Au atoms for every metallacarborane-based thioligand (**[44]⁻**, **[94]⁻** and **95**).

Sample	Experimental values			Theoretical S:B ratio
	Au	S	B	
MPCs modified with ligand 89	3	0.91	9.4	1:10
MPCs modified with ligand 90	2.8	0.93	10.8	1:10
MPCs modified with ligand 91	4	1,6	9,25	2:10
MPCs modified with ligand [44]⁻	4	0.5	17.67	1:18
MPCs modified with ligand [94]⁻	2,8	0.4	18,94	1:18
MPCs modified with ligand 95	3,8	0.95	17.05	1:18

Table 12. ICP-AES analysis for MPCs functionalized with neutral and anionic thioligands

2.6.3. Preparation of MPCs capped with thioligands *via* the method of sonication

The preparation of highly disperse MPCs by different techniques still attracts a significant interest; moreover, many methods of synthesis have been developed and tested with success. During our research, we came across an alternative route to the preparation of monodisperse MPCs, by sonicating ligand **88** as a solid, at 55 °C, with aqueous solution of Au-citrate solution prepared according to the method reported by Turkevich-Frens.^{109,110}

Samples were taken out every hour and analyzed by UV-vis spectroscopy, indicating the “fragmentation” of the initial MPCs from about 14 nm to approximately 3 nm.

Results and discussions

Figure 79. UV-vis of initial Au-citrate solution

2.6. Preparation and characterization of MPCs capped with thiol-based boron clusters

Based on the absorbance values depicted in Figure 78a, the particle size was determined using Haiss *et al.* tables²⁵¹ and represented in Figure 78b with respect to the sonication time.

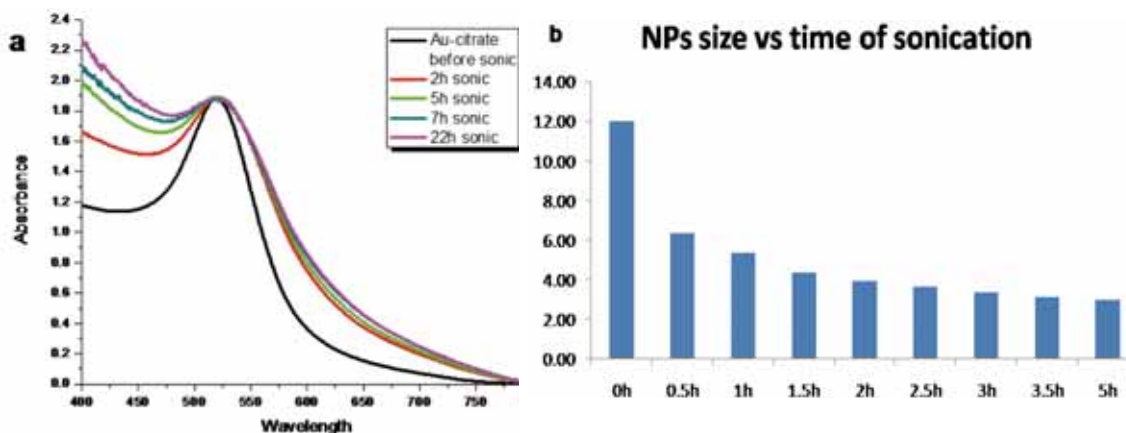
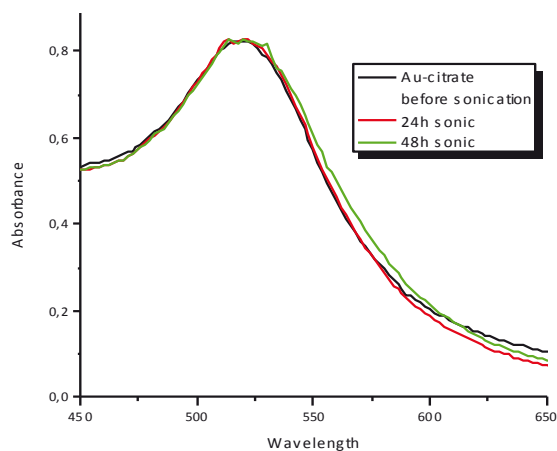


Figure 78. a) UV-vis spectrum of mercaptocarborane, sonicated at 55 °C for different periods of time; b) MPCs size function of sonication times

The possibility of the sonication itself inducing “fragmentation” of the particles was discarded after sonicating Au-citrate solution alone at about 55 °C. No “fragmentation” was observed, not even after 48h of sonication, as illustrated in Figure 79.



TEM provided additional information regarding the “fragmentation” of nanoparticles in presence of mercaptocarborane **88** as shown in Figure 80 below.

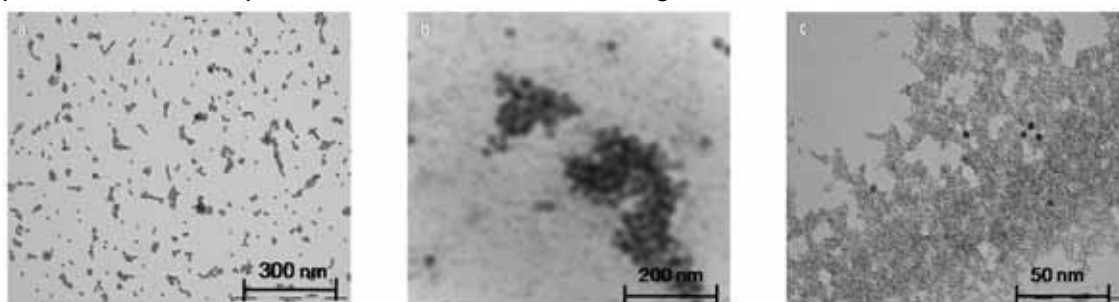


Figure 80. TEM images illustrating the fragmentation process: a) Au-citrate solution before sonication; b) after 3h sonication; c) after 15h sonication

Results and discussions

After only three hours of sonication at 55 °C, in the reaction mixture there are present both initial MPCs of about 14 nm as well as smaller ones of ca. 3 nm. However, after 15 hours of sonication, we can find a vast majority of monodispersed 3 nm MPCs and only a few initial particles.

Table 13. Au:B molar ratios determined by ICP-AES

Time of sonication	Au	B
10 min	2	10.34
1h	2	19.82
6h	2	42.72
15h	2	58.52

In addition to these characterization techniques, ICP-AES analysis also confirms the “fragmentation” of the initial nanoparticles, since after 10 minutes sonicating the molar ratio was of 2Au : 10.34B, whereas after 15 hours of sonication, the ratio was 2Au : 58.52B (See Table 13).

We also wanted to investigate if the temperature alone could cause the same “fragmentation” effect on the nanoparticles. Therefore, mercaptocarborane, **88**, in solid was added to Au-citrate solution and refluxed for 9 hours. The results are shown in Figure 81.

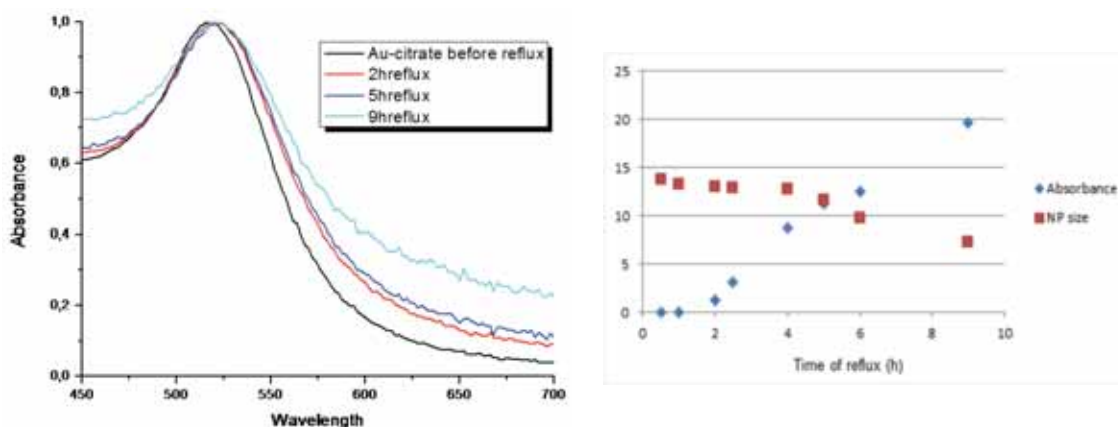
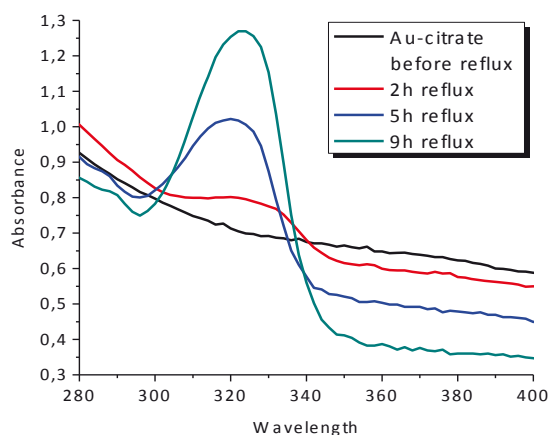
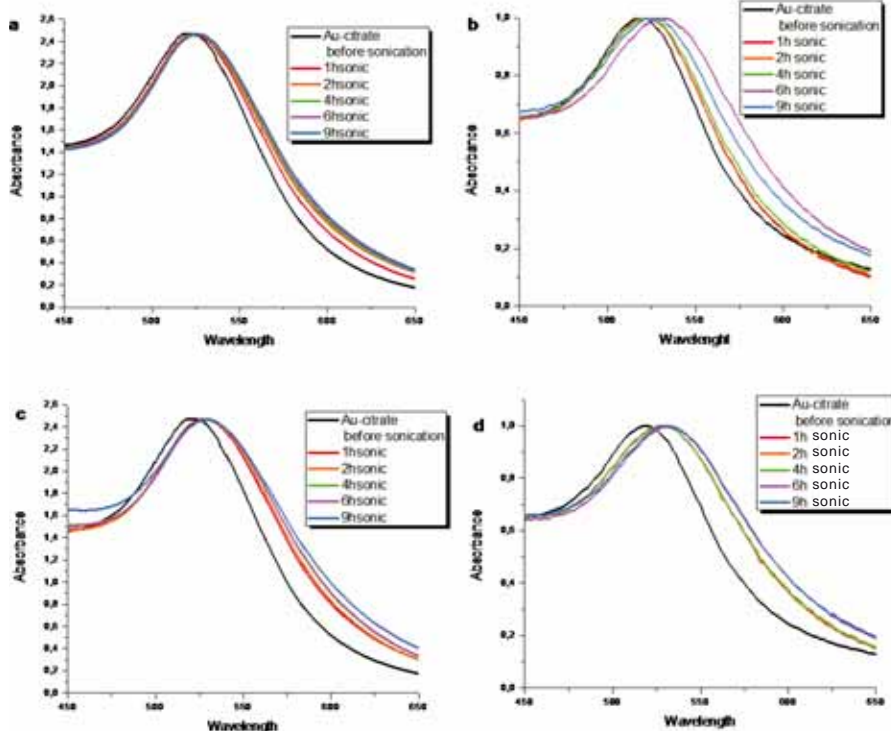


Figure 81. “Fragmentation” of nanoparticles with time of reflux



However, this method does not produce the same degree of nanoparticle “fragmentation” as the sole sonication method did; the size decreases from about 15.5 nm to aprox. 7.3 nm. Moreover, Au (I) can also be observed in the UV-vis spectra, at about 320 nm as presented in Figure 82.



After seeing these results we can conclude that both sonication and a temperature no higher than 60° C are required to have a “fragmentation” process without by-products. The next step was to determine if other carborane-

based ligands were also able to induce nanoparticle “fragmentation”; to achieve this, compounds **89**, **90**, **92** (not water-soluble) and [**94**]⁻ (water-soluble) were added in solid to Au-citrate solutions and sonicated for 9 hours at 55 °C. Samples were taken out every hour and analysed by UV-vis. The results are described in Figure 83. As one can observe, the other boron-based compounds, both neutral (**89**, **90**) as well as anionic ([**94**]⁻) were not able to reduce the size of initial nanoparticles by sonication. Compound **92** induces very little “fragmentation”, namely from approx. 16 nm to about 10 nm after 9 hours of sonication, which cannot be comparable to the degree of ripening produced by sonicating the Au-citrate solution with **88**.

For a more complete study, various ligands were sonicated together with Au-citrate solution and analyzed by UV-vis. Sulphur (S₈), bis(□-sulfonatophenyl)phenylphosphane dihydrate dipotassium salt (BSSP), a peptide (CALNN) and PEG (these last three being water-soluble) were submitted to sonication after previous addition to the Au-citrate solution. The gathered results indicate that in presence of the water-soluble species, no “fragmentation” takes place, whereas with S₈ the decrease in size is observed, however, in a much lesser degree than for thioligand **88** (from 12 nm to about 9.5 nm) (Figure 84).

Results and discussions

2.6. Preparation and characterization of MPCs capped with thiol-based boron clusters

Once the preparation part was completed, we focused on determining the

MPCs properties:

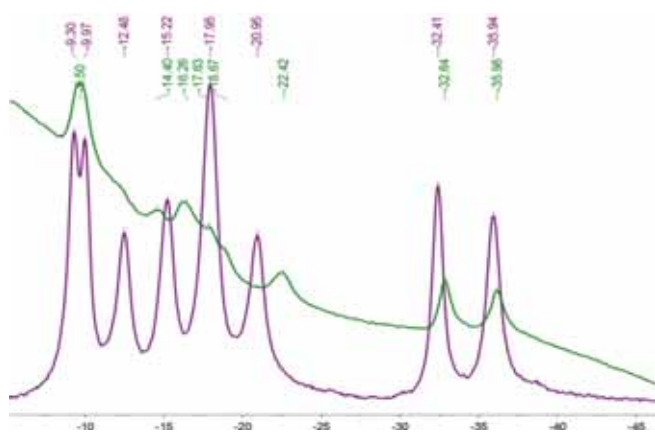
particles obtained by this sonication method were the ones capped with

88, we expected

them to exhibit the same

properties as the ones prepared *via*

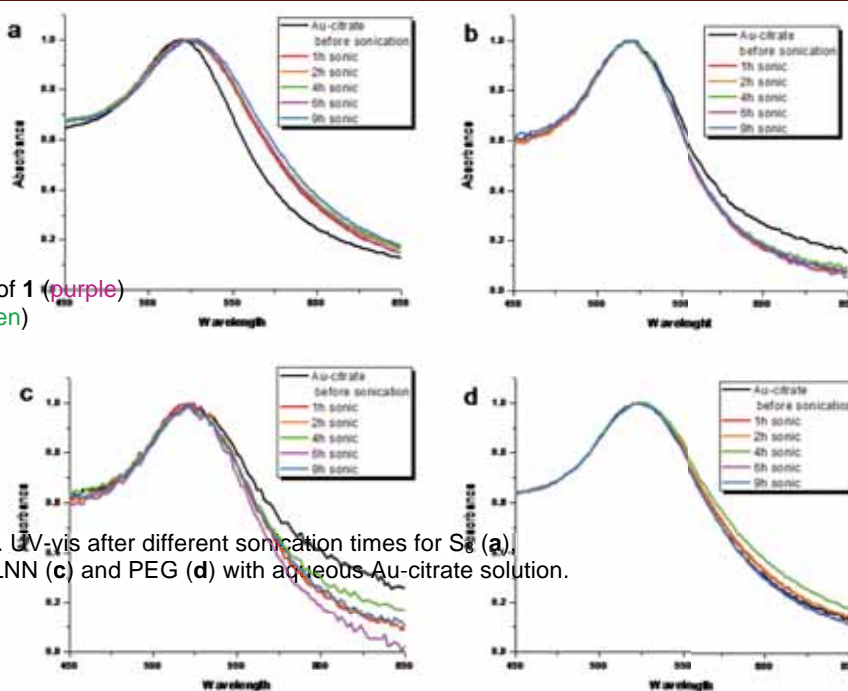
reduction with sodium borohydride, namely the reversible phase transfer from aqueous to organic phases. However, these newly prepared materials did not show this unique properties and the answer to this was to arrive after looking at the ^{11}B -NMR spectra. As indicated in Figure 85, the cluster is partially deboronated during the sonication process (probably because the resulting citrate acts as a nucleophile, eliminating one B-H vertex), resulting in the capping of the MPCs not by the initial neutral thioligand, but by its corresponding, anionic species.



The peaks at about -32 and -35 ppm clearly show the formation of the *nido* cluster, but also confirm the capping of the MPCs with the boron thioligand, based on the broadening of signals as well as to the slight shift to lower field values, due to interactions between the sulphur atom of the cluster and the Au core.

Figure 85. ^{11}B (^1H)-NMR of the *nido* species of **1** (purple) and the MPCs capped with **88** (green).

Figure 84. UV-vis after different sonication times for Se (a), BSSP (b), CALNN (c) and PEG (d) with aqueous Au-citrate solution.



A parallel study was performed to determine if sonication alone could induce the partial deboronation of the *closo* mercaptocarborane cluster, **88**. For this, **88** was added to various reaction mixtures and sonicated at 55 °C for 22 hours, and the result is illustrated in Figure 86. From the NMR data obtained for the sonication of **88** with milliQ water (red), we can clearly see that the deboronation process is practically inexistent, since the peaks indicating the formation of the *nido* species are barely visible at -32 and -35 ppm. On the other hand, the result of the sonication of 1 Eq. of **88** with 6 Eq. sodium citrate dehydrate, for 22 hours, at 55° C (depicted in blue) demonstrates without any doubt the formation of the *nido* cluster of **88**, as a consequence of the nucleophilic attack of the citrate species present in the medium. The NMR spectra represented in green was discussed just above (Figure 85).

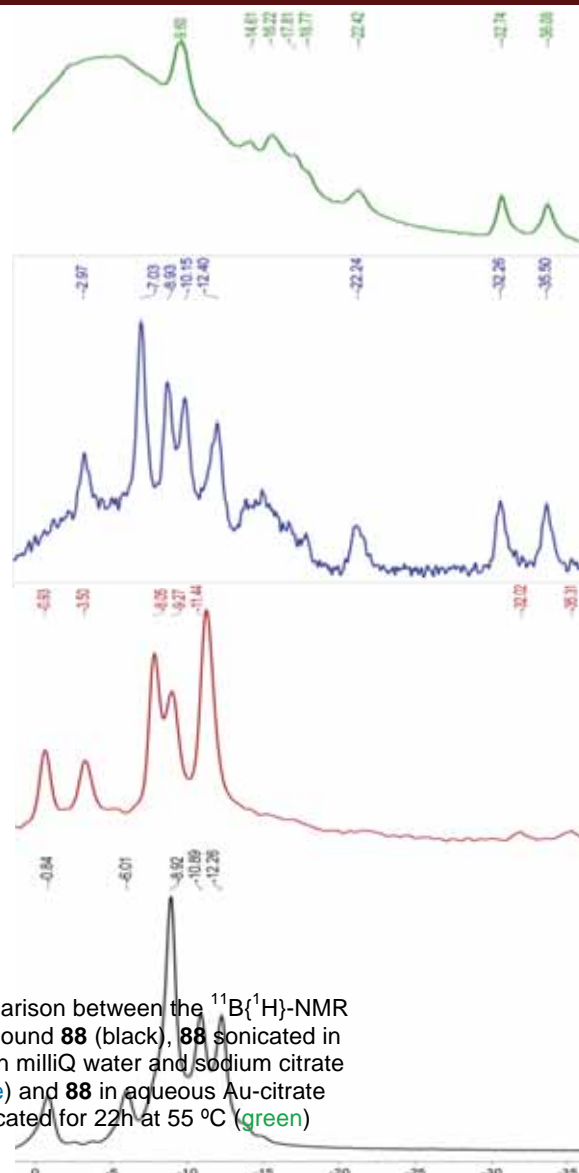


Figure 86. Comparison between the $^{11}\text{B}\{^1\text{H}\}$ -NMR spectra of compound **88** (black), **88** sonicated in milliQ (red), **88** in milliQ water and sodium citrate present in the medium (blue) and **88** in aqueous Au-citrate solution sonicated for 22h at 55 °C (green)

2.6.4. Preparation of MPCs capped with thioligands *via* the acetone method

Numerous methods for the preparation of nanoparticles (NPs) have been described in the literature; however, the synthesis of metallic NPs usually proceeds *via* the reduction of a precursor. Fine control over size and shape is of tremendous importance for many applications because these parameters are critical to both physical and chemical properties of NPs. Therefore, one-step and room temperature synthetic procedures allowing access to NPs dispersible in a large range of solvents (in particular in water) are desirable, especially when considering formulation issues. In this paper we report a very simple room temperature synthesis procedure, namely functionalization of ca. 12

nm citrate-stabilized MPCs with boron-based thioligands, yielding MPCs dispersible in almost any solvent, and particularly in water. The almost spherical shape and the quasi-aromatic character of carborane structures are key advantages, converting these species into rather exceptional materials. Moreover, carboranethiols have proven to be useful building blocks as they combine synthetic accessibility with a large number of sites for polyfunctionalization and extraordinarily thermal and chemical stability.

The preparation of the initial Au-citrate solution is based on the method reported by Turkevich-Frens.^{109,110} In a 250 mL round-bottom flask equipped with a reflux condenser, 950.6 µL H₂AuCl₄ aqueous solution (0.21 M) were added over 200 mL milliQ water and brought to boil. When the mixture started to reflux, 235.28 mg (0.8 moles, 294.1 g/mol) sodium citrate dihydrate in 20 mL milliQ water were added in one quick movement. The color changed from slight yellow to dark-blue almost immediately, and turned dark-red after 2 minutes of reflux. The mixture was left under reflux and stirring for 1 hour, then left at room temperature overnight. The Au-citrate solution was then filtered and analyzed by UV-vis spectroscopy, showing a MPCs diameter of about 12 nm.

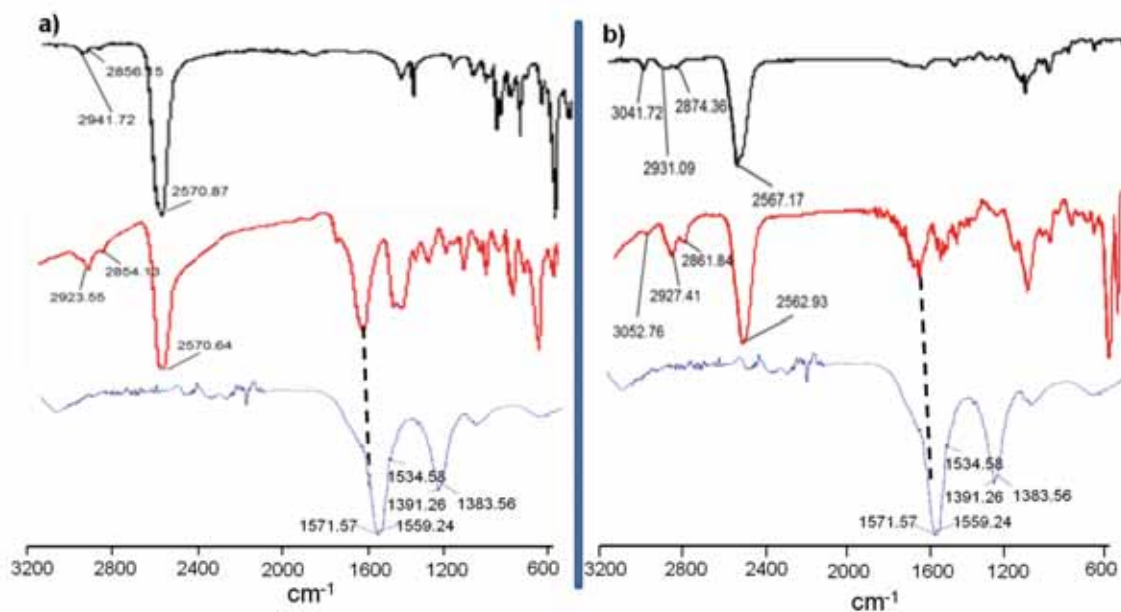
Water-soluble gold nanoparticles of approximately 10 nm in diameter were prepared by modification of citrate-capped gold nanoparticles with boron-rich clusters, as indicated below:

- a) In the case of neutral thiocarboranes **88-91** and **93**, 8 mg of boron-based thioligands dissolved in 6 mL acetone were added dropwise over 40 mL of previously prepared Au-citrate solution. The resulting dark-red mixture was shaken for 1 hour at room temperature, then centrifuged four times for 20 minutes at 13500 rpm and 10° C using a water: ether 1:1 mixture to remove unreacted thiocarboranes.
- b) In the case of metallocarborane-based ligands [**44**], [**94**] and **95**, no acetone is required since they are water soluble, so the ligands are simply added to the Au-citrate aqueous solution. After shaking the dark-red solution for 1 hour, the excess ligands are removed by centrifuging four times for 20 minutes at 13500 rpm and 10° C, using just milliQ water to take away the unreacted thioligands.

After purification, a dark-red water soluble product was obtained and characterized by FTIR, NMR, ICP-AES, UV-vis, CPS and, in some cases, cyclic voltammetry (CV). Although these newly obtained materials were soluble in organic solvents but most importantly in water, there was no reversible phase transfer phenomenon as in the case of the already reported MPCs.²⁵² However, another interesting property emerged, which will be commented upon later on.

The coordination of thioligand molecules with gold surfaces was observed using FTIR spectroscopy. The spectra presented in Figure 85 show the main characteristic bands labeled in both cases. Strong broad absorptions at $2562\text{--}2570\text{ cm}^{-1}$ are present in both the pure neutral/anionic ligands and their corresponding final MPCs, due to B–H stretches, also supporting a *closo* cluster structure.²⁰⁶ In addition, the FTIR spectrum of MPCs functionalized with ligand [94][−] exhibits $\nu(\text{C–H})$ stretch absorption at 3052 cm^{-1} confirming the presence of $\text{C}_{\text{cluster}}\text{–H}$ bonds²³⁸ in the gold nanoparticles; however, this bond does not appear in the FTIR spectra of either one of the MPCs modified with neutral ligands, since all carbon atoms are substituted.

Moreover, we can see that the citrate absorption bands are also present in the FTIR spectrum of the MPCs functionalized with ligands 89 (a) and [94][−] respectively (b) (Figure 87a), whereas in the case of the MPCs capped with the anionic thioligand [94][−] (Figure 87b) these bands are present in a much lower intensity, due to electronic repulsions between [94][−] and the citrate itself.

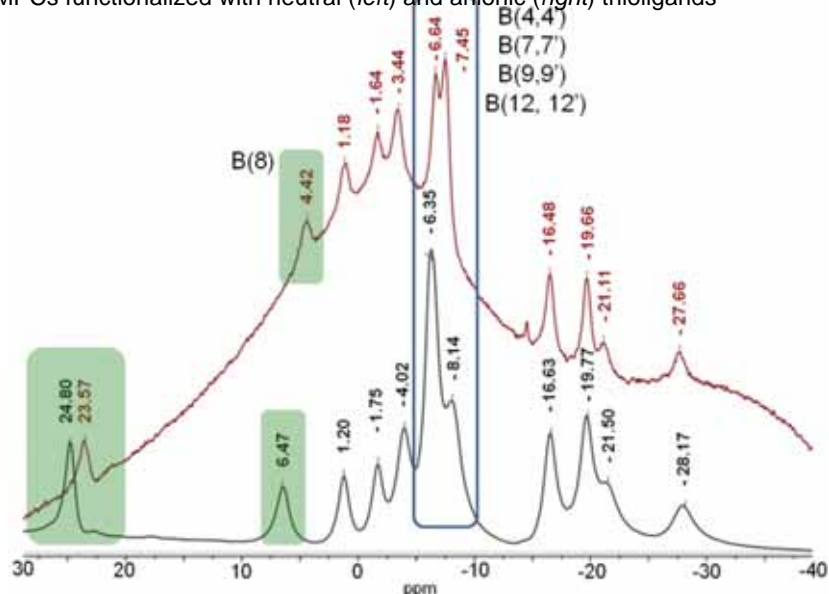


Regarding ¹¹B-NMR spectra, an interesting observation resides in the upfield shift of the signals corresponding to MPCs functionalized with ligand [94][−], as observed from Figure 88. This chemical shift is most probably due to interactions between the metal core of the nanoparticle and the sulfur atom belonging to the anionic thioligand.

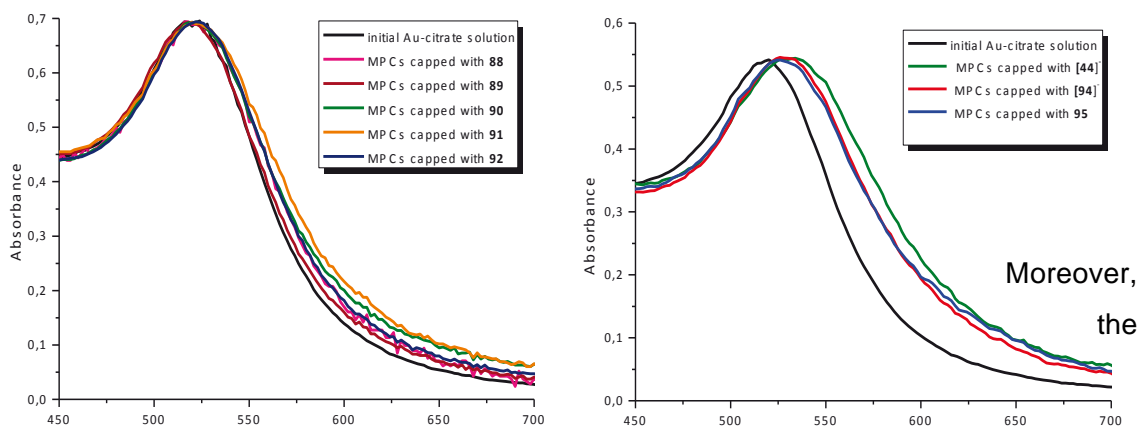
Figure 88. Comparison between ^{11}B NMR spectra of ligand [94] before (black) and after (red)

Results and discussions

Figure 89. UV-vis spectra of MPCs functionalized with neutral (left) and anionic (right) thioligands



The slight shift between the absorbance of the initial Au-citrate solution and the one showed by the MPCs functionalized with anionic thiometallacarboranes could be the result of possible interactions between the gold core and the metal contained by our sandwich-type ligands, conclusion based on the fact that in the case of neutral carboranethiols, no such shift is present, as shown in Figure 89.



typical plasmon

band present at 520 nm indicates the absence of aggregation before and after modification with ligands also supported by the red color of the dispersions.

The attachment of the stabilizing neutral thioligands **88-91** and **93** was confirmed by analytical centrifugation, showing a decrease in apparent particle size upon formation of the new ligand shell, due to the decrease in density of the nanoparticles (Figure 90).

Results and discussions

The shift to the left with respect to the peak of the initial Au-citrate solution confirms the replacement of the citrate shell with our thioligands.

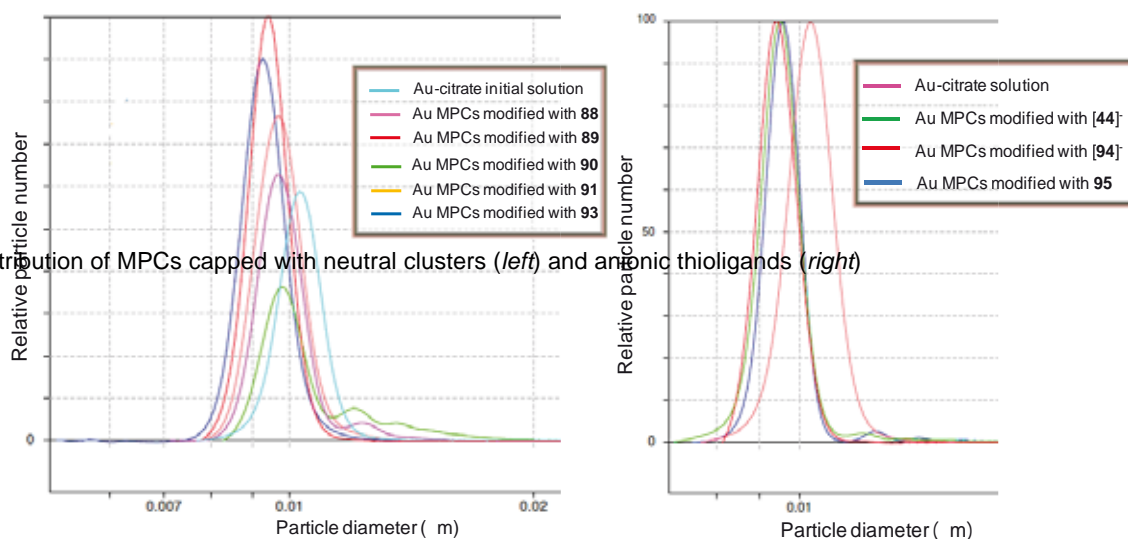


Figure 90. Size distribution of MPCs capped with neutral clusters (*left*) and anionic thioligands (*right*)

Cyclic Voltammetry (CV) can be used to study qualitative information about electrochemical processes under various conditions, such as the presence of intermediates in oxidation-reduction reactions, the reversibility of a reaction, to determine the electron stoichiometry of a system, the diffusion coefficient of an analyte, and the formal reduction potential, which can be used as an identification tool. In addition, because concentration is proportional to current in a reversible, nernstian

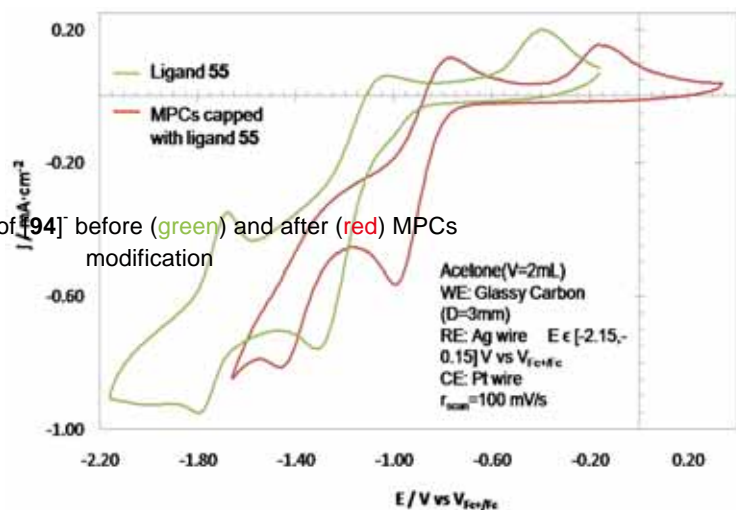


Figure 91. CV of [94] before (green) and after (red) MPCs modification

system, concentration of an unknown solution can be determined by generating a calibration curve of current *versus* concentration. In this case we used CV to determine the reversibility of a reaction, as well as to see if the presence of both Co and Au within the same molecule may affect the reductive/oxidative

potentials. There is a difference of about 0.2V between the reductive value of the cobalt-based compound and the MPCs, as indicated in Figure 91 above.

Regarding the properties of these water soluble 10 nm MPCs an interesting observation is that when ether is added to the aqueous solution followed by a few drops of dilute HCl acid, the MPCs precipitate from water, redissolve readily in the etheric phase and end up forming a thin Au film at the interphase. If acetone is added to this mixture, the color of the solution changes from gray to dark red. This is a unique property of MPCs since the Au film, once formed, redissolves upon shaking in the aqueous mixture and the phenomenon repeats itself at infinitum.

2.6.5. Applications of MPCs with boron-based thioligands

Nanoparticles can be very useful in medical applications, such as cancer diagnosis,²²¹ due to their shape, charge, stability and relationship with water, and also because of the ability to functionalize them. Because of their small size and properties, nanoparticles can have long half/lives during circulation in the body and reach very deep sites that other drugs or contrast agents cannot usually access. Moreover, they can cross barriers such as blood/brain barrier or gastro/intestinal barrier. This can be a major advantage for the detection and visualization of tumor cells at very early stages of disease. Additionally, Merkoçi *et al*¹⁰⁵ have developed a rapid electrochemical biosensing strategy for cancer cells identification/quantification using antibody-functionalized gold nanoparticles as labels. This type of labels was used for the marking of circulating tumor cells (CTC), which are blood-travelling cells detached from a tumor or from metastasis. Their quantification is under intensive research for examining cancer metastasis, and monitoring the therapeutic outcomes of cancer.²⁵³ In a recent study,¹⁰⁶ a novel magnetosandwich assay based biosensor based on gold nanoparticles labels has been developed and applied for the detection of antibodies anti-hepatitis surface antigen in human serum. The reported assay takes advantage of the properties of the magnetic beads used as platforms of the immunoreactions and the nanoparticles used as electrocatalytic labels. The final detection of these gold nanoparticles tags is performed in a rapid and simple way approaching their catalytic properties towards the hydrogen ions electroreduction in an acidic medium.

In addition to the biosensing applications,²⁵⁴ the use of nanoparticles as carriers of biomolecules and their application in biomedical and nutritional technologies is an emerging research field in the last years. Future potential applications for both biosensing and therapeutic purposes were found for gold nanoparticles modified with k-casein derived peptides, due to the binding properties of these peptides with the bacteria responsible for enteric diseases (*Enterotoxigenic E. coli*).²⁵⁵

Out of all the types and sizes of our preparations of MPCs, the most interesting from the medical point of view are the MPCs capped with mercaptocarborane, **88**. This new type of MPC is hydrophobic and completely insoluble in water when uncharged, but, when offered electrons by a suitable reducing agent, transfers readily to an aqueous phase where it behaves as a Henglein-type electron pool. In addition, exchangeable cations can be stored in the ligand shell. When discharged, the particles precipitate in water and redissolve readily in less polar solvents. These unprecedented properties are due to the nanoparticle preparation method as well as to the use of mercaptocarborane clusters as capping agents, which, like other thiol ligands, effectively stabilize the gold core, but owing to their spherical shape necessarily leave gaps that allow direct access of reactants and solvent molecules to the gold surface. The design of water-soluble boron rich macromolecules or particles is of significance for Boron Neutron Capture Therapy (BNCT) and for drug delivery.

To illustrate potential biomedical applications of their unique solubility characteristics, we have demonstrated the cellular uptake of these MPCs from aqueous solution by a human cancer cell line and show that the particles penetrate membrane structures as they are oxidized and become more hydrophobic within the biological environment. The cellular uptake of nanoparticles was performed on HeLa cells by incubating them for 2 hours with MPCs dispersed in cell culture medium. We have also shown that the uptake of these MPCs causes significant stress by the generation of reactive oxygen species (ROS). Taking all the above into consideration we believe that these new materials offer a broad scope for exciting research and future applications.

Cellular Uptake and Intracellular Fate

In order to investigate how our hydrophilic MPCs, that have the unique property of becoming hydrophobic when oxidized, interact with biological cells we conducted some preliminary experiments on HeLa cells. This is of interest since a cell represents a medium that is strongly compartmentalized into aqueous microenvironments separated from each other by hydrophobic membrane barriers. Our expectation was that the MPCs can cross these barriers easier than purely hydrophilic particles and that they eventually end up as hydrophobic inclusions in membranes.

Results and discussions

Although the intracellular environment is generally described as reductive, it should be oxidative with respect to the MPCs that have been prepared in the presence of a high concentration of sodium borohydride. The results discussed below suggest that this is

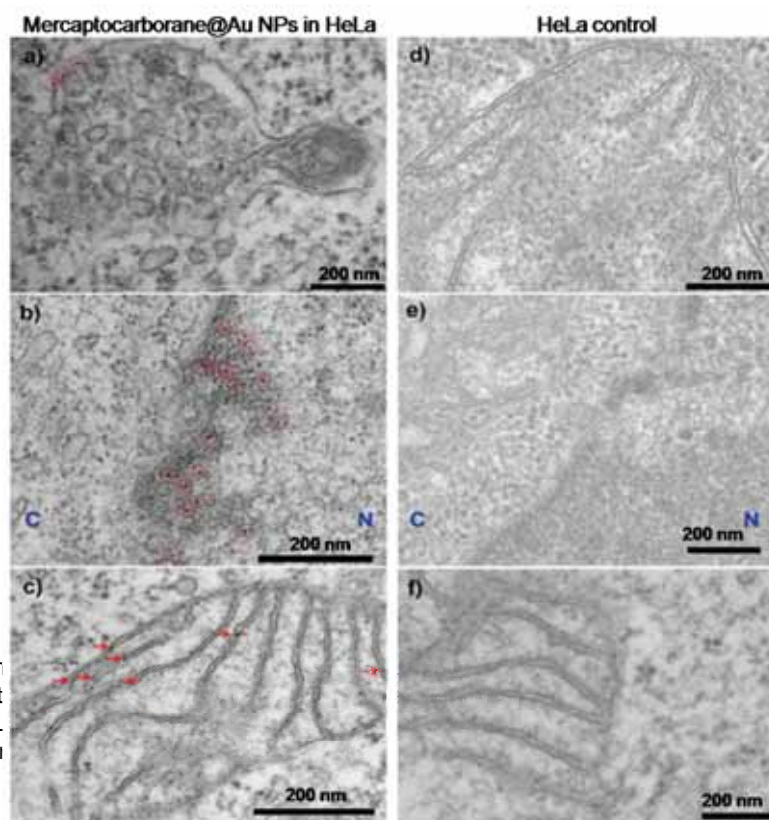


Figure 92. Correlating aggregating features in HeLa cells under control conditions.

indeed the case. We chose HeLa cells, because they are a common human fibroblast cell line, which has frequently been used to investigate cellular uptake of nanoparticles. The first clear difference compared to standard gold nanoparticles is that our MPCs are relatively toxic so that all cells died after 24 hours of incubation with them. We therefore restricted the time the cells were in contact with the particles to 2 hours. Under these conditions the cells

remained alive even 48 hours after they had been incubated. TEM images of cell sections prepared immediately after the 2 hours incubation time are shown in Figure 92a-c.

Due to the size of the particles, which are very small, it is not possible to undoubtedly identify individual ones in these images. Nevertheless, aggregates composed of several particles can be clearly distinguished. It is a general problem with standard TEM imaging of intracellular metal particles below about 5 nm that these are often indistinguishable from stained proteins and other subcellular structures of comparable size. Figure 92d-f shows a comparison between similar images obtained in the absence of MPCs, in order to demonstrate that the excellent contrast provided by the gold, in this case does indeed provide us with confidence to identify and locate aggregates of MPCs, some of which have been labeled for clarity with red circles or arrows. The images in Figure 92a-c show features belonging to three different compartments, a multivesicular body, the nuclear envelope, and a mitochondrion. In all

cases, most of the aggregated particles are clearly identified and reside within membrane structures, fact particularly clear in the case of the nuclear envelope, part of which is densely decorated with aggregates. A number of aggregates are also found in the cytosol and in the nucleus. These findings support the hypothesis

that the particles are initially dispersed in the aqueous phase of the cell, where they appear to be

able to diffuse freely into various organelles, and then gradually become oxidized and rendered hydrophobic, which leads to

aggregation followed by precipitation of the aggregates into membrane structures.

To confirm the involvement of redox processes in this behavior, we have investigated the formation of ROS, which include OH radicals formed as a consequence of enhanced redox activity within the cell. The confocal microscopy image in Figure 91 clearly shows significantly enhanced ROS levels after incubation with MPCs, indicating the formation of radicals and subsequent oxidative stress that we attribute to the loss of electrons (and sodium ions) from the MPCs, as shown in Scheme 20.

The behavior of our MPCs in the biological environment is highly unusual and further confirms that these particles have properties that differ significantly from those of standard preparations. Most commonly, nanoparticles are taken up by endocytosis and are not able to transfer spontaneously across membrane boundaries.²⁵⁶ They tend to remain confined to endocytic vesicles, such as those shown in Figure 93a, and do not reach the cytoplasm or the nucleus and least of all the mitochondria, which have no mechanisms for the direct uptake of particular matter and, like the nucleus, are surrounded by a double membrane.

The toxicity of these new MPCs and their ability to readily reach intracellular targets makes them attractive candidates for further studies in view of potential anticancer activity or as boron-rich agents for BNCT. The above observations together suggest that in this system, ligand exchange with intracellular glutathione, as reported by Rotello and coworkers,^{229b} within the time scale of our experiments only plays - a minor

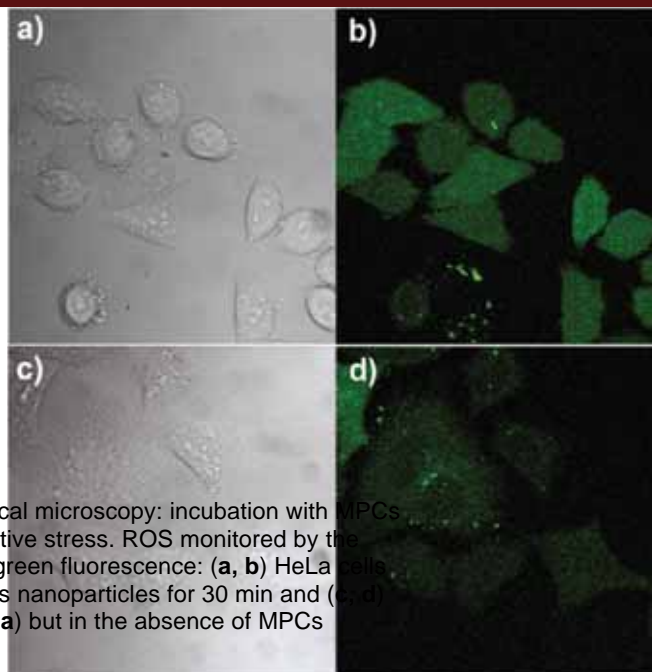
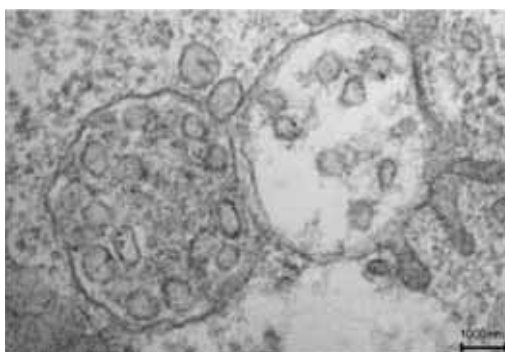


Figure 93. Confocal microscopy: incubation with MPCs causes oxidative stress. ROS monitored by the appearance of green fluorescence: (a, b) HeLa cells incubated with MPCs nanoparticles for 30 min and (c, d) same as (a) but in the absence of MPCs

role, if any, since it would render the particles hydrophilic and prevent their precipitation into membrane structures. Resisting ligand exchange is quite common and has been observed before for particles stabilized with peptides and/or polyethylene glycol-based ligands.²⁵⁷ Further extended work should be carried out in the future in order to determine if these materials undergo chemical modifications and

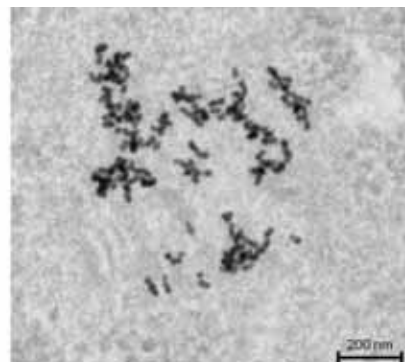
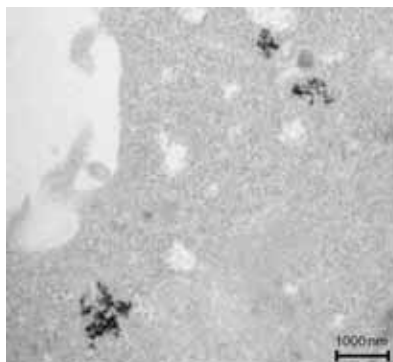
It should also be mentioned that these new mercaptocarborane-capped MPCs display a host of fascinating properties which suggest applications in catalysis and electrocatalysis and the possibility of new nanoscopic electron and ion valves to be integrated in artificial and biological membranes. In addition, new electrochemical sensors and diagnostic tools may arise from such nanoparticles.



Regarding the cellular uptake of the other 3 nm MPCs prepared *via* reduction with sodium borohydride, preliminary studies on HeLa cells using compound **95** were conducted showing that after a period of incubation of 2 hours, Au NPs were found in late endosomes. A TEM representative image is presented in Figure 94. However, even if the particles finally reside in endosomes, the positive result of this study is the fact that the

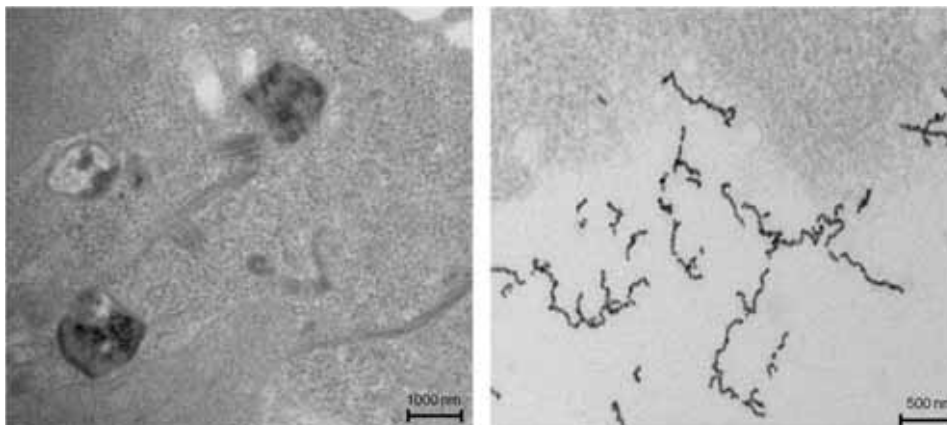
cells were still alive after the incubation period. Therefore, as a follow-up study we should vary the incubation time, and observe the effect it has on the cellular uptake.

On the topic of 10 nm MPCs capped with neutral **88**, studies were performed on HeLa cells, with an incubation time of four hours. These



MPCs were found to be taken up in the cells cytoplasm as quite aggregated features mostly found without the surrounding membrane but in some cases *via* endocytosis. In addition, no particles were found in the cell nucleus or mitochondria, as presented in Figure 95.

Another study on HeLa cells uptake was performed with MPCs capped with thioligand **95**. Still, no nanostructures were to be found neither in the nucleus, nor in the mitochondria; the only difference with respect to the previous test with **88** is that MPCs present in the HeLa cells cytoplasm and taken up as wired structures that could be seen on the outside of the cell membrane (Figure 96).



More studies on the uptake by HeLa cells the MPCs capped with **90**, **[44]** and **[94]** are currently in progress.

3. Conclusions

Conclusions

9

1. We discovered a faster and simpler method with very high yields for the obtaining of $[3,3'\text{-M}(\text{C}_2\text{B}_9\text{H}_{11})_2]$ complexes ($\text{M} = \text{Co}, \text{Fe}$), by plainly heating the metal salt (CoCl_2 or FeCl_2) with the trimethylammonium salt of the corresponding *nido* species.

2. We synthesized and characterized $[3,3'\text{-Fe}(8\text{-(OCH}_2\text{CH}_2)_2\text{X-(1,2-C}_2\text{B}_9\text{H}_{10})(1',2'\text{-C}_2\text{B}_9\text{H}_{11})]$ bearing organic alkyl end groups. **Cyclic voltammetry** was used for the first time in order to determine the type of metallacarborane present, as well as to differentiate between a closed dioxane ring system and an open one.

Other subject of interest alongside this PhD thesis was the preparation of $[3,3'\text{-Fe}(8\text{-(OCH}_2\text{CH}_2)_2\text{X-(1,2-C}_2\text{B}_9\text{H}_{10})(1',2'\text{-C}_2\text{B}_9\text{H}_{11})]$ ($\text{X} = \text{F}, \text{Cl}, \text{Br}, \text{I}, \text{SH}$), an atom efficient and environmental friendly transformation that would facilitate the use of such anionic monobranched polyethoxylated metallacarborane synthons in posterior derivatization. Furthermore, the thiol-terminated synthon opened the way to **surface functionalization** of gold nanoparticles.

3. Me-carboranyl, Ph-carboranyl and di-carboranyl were used as nucleophiles in the cobaltabis(dicarbollide) functionalization *via* dioxane ring opening reaction of $[3,3'\text{-M}(8\text{-(OCH}_2\text{CH}_2)_2\text{-(1,2-C}_2\text{B}_9\text{H}_{10})(1',2'\text{-C}_2\text{B}_9\text{H}_{11})]$ ($\text{M} = \text{Co}, \text{Fe}$), compounds **6** and **7**, yielding mono- and dianionic macromolecules.

The partial deboronation of these previously synthesized *closo* compounds led to the corresponding di- and tri-anionic *nido* species. This reaction allowed the obtaining of a novel type of high boron content (almost 50%) polyanionic macromolecules. The fact that these compounds are polyanionic makes them more soluble in water, which therefore increases their potential for **biological uses**.

The complexation reaction **in solution** with anhydrous CoCl_2 or FeCl_2 of the *nido* clusters yielded mono- and hetero- M(III) ($\text{M} = \text{Co}, \text{Fe}$) sandwich-type coordination complexes. **UV-Visible analysis** was successfully used to quantify the number of cobaltabis(dicarbollide) units within a macromolecule. Since these macromolecules are soluble in water and present an elevated number of boron atoms, they could be important candidates for possible applications in the treatment of tumor cells by the technique of **Boron Neutron Capture Therapy**.

4. The cleavage of the dioxane ring of the zwitterionic derivative of cobaltabis(dicarbollide), **6**, was achieved by employing biomolecules such as aminoacids and antibiotics (sodium salicylate, nicotinamide, nicotinic acid, arginine, histidine and pyrazinamide among others). The resulting species were characterized using FTIR, MALDI-TOF and ^1H , ^{11}B and ^{13}C NMR techniques.

3. Conclusions

5. Another subject was the synthesis and characterization of both neutral and anionic boron-based thioligands for their posterior use in surface functionalization.

We prepared ca. 3 nm MPCs capped with the above described thioligands *via* a simple procedure consisting in reduction of a chlorauric acid and thioligand methanolic solution with sodium borohydride. All of these MPCs showed very good solubility in water, acetone and isopropanol, an unexpected finding considering the hydrophobic nature of the carborane-based shell. Moreover, in the case of the Au NPs modified with the neutral mercaptocarborane cluster, **88**, a **unique reversible phase-transfer property** (from polar to non-polar solvents) was observed.

This newly synthesized material was characterized by using both more common characterization techniques, such as FTIR, ^1H and ^{11}B NMR, elemental analysis, UV-Visible, as well as techniques more specialized on Au NPs characterization, as for instance CPS, TEM, XPS and ICP-AES.

6. The fragmentation of 10 nm MPCs in presence of mercaptocarborane, **88**, was achieved, leading to **monodispersed MPCs** with a diameter of around 3 nm *via* sonication, a viable method, with practical interest. Other boron-based thioligands, both neutral and anionic, namely **89**, **90**, **92** and [**94**], as well as ligands different from the ones based on carboranes (S_8 , bis(\square -sulfonatophenyl)phenylphosphane dihydrate dipotassium salt (BSSP), a peptide (CALNN) and PEG) did not show the same degree of fragmentation as the one induced by **88**.

7. 10 nm MPCs were also prepared by a rapid and simple method, MPCs showing new and interesting properties, with applications in Au thin films deposition.

8. To illustrate potential biomedical applications of their unique solubility characteristics, we have demonstrated the cellular uptake of these MPCs capped with **88** from aqueous solution by a human cancer cell line and show that the **particles penetrate membrane structures** as they are oxidized and become more hydrophobic within the biological environment. The cellular uptake of nanoparticles was performed on HeLa and showed that the uptake of these MPCs causes significant stress by the generation of reactive oxygen species (ROS).

Regarding the cellular uptake of the other 3 nm MPCs prepared *via* reduction with sodium borohydride, preliminary studies on HeLa cells using compound **95** were conducted showing that after a period of incubation of 2 hours, MPCs were found in late endosomes. A follow-up study should be carried out varying the incubation time, and observe the effect it has on the cellular uptake.

4. Bibliography

Bibliography

- ¹ I. Shapiro, C. D. Good, R. E. Williams, *J. Am. Chem. Soc.*, **1962**, *84*, 3837.
- ² R. N. Grimes, *Carboranes*, Academic Press New York, **1974**.
- ³ T. Onak, *Boron Hydride Chemistry*, E. L. Muetterties, Ed., Academic Press New York, **1973**, 349.
- ⁴ http://www.nobelprize.org/nobel_prizes/chemistry/laureates/1976/
- ⁵ N. W. Lipscomb, *Boron Hydrides*, Benjamin, New York, **1963**.
- ⁶ R. Hoffmann, W. N. Lipscomb, *J. Chem. Phys.*, **1962**, *36*, 3489; Z. F. Chen, R. B. King, *Chem. Rev.*, **2005**, *105*, 3613.
- ⁷ H. C. Brown, *Science*, **1980**, *210*, 485.
- ⁸ a) H. I. Schlesinger, H. C. Brown, H. R. Hoekstra, L. R. Rapp, *J. Am. Chem. Soc.*, **1953**, *75*, 199; b) H. C. Brown, H. I. Schlesinger, A. B. J. Burg, *J. Am. Chem. Soc.*, **1939**, *61*, 673; c) K. P. C. Vollhardt, *Organic Chemistry*, W. H. Freeman and Co., New York, **1987**.
- ⁹ a) R. N. Grimes, *Carboranes*, Academic Press New York, **1971**; b) S. Papetti, T. L. Heying, *J. Am. Chem. Soc.*, **1964**, *86*, 2295.
- ¹⁰ R. W. Rudolph, *Acc. Chem. Res.*, **1976**, *9*, 446.
- ¹¹ R. E. Williams, *Inorg. Chem.*, **1971**, *10*, 210.
- ¹² a) K. Wade, *Adv. Inorg. Radiochem.*, **1976**, *18*, 1; b) D. M. P. Mingos, *Nature (Phy. Science)*, **1972**, 236, 99; c) R. W. Rudolph, W. R. Pretzer, *Inorg. Chem.*, **1972**, *11*, 1974; d) K. Wade, *Chem. Commun.*, **1971**, 792.
- ¹³ a) M. F. Hawthorne, D. C. Young, P. M. Garret, D. A. Owen, S. G. Schwerin, F. N. Tebbe, P. A. Wegner, *J. Am. Chem. Soc.*, **1968**, *90*(4), 862; b) R. A. Wiesboeck, M. F. Hawthorne, *J. Am. Chem. Soc.*, **1964**, *86*, 1642.
- ¹⁴ a) J. Buchanan, E. M. J. Hamilton, D. Reed, A. J. Welch, *J. Chem. Soc., Dalton Trans.*, **1990**, 677; b) X. L. R. Fontaine, N. N. Greenwood, J. D. Kennedy, K. Nestor, M. Thornton-Pett, S. Hermánek, T. Jelinek, B. Stibr, *J. Chem. Soc., Dalton Trans.*, **1990**, 681.
- ¹⁵ M. F. Hawthorne, D. C. Young, P. A. Wegner, *J. Am. Chem. Soc.*, **1965**, *87*, 1818.
- ¹⁶ M. F. Hawthorne, T. D. Andrews, *J. Chem. Soc., Chem. Comm.*, **1965**, 443.
- ¹⁷ C. Masalles, S. Borrós, C. Viñas, F. Teixidor, *Adv. Mater.*, **2000**, *16*, 1199
- ¹⁸ C. Viñas, J. Pedrajas, J. Bertran, F. Teixidor, R. Kivekäs, R. Sillanpää, *Inorg. Chem.*, **1997**, *36*, 2482
- ¹⁹ R. M. Chamberlin, B. L. Scott, M. M. Melo, K. D. Abney, *Inorg. Chem.*, **1997**, *36*, 809.
- ²⁰ a) A. N. Gashti, J. C. Huffman, A. Edwards, G. Szekeley, A. R. Siedle, J. A. Karty, J. P. Reilly, L. J. Todd, *J. Organomet. Chem.*, **2000**, *614*, 120; b) P. K. Hurlburt, R. L. Miller, K. D. Abney, T. D. Foreman, R. J. Butcher, S. A. Kinkead, *Inorg. Chem.*, **1995**, *34*, 5215; c) L. Matel, F. Macásek, P. Rajec, S. Harmanek, J. Plešek, *Polyhedron*, **1982**, *1*, 511.
- ²¹ A. W. Bauer, W. M. Kirby, J. C. Cherris, M. Truck, *Am. J. Clin. Pathol.*, **1966**, *45*, 493.
- ²² a) I. P. Beletskaya, V. I. Bregadze, V. A. Ivushkin, P. V. Petrovskii, I. B. Sivaev, G. G. Zhigareva, *J. Organomet. Chem.*, **2004**, *689*, 2920; b) I. Rojo, F. Teixidor, C. Viñas, R. Kivekäs, R. Sillanpää, *Chem. Eur. J.*, **2003**, *9*, 4311; c) I. Rojo, F. Teixidor, R. Kivekäs, R. Sillanpää, C. Viñas, *J. Am. Chem. Soc.*, **2003**, *125*, 14720; d) I. Rojo, F. Teixidor, R. Kivekäs, R. Sillanpää, C. Viñas, *Organometallics*, **2003**, *22*, 4642; e) M. D. Mortimer, C. B. Knobler, M. F. Hawthorne, *Inorg. Chem.*, **1996**, *35*, 5750.
- ²³ a) I. Rojo, J. Pedrajas, F. Teixidor, C. Viñas, R. Kivekäs, R. Sillanpää, I. Sivaev, V. Bregadze, S. Sjöberg, *Organometallics*, **2003**, *22*, 3414; b) J. Plešek, B. Grüner, J. Macháček, I. Cisačová, J. Čáslavský, *J. Organomet. Chem.*, **2007**, *692*, 4801.
- ²⁴ J. Llop, C. Masalles, C. Viñas, F. Teixidor, R. Sillanpää, R. Kivekäs, *Dalton Trans.*, **2003**, 556.
- ²⁵ a) I. B. Sivaev, Z. A. Starikova, S. Sjöberg, V. I. Bregadze, *J. Organomet. Chem.*, **2002**, *649*, 1. b) I. B. Sivaev, S. Sjöberg, V. I. Bregadze, *International Conference Organometallic Compounds - Materials of the Next Century*, Nizhny Novgorod, Russia, May 29-June 2, **2000**.
- ²⁶ J. Plešek, B. Grüner, S. Heřmánek, J. Báča, V. Mareček, J. Jänchenová, A. Lhotský, K. Holub, P. Selucký, J. Rais, I. Cisačová, J. Čáslavský, *Polyhedron*, **2002**, *21*, 975.
- ²⁷ a) B. Grüner, L. Mikulašek, J. Bača, I. Cisačová, V. Böhmer, C. Danila, M. M. Reinoso-Garcia, W. Verboom, D. N. Reinhoudt, A. Casnati, R. Ungaro, *Eur. J. Org. Chem.*, **2005**, 2022. b) L. Mikulašek, B. Grüner, C. Danila, V. Böhmer, J. Čáslavský, P. Selucky, *Chem. Commun.*, **2006**, 4001.
- ²⁸ a) A. B. Olejniczak, J. Plešek, O. Kříž, Z. J. Lesnikowski, *Angew. Chem., Int. Ed.* **2003**, *42*, 5740. b) Z. J. Lesnikowski, E. Paradowska, A. B. Olejniczak, M. Studzinska, P. Seekamp, U. Schüßler, D. Gabel, R. F.

4. Bibliography

- Schinazi, J. Plešek, *Bioorg. Med. Chem.*, **2005**, 13, 4168. c) A. B. Olejniczak, J. Plešek, Z. J. Lesnikowski, *Chem. Eur. J.*, **2007**, 13, 311.
- ²⁹ A. A. Semioshkin, I. B. Sivaev, V. I. Bregadze, *Dalton Trans.*, **2008**, 8, 977.
- ³⁰ J. Plešek, *Chem. Rev.*, **1992**, 92, 269.
- ³¹ a) J. Rais, M. Kyus, S. Hermánek, *Czech Patent* 153 933, **1974**; Chem. Abst. **1975**, 82 23370c; b) J. Rais, P. Selucky, M. Kyus, *J. Inorg. Nucl. Chem.*, **1976**, 38, 1376.
- ³² a) C. Viñas, S. Gómez, J. Bertran, F. Teixidor, J. Barron, R. Sillanpää, R. Kivekäs, J. F. Dozol, H. Rouquette, *J. Organomet. Chem.*, **1999**, 581, 188; b) C. Viñas, S. Gómez, J. Bertran, F. Teixidor, J. F. Dozol, H. Rouquette, *Chem. Comm.*, **1998**, 191; c) C. Viñas, S. Gómez, J. Bertran, F. Teixidor, J. F. Dozol, H. Rouquette, *Inorg. Chem.*, **1998**, 43, 3640; d) C. Viñas, J. Bertran, S. Gómez, F. Teixidor, R. Sillanpää, R. Kivekäs, J. F. Dozol, H. Rouquette, *J. Chem. Soc., Dalton Trans.*, **1998**, 17, 2849.
- ³³ F. Teixidor, M. A. Flores, C. Viñas, R. Kivekäs, R. Sillanpää, *Angew. Chem.*, **1996**, 108, 2388.
- ³⁴ F. Teixidor, M. A. Flores, C. Viñas, R. Sillanpää, R. Kivekäs, *J. Am. Chem. Soc.*, **2000**, 122, 1963.
- ³⁵ M.F. Hawthorne, *Advances on Boron and the Boranes*, eds. J.F. Liebman, A. Greenberg, R.E. Williams, VCH Publishers, New York, **1988**, Capítol 10, p. 225.
- ³⁶ a) A. Demonceau, F. Simal, A. F. Noels, C. Viñas, R. Nuñez, F. Teixidor, *Tetrahedron Letters*, **1997**, 38, 7879; b) A. Demonceau, F. Simal, A. F. Noels, C. Viñas, R. Nuñez, F. Teixidor, *Tetrahedron Letters*, **1997**, 38, 4079; c) O. Tutusaurus, S. Delfosse, A. Demonceau, A. F. Noels, R. Nuñez, C. Viñas, F. Teixidor, *Tetrahedron Letters*, **2002**, 43, 983.
- ³⁷ F. Simal, S. Sebillé, A. Demonceau, A. F. Noels, R. Nuñez, M. Abad, F. Teixidor, C. Viñas, *Tetrahedron Letters*, **2000**, 41, 5347.
- ³⁸ C. Masalles, J. Llop, C. Viñas, F. Teixidor, *Adv. Mater.*, **2002**, 14, 826.
- ³⁹ a) F. Lerouge, C. Viñas, F. Teixidor, R. Núñez, A. Abreu, E. Xochitiotzi, R. Santillán, N. Farfán, *Dalton Trans.*, **2007**, 1898; b) F. Lerouge, C. Viñas, F. Teixidor, R. Sillanpää, A. Abreu, E. Xochitiotzi, N. Farfán, R. Santillán, R. Núñez, *Dalton Trans.*, **2011**, 40 (29), 7541; c) A. Ferrer-Ugalde, E. J. Juárez-Pérez, F. Teixidor, C. Viñas, R. Sillanpää, E. Pérez-Inestrosa, R. Núñez. *Chemistry A European Journal, Chem. Eur. J.*, **2012**, 18, 544.
- ⁴⁰ a) K. Kokado, Y. Chujo, *Polymer Journal*, **2010**, 42, 363; b) K. Kokado, M. Tominaga, Y. Chujo, *Macromolecular Rapid Comm.*, **2010**, 15, 1389; c) K. Kokado, Y. Chujo, *Dalton Trans.*, **2003**, 9, 1919.
- ⁴¹ a) K. Ohta, A. Januszko, P. Kaszynski, T. Nagamine, G. Sasnouski, Y. Endo, *Liq. Cryst.*, **2004**, 31, 671; b) W. Piecek, J. M. Kaufman, P. Kaszynsky, *Liq. Cryst.*, **2003**, 30, 39. (c) P. Kaszynski, S. Pakhomov, K. F. Tesh, *Inorg. Chem.*, **2001**, 40, 6622; c) P. Kaszynsky, *Collect. Czech. Chem. Commun.*, **1999**, 64, 895; d) A.G. Douglass, K. Czuprynski, M. Mierzwa, P. Kaszynski, *Chem. Mater.*, **1998**, 10, 2399.
- ⁴² a) M. Nieuwenhuyzen, K. R. Seddon, F. Teixidor, A. V. Puga, C. Viñas, *Inorg. Chem.*, **2009**, 48, 889; b) A. S. Larsen, J. D. Holbrey, F. S. Tham, C. A. Reed, *J. Am. Chem. Soc.*, **2000**, 122, 7264; c) B. Ronig, I. Pantenburg, L. Wesemann, *Eur. J. Inorg. Chem.*, **2002**, 319; d) E. Justus, K. Rischka, J. F. Wishart, K. Werner, D. Gabel, *Chemistry A European Journal*, **2008**, 14, 1918.
- ⁴³ a) C. Masalles, F. Teixidor, S. Borrós, C. Viñas, *Anal. Bioanal. Chem.*, **2002**, 372, 513; b) I. A. Marques, E. Crespo, F. Teixidor, N. Zine, J. Bausells, J. Samitier, A. Errachid, *Sensors and Actuators B: Chemical*, **2008**, 130, 295; c) N. Zine, J. Bausells, F. Teixidor, C. Viñas, C. Masalles, J. Samitier, A. Errachid, *Materials Science & Engineering C*, **2006**, 26, 399; d) N. Zine, J. Bausells, F. Vocanson, R. Lamartine, Z. Asfari, F. Teixidor, E. Crespo, I. A. Marques de Oliveira, J. Samitier, A. Errachid, *Electrochimica Acta*, **2006**, 51, 5075; e) A. Errachid, D. Caballero, E. Crespo, F. Bessueille, M. Pla-Roca, C. A. Mills, F. Teixidor, J. Samitier, *Nanotechnology*, **2007**, 18, 485301.
- ⁴⁴ a) A. I. Stoica, C. Viñas, F. Teixidor, *Chem. Comm.*, **2009**, 33, 4988; b) A. Stoica, C. Viñas, F. Teixidor, *Chem. Comm.*, **2008**, 48, 6492.
- ⁴⁵ C. Guardiola, C. Fleta, D. Quirion, J. Rodríguez, M. Lozano, F. Teixidor, C. Viñas, A. R. Popescu, C. Domingo, K. Amgarou, *Journal of Instrumentation*, **2011**, 6, 11001.
- ⁴⁶ a) W. N. Sweet, A. H. Soloway, R. L. Wright, *J. Pharmac. Exp. Ther.*, **1962**, 137, 263; b) H. Hatanaka, *Borax Rev.*, **1991**, 9, 5.
- ⁴⁷ I. H. Hall, A.E. Warren, C.C Lee, M.D. Wasczszak, L.G. Sneddon, *Anticancer Res.*, **1998**, 18, 951.
- ⁴⁸ P. Cígler, M. Koříšek, P. Čezáková, J. Brynda, Z. Otwinowski, J. Pokorná, J. Plešek, B. Grüner, L. Doležalová-Marešová, M. Máša, J. Sedláček, J. Bodem, H.-G. Kräusslich, V. Král, J. Konvalinka, *Proc. Natl. Acad. Sci.*, **2005**, 102, 15394.
- ⁴⁹ C. T. Peng, *Radiopaques, a Burger's Medicinal Chemistry*, ed. M. E. Wolff, Nova York, **1981**.
- ⁵⁰ W. Krause, P. W. Schneider, *Top. Curr. Chem.*, **2002**, 222, 107.
- ⁵¹ R. R. Srivastava, D. K. Hamlin, D. S. Wilbur, *J. Org. Chem.*, **1996**, 61, 9041.

- ⁵² G. Barberà, F. Teixidor, C. Viñas, R. Sillanpää, R. Kivekäs, *Eur. J. Inorg. Chem.*, **2003**, 1511.
- ⁵³ A. Pepioli, F. Teixidor, K. Saralidze, C. van der Marel, P. Williams, L. Voss, M. L. W. Knetsch, C. Viñas, L. H. Koole, *Biomaterials*, **2011**, 3, 6389.
- ⁵⁴ *CRC Handbook of Chemistry and Physics*, ed. D. R. Lide, CRC Press Boca Raton, Londres, **2003**.
- ⁵⁵ a) W. H. Knoth, H. C. Miller, J. C. Sauer, J. H. Balthis, Y. T. Chia, E. L. Muetterties, *Inorg. Chem.*, **1964**, 3, 159; b) W. Preetz, G. Peters, *Eur. J. Inorg. Chem.*, **1999**, 1831.
- ⁵⁶ a) M. F. Hawthorne, A. Maderna, *Chem. Rev.*, **1999**, 99, 3421; b) V. Bregadze, I. Sivaev, S. Glazun, *Anti Cancer Agents in Medicinal Chemistry*, **2006**, 6, 75.
- ⁵⁷ G. L. Locher, *Am. J. Roentgenol.*, **1936**, 36, 1.
- ⁵⁸ a) M. F. Hawthorne, M. W. Lee, *J. Neuro-Oncol.*, **2003**, 62, 33; b) A. H. Soloway, J. C. Zhuo, F. G. Rong, A. J. Lunato, D. H. Ives, R. F. Barth, A. K. M. Anisuzzaman, C. D. Barth, B. A. Barnum, *J. Organometal. Chem.*, **1999**, 581, 150; c) M. F. Hawthorne, *Mol. Med. Today*, **1998**, 4, 174.
- ⁵⁹ G. Calabrese, J. J. Nesnas, E. Barbu, D. Fatouros, J. Tsibouklis, *Drug Discov. Today*, **2011**, 17, 153.
- ⁶⁰ J. A. Coderre, G. M. Morris, *Radiat. Res.*, **1999**, 151, 1.
- ⁶¹ a) W. Sauerwein, J. Rassow, B. Mijneer, *New York: Plenum Press*, Vol 2, **1997**, 531; b) D. Gabel, S. Foster, R. G. Fairchild, *Radiat. Res.*, **1987**, 111, 25.
- ⁶² a) Y. Nakagawa, H. Hatanaka, *J. Neurooncol.*, **1997**, 33, 105; b) A. H. Soloway, H. Hatanaka, M. A. Davis, *J. Med. Chem.*, **1967**, 10, 714.
- ⁶³ a) Y. Mishima, M. Ichihashi, S. Htta, C. Honda, K. Yamamura, T. Nakagawa, *Cell Res.*, **1989**, 2, 226; b) H. R. Synder, A. J. Reedy, W. J. Lennarz, *J. Am. Chem. Soc.*, **1958**, 80, 835.
- ⁶⁴ Y. Imahori, S. Ueda, Y. Ohmori, K. Sakae, T. Kusuki, T. Kobayashi, M. Takagaki, K. Ono, T. Ido, R. Fujii, *Clin. Cancer Res.*, **1998**, 4, 1825.
- ⁶⁵ a) T. Aihata, J. Hiratsuka, N. Morita, M. Uno, Y. Sakurai, A. Maruhashi, K. Ono, T. Harada, *Head Neck*, **2006**, 28, 850; b) I. Kato, K. Ono, Y. Sakurai, M. Ohmae, A. Maruhashi, Y. Imahori, M. Kirihata, M. Nakazawa, Y. Yura, *Appl. Radiat. Isot.*, **2004**, 61, 1069; c) M. Suzuki, Y. Sakurai, S. Hagiwara, S. Masunaga, Y. Kinashi, K. Nagata, A. Maruhashi, M. Kudo, K. Ono, *Jpn. J. Oncol.*, **2007**, 37, 376.
- ⁶⁶ a) J. Cai, A. H. Soloway, R. F. Barth, D. M. Adams, J. R. Hariharan, I. M. Wyzlic, K. Radcliffe, *J. Med. Chem.*, **1997**, 40, 3887; b) L. Gedda, M. Silvander, S. Sjoberg, W. Tjarks, J. Carlsson, *Anticancer Drug Des.*, **1997**, 12, 671; c) D. P. Kelly, S. A. Bateman, R. F. Martin, M. E. Reum, M. Rose, A. D. Whittaker, *Aust. J. Chem.*, **1994**, 47, 247; d) H. Nakamura, M. Sekido, Y. Yamamoto, *J. Med. Chem.*, **1997**, 40, 2825; e) Y. Yamamoto, H. Nakamura, *J. Med. Chem.*, **1993**, 36, 2232; f) Y. Yamamoto, J. Cai, H. Nakamura, N. Sadayori, N. Asao, H. Nemoto, *J. Org. Chem.*, **1995**, 60, 3352.
- ⁶⁷ a) F. Alam, A. H. Soloway, B. V. Bapat, R. F. Barth, D. M. Adams, *Basic Life Sci.*, **1989**, 50, 107; b) S. B. Kahl, J. Li, *Inorg. Chem.*, **1996**, 35, 3878; c) S. B. Kahl, D. D. Joel, M. M. Nawrocky, P. L. Micca, K. P. Tran, G. C. Finkel, D. N. Slatkin, *Proc. Natl. Acad. Sci. USA*, **1990**, 87, 7265; d) M. Miura, P. L. Micca, C. D. Fisher, J. C. Heinrichs, J. A. Donaldson, G. C. Finkel, D. N. Slatkin, *Int. J. Cancer*, **1996**, 68, 114; e) H. Murakami, T. Nagasaki, I. Hamachi, S. Shinkai, *Tetrahedron Lett.*, **1993**, 34, 6273; f) K. Woodburn, A. S. Phadke, A. R. Morgan, *Bioorg. Med. Chem.*, **1993**, 3, 2017; g) E. Hao, M. Vicente, *Chem. Commun.*, **2005**, 1306; h) E. Hao, M. Sibrian-Vazquez, W. Serem, J. Garno, F. Fronczek, M. G. H. Vicente, *Chem. Eur. J.*, **2007**, 13, 9035; i) H. Li, F. Fronczek, M. Vicente, *Tetrahedron Lett.*, **2008**, 49, 4828; j) V. Gottumukkala, O. Ongayi, D. Baker, L. Lomax, M. Vicente, *Bioorganic & medicinal chemistry*, **2006**, 14, 1871; k) J. Wang, L. Ren, C. Weng, G. Jin, *Chem. Commun.*, **2006**, 162.
- ⁶⁸ a) F.-G. Rong, A. H. Soloway, *Nucleosides Nucleotides*, **1994**, 13, 2021; b) R. F. Schinazi, W. H. Prusoff, *J. Org. Chem.*, **1985**, 50, 841; c) A. Sood, B. R. Shaw, B. F. Spielvogel, *J. Am. Chem. Soc.*, **1989**, 111, 9234; d) Y. Yamamoto, T. Seko, H. Nakamura, H. Nemoto, H. Hojo, N. Mukai, Y. Hashimoto, *J. Chem. Soc., Chem. Commun.*, **1992**, 157; e) P. Matejicek, P. Cígler, A. Olejniczak, A. Andrysiak, B. Wojtczak, K. Prochazka, Z. Lesnikowski, *Langmuir*, **2008**, 24, 2625.
- ⁶⁹ a) S. B. Kahl, R. A. Kasar, *J. Am. Chem. Soc.*, **1996**, 118, 1223; b) M. Kirihata, T. Morimoto, T. Mizuta, I. Ichimoto, *Biosci. Biotechnol. Biochem.*, **1995**, 59, 2317; c) C. Malan, C. Morin, *Synletters*, **1996**, 2, 167; d) H. Nakamura, M. Fujiwara, Y. Yamamoto, *J. Org. Chem.*, **1998**, 63, 7529; e) H. Nakamura, M. Fujiwara, Y. Yamamoto, *Bull. Chem. Soc. Jpn.*, **2000**, 73, 231; f) R. R. Srivastava, R. R. Singhaus, G. W. Kabalka, *J. Org. Chem.*, **1997**, 62, 4476; g) M. Takagaki, K. Ono, Y. Oda, H. Kikuchi, H. Nemoto, S. Iwamoto, J. Cai, Y. Yamamoto, *Cancer Res.*, **1996**, 56, 2017.
- ⁷⁰ a) J. K. Prashar, D. E. Moore, *J. Chem. Soc. Perkin Trans.*, **1993**, 1051; b) J. J. Schaeck, S. B. Kahl, *Inorg. Chem.*, **1999**, 38, 204.
- ⁷¹ a) F. Alam, A. H. Soloway, J. E. McGuire, R. F. Barth, W. E. Carey, D. Adams, *J. Med. Chem.*, **1985**, 28, 522; b) D. M. Goldenberg, R. M. Sharkey, F. J. Primus, E. Mizusawa, M. F. Hawthorne, *Proc. Natl. Acad.*

4. Bibliography

- Sci. USA*, **1984**, *81*, 560; c) R. H. Pak, F. J. Primus, K. J. Rickard-Dickson, L. L. Ng, R. R. Kane, M. F. Hawthorne, *Proc. Natl. Acad. Sci. USA*, **1995**, *92*, 6986.
- ⁷² a) J. Capala, R. F. Barth, M. Bendayan, M. Lauzon, D. M. Adams, A. H. Soloway, R. A. Fenstermaker, J. Carlsson, *Bioconjug. Chem.*, **1996**, *7*, 7; b) L. Gedda, P. Olsson, J. Carlsson, *Bioconjug. Chem.*, **1996**, *7*, 584; c) W. Yang, R. F. Barth, D. M. Adams, A. H. Soloway, *Cancer Res.*, **1997**, *57*, 4333.
- ⁷³ a) G. Fulcrand-El Kattan, Z. J. Lesnikowski, S. Yao, F. Tanious, W. D. Wilson, R. F. Schinazi, *J. Am. Chem. Soc.*, **1994**, *116*, 7494; b) A. Nakanishi, L. Guan, R. R. Kane, H. Kasamatsu, M. F. Hawthorne, *Proc. Natl. Acad. Sci. USA*, **1999**, *96*, 238; c) A. Sood, B. R. Shaw, B. F. Spielvogel, *J. Am. Chem. Soc.*, **1990**, *112*, 9000.
- ⁷⁴ Q. Wei, E. B. Kullberg, L. Gedda, *Int. J. Oncol.*, **2003**, *23*, 1159.
- ⁷⁵ a) M. V. Backer, T. I. Gaynutdinov, V. Patel, A. K. Bandyopadhyaya, B. T. Thirumamagal, W. Tjarks, R. F. Barth, K. Claffey, J. M. Backer, *Mol. Cancer Ther.*, **2005**, *4*, 1423; b) S. Shukla, G. Wu, M. Chatterjee, W. Yang, M. Sekido, L. A. Diop, R. Müller, J. J. Sudimack, R. J. Lee, R. F. Barth, W. Tjarks, *Bioconjug. Chem.*, **2003**, *14*, 158; c) G. Wu, R. F. Barth, W. Yang, M. Chatterjee, W. Tjarks, M. J. Ciesielski, R. A. Fenstermaker, *Bioconjug. Chem.*, **2004**, *15*, 185.
- ⁷⁶ V. A. Trivillin, E. M. Heber, D. W. Nigg, M. E. Itoiz, O. Calzetta, H. Blaumann, J. Longhino, A. E. Schwint, *Rad. Res.*, **2006**, *166*, 387.
- ⁷⁷ E. Heber, V. Trivillin, D. Nigg, E. L. Kreimann, M. E. Itoiz, R. J. Rebagliati, D. Batistoni, A. E. Schwint, *Arch. Oral Biol.*, **2004**, *49*, 313.
- ⁷⁸ P. Li, B. R. Shaw, *J. Org. Chem.*, **2005**, *70*, 2171; b) A. H. S. Hall, J. Wan, E. E. Shaughnessy, B. R. Shaw, K. A. Alexander, *Nucleic Acids Res.*, **2004**, *32*, 5991; c) M. I. Dobrikov, K. M. Grady, B. R. Shaw, *Nucleos. Nucleot. Nucleic Acids*, **2003**, *22*, 275; d) B. Spielvogel, V. Powell, A. Sood, *Main Group Metal Chem.*, **1996**, *19*, 699.
- ⁷⁹ A. H. Soloway, W. Tjarks, B. A. Barnum, F. G. Rong, R. F. Barth, I. M. Codogni, J. G. Wilson, *Chem. Rev.*, **1998**, *98*, 1515.
- ⁸⁰ I. B. Sivaev, V. V. Bregadze, *Eur. J. Inorg. Chem.*, **2009**, *11*, 1433.
- ⁸¹ J. F. Valliant, K. J. Guenther, A. S. King, P. Morel, P. Schaffer, O. O. Sogbein, K. A. Stephenson, *Coord. Chem. Rev.*, **2002**, *232*, 173.
- ⁸² a) B. D. Anderson, *Adv. Drug Deliv. Rev.*, **1996**, *19*, 171; b) K. Hoste, K. De Winne, E. Schacht, *Int. J. Pharm.*, **2004**, *277*, 119.
- ⁸³ a) I. J. Majoros, C. R. Williams, J. R. Baker, *Curr. Top. Med. Chem.*, **2008**, *8*, 1165; b) Y. Gao, G. Gao, Y. He, T. Liu, R. Qi, *Mini-Rev. Med. Chem.*, **2008**, *8*, 889; c) I. Singh, A. K. Rehni, R. Kalra, G. Joshi, M. Kumar, *Pharmazie*, **2008**, *63*, 491; d) A. Agarwal, A. Asthana, U. Gupta, N. K. Jain, *J. Pharm. Pharmacol.*, **2008**, *60*, 671; e) Y. Cheng, T. Xu, *Eur. J. Med. Chem.*, **2008**, *43*, 2291; f) M. Najlah, A. D'Emanuele, *Curr. Opin. Drug Discovery Dev.*, **2007**, *10*, 756; g) H. S. Parekh, *Curr. Pharm. Des.*, **2007**, *13*, 2837; h) Y. Cheng, Y. Gao, T. Rao, Y. Li, T. Xu, *Comb. Chem. High Throughput Screen*, **2007**, *10*, 336; i) H. Yang, W. Y. Kao, *J. Biomater. Sci., Polym. Ed.*, **2006**, *17*, 3; j) S. Svenson, *Eur. J. Pharm. Biopharm.*, **2009**, *71*, 445; k) A. Florence, *Adv. Drug Delivery Rev.*, **2005**, *57*, 2104.
- ⁸⁴ a) G. R. Newkome, C. N. Moorefield, F. Vögtle, *Dendrimers and Dendrons: Concepts, Syntheses, Applications*, Wiley-VCH, Weinheim, **2001**; b) J. M. J. Fréchet, D. A. Tomalia, *Dendrimers and Other Dendritic Polymers*, Wiley, Chichester, **2001**; c) C. A. Shalley, F. Vögtle, *Dendrimers V: Functional and Hyperbranched Building*, Springer, Berlin, **2003**; d) G. R. Newkome, C. D. Shreiner, *Polymer*, **2008**, *49*, 1; e) D. Astruc, E. Boisselier, C. Ornelas, *Chem. Rev.*, **2010**, *110*, 1857; f) G. R. Newkome, C. Shreiner, *Chem. Rev.*, **2010**, *110*, 6338.
- ⁸⁵ a) N. Nishiyama, W.-D. Jang, K. Kataoka, *New J. Chem.*, **2007**, *31*, 1074; b) J. P. Collman, L. Fu, A. Zingg, F. Diederich, *Chem. Commun.*, **1997**, 193; c) D. K. Smith, F. Diederich, *Chem. Commun.*, **1998**, 2501; d) G. M. Dykes, D. K. Smith, *Tetrahedron*, **2003**, *59*, 3999; e) S. Shinoda, *J. Inclusion Phenom. Macrocyclic Chem.*, **2007**, *59*, 1.
- ⁸⁶ a) E. Badetti, A.-M. Caminade, J.-P. Majoral, M. Moreno- Mañas, R. M. Sebastián, *Langmuir*, **2008**, *24*, 2090; b) P. Gamez, P. De Hoog, M. Lutz, A. L. Spek, J. Reedijk, *Inorg. Chem. Acta*, **2003**, *351*, 319.
- ⁸⁷ E. Badetti, G. Franc, J.-P. Majoral, A.-M. Caminade, R. M. Sebastián, M. Moreno-Mañas, *Eur. J. Org. Chem.*, **2011**, 1256.
- ⁸⁸ R. F. Barth, D. M. Adams, A. H. Soloway, F. Alam, M. V. Darby, *Bioconj. Chem.*, **1994**, *5*, 58.
- ⁸⁹ G. Wu, R. F. Barth, W. Yang, M. Chatterjee, W. Tjarks, M. J. Ciesielski, R. Fenstermaker, *Bioconjugate Chem.*, **2004**, *15*, 185.

4. Bibliography

- ⁹⁰ R. F. Barth , W. Yang , D. M. Adams , J. H. Rotaru , S. Shukla , M. Sekido , W. Tjarks , R. A. Fenstermaker, M. Ciesielski , M. M. Nawrocky , J. A. Coderre, *Cancer Res.*, **2002**, 6, 3159.
- ⁹¹ W. Yang , R.F. Barth , G. Wu , A. K. Bandyopadhyaya , B. T. Thirumamagal , W. Tjarks , P. J. Binns , K. Riley, H. Patel , J. A. Coderre , M. J. Ciesielski , R. A. Fenstermaker, *Appl., Radiat. Isotop.*, **2004**, 61, 981.
- ⁹² W. Yang, R. F. Barth, G. Wu, W. Tjarks, P. Binns, K. Riley, *Appl. Radiat. Isotop.*, **2009**, 67, 328.
- ⁹³ A. M. Schrand, M. F. Rahman, S. M. Hussain, J. J. Schlager, D. A. Smith, A. F. Syed, *Nanomed. nanobiotechnol.*, **2010**, 2, 544.
- ⁹⁴ Huang X, Jain PK, I. H. El-Sayed, M. A. El-Sayed, *Nanomedicine*, **2007**, 2, 681.
- ⁹⁵ G. Han, P. Ghosh, V. M. Rotello, *Nanomedicine*, **2007**, 2, 113; b) C. S. Thaxton, N. L. Rosi, C. A. Mirkin, *MRS Bull*, **2005**, 30, 376; c) I. H. El-Sayed, X. Huang, M. A. El-Sayed, *Nano Lett*, **2005**, 5, 829.
- ⁹⁶ J. J. Storhoff, C. A. Mirkin, *Chem Rev*, **1999**, 99, 1849.
- ⁹⁷ H. Yi, J. L. M. Leunissen, G. M. Shi, C. A. Gutekunst, S. M. Hersch, *J Histochem Cytochem*, **2001**, 49, 279.
- ⁹⁸ a) G. Voskerician, M. S. Shive, R. S. Shawgo, H. von Recum, J. M. Anderson, M. J. Cima, R. Langer, *Biomaterials*, **2003**, 24, 1959; b) G. Tkachenko, H. Xie, D. Coleman, W. Glomm, J. Ryan, M. F. Anderson, S. Franzen, D. L. Feldheim, *J. Am. Chem. Soc.*, **2003**, 125, 4700.
- ⁹⁹ A. G. Tkachenko, H. Xie, D. Coleman, W. Glomm, J. Ryan, M. F. Anderson, S. Franzen, D. L. Feldheim, *J. Am. Chem. Soc.*, **2003**, 125, 4700.
- ¹⁰⁰ a) P. Sharma, S. C. Brown, N. Bengtsson, Q. Zhang, G. A. Walter, S. R. Grobmyer, S. Santra, H. Jiang, E. W. Scott, B. M. Moudgil, *Bioimaging Chem Mater*, **2008**, 20, 6087; b) M. Bruchez, Jr., M. Moronne, P. Gin, S. Weiss, A. P. Alivisatos, *Science*, **1998**, 281, 2013.
- ¹⁰¹ M. Bruchez, Jr., M. Moronne, P. Gin, S. Weiss, A. P. Alivisatos, *Science*, **1998**, 281, 2013.
- ¹⁰² R. Hong, N. O. Fischer, A. Verma, C. M. Goodman, T. Emrick, V. M. Rotello, *J. Am. Chem. Soc.*, **2004**, 126, 739.
- ¹⁰³ a) L. R. Hirsch, R. J. Stafford, J. A. Bankson, S. R. Sershen, B. Rivera, R. E. Price, J. D. Hazle, N. J. Halas, J. L. West, *Proc Natl Acad Sci U S A*, **2003**, 100, 1549; b) C. Loo, A. Lin, L. Hirsch, M. H. Lee, J. Barton, N. Halas, J. West, R. Drezek, *Technol Cancer Res Treat*, **2004**, 3, 33; c) J. F. Hainfeld, D. N. Slatkin, H. M. Smilowitz, *Phys Med Biol*, **2004**, 49, 309; d) D. Pissuwan, S. M. Valenzuela, M. C. Killingsworth, X. Xu, M. B. Cortie, *J Nanopart Res.*, **2006**, 9, 1109.
- ¹⁰⁴ J. Chen, B. Wiley, D. Campbell, F. Saeki, L. Cang, L. Au, J. Lee, X. Li, Y. Xia, *Adv Mater*, **2005**, 17, 2255; b) R. S. De M, H. Akpınar, O. R. Miranda, R. R. Arvizo, U. H. F. Bunz, V. M. Rotello, *Nat. Chem.*, **2009**, 461.
- ¹⁰⁵ M. Maltez-da Costa, A. de la Escosura-Muñiz, C. Nogués, L. Barrios , E. Ibáñez, A. Merkoçi, *Small*, **2012**, 8, 3605.
- ¹⁰⁶ A. de la Escosura-Muñiza, M. Maltez-da Costa, Ch. Sánchez-Espinel, B. Díaz-Freitas, J. Fernández-Suarez, Á. González-Fernández, A. Merkoçi, *Biosensors and Bioelectronics*, **2010**, 26, 1710.
- ¹⁰⁷ R. Koch, *On bacteriological research*, August Hirsch Forest, Berlin, **1890**.
- ¹⁰⁸ J. Forestier, *Lancet*, **1934**, 224, 646.
- ¹⁰⁹ J. Turkevich, P. C. Stevenson, J. Hillier, *Discuss. Faraday Soc.*, **1951**, 11, 55.
- ¹¹⁰ G. Frens, *Nature: Phys. Sci.*, **1973**, 241, 20.
- ¹¹¹ X. Ji, X. Song, J. Li, Y. Bai, W. Yang, X. Peng, *J. Am. Chem. Soc.*, **2007**, 129, 13939.
- ¹¹² I. Ojea-Jimenez, F. M. Romero, N. G. Bastus, V. Puentes, *J. Phys. Chem. C*, **2010**, 114, 1800.
- ¹¹³ N. G. Bastus, J. Comenge, V. Puentes, *Langmuir*, **2011**, 27, 11098.
- ¹¹⁴ M. Brust, M. Walker, D. Bethell, D. J. Schiffrin, R. Whyman, *J. Chem. Soc., Chem. Commun.*, **1994**, 801.
- ¹¹⁵ R. R. Arvizo, S. Bhattacharyya, R. A. Kudgus, K. Giri, R. Bhattacharyya, P. Mukkerjee, *Chem. Soc. Rev.*, **2012**, 41, 2943.
- ¹¹⁶ M.-C. Daniel, D. Astruc, *Chem. Rev.*, **2004**, 104, 293.
- ¹¹⁷ K. R. Brown, D. G. Walter, M. J. Natan, *Chem. Mater.*, **1999**, 12, 306.
- ¹¹⁸ J. Kreuter, *Adv. Drug Deliv. Rev.*, **2001**, 47, 65.
- ¹¹⁹ a) R. N. Alyaudtin , A. Reichel , R. Löbenberg , P. Ramge , J. Kreuter , D. J. Begley, *J. Drug. Targ.*, **2001**, 9, 209; b) P. R. Lockman , R. J. Mumper , M. A. Khan , D. D. Allen, *Drug Deliv. Ind. Pharm.*, **2002**, 25, 1.
- ¹²⁰ S. Mandal, G. J. Bakeine, S. Krol, C. Ferrari, A. M. Clerici, C. Zonta, L. Cansolino, F. Ballarini, S. Bortolussi, S. Stella, N. Protti, P. Bruschi, S. Altieri, *Appl. Radiat. Isotop.*, **2011**, 69, 12, 1692.

4. Bibliography

- ¹²¹ A. L. Pickering, C Mitterbauer, N. D. Browning, S. M. Kauzlarich, P. P. Power, *Chem. Commun.*, **2007**, 6, 580.
- ¹²² R. R. Arvizo, S. Rana, O. R. Miranda, R. Bhattacharya, V. M. Rotello, P. Mukherjee, *Nanomed.: Nanotechnol., Biol. Med.*, **2010**, 7, 580.
- ¹²³ S. Gurunathan, K.-J. Lee, K. Kalishwaralal, S. Sheikpranbabu, R. Vaidyanathan, S. H. Eom, *Biomaterials*, **2009**, 30, 6341.
- ¹²⁴ M. I. Sriram, S. B. M. Kanth, K. Kalishwaralal, S. Gurunathan, *Int. J. Nanomedicine*, **2010**, 5, 753.
- ¹²⁵ a) V. L. Colvin, *Nat Biotechnol*, **2003**, 21, 1166; b) K. L. Dreher, *Toxicol Sci*, **2004**, 77, 3; c) G. Oberdorster, A. Maynard, K. Donaldson, V. Castranova, J. Fitzpatrick, K. Ausman, J. Carter, B. Karn, W. Kreyling, D. Lai, *Part Fibre Toxicol.*, **2005**, 2, 8; d) G. Oberdorster, E. Oberdorster, J. Oberdorster, *Environ Health Perspect*, **2005**, 113, 823; e) A. Nel, T. Xia, L. Madler, N. Li, *Science*, **2006**, 311, 622; f) A. E. Nel, L. Madler, D. Velegol, T. Xia, E. M. V. Hoek, P. Somasundaran, F. Klaessig, V. Castranova, M. Thompson, *Nat Mater*, **2009**, 8, 543; g) Royal Society. Nanoscience and Nanotechnologies: Opportunities and Uncertainties. London: Royal Society; **2004**. Available at: www.nanotec.org.uk/finalReport.htm; h) K. W. Powers, S. C. Brown, V. B. Krishna, S. C. Wasdo, B. M. Moudgil, S. M. Roberts, *Toxicol Sci*, **2006**, 90, 296; i) K. Tiede, A. B. A. Boxall, S. P. Tear, J. Lewis, H. David, M. Hasselov, *Food Addit Contam*, **2008**, 25, 795.
- ¹²⁶ A. Nel, T. Xia, L. Madler, N. Li, *Science*, **2006**, 311, 622.
- ¹²⁷ G. Oberdorster, J. Fern, B. Lehnert, *Environ Health Perspect*, **1994**, 102, 173.
- ¹²⁸ R. W. Tarnuzzer, J. Colon, S. Patil, S. Seal, *Nano Lett*, **2005**, 5, 2573.
- ¹²⁹ a) Y. Pan, S. Neuss, A. Leifert, M. Fischler, F. Wen, U. Simon, G. Schmid, W. Brandau, W. Jahnen-Dechent, *Small*, **2007**, 3, 1941; b) W. H. De Jong, W. I. Hagens, P. Krystek, M. C. Burger, A. J. Sips, R. E. Geertsma, *Biomaterials*, **2008**, 29, 1912.
- ¹³⁰ B. D. Chithrani, W. C. W. Chan, *Nano Lett.*, 2007, 7, 1542.
- ¹³¹ a) S. G. Wang, W. T. Lu, O. Tovmachenko, U. S. Rai, H. T. Yu, P. C. Ray, *Chem Phys Lett*, **2008**, 463, 145; b) B. D. Chithrani, A. A. Ghazani, W. C. W. Chan, *Nano Lett*, **2006**, 6, 662; c) T. S. Hauck, A. A. Ghazani, C. W. C. Chan, *Small*, **2008**, 4, 153; d) H. J. Parab, H. M. Chen, T. C. Lai, J. H. Huang, P. H. Chen, R. S. Liu, M. Hsiao, C. H. Chen, D. P. Tsai, Y. K. Hwu, *J Phys Chem C*, **2009**, 113, 7574.
- ¹³² a) C. Goodman, C. McCusker, T. Yilmaz, V. Rotello, *Bioconjugate Chem.*, **2004**, 15, 897; b) A. Verma, F. Stellacci, *Small*, **2010**, 6, 12.
- ¹³³ J.A. Khan, R. A. Kudgus, A. Szabolcs, S. Dutta, E. Wang, S. Cao, G. L. Curran, V. Shah, S. Curley, D. Mukhopadhyay, J. D. Robertson, R. Bhattacharya, P. Mukherjee, *PLoS One*, **2011**, 6, e20347.
- ¹³⁴ a) C. K. Kim, P. Ghosh, C. Pagliuca, Z.-J. Zhu, S. Menichetti, V. M. Rotello, *J. Am. Chem. Soc.*, **2009**, 131, 1360; b) S. S. Agasti, A. Chomposor, C.-C. You, P. Ghosh, C. K. Kim, V. M. Rotello, *J. Am. Chem. Soc.*, **2009**, 131, 5728.
- ¹³⁵ M. A. El-Sayed, *Acc. Chem. Res.*, **2001**, 34, 257.
- ¹³⁶ J. Chen, D. Wang, J. Xi, L. Au, A. Siekkinen, A. Warsen, Z.-Y. Li, H. Zhang, Y. Xia, X. Li, *Nano Lett.*, **2007**, 7, 1318.
- ¹³⁷ H. S. Cho, *Phys. Med. Biol.*, **2005**, 50, N163.
- ¹³⁸ a) J. F. Hainfeld, D. N. Slatkin, T. M. Focella, H. M. Smilowitz, *Br. J. Radiol.*, **2006**, 79, 248; b) T. Kong, J. Zeng, X. Wang, X. Yang, J. Yang, S. McQuarrie, A. McEwan, W. Roa, J. Chen, J. Z. Xing, *Small*, **2008**, 4, 1537.
- ¹³⁹ T. Baše, Z. Bastl, Z. Plzák, T. Grygar, J. Plešek, M. J. Carr, V. Malina, J. Šubrt, J. Boháček, E. Veřnířková, O. Kříž, *Langmuir*, **2005**, 21, 7776.
- ¹⁴⁰ a) A. C. Templeton, W. P. Wuelfing, R. Murray, *Acc. Chem. Res.*, **2000**, 33, 27 and references therein; b) A. J. Henglein, *Phys. Chem.*, **1979**, 83, 2209.
- ¹⁴¹ a) R. G. Nuzzo, L. H. Dubois, D. L. Allara, *J. Am. Chem. Soc.*, **1990**, 112, 558; b) M. D. Porter, T. B. Bright, D. L. Allara, C. E. D. Chidsey, *J. Am. Chem. Soc.*, **1987**, 109, 3559; c) A. Ulman, *Chem. Rev.*, 1996, 96, 1533; d) R. G. Nuzzo, D. L. Allara, *J. Am. Chem. Soc.*, **1983**, 105, 4481; e) H. A. Biebuyck, C. D. Bain, G. M. Whitesides, *Langmuir*, **1994**, 10, 1825; f) H. Grönbeck, A. Curioni, W. Andreoni, *J. Am. Chem. Soc.*, **2000**, 122, 3839; g) R. G. Nuzzo, B. R. Zegarski, L. H. Dubois, *J. Am. Chem. Soc.*, **1987**, 109, 733.
- ¹⁴² M. Brust, J. Fink, D. Bethell, D. J. Schiffrin, C. J. Kiely, *Chem. Soc., Chem. Commun.*, **1995**, 1655.
- ¹⁴³ a) M. J. Hostetler, J. E. Wingate, C.-Z. Zhong, J. E. Harris, R. W. Vachet, M. R. Clark, J. D. Londono, S. J. Green, J. J. Stokes, G. D. Wignall, G. L. Glish, M. D. Porter, N. D. Evans, R. W. Murray, *Langmuir*, **1998**, 14, 17; b) D. V. Leff, P. C. O'Hara, J. R. Heath, W. M. Gelbart, *J. Phys. Chem.*, **1996**, 99, 7036.
- ¹⁴⁴ R. L. Whetten, J. T. Houry, M. M. Alvarez, S. Murthy, I. Vezmar, Z. L. Wang, P. W. Stephen, C. L. Cleveland, W. D. Luedtke, U. Landman, *Adv. Mater.*, **1996**, 5, 428.

4. Bibliography

- ¹⁴⁵ a) T. G. Schaaff, M. N. Shafigullin, J. T. Khoury, I. Vezmar, R. L. Whetten, W. Cullen, P. N. First, C. Gutierrez-Wing, J. Ascensio, M. J. Jose-Yacamán, *J. Phys. Chem. B*, **1997**, *101*, 7885; b) M. M. Alvarez, J. T. Khoury, T. G. Schaaff, M. Shafigullin, I. Vezmar, R. L. Whetten, *Chem. Phys. Lett.*, **1997**, *266*, 91.
- ¹⁴⁶ a) M. J. Hostetler, S. J. Green, J. J. Stokes, R. W. Murray, *J. Am. Chem. Soc.*, **1996**, *118*, 4212; b) R. S. Ingram, M. J. Hostetler, R. W. Murray, *J. Am. Chem. Soc.*, **1997**, *119*, 9175; c) M. J. Hostetler, A. C. Templeton, R. W. Murray, *Langmuir*, **1999**, *15*, 3782.
- ¹⁴⁷ A. C. Templeton, M. J. Hostetler, C. T. Kraft, R. W. Murray, *J. Am. Chem. Soc.*, **1998**, *120*, 1906.
- ¹⁴⁸ A. C. Templeton, M. J. Hostetler, E. K. Warmoth, S. Chen, C. M. Hartshorn, V. M. Krishnamurthy, M. D. E. Forbes, R. W. Murray, *J. Am. Chem. Soc.*, **1998**, *120*, 4845.
- ¹⁴⁹ G. R. Newkome, C. N. Moorefield, F. Vogtle, *VCH: New York*, **1996** and references therein.
- ¹⁵⁰ R. F. Barth, A. H. Soloway, R. G. Fairchild, *Cancer Res.*, **1990**, *50*, 1061.
- ¹⁵¹ a) R. F. Barth, J. A. Coderre, M. G. Vicente, T. E. Blue, *Clin. Cancer Res.*, **2005**, *11*, 3987; b) M. F. Hawthorne, *Angew. Chem., Int. Ed. Engl.*, **1993**, *32*, 950; c) Z. Yinghuai, K. Cheng Yan, J. A. Maguire, N. S. Hosmane, *Curr. Chem. Biol.*, **2007**, *1*, 141.
- ¹⁵² R. F. Barth, A. H. Soloway, R. G. Fairchild, R. M. Brugger, *Cancer*, **1992**, *70*, 2995.
- ¹⁵³ H. Nakamura, *Methods in Enzymology*, **2009**, *465*, 179.
- ¹⁵⁴ H. Yanagië , T. Tomita , H. Kobayashi , Y. Fujii , T. Takahashi , K. Hasumi , H. Nariuchi , M. Sekiguchi, *Br. J. Cancer*, **1991**, *63*, 522.
- ¹⁵⁵ a) K. Shelly, D. A. Feakes, M. F. Hawthorne, P. G. Schmidt, T. A. Krisch, W. F. Bauer, *PNAS*, **1992**, *89*, 9039; b) D. A. Feakes, K. Shelly, C. B. Knobler, M. F. Hawthorne, *PNAS*, **1994**, *91*, 3029; c) S. Martini, S. Ristori, A. Pucci, C. Bonechi, A. Becciolini, G. Martini, C. Rossi, *Biophys. Chem.*, **2004**, *111*, 27.
- ¹⁵⁶ X. Q. Pan, H. Wang, S. Shukla, M. Sekido, D. M. Adams, W. Tjarks, R. F. Barth, R. Lee, *J. Bioconjugate Chem.*, **2002**, *13*, 435.
- ¹⁵⁷ E. B. Kullberg, J. Carlsson, K. Edwards, J. Capala, S. Sjoberg, L. Gedda, *Int. J. Oncol.*, **2003**, *23*, 461.
- ¹⁵⁸ a) K. Maruyama, O. Ishida, S. Kasaoka, T. Takizawa, N. Utoguchi, A. Shinohara, M. Chiba, H. Kobayashi, M. Eriguchi, H. Yanagië, *J. Controlled Release*, **2004**, *98*, 195; b) H. Yanagië, K. Ogura, K. Takagi, K. Maruyama, T. Matsumoto, Y. Sakurai, J. Skvarc, R. Illic, G. Kuhne, T. Hisa, I. Yoshizaki, K. Kono, Y. Furuya, H. Sugiyama, H. Kobayashi, K. Ono, K. Nakagawa, M. Eriguchi, *Appl. Radiat. Isot.*, **2004**, *61*, 639.
- ¹⁵⁹ A. Doi , S. Kawabata , K. Iida , K. Yokoyama , Y. Kajimoto , T. Kuroiwa , T. Shirakawa , M. Kirihaata , S. Kasaoka , K. Maruyama , H. Kumada , Y. Sakurai , S. Masunaga , K. Ono , S. Miyatake, *J. Neurooncol.*, **2008**, *87*, 287.
- ¹⁶⁰ Y. Endo, T. Iijima, Y. Yamakoshi, H. y. Fukasawa, C. Miyaura, M. Inada, A. Kubo, A. Itai, *Chem. Biol.*, **2001**, *8*, 341.
- ¹⁶¹ a) D. A. Feakes, K. Shelly, M. F. Hawthorne, *PNAS*, **1995**, *92*, 1367; b) R. A. Watson-Clark, M. L. Banquerigo, K. Shelly, M. F. Hawthorne, E. Brahn, *PNAS*, **1998**, *95*, 2531.
- ¹⁶² H. Nakamura, Y. Miyajima, T. Takei, S. Kasaoka, K. Maruyama, *Chem. Commun.*, **2004**, 1910.
- ¹⁶³ Y. Miyajima, H. Nakamura, Y. Kuwata, J.-D. Lee, S. Masunaga, K. Ono, K. Maruyama, *Bioconjugate Chem.*, **2006**, *17*, 1314.
- ¹⁶⁴ T. Li, J. Hamdi, M. F. Hawthorne, *Bioconjugate Chem.*, **2006**, *17*, 15.
- ¹⁶⁵ D. Gabel, D. Preusse, D. Haritz, F. Grochulla, K. Haselsberger, H. Fankhauser, C. Ceberg, H.-D. Peters, U. Klotz, *Acta Neurochirurgica*, **1997**, *139*, 606.
- ¹⁶⁶ a) A. Holmberg, L. Meurling, *Bioconjugate Chem.*, **1993**, *4*, 570; b) D. H. Swenson, B. H. Laster, R. L. Metzger, *J. Med. Chem.*, **1996**, *39*, 1540; c) T. Sano, *Bioconjugate Chem.*, **1999**, *10*, 905; d) S. Hoffmann, E. Justus, M. Ratajski, E. Lork, D. Gabel, *J. Organomet. Chem.*, **2005**, *690*, 2757; e) R. G. Kultyshev, J. Liu, S. Liu, W. Tjarks, A. H. Soloway, S. G. Shore, *J. Am. Chem. Soc.*, **2002**, *124*, 2614.
- ¹⁶⁷ J.-D. Lee, M. Ueno, Y. Miyajima, H. Nakamura, *Org. Lett.*, **2007**, *9*, 323.
- ¹⁶⁸ a) W. J. Tjarks, *Organomet. Chem.*, **2000**, *614*, 37; b) Z. J. Lesnikowski, J. Shi, R. F. Schinazi, *J. Organomet. Chem.*, **1999**, *581*, 156; c) Y. Byun, J. H. Yan, A. S. Al-Madhoun, J. Johnsamuel, W. L. Yang, R. F. Barth, S. Eriksson, W. J. Tjarks, *Med. Chem.*, **2005**, *48*, 1188; d) A. S. Al-Madhoun, J. Johnsamuel, J. H. Yan, W. H. Ji, J. H. Wang, J. C. Zhuo, A. J. Lunato, J. E. Woollard, A. E. Hawk, G. Y. Cosquer, T. E. Blue, S. Eriksson, W. J. Tjarks, *Med. Chem.*, **2002**, *45*, 4018; e) A. J. Lunato, J. H. Wang, J. E. Woollard, A. K. M. Anisuzzaman, W. H. Ji, F. G. Rong, S. Ikeda, A. H. Soloway, S. Eriksson, D. H. Ives, T. E. Blue, W. J. Tjarks, *Med. Chem.*, **1999**, *42*, 3378.
- ¹⁶⁹ a) R. A. Spryshkova, L. I. Karaseva, V. A. Brattsev, N. G. Serebryakov, *Med. Radiol.*, **1981**, *26*, 62; b) R. A. Spryshkova, V. A. Brattsev, T. L. Sherman, V. I. Stanko, *Med. Radiol.*, **1981**, *26*, 51; c) Miadokova, E.; Trebaticka, M.; Podstavkova, S.; Vlcek, D. *Biologia (Bratislava)* **1990**, *45*, 917.

4. Bibliography

- ¹⁷⁰ M. Gielen, A. Bouhdid, R. Willem, V. I. Bregadze, L. V. Ermanson, E. R. T. Tiekink, *J. Organomet. Chem.*, **1995**, 501, 277.
- ¹⁷¹ a) I. H. Hall, C. E. Tolmie, B. J. Barnes, M. A. Curtis, J. M. Russel, J. M. Finn, R. N. Grimes, *Appl. Organomet. Chem.*, **2000**, 14, 108; b) H. I. Hall, C. B. Lackey, T. D. Kistler, R. W. Durham, Jr.; M. Russel, R. N. Grimes, *Anticancer Res.*, **2000**, 20, 2345.
- ¹⁷² R. L. Juliano, *Prog Clin Biol Res*, **1976**, 9, 21.
- ¹⁷³ T. M. Allen, *Chonn A. FEBS Lett.*, **1987**, 223, 42; b) J. H. Senior, *Crit Rev Ther Drug Carrier Syst.*, **1987**; 3, 123; c) A. Gabizon, D. Papahadjopoulos, *Proc Natl Acad Sci USA*, **1988**, 85, 6949.
- ¹⁷⁴ D. C. Drummond, O. Meyer, K. Hong D. B. , Kirpotin, D. Papahadjopoulos, *Pharmacol Rev.*, **1999**, 51, 691.
- ¹⁷⁵ R. K. Jain, *J Control Release*, **1998**, 53, 49.
- ¹⁷⁶ T. L. Andersen, S. S. Jensen, K. Jorgensen, *Prog. Lip. Res.*, **2005**, 44, 68.
- ¹⁷⁷ Y. Barenholz, *Curr Opin Colloid Interface Sci*, **2001**, 6, 66.
- ¹⁷⁸ a) J. A. Harding, C. M. Engbers, M. S. Newman, N. I. Goldstein, S. Zalipsky, *Biochim Biophys Acta*, **1997**;1327, 181; b) G. A. Koning, J. A. A. M. Kamps, G. L. Scherphof, *J Liposome Res*, **2002**;12, 107.
- ¹⁷⁹ a) T. Ishida, M. J. Kirchmeier, E. H. Moase, S. Zalipsky, T. M. Allen, *Biochim Biophys Acta*, **2001**;1515; b) M. B. Yatvin, W. Kreutz, B. A. Horwitz, M. Shinitzky, *Science*, **1980**, 210, 1253; c) J. Connor, M. B. Yatvin, L. Huang, *Proc Natl Acad Sci USA*, **1984**, 81, 1715; d) H. Ellens, J. Bentz, F. C. Szoka, *Biochemistry*, **1984**, 23, 1532; e) D. Collins, D. C. Litzinger, L. Huang, *Biochim Biophys Acta*, **1990**, 1025, 234; f) K. Kono, K. Zenitani, T. Takagishi, *Biochim Biophys Acta*, **1994**, 1193, 1; g) D. C. Drummond, M. Zignani, J. Leroux, *Prog Lipid Res*, **2000**, 39, 409; h) P. Venugopalan, S. Jain, S. Sankar, P. Singh, A. Rawat, S. P. Vyas, *Pharmazie*, **2002**, 57, 659; i) J. Shin, P. Shum, D. H. Thompson, *J Control Release*, **2003**, 91, 187.
- ¹⁸⁰ a) M. B. Yatvin, J. N. Weinstein, W. H. Dennis, R. Blumenthal, *Science*, **1978**, 202, 1290; b) J. N. Weinstein, R. L. Magin, M. B. Yatvin, D. S. Zaharko, *Science*, **1979**, 204, 188; c) M. H. Gaber, K. Hong, S. K. Huang, D. Papahadjopoulos, *Pharm Res*, **1995**, 12, 1407; d) K. Kono, R. Nakai, K. Morimoto, T. Takagishi, *FEBS Lett.*, **1999**, 456, 306; e) G. Kong, G. Anyarambhatla, W. P. Petros, R. D. Braun, O. M. Colvin, D. Needham, et al. *Cancer Res*, **2000**, 60, 6950; f) K. Kono, *Adv Drug Del Rev*, **2001**, 53, 307; g) D. Needham, M. W. Dewhirst, *Adv Drug Del Rev.*, **2001**, 53, 285.
- ¹⁸¹ a) V. C. Anderson, D. H. Thompson, *Biochim Biophys Acta*, **1992**, 1109, 33; b) H. Lamparski, U. Liman, J. A. Barry, D. A. Frankel, V. Ramaswami, M. F. Brown, D. F. O'Brien, *Biochemistry*, **1992**, 31, 685; c) C. G. Morgan, Y. P. Yianni, S. S. Sandhu, A. C. Mitchell, *Photochem Photobiol*, **1995**, 62, 24; d) C. R. Miller, D. E. Bennett, D. Y. Chang, D. F. O'Brien, *Biochemistry*, **1996**, 35, 11782; e) B. Bondurant, A. Mueller, D. F. O'Brien, *Biochim Biophys Acta*, **2001**, 1511, 113; f) P. Shum, J. M. Kim, D. H. Thompson, *Adv Drug Del Rev*, **2001**, 53, 273.
- ¹⁸² a) C. C. Pak, S. Ali, A. S. Janoff, P. Meers, *Biochim Biophys Acta*, **1998**, 1372, 13; b) C. C. Pak, R. K. Erukulla, P. L. Ahl, A. S. Janoff, P. Meers, *Biochim Biophys Acta*, **1999**, 1419, 111; c) P. Meers, *Adv Drug Del Rev*, **2001**, 53, 265; d) K. Jørgensen, J. Davidsen, O. G. Mouritsen, *FEBS Lett*, **2002**, 531, 23; e) J. Davidsen, K. Jørgensen, T. L. Andresen, O. G. Mouritsen, *Biochim Biophys Acta*, **2003**, 1609, 95.
- ¹⁸³ D. Gabel, D. Awad, T. Schaffran, D. Radovan, D. Dabaran, L. Damian, M. Winterhalter, G. Karlsson, K. Edwards, *Chem. Med. Chem.*, **2007**, 2, 51.
- ¹⁸⁴ X. Li, Y. Zhao, *Langmuir*, **2012**, 28, 4152.
- ¹⁸⁵ G. Shi, W. Guo, S. M. Stephenson, R. J. Lee, *J. Contrl. Rel.*, **2002**, 80, 309.
- ¹⁸⁶ a) I. B. Sivaev, V. I. Bregadze, *Collect. Czech. Chem. Commun.*, **1999**, 64, 783; b) A. Franken, J. Plešek, C. Nachtigal, *Collect. Czech. Chem. Commun.*, **1997**, 62, 746; c) M. R. Churchill, K. Gold, J. N. Francis, M. F. Hawthorne, *J. Am. Chem. Soc.*, **1969**, 91, 1222.
- ¹⁸⁷ a) J. Plešek, S. Hermánek, A. Franken, I. Císařová, C. Nachtigal, *Collect. Czech. Chem. Commun.*, **1997**, 62, 47; b) B. Grüner, J. Plešek, J. Bářa, I. Císařová, J. F. Dozol, H. Rouquette, C. Viñas, P. Selucký, J. Rais, *New J. Chem.*, **2002**, 26, 1519; c) P. Selucký, J. Plešek, J. Rais, M. Kyrs, L. Kadlecova, *J. Radioanal. Nucl. Chem.*, **1991**, 149, 131.
- ¹⁸⁸ a) I. Rojo, F. Teixidor, C. Viñas, R. Kivekäs, R. Sillanpää, *Chem Eur. J.*, **2004**, 10, 5376; b) E. J. Juarez, C. Viñas, A. Gonzalez-Campo, F. Teixidor, R. Sillanpää, R. Kivekäs, R. Nunez, *Chem Eur. J.*, **2008**, 14, 4924.
- ¹⁸⁹ P. Farràs, F. Teixidor, R. Sillanpää, C. Viñas, *Dalton Trans.*, **2010**, 39, 1716.
- ¹⁹⁰ H. Li, Y.-Y. Luk, M. Mrksich, *Langmuir*, **1999**, 15, 4957.
- ¹⁹¹ L. Pasquato, F. Rancan, P. Scrimin, F. Mancin, C. Frigeri, *Chem. Commun.*, **2000**, 2253.

4. Bibliography

- ¹⁹² a) R. Bernard, D. Cornu, M. Perrin, J. P. Schaff, P. Miele, *J. Organomet. Chem.*, **2004**, 689, 2581.; b) K. Y. Zhizhin, V. N. Mustyatsa, E. A. Malinina, N. A. Votinova, E. Y. Matveev, L. V. Goeva, I. N. Polyakova, N. T. Kuznetsov, *Russ. J. Inorg. Chem.*, **2005**, 50, 203.
- ¹⁹³ I. B. Sivaev, A. A.; Semioshkin, B. Brellochs, S. Sjöberg, V. I. Bregadze, *Polyhedron*, **2000**, 19, 627.
- ¹⁹⁴ a) J. Plešek, S. Hermánek, K. Base, L. J. Todd, W. F. Wright, *Collect. Czech. Chem. Commun.*, **1976**, 41, 3509; b) A. Petina, V. Petříšek, K. Malý, V. Šubrtová, A. Línek, L. Hummel, *Z. Kristallogr.*, **1981**, 154, 217; c) V. Šubrtová, V. Petříšek, L. Hummel, *Acta Crystallogr., Sect. C*, **1989**, 45, 1964.
- ¹⁹⁵ a) S. H. Strauss, *Chem. Rev.*, **1993**, 93, 927; b) C. A. Reed, *Acc. Chem. Res.*, **1998**, 31, 133.
- ¹⁹⁶ I. B. Sivaev, S. Sjöberg, V. Bregadze, *J. Organomet. Chem.*, **2003**, 680, 106.
- ¹⁹⁷ P. Farràs, F. Teixidor, R. Kivekäs, R. Sillanpää, C. Viñas, G. Bohumir, I. Císarová, *Inorg. Chem.*, **2008**, 47, 9497.
- ¹⁹⁸ V. Šícha, P. Farràs, B. Štíbr, F. Teixidor, B. Grüner, C. Viñas, *J. Organomet. Chem.*, **2009**, 694, 1599.
- ¹⁹⁹ J. C. Fanning, *Coord. Chem. Rev.*, **1995**, 140, 27.
- ²⁰⁰ V. I. Bregadze, *Chem. Rev.*, **1992**, 209.
- ²⁰¹ a) M. Karas, F. Hillenkamp, *Anal. Chem.*, **1988**, 60, 2299; b) M. Karas, D. Bachmann, F. Hillenkamp, *Anal. Chem.*, **1985**, 57, 2935; c) K. Tanaka, H. Waki, Y. Ido, S. Akita, Y. Yoshida, T. Yoshida, *Rapid Commun. Mass Spectrom.*, **1988**, 2, 151.
- ²⁰² a) F. Teixidor, J. Casabó, C. Viñas, E. Sanchez, L. Escriche, R. Kivekäs, *Inorg. Chem.*, **1991**, 30, 3053; b) F. Teixidor, R. Núñez, C. Viñas, R. Sillanpää, R. Kivekäs, *Inorg. Chem.*, **2001**, 40, 2587.
- ²⁰³ a) F. Teixidor, A. Romerosa, C. Viñas, J. Rius, C. Miravittles, J. Casabó, *J. Chem. Soc., Chem. Commun.*, **1991**, 192; b) F. Teixidor, J. A. Ayllón, C. Viñas, J. Rius, C. Miravittles, J. Casabó, *J. Chem. Soc., Chem. Commun.*, **1992**, 1279; c) F. Teixidor, J. Casabó, A. M. Romerosa, C. Viñas, J. Rius, C. Miravittles, *J. Am. Chem. Soc.*, **1991**, 113, 9895.
- ²⁰⁴ P. Farràs, A. M. Cioran, Václav Šícha, F. Teixidor, Bohumil Štíbr, Bohumír Grüner, Clara Viñas, *Inorg. Chem.*, **2009**, 48, 8210.
- ²⁰⁵ D. Massiot, F. Fayon, M. Capron, I. King, S. Le Calvé, B. Alonso, J.-O. Durand, B. Bujoli, Z. Gan, G. Hoatson, *Magn. Reson. Chem.*, **2002**, 40, 70.
- ²⁰⁶ L. A. Leites, *Chem. Rev.*, **1992**, 92, 279.
- ²⁰⁷ I. B. Sivaev, V. Bregadze, S. Sjöberg, In *Research and Development in Neutron Capture Therapy*; W. Sauerwein, R. Moss, A. Wittig, Eds.; Monduzzi Editore S.p.A.: Bologna, **2002**; 19.
- ²⁰⁸ M. F. Hawthorne, D.C. Young, T. D. Andrews, D. V. Howe, R. L. Pilling, A. D. Pitts, M. Reintjes, L. F. Warren Jr, P. A. Wegner, *J. Am. Chem. Soc.*, **1968**, 90, 879.
- ²⁰⁹ V. Cerný, I. Pavlík, E. Kustková-Maxová, *Collect. Czech. Chem. Commun.*, **1976**, 41, 3232
- ²¹⁰ P. González-Cardoso, A-I Stoica, P. Farràs, A. Pepioli, C. Viñas, F. Teixidor, *Chem. Eur. J.*, **2010**, 16, 6660.
- ²¹¹ a) J.-Q. Wang, C.-X. Ren, L.-H. Weng, G.-X. Jin, *Chem. Commun.*, **2006**, 162; b) K. J. Winberg, G. Barberà, L. Eriksson, F. Teixidor, V. Tolmachev, C. Viñas, S. Sjöberg, *J. Organomet. Chem.*, **2003**, 680, 188.
- ²¹² a) E. Hao, T. J. Jensen, B. H. Courtney, M. G. H. Vicente, *Bioconjugate Chem.*, **2005**, 16, 1495; b) M. Sibrian-Vazquez, E. Hao, T. J. Jensen, M. G. H. Vicente, *Bioconjugate Chem.*, **2006**, 17, 928; c) E. Hao, M. Zhang, W. E. , K. M. Kadish, F. R. Fronczek, B. H. Courtney, M. G. H. Vicente, *Bioconjugate Chem.*, **2008**, 19, 2171.
- ²¹³ A) A. B. Olejniczak, P. Mucha, B. Grüner, Z. J. Lesnikowski, *Organometallics*, **2007**, 26, 3272; b) B. A. Wojtczak, A. Andrysiak, B. Grüner, Z. J. Lesnikowski, *Chem. Eur. J.*, **2008**, 14, 10675.
- ²¹⁴ R. B. King, *Chem. Rev.*, **2001**, 101, 1119.
- ²¹⁵ D. C. Young, D. V. Howe, M. F. Hawthorne, *J. Am. Chem. Soc.*, **1969**, 91, 859.
- ²¹⁶ a) M. Yu. Stogniy, E. N. Abramova, I. A. Lobanova, I. B. Sivaev, V. I. Bragin, P. V. Petrovskii, V. N. Tsupreva, O. V. Sorokina, V. I. Bregadze, *Collect. Czech. Chem. Commun.*, **2007**, 72, 1676; b) J. Plešek, T. Jelínek, F. Mares, S. Heřmanek, *Collect. Czech. Chem. Commun.*, **1993**, 58, 1534.
- ²¹⁷ T. Peymann, K. Kück, D. Gabel, *Inorg. Chem.*, **1997**, 36, 5138.
- ²¹⁸ E. L. Crossley, L. M. Rendina, presented at the *RACI Inorganic Conference*, Hobart (Tasmania), February **2007**.
- ²¹⁹ a) Ya. Z. Voloshin, O. A. Varzatskii, K. Yu. Zhizhin, N. T. Kuznetsov, presented at *XXIII Chugaev International Conference on Coordination Chemistry*, Odessa (Ukraine), September **2007**; b) Ya. Z. Voloshin, O. A. Varsatskii, Yu. N. Bubnov, *Russ. Chem. Bull.*, **2007**, 56, 577.
- ²²⁰ a) M. Brust, M. Walker, D. Bethell, D. J. Schiffrin, *J. Chem. Soc. Chem. Commun.*, **1994**, 7, 801; b) M. Brust, J. Fink, D. Bethell, D. J. Schiffrin, C. Kiely, *J. Chem. Soc. Chem. Commun.*, **1995**, 16, 1655; c) R. H.

4. Bibliography

- Terrill, T. A. Postlethwaite, C. H. Chen, C. D. Poon, A. Terziz, A. D. Chen, J. E. Hutchison, M. R. Clark, G. Wignall, J. D. Londono, R. Superfine, M. Falvo, C. S. Johnson, E. T. Samulski, R. W. Murray, *J. Am. Chem. Soc.*, **1995**, *117*, 12537; d) A. Badia, S. Singh, L. Demers, L. Cuccia, G. R. Brown, R. B. Lennox, *Chem-Eur. J.*, **1996**, *2*, 359; e) M. J. Hostetler, J. J. Stokes, R. W. Murray, *Langmuir*, **1996**, *12*, 3604; f) M. C. Daniel, D. Astruc, *Chem. Rev.*, **2004**, *104*, 293; g) E. Boisselier, D. Astruc, *Chem. Soc. Rev.*, **2009**, *38*, 1759; h) R. Sardar, A. M. Funston, P. Mulvaney, R. W. Murray, *Langmuir*, **2009**, *25*, 13840.
- ²²¹ a) H. Wohltjen, A. W. Snow, *Anal. Chem.*, **1998**, *70*, 2856; b) Y. Joseph, A. Peic, X. D. Chen, J. Michl, T. Vossmeier, A. Yasuda, *J. Phys. Chem. C*, **2007**, *111*, 12855; c) O. Barash, N. Peled, F. R. Hirsch, H. Haick, *Small*, **2009**, *5*, 2618; d) G. Peng, U. Tisch, O. Adams, M. Hakim, N. Shehada, Y. Y. Broza, S. Billan, R. Abdah-Bortnyak, A. Kuten, H. Haick, *Nat. Nanotechnol.*, **2009**, *4*, 669; e) E. Chow, T. R. Gengenbach, L. Wiczorek, B. Raguse, *Sens. Actuators B*, **2010**, *143*, 704; f) E. Covington, F. I. Bohrer, C. Xu, E. T. Zellers, C. Kurdak, *Lab Chip*, **2010**, *22*, 3058.
- ²²² P. D. Jadzinsky, G. Calero, C. D. Ackerson, D. A. Bushnell, R. D. Kornberg, *Science*, **2007**, *318*, 430.
- ²²³ a) F. Wen, U. Englert, B. Gutrat, U. Simon, *Eur. J. Inorg. Chem.*, **2008**, *1*, 106; b) M. Zhu, C. M. Aikens, F. J. Hollander, G. C. Schatz, R.C. Jin, *J. Am. Chem. Soc.*, **2008**, *130*, 5883; c) H. F. Qian, W. T. Eckenhoff, Y. Zhu, T. Pintauer, R. C. Jin, *J. Am. Chem. Soc.*, **2010**, *132*, 8280; d) J. F. Parker, C. A. Fields-Zinna, R. W. Murray, *Acc. Chem. Res.*, **2010**, *43*, 1289.
- ²²⁴ Y. Shichibu, Y. Negishi, T. Watanabe, N. K. Chaki, H. Kawaguchi, T. Tsukuda, *J. Phys. Chem. C*, **2007**, *111*, 7845.
- ²²⁵ X.-K. Wan, Z.-W. Lin, Q.-M. Wang, *J. Am. Chem. Soc.*, **2012**, *134*, 14750.
- ²²⁶ B. K. Teo, X. Shi, H. Zhang, *J. Am. Chem. Soc.*, **1992**, *114*, 2743.
- ²²⁷ a) J. Akola, M. Walter, R. L. Whetten, H. Hakkinen, H. Gronbeck, *J. Am. Chem. Soc.*, **2008**, *130*, 3756; b) M. Walter, J. Akola, O. Lopez-Acevedo, P. D. Jadzinsky, G. Calero, C. J. Ackerson, R. L. Whetten, H. Gronbeck, H. Hakkinen, *Proc. Natl. Acad. Sci. U.S.A.*, **2008**, *105*, 9157; c) D. E. Jiang, M. Walter, J. Akola, *J. Phys. Chem. C*, **2010**, *114*, 15883; d) C. M. Aitkens, *J. Phys. Chem. Lett.*, **2010**, *2*, 99.
- ²²⁸ J. Pedersen, S. Bjornholm, J. Borggreen, K. Hansen, T. P. Martin, H. D. Rasmussen, *Nature*, **1991**, *353*, 733.
- ²²⁹ a) G. F. Paciotti, L. Myer, D. Weinreich, D. Goia, N. Pavel, R. E. McLaughlin, L. Tamarkin, *Drug Delivery*, **2004**, *11*, 169; b) R. Hong, G. Han, J. M. Fernandez, B. J. Kim, N. S. Forbes, V. M. Rotello, *J. Am. Chem. Soc.*, **2006**, *128*, 1078; c) B. D. Chithrani, W. C. W. Chan, *Nano Lett.*, **2007**, *7*, 1542; d) P. Podsiadlo, V. A. Sinani, J. H. Bahng, N. W. S. Kam, J. Lee, N. A. Kotov., *Langmuir*, **2008**, *24*, 568; e) P. S. Ghosh, C. K. Kim, G. Han, N. S. Forbes, V. M. Rotello, *ACS Nano*, **2008**, *2*, 2213; f) C. Kim, S. S. Agasti, Z. J. Zhu, L. Isaacs, V. M. Rotello, *Nat. Chem.*, **2010**, *2*, 962; g) Z. Krpetic, P. Nativo, V. See, I. A. Prior, M. Brust, M. Volk, *Nano Lett.*, **2010**, *10*, 4549; h) J. Gil-Tomas, L. Dekker, N. Narband, I. P. Parkin, S. P. Nair, C. Street, M. J. Wilson, *Mater. Chem.*, **2011**, *21*, 4189.
- ²³⁰ a) J. M. de la Fuente, A. G. Barrientos, T. C. Rojas, J. Rojo, A. Fernandez, S. Penades, *Angew. Chem., Int. Ed.*, **2001**, *40*, 2258; b) A. G. Barrientos, J. M. de la Fuente, T. C. Rojas, A. Fernandez, S. Penades, *Chem.-Eur. J.*, **2003**, *9*, 1909; c) J. Rojo, V. Diaz, J. M. de la Fuente, I. Segura, A. G. Barrientos, H. H. Riese, A. Bernade, S. Penades, *ChemBioChem*, **2004**, *5*, 291; d) I. Garcia, M. Marradi, S. Penades, *Nanomedicine*, **2010**, *5*, 777.
- ²³¹ a) R. Levy, N. T. K. Thanh, R. C. Doty, I. Hussain, R. Nichols, D. J. Schiffrin, M. Brust, D. G. Fernig, *J. Am. Chem. Soc.*, **2004**, *126*, 10076; b) P. Pengo, S. Polizzi, L. Pasquato, P. Scrimin, *J. Am. Chem. Soc.*, **2005**, *127*, 1616; c) J. M. Slocik, M. O. Stone, R. R. Naik, *Small*, **2005**, *1*, 1048; d) R. Levy, *ChemBioChem*, **2006**, *7*, 1145; e) P. Pengo, L. Baltzer, L. Pasquato, P. Scrimin, *Angew. Chem., Int. Ed.*, **2007**, *46*, 400; f) Z. Krpetic, P. Nativo, F. Porta, M. Brust, *Bioconjugate Chem.*, **2009**, *20*, 1619.
- ²³² a) I. Hussain, S. Graham, Z. X. Wang, B. Tan, D. C. Sherrington, S. P. Rannard, A. I. Cooper, M. Brust, *J. Am. Chem. Soc.*, **2005**, *127*, 16398; b) Z. X. Wang, B. E. Tan, I. Hussain, N. Schaeffer, M. F. Wyatt, M. Brust, A. I. Cooper, *Langmuir*, **2007**, *23*, 885.
- ²³³ a) W. P. Wuelfing, S. M. Gross, D. T. Miles, R. W. Murray, *J. Am. Chem. Soc.*, **1998**, *120*, 12696; b) M. Bartz, J. Kuther, G. Nelles, N. Weber, R. Seshadri, W. J. Tremel, *Mater. Chem.*, **1999**, *9*, 121; c) A. G. Kanaras, F. S. Kamounah, K. Schaumburg, C. J. Kiely, M. Brust, *Chem. Commun.*, **2002**, *20*, 2294; d) T. Ishii, H. Otsuka, K. Kataoka, Y. Nagasaki, *Langmuir*, **2004**, *20*, 561; e) T. R. Tshikhudo, D. Demuru, Z. X. Wang, M. Brust, A. Secchi, A. Arduini, A. Pochini, *Angew. Chem., Int. Ed.*, **2005**, *44*, 2913; f) L. Duchesne, D. Gentili, M. Comes-Franchini, D. G. Fernig, *Langmuir*, **2008**, *24*, 13572.
- ²³⁴ a) R. S. Ingam, M. J. Hostetler, R. W. Murray, T. G. Schaaf, J. T. Khoury, R. L. Whetten, T. P. Bigioni, D. K. Guthrie, P. N. First, *J. Am. Chem. Soc.*, **1997**, *119*, 9279; b) S. W. Chen, R. S. Ingram, M. J. Hostetler, J. J. Pietron, R. W. Murray, T. G. Schaaf, J. T. Khoury, M. M. Alvarez, R. L. Whetten, *Science*,

4. Bibliography

- 1998, 220, 2098; c) J. F. Hicks, A. C. Templeton, S. W. Chen, K. M. Sheran, R. Jasti, R. W. Murray, J. Debord, T. G. Schaaf, R. L. Whetten, *Anal. Chem.*, **1999**, 71, 3703; d) B. M. Quinn, P. Liljeroth, V. Ruiz, T. Laaksonen, K. Kontturi, *J. Am. Chem. Soc.*, **2003**, 125, 6644.
- ²³⁵ B. M. Quinn, K. Kontturi, *J. Am. Chem. Soc.*, **2004**, 126, 7168.
- ²³⁶ a) A. Henglein, J. Lilie, *J. Am. Chem. Soc.*, **1981**, 103, 1059; b) A. Henglein, *Top. Curr. Chem.*, **1988**, 143, 113; c) A. Henglein, *Chem. Rev.*, **1989**, 89, 1861.
- ²³⁷ a) V. Gottumukkala, O. Ongayi, D. G. Baker, L. G. Lomax, M. G. H. Vicente, *Bioorg. Med. Chem.*, **2006**, 14, 1871; b) J.-Q. Wang, C.-X. Ren, L.-H. Weng, G.-X. Jin, *Chem. Commun.*, **2006**, 162.
- ²³⁸ L. A. Leites, L. E. Vinogradova, *J. Organomet. Chem.*, **1977**, 125, 37.
- ²³⁹ a) H. D. Smith, C. O. Obenland, S. Papetti, *Inorg. Chem.*, **1966**, 5, 1013; b) C. Viñas, R. Benakki, F. Teixidor, J. Casabó, *Inorg. Chem.*, **1995**, 34, 3844.
- ²⁴⁰ a) F. Teixidor, C. Viñas, R. Sillanpää, R. Kivekäs, *Inorg. Chem.*, **1994**, 33, 2645.; b) F. Teixidor, J. Pedradas, C. Viñas, *Inorg. Chem.*, **1995**, 34, 1726; c) R. Kivekäs, R. Sillanpää, F. Teixidor, C. Viñas, R. Núñez, *Acta Crystallogr., Sect. C*, **1994**, 50, 2027; d) J. Llop, C. Viñas, J. M. Oliva, F. Teixidor, M. A. Flores, R. Kivekäs, R. Sillanpää, *J. Organomet. Chem.*, **2002**, 657, 232; e) J. M. Oliva, N. L. Allan, P. V. Schleyer, C. Viñas, F. Teixidor, *J. Am. Chem. Soc.*, **2005**, 127 (39), 13538.
- ²⁴¹ Cation exchange resin strongly acidic PA (provided by Panreac) with a total exchange capacity of 2.0 meq/mL and a water content of 46–52%, loaded with lithium chloride.
- ²⁴² H. Qian, W. T. Eckenhoff, Y. Zhu, T. Pintauer, R. Jin, *J. Am. Chem. Soc.*, **2010**, 132, 8280.
- ²⁴³ B. Kivekäs, R. Benakki, C. Viñas, R. Sillanpää, *Acta Crystallogr.*, **1999**, C55, 1581.
- ²⁴⁴ P. D. Jadzinsky, G. Calero, C. D. Ackerson, D. A. Bushnell, R. D. Kornberg, *Science*, **2007**, 318, 430.
- ²⁴⁵ O. Lopez-Acevedo, J. Akola, R. L. Whetten, H. Grönbeck, H. Häkkinen, *J. Phys. Chem. C*, **2009**, 113 (13), 5035.
- ²⁴⁶ a) A. S. Batsanov, M. A. Fox, T. G. Hibbert, J. A. K. Howard, R. Kivekäs, A. Laromaine, R. Sillanpää, C. Viñas, K. Wade, *Dalton Trans.*, **2004**, 3822; b) J. G. Planas, C. Viñas, F. Teixidor, A. Comas-Vives, G. Ujaque, A. Lledós, M. E. Light, M. B. Hursthouse, *J. Am. Chem. Soc.*, **2005**, 127, 15976.
- ²⁴⁷ F. Teixidor, C. Viñas, A. Demonceau, R. Núñez, *Pure Appl. Chem.*, **2003**, 75, 1305.
- ²⁴⁸ A. V. Puga, F. Teixidor, R. Sillanpää, R. Kivekäs, C. Viñas, *Chem. Eur. J.*, **2009**, 15, 9764.
- ²⁴⁹ a) R. Núñez, P. Farràs, F. Teixidor, C. Viñas, R. Sillanpää, R. Kivekäs, *Angew. Chem., Int. Ed.*, **2006**, 45, 1270. b) F. Teixidor, R. Núñez, C. Viñas, R. Sillanpää, R. Kivekäs, *Angew. Chem. Int. Ed.*, **2000**, 39, 4290.
- ²⁵⁰ P. Mulvaney, *Langmuir*, **1996**, 12, 788.
- ²⁵¹ W. Haiss, N. T. K. Thanh, J. Aveyard, D. G. Fernig, *Anal. Chem.*, **2007**, 79, 4215.
- ²⁵² A. M. Cioran, A. D. Musteti, F. Teixidor, Z. Krpetić, I. A. Prior, Q. He, Ch. J. Kiely, M. Brust, C. Viñas, *J. Am. Chem. Soc.*, **2012**, 134, 212.
- ²⁵³ a) T. G. Lugo, S. Braun, R. J. Cote, K. Pantel, V. Rusch, *J. Clinical Oncology*, **2003**, 21, 2609; b) S. Nagrath, L. V. Sequist, S. Maheswaran, D. W. Bell, D. Irimia, L. Ulkus, M. R. Smith, E. L. Kwak, S. Digumarthy, A. Muzikansky, P. Ryan, U. J. Balis, R. G. Tompkins, D. A. Haber, M. Toner, *Nature*, **2007**, 450, 1235; c) P. Paterlini-Brechot, N. L. Benali, *Cancer Letters* 2007, 253, 180. [4] K. Pantel, C. Alix-Panabières, *Trends in Molecular Medicine*, **2010**, 16, 398; d) N. Bednarz-Knoll, C. Alix-Panabières, K. Pantel, *Breast Cancer Research*, **2011**, 13, 228.
- ²⁵⁴ a) A. De la Escosura-Munñiz, A. Ambrosi, A. Merkoçi, *Trends in Analytical Chemistry*, **2008**, 27, 568; b) A. Merkoçi, *Biosensors and Bioelectronics*, **2010**, 26, 1164; c) B. Pérez-López, A. Merkoçi, *Analytical and Bioanalytical Chemistry*, **2011**, 399, 1577.
- ²⁵⁵ M. Espinoza-Castañeda, A. de la Escosura-Munñiz, G. González-Ortiz, S. M. Martín-Orúe, J. F. Pérez, A. Merkoçi, *Biosensors and Bioelectronics*, **2013**, 40, 1, 271.
- ²⁵⁶ C. Brandenberger, C. Muhlfeld, Z. Ali, A. G. Lenz, O. Schmid, W. J. Parak, P. Gehr, B. Rothen-Rutishauser, *Small*, **2010**, 6, 1669.
- ²⁵⁷ a) W. P. Wuelfing, S. M. Gross, D. T. Miles, R. W. Murray, *J. Am. Chem. Soc.*, **1998**, 120, 12696; b) L. Duchesne, D. Gentili, M. Comes-Franchini, D. G. Fernig, *Langmuir*, **2008**, 24, 13572.